HANDBOOK
OF CHEMICAL AND BIOCHEMICAL TECHNOLOGIES

Edited by: Jurex Cuenca Gallo

ARCLER PRESS

HANDBOOK OF CHEMICAL AND BIOCHEMICAL TECHNOLOGIES

HANDBOOK OF CHEMICAL AND BIOCHEMICAL TECHNOLOGIES

Edited by

Jurex Cuenca Gallo

ARCLER PRESS

www.arclerpress.com

Handbook of Chemical and Biochemical Technologies

Jurex Cuenca Gallo

Arcler Press
2010 Winston Park Drive,
2nd Floor
Oakville, ON L6H 5R7
Canada
www.arclerpress.com
Tel: 001-289-291-7705
001-905-616-2116
Fax: 001-289-291-7601
Email: orders@arclereducation.com

e-book Edition 2019
ISBN: 978-1-77361-611-7 (e-book)

ISBN: 978-1-77361-466-3 (Hardcover)

Arcler Press publishes wide variety of books and eBooks. For more information about Arcler Press and its products, visit our website at www.arclerpress.com

ABOUT THE EDITOR

Dr. Jurex Gallo was conferred with his PhD degree in Chemical Engineering from De La Salle University – Manila in 2014. His expertise revolved in the fields of Material Science and Environmental Engineering focused on industrial and hazardous waste treatment and management. Presently, Dr. Gallo is affiliated as Senior Science Research Specialist of the Department of Science and Technology e-Asia Joint Research Program in the Philippines on developing functional carbon-based nanomaterials such as carbon nanotubes and graphene for energy and environmental applications.

TABLE OF CONTENTS

LIST OF FIGURES

synthesized through biosynthesis of fatty acid. Enzyme designations: 2-enoyl-CoA hydratase (5), fatty acyl-CoA dehydrogenase (4), β-ketothiolase (7), and 3-hydroxyacyl-CoA dehydrogenase (6).

Figure. 12. Applications of PHA in manufacturing of various composite materials

Figure. 13. Production of biodiesel from triglyceride and alcohol

Figure. 14. The growth of *R. opacus* PD630 from high concentrations of glucose concentrations in flask cultures. The concentrations of glucose tested in defined media containing 1.4 g l^{-1}

Figure. 15. The effects of $(NH_4)_2SO_4$ and glucose concentrations on pH of the culture. (a) Representation of fatty acid content, (b) representation of CDW, and (c) representation of fatty acid creation (d) by *R. opacus* PD630 in flask culture

Figure. 16. The response surface curve showing the varying concentrations of $(NH_4)_2SO_4$ and glucose on fatty acid synthesis by *R. opacus* PD630

Figure. 17. Saccharification of corn silage with industrial enzymes; the adjustment of homogenized feedstock (i.e., 67 g l^{-1} of dried material stuff) was carried out adjusted to the pH value of 5.0. The addition of Novozymes (0.5 ml Celluclast sand 2 ml Viscozyme L) into the suspension of 100 ml was carried out followed by the hydrolysis at 200 rpm at 45°C. The error bars show the standard deviations of the three (3) independent replicates.

Figure. 18. Production and growth of lipids from *R. opacus* PD630 with different saccharified corn silage in flasks. The inoculation of the strain in the saccharified solution was around 100 (▲), 75 (□), and 50% (○). The solutions along with a defined media (x) comprising of 1 g l^{-1} $(NH_4)_2SO_4$ and 18 g l^{-1} glucose at an initial OD 660 of about 0.3. A diluted saccharified stock, having a dilution ratio of 3:1 with the addition of water, is categorized as 75%, while a diluted saccharified stock, having a dilution ratio of 1:1 with the addition of water, is categorized as 50%. The error bars show the standard deviations of the three (3) independent replicates.

Figure. 19. Effect of glucose addition on the production of lipid by *R. opacus* PD630 developed from the saccharified corn silage in flasks. The inoculation of the strain in the saccharified solution was around 75% solution appended with 30 (▲), 20 (□), or 10 g l^{-1} glucose at an initial OD 660 of about 0.3 without a medium (x). The error bars show the standard deviations of the three (3) independent replicates.

Figure. 20. Fluorescent image of stained cells of *R. opacus* PD630 tainted with the lipophilic fluorophore, that is, Nile Red. Cells were produced in a nominal

by manufacturing in a nanostructure hole.

Figure. 71. Complete development of Complete Genomics' nanoballs after magnification of the rolling cycle. Ligation is used for carrying out sequencing of these DNB

Figure. 72. Ion Torrent technology illustrating the release of proton after the incorporation of the nucleotide by the DNA

Figure. 73. Advanced Ion Torrent technology. (a) The Ion Torrent exclusive microchip design. (b) Cross-sectional outlook of a single well which houses ionic sphere particles possessing a clonal amplified template of DNA. The incorporation of nucleotide by DNA poly

Figure. 74. A typical schematic of whole-genome sequencing

LIST OF TABLES

PREFACE

The enthusiastic approach of scientists and researchers toward green chemical and biochemical technologies inspired me to write this book with a desire to satisfy the current demand for a systematic handbook on chemical and biochemical technologies. This book is mainly intended not only for the students of chemistry having completed their organic–synthetic, inorganic–analytical, and physicochemical courses but also for machine engineering students who are inclined toward process engineering and chemical technology. This book can be considered a bridge between academic and industrial prospects of young chemists and biochemists. Moreover, numerous people from various backgrounds can also benefit from this book. For instance, sales persons, doctors, and medical students can acquire fundamental knowledge of the chemistry and biology of different chemical products available in the market. This book will not focus on memorizing the stuff; instead, it will instigate meditating and creative thinking among engineers, chemists, and biochemists.

The Handbook of Chemical and Biochemical Technologies contains a set of guidelines and information regarding different applications of chemistry and biochemistry. By offering a modern and applied approach, this book will assist the readers to comprehend the values and relevance of innovative chemical technologies. This book is designed to provide a deep insight into chemical phenomena (natural or human driven) and technological breakthroughs taking place in the world. The Handbook of Chemical and Biochemical Technologies consists of broad-ranging views on the current advancements in applied chemical and biochemical methodologies which include diverse aspects of modern chemical and biochemical processes and experimentations. This book focuses on the applications of chemistry in different areas of human activity. Moreover, this book presents viable solutions to a variety of challenges and problems which are encountered in engineering and research sector. This book also focuses on both the theoretical and the experimental aspects of various chemical and biochemical technologies.

Sustainability and environment stability are key factors controlling the overall health of our planet. Chapter 1 of this book contains a detailed introduction of modern chemical and biochemical technologies and their relationships with environment sustainability. The second chapter of this book deals with

the microbial and biochemical technologies. Applications of modern microbial and biochemical technologies in different consumer products are also discussed in Chapter 2. Pollution-free environment is essential for the well-being of living species on the Earth. The applications of green chemical technologies in various industrial processes are illustrated in Chapter 3. Chapter 4 discusses various chemical routes for the synthesis of different nanostructures based on gallium oxide. Solgel process is recognized as a fundamental process to synthesize nanomaterials and chemical products via chemical routes, which are illustrated in Chapter 5. The world is shifting toward sustainable and renewable energy resources to combat the increasing gap between energy demands and supplies. Chapter 6 contains a detailed presentation of dye-sensitized solar cells (DSSCs) prepared via chemical routes. Chapters 7 and 8 focus on different chemical looping and sequencing technologies for improving the chemical process industry. This book also contains a detailed presentation of different industrial products such as polymeric consumer goods, solar cells, plastics, elastomers, and some synthetic building materials. This book is an ideal source of information for the graduate-level research in different areas of chemistry, biochemistry, chemical engineering, and sustainable chemical technologies.

CHAPTER 1

SUSTAINABLE CHEMICAL AND BIOCHEMICAL TECHNOLOGIES

CONTENTS

1.1 INTRODUCTION

This chapter contains detailed discussions regarding the development trends in modern chemical technologies and fundamental changes in technology for eco-sustainability. The basic strategies of sustainable development and potential alternatives are also identified. Some predictions and opinions are offered regarding the prospective progress in the growth of advanced and sustainable chemical technologies.

The eras of the industrial, agricultural, and modern scientific–technical development have shaped the destiny of human civilization. Currently, we are living in the era of modern information technology and environmental sustainability. The society is shifting toward a new era of sustainable development (Hongbo, Yuancheng, Chengwei, Yutie, & Lin, 2010; Rahmani, Haghighi, Estifaee, & Rahimpour, 2012; Suraweera et al., 2014). The term "sustainable development" is perceived as a balanced or a stable development. The different understanding of sustainable development is reflected by different words used in various languages, for example, trwały rozwj, zrównoważony rozwj, nachhaltige Entwicklung, and development durable. The concept of sustainable development has evolved since its origin. The ultimate aim, characteristics, and the definition of sustainable development have changed significantly in the last 20 years (Fukui, Murakami, & Ichikawa, 1994; Nishikawa, Yanagawa, Morikawa, Sakata, & Kojima, 2001; Levenspiel, 2005; Jena, 2009). The concept of environmental sustainability has been proposed by various environmentalists and scientists (Meadows, Meadows, Randers, & Behrens, 1972; Keeble, 1988; Butlin, 1989). A more promising version was announced in a seminar by United Nation Conference on Environment and Development (Houghton, Callander, & Varney, 1992; Grubb, 1993; Elkington, 1994). Many authors have discussed the modern sustainability concepts in detail (Borowiecki, Gołębiowski, & Skowroński, 1998; Taniewski, 1999; 2012). Sustainable development is a human concept directed at the enhancement of the living quality and human welfare. The advances in sustainable development are meant for meeting the necessities of future generations under challenging circumstances, that is, with limited resources and abundant industrial activities. A progressive vision associates social justice, environmental protection, and economic growth (Taniewski, 2004; 2005; 2006; 2008). Despite numerous barriers and obstacles, it is strongly believed that sustainable development can be implemented gradually. The implementation of sustainable development strategies will replace the old models of civilization development to maximize manufacturing and

profits. Presently, sustainability is a primary necessity (not an option) of the human race (Ismagilov et al., 2011; Bednarek-Gejo, Mianowany, Skoczylas, & Głowacka, 2012).

Implementation of the novel and sustainable strategies requires major modifications in economic structure, consumption and production profiles, technologies, organizations and institutions, environmental and industrial ethics, and so on. Novelties in technology play an essential role which serves as critical drivers for the transformation of basic development models (Degnan, 2000; 2003; Catani, Mandreoli, Rossini, & Vaccari, 2002; Marcilly, 2003).

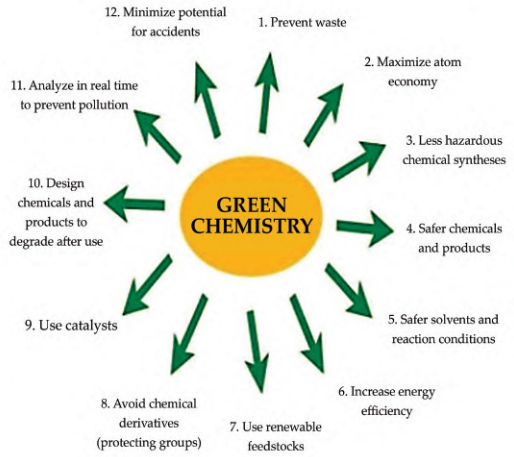

Figure 1. Benefits of green chemistry and its applications

[Source: https://www.slideshare.net/amitkumarchoudhary17/green-technology-42692950]

Presently, the world's leading chemical industries have gauged the importance of sustainable development strategies (Arpentinier et al., 2005; Cavani, Centi, Perego, & Vaccari, 2005; Muda, 2014). Several special programs are being announced to support environmental sustainability and the expansion of sustainable chemical technologies, that is, Responsible Care, Product Stewardship, Life Cycle Assessment and cradle to grave (Bozell, 2001; Wilson & Schwarzman, 2009). It is firmly believed that steadily introduced and constantly improved sustainable models of the chemical industries will inevitably result in tremendous technological breakthroughs. For instance, Chum and Overend (2001) predicted a 90%

reduction in feedstock losses due to wastes and by-products by 2020. Moreover, the use of carbon compounds and renewable energy resources is expected to increase by 20 and 13%, respectively (Anastas & Kirchhoff, 2002; Trost, 2002; Anastas & Zimmerman, 2003).

Numerous presentations, general reviews, and research articles have been published to address the following trends in modern sustainable chemical technologies (Metzger, 2006; Guillena, Ramón, & Yus, 2007; Chen et al., 2008; Biermann, Bornscheuer, Meier, Metzger, & Schäfer, 2011). Some major reviews published in the area of sustainability deal with green chemistry, renewable raw materials, methane, and carbon chemistry (Lunsford, 1995; 2000; Xu, Bao, & Lin, 2003; Holmen, 2009). Additional sustainability areas include clean fuels, syngas, catalysis trends, nanotechnology, miniaturization, separation, and innovations for sustainability (Kioes & Liebner, 2004; Koempel, Liebner, & Wagner, 2005; Liebner & Koempel, 2005; Pushparaj et al., 2013). Certain publications contain detailed sustainability concepts amalgamated by both ancient and modern theories (Taniewski, 2002; Aramendía et al., 2004; Skutil & Taniewski, 2006; Nouralishahi, Pahlavanzadeh, & Daryan, 2008). The theme of this chapter is to explore the modern chemical technologies in detail. The principles of green engineering technologies are also addressed in the subsequent sections of this chapter.

1.2 CHEMICAL TECHNOLOGIES IN DEVELOPMENT

The global trends toward sustainable (green) chemical technologies mainly focus on the following areas:

- Minimization of raw material usage facilitated by the increment in selectivity due to a wide range of choices for suitable processes, optimal operating parameters, feedstock, recirculation of by-products, highly selective catalysts, etc. (Van-Hove, 2006; Gawlitza, Braun, Leson, Lipfert, & Nestler, 2007; Erdély et al., 2009; Wang, Deng, Chu, & Yang, 2009)
- Minimization of power consumption facilitated by the increment in selectivity due to a wide range of choices which involve the substitution of endothermic processes by exothermic ones, development of exothermic and endothermic operations and processes, a gradual substitution of extraordinary energy-

consuming cryogenic separation processes by adsorption and membranes, an improvement in the development of heat exchangers and reactors, innovations in steering and process control, etc. (Charpentier, 2005; Sell, Ott, & Kralisch, 2014; Zhang et al., 2014; Francisco, Franco, Zepka, & Jacob-Lopes, 2015; Shanmugam & Donaldson, 2015).

- Increasing environmental safety standards by the following environmental codes which involve the minimizing the emission volumes, proper dumping of wastes and sewage, development of zero-waste or low-waste technologies, enhanced safety of the processes, etc.
- Waste management industrial processes which involve processing, destruction, recycling, combustion, and safe deposition of industrial wastes.

The above actions and tendencies accord with the fundamental ethical principles. The role of ethics is vital to regulate various industrial processes being carried out today. The ethical issues are linked to the constant risk and responsibilities for chemical processes, products, and their safety. Therefore, it is essential to practice ethics to ensure self-improvement, eradication of hazards and threats, transparent relationships with society, and dependable information practice, for progression of chemical industries.

There are various tools which can be employed for the improvement of recognized technologies and the development of sustainable (green) and novel chemical technologies. Some basic tools essential for the achievement of technological sustainability are given below:

- Selection of the most suitable substitute primary resources,
- Selection of the most suitable alternative feedstocks,
- Selection of the most suitable processes and operating conditions,
- Selection of the most suitable energy sources and energy management systems,
- Selection of the most suitable catalysts,
- Selection of the most suitable reactor/equipment systems,
- Selection of the most suitable methods to manage sewage and waste, emissions, and by-products, and
- Selection of the most suitable and safe products.

These basic tools are mutually interdependent. The selection made in one category usually predetermines the selection in the other. The change in

feedstocks and primary resources often involves alterations in manufacturing processes and routes. The transformation of prevalent technologies into sustainable, environmentally benign, technically optimal, and economically feasible technologies will always require continuous efforts. Various assessment techniques such as best available techniques (BAT) are useful in selecting the most sustainable technologies among presently available techniques.

1.3 PRIMARY RESOURCES AND FEED

The fundamental resources which can be utilized as the starting materials for the synthesis of intermediates (e.g., feedstocks, synthetic fuels, or chemical compounds) are refinery gas streams, crude oil fractions, natural gasoline, natural gas, LPG, coal liquids, biomass, coal gases, minerals, and atmospheric CO_2.

It is strongly believed that petrochemical-based refinery gas streams, crude oil fractions, natural gasoline, natural gas, and LPG will remain the major bulk products of commercial inorganic manufacturing (hydrogen, nitrogen, ammonia, fertilizers, etc.) and the essential part of commercial organic manufacturing (polymers, synthetic rubbers, synthetic fibers, detergents, etc.). On the other hand, the gradual rise in the oil prices will instigate the growth and development of alternate energy resources. The crude oil fraction group deals with the processing and application of heavy and superheavy products of crude oil. These foreseeable tendencies will be triggered by a growing need to use heavy fractions and residues along with the synthesis of heavy and superheavy crude oil products in place of steadily exhausting traditional oils.

It is estimated that within primary resources of hydrocarbons, the relative contribution of methane (natural gas) will increase at the expense of oil in various applications such as energetics, petrochemical production, and transportable liquid fuels (gas-to-liquids, GTL). This major shift is only possible to die to the availability of large natural gas reserves (higher annual production ratio/proved reserves) and recent developments in CH_4 chemical technology. Plentiful resources of flared gas and remote natural gas that are not much utilized and even large resources of methane hydrates that have not yet been explored will instigate their general processing and utilization.

The contribution of coal (as a principal raw material) toward the energy sector was extremely high in late 18th century and early 19th century.

However, the contribution of coal and its derivatives (coal tar and coke-oven gas) significantly declined in favor of natural gas and petroleum. Presently, the role of coal is limited to the short-scale production of aromatics and hydrogen from natural gas and oil. The large-scale Fischer–Tropsch synthesis and coal gasification practiced in South Africa (since the 1950s) are unusual phenomena triggered by specific circumstances. However, the coal-based synthesis routes (Mossel Bay) experienced drastic depreciation due to the advent of gas-based synthesis routes since the 1990s. Despite all the facts, one can assume that in the years to come, the commercial coal industry will revive gradually, particularly in the area of novel gasification methods leading to advanced coal-based materials (composites, fibers, sorbents, carbon nanomaterials), coal bed methane processing, and SNG (substitute natural gas). Substantial advancement has been recently witnessed in these new fields. On the other hand, the revival of carbonization (coal degassing), including coal hydro-liquefaction or coking processes, is highly unlikely.

Chemical processing of renewables/biomass (fats, cellulose, vegetable oils, agricultural residues, municipal wastes, agroindustrial products, etc.) is becoming progressively essential in the synthesis of biofuel fine chemicals or products with improved environmental biodegradability, for example, polymers. Therefore, these processes should be considered as alternative routes for processing of energy products. Bulk production of chemicals from these unique resources will be a matter of prospective process considerations.

1.4 FEEDSTOCK

Presently, the best feedstock raw materials are those which can be converted into desirable products with the maximum selectivity. Various alternate feedstock raw materials can be utilized for the manufacture of higher and lower olefins, diolefins, surfactant intermediates, alkyl aromatics, oxygen compounds, heterocyclic compounds, etc. (Noble & Agrawal, 2005; Broering et al., 2006). Commercial organic synthesis typically involves a significant number of alternative feedstocks, which results in an extremely large number of processing routes leading to isoprene. Some substitute feedstocks and alternative processing technologies employed in the petrochemical industry have been discussed earlier in this chapter (Taniewski, 2002; Koros et al., 2004). The increasing applications of renewable (novel) feedstocks have been discussed above. The indications of the feedstock transformation processes are discussed in the subsequent sections. Some examples of

alternate feedstocks and primary resources used for the synthesis of the bulk intermediates are listed below:

- Ethylene (steam cracking of LPG, gasoline, ethane, and heavy and middle oil fractions; oxidative dehydrogenation or dehydrogenation of ethane and oxidative coupling of methane);
- Propylene (steam cracking of liquid hydrocarbon fractions or LPG, separation from FCC gases, oxidative dehydrogenation or dehydrogenation of propane and conversion of methanol);
- Butadiene (dehydrogenation of n-butenes and n-butane and steam cracking of liquid fractions of hydrocarbons);
- Benzene (steam cracking of liquid fractions of hydrocarbons, catalytic reforming of gasoline, hydrotreated pyrogasoline fraction or hydrodealkylation of toluene and disproportionation of toluene);
- Toluene (steam cracking of liquid fractions of hydrocarbons and catalytic reforming of gasoline);
- Xylenes (steam cracking of liquid fractions of hydrocarbons, catalytic reforming of gasoline, and alkylation or disproportionation of toluene);
- Synthesis gas, SNG (partial oxidation or steam reforming of natural gas, processing of biomass, reforming of heavy fractions, residues of oil, and gasification of coal);
- Hydrogen (reforming of oil residues or natural gas, gasification of biomass or coal, reforming of renewable liquid fuel (bio-oils, bioethanol, etc.), reforming of DME, ethanol, methanol, hydrocarbon fuels for cells, water decomposition by high-temperature splitting process, catalytic breakdown of natural gas, electrolysis of water via renewable sources of molecular or electrical energy, photolytic splitting of water via photoelectrolytic or photobiological methods, etc. (Dijkema, Ferrão, Herder, & Heitor, 2006; Davood Abadi Farahani, Rabiee, Vatanpour, & Borghei, 2016).

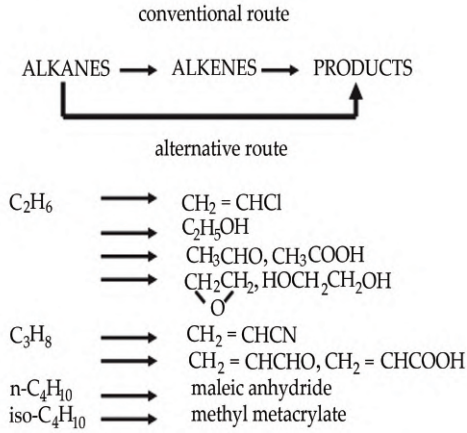

Figure. 2. Alkenes versus alkanes alternatives

[Source: http://onlinelibrary.wiley.com/doi/10.1002/ceat.200600178/]

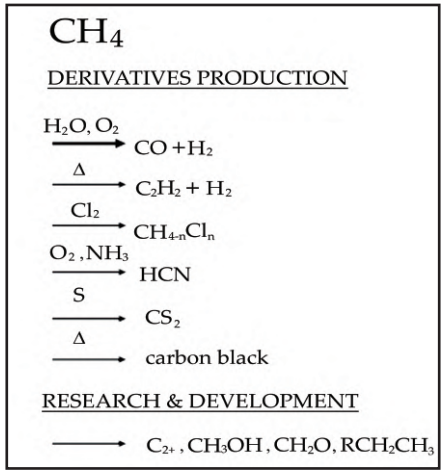

Figure. 3. Production and R&D of methane derivatives

[Source: http://onlinelibrary.wiley.com/doi/10.1002/ceat.200600178/]

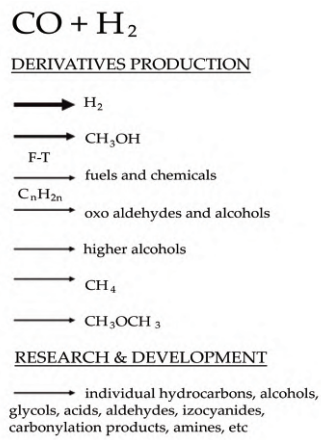

Figure. 4. Production and R&D of synthesis gas derivatives, that is, F-T—Fischer–Tropsch synthesis.

[Source: http://onlinelibrary.wiley.com/doi/10.1002/ceat.200600178/]

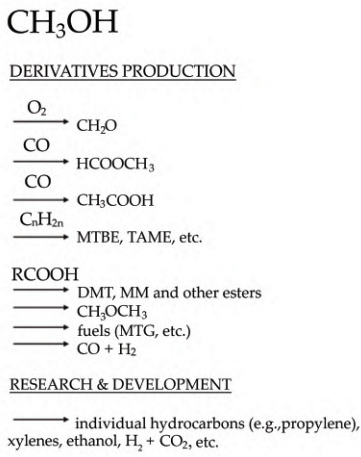

Figure. 5. Production and R&D of methanol derivatives. (a) Methyl tetrabutyl ether—MTBE; tetra-amyl methyl ether—TAME; dimethyl terephthalate—DMT; methyl methacrylate—MM; methanol-to-gasoline (MTG) synthesis.

[Source: http://onlinelibrary.wiley.com/doi/10.1002/ceat.200600178/]

The selection of the particular feedstock material may sometimes result in the desirable decline in the number of synthesis steps, thus evading the production of intermediate compounds, for example, production of alkene

derivatives from alkanes in place of alkenes and synthesis of C_1 derivatives from methane in place of syngas and vice versa). The application of some alternate routes to produce alkane-based derivatives of alkenes has been observed in the last two decades. These simple yet robust synthesis approaches will compete with conventional alkene-based methods (Lepoutre, 2008; White, 2009).

Figure 3 to Figure 5 demonstrate the synthesis of C_1 derivatives from syngas, methane, or methanol (Aramendía et al., 2004; Skutil, & Taniewski, 2006). These examples illustrate another critical problem associated with the selection of feedstock, viz. the prospect of employing the same feedstock to the same industry for the synthesis of different products, that is, of the need to select the optimal production profile (Lorenz & Eck, 2005; Nouralishahi et al., 2008).

1.5 TECHNOLOGICAL PROCESSES

Some major technological processes can be categorized as petrochemical, carbochemical, refining, biochemical, environmental, mineral-based (including hydrometallurgy and ceramics), and specialty chemical processes involving membranes, fuel cells, and ionic liquids. The quest for selection of the best technological process is typically based on the tendency to develop highly selective zero-waste or low-waste technology. It often necessitates the selection of the best processing route among various procedures leading to the construction of same products even from the same set of raw materials. For instance, Figure 6 displays the state-of-the-art synthetic technology in the area of transportable liquid fuels' production from natural gas via different (existing/novel) alternative routes (Lorenz & Zinke, 2005; Paula & Birrer, 2006)

1.5.1 Operating Conditions

After the choice of the best processing route, it is essential to designate the type of process and its typical operating conditions. Process types include low pressure, high pressure, liquid phase, gas phase, multiphase (mainly perspective in a few cases), catalytic, non-catalytic, or multicatalytic (mainly perspective in some cases). On the other hand, the optimum operating conditions are set according to the process requirements involving supercritical fluids and other alternate materials.

1.5.2 Catalytic Technologies

The modern catalytic technologies are applicable in particular chemical branches such as petrochemical and refining. The rapid advancement in the assessment and application of the new selective catalysts (regioselective and stereoselective) creates likelihoods for the best selection and constant development. Some common catalysts include shape-selective zeolites, nanostructured, monolithic, mesoporous, blocks, metallocenes and various one-centered catalysts, heterogenized homogeneous, polyfunctional, bio, phase transfer, membrane, etc. (Sheldon & Dakka, 1994; Sheldon, 1996; Sheldon, Wallau, Arends, & Schuchardt, 1998).

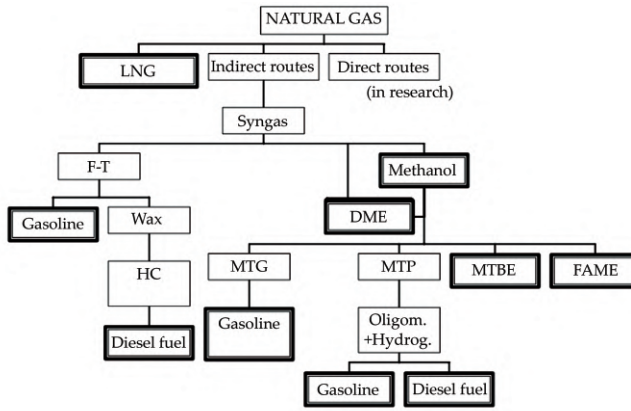

Figure. 6. Portable liquid fuels obtained from natural gas (GTL, gas-to-liquids). liquefied natural gas (LNG); Fischer–Tropsch (F-T) synthesis; dimethyl ether (DME); mild hydrocracking (HC); methanol-to-gasoline (MTG) synthesis; methanol-to-propylene (MTP) synthesis; methyl tetrabutyl ether (MTBE); fatty acid methyl esters (FAME); oligomerization (oligom.); hydrogenation (hydrog.)

[Source: http://onlinelibrary.wiley.com/doi/10.1002/ceat.200600178/]

It is imperative to note that chemical technologies primarily focused on high catalytic activities in the 20th century. However, modern chemical technologies are more apprehensive about the high selectivity of the catalysts. This priority shift is comprehensible in respect of both a high catalyst activity typically associated with the past technologies and the higher selectivity associated with the current sustainability trends. The critical role of the increase in process selectivity arises from the fact that the consumption of energy and raw materials can be reduced by following this technology.

Moreover, the costs of waste management and product separation also play an important role in defining the role of catalytic selectivity.

On the contrary, there are a few catalytic unit processes (e.g., hydrogenation, stereospecific polymerization, and partial oxidation), which take place with poor selectivity standards. The catalytic technologies are still waiting for uprise of their role in the synthesis of green chemicals and pharmaceuticals products. Presently, there is an obvious prevalence of non-catalytic routes in fine chemical productions and various similar products, which leads to undesirably higher values of Sheldon's E-factor (cumulative waste mass/cumulative mass of the desired product) equivalent to 5100 (Anastas, Heine, & Williamson, 2000; Anastas & Kirchhoff, 2002).

Strong tendencies to cultivate safer and cleaner technologies (non-solvent, catalytic, etc.) are witnessed in the synthesis of all fine and specialty chemicals such as pharmaceuticals, intermediates, dyes, agrochemicals, pigments, fragrances, flavors, liquid crystals for displays, chemical compounds for cosmetic and food industries, and electronic chemicals for the synthesis of chips (Anastas & Zimmerman, 2003; McDonough, Braungart, Anastas, & Zimmerman, 2003; Anastas, 2008).

1.6 BIOTECHNOLOGY

Currently, the importance of industrial biotechnology associated with the chemical handling of renewable/biomass as an alternative to the traditional technology based on minerals and fossil fuels is being explored extensively (Anastas, 1998; Ballini, 2009; Sharma, 2010. The novel biotechnology involves the transformation of renewable resources via fermentation, transesterification, or hydrolysis to produce biofuels (esters, alcohols, etc.). Additionally, the enzymatic productions of intermediates, fine chemicals, pharmaceuticals (e.g., vaccines, biomolecule manufacturing, stereoselective biocatalysts, and chiral technologies) and various biodegradable products from renewable resources are being carried out. Biomass processing or the use of biotechnological routes for bulk chemical synthesis and chemical operations exhibits significant but slow progress (e.g., biodesulfurization of solids or liquids and enzymatic manufacture of 1, 3-propanediol from glucose molecules).

1.7 CHEMICAL NANOTECHNOLOGY

The field of chemical nanotechnology is a subdivision of nanotechnology resulting as a by-product of nanoscience evolution derived from the general science of surfaces and thin films (Tang & Zhao, 2009; Soetaert & Vandamme, 2010). This multidisciplinary novel new field is associated with nanomaterials (nanowires, nanofibers, nanotubes, etc.), catalysts, surfactants, sensors, membranes, coatings, polymers, etc. This multidisciplinary area of research focuses on the development of rapidly growing alternative synthesis routes leading to the construction of novel and customized products (Hopwood, Mellor, & O'Brien, 2005; Cheng & Gross, 2011).

1.8 CHEMISTRY AND ENVIRONMENT

There are climate and environmental issues facing across the world which are widely recognized as daunting problems. As the quality of life is declining therefore environmental and green technologies, sustainable development is important. In technology, there has been a major progress, especially clean water and air causing depletion of natural life resources (Lélé, 1991; Sneddon, Howarth, & Norgaard, 2006). Their problems are causing serious social, environmental, and economic impairment across the globe. Sustainable resources suggest that non-renewable resources should be husbanded (e.g., recycled and reduced) and renewable resources should be used wherever possible to increase their life for next generations to come (Irwin, 1995; Patil, 2013; 2014).

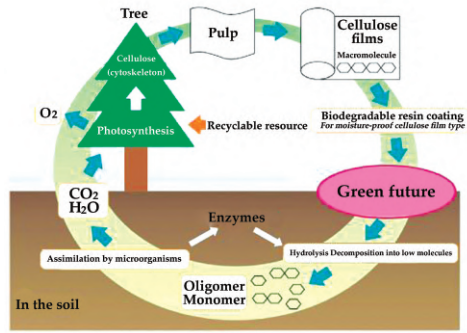

Figure. 7. Future trends in chemistry and its impact on environmental sustainability

[Source: http://www.futamura.co.jp/english/cellophane/greenfuture/index.html]

A review on the trend toward green technologies and sustainability in chemical process industry has been given in this chapter. In applications and understanding of sustainability, a broad review of state-of-the-art green technologies with some case studies that highlight the economic benefits implementing green technologies from chemical engineering viewpoints is discussed. Renewable resources are being used by green technologies to reduce pollutants, emissions, and waste; reuse, recover, and recycle; restore the balance of biosphere and ecosystem; and reduce the pressure on natural resources and ultimately aid in giving "ecologically sustainable development." These green technologies are, hence, cost-effective, feasible, appropriate to climate, environmentally advanced, geographic, social, ecological, and economic conditions of the country (Dalton, 1998; Renn, 2008). The development of new safe, environment-friendly and non-toxic can be the only way to achieve this aim (Pace, 2012). Therefore, by investing in green technologies, CPI must encourage sustainable development and ensure improved adherence to health, safety, and environment standards (Albrecht, Evans, & Raston, 2006; Polshettiwar, Nadagouda, & Varma, 2009).

In the past, the environmental problems were considered as a part of the rapid utilization of the natural resources and the economic system (Horváth & Anastas, 2007; Anastas & Eghbali, 2010). It took many years to consider the recognized ways that the initial design of the CPI, materials used (feedstocks), the energy consumption, the hazardous properties of products and other some other parameters that are involved in the manufacturing of the products (recycling, life cycle, etc.)

The increased development of some innovative chemical products and new chemical technologies in last few decades has gained the attention of the environmentalists to remedial actions for the detrimental impacts (environmental pollution, monitoring, recycling, reduction of pollutants, etc.). It should be noted that the most effective way to decrease the harmful impacts is to innovate the design in the manufacturing process taking into account the materials, use, energy, generation of secondary and atom economy, and at the end life cycle of the products and their recycling into new materials.

A more environment-friendly synthetic route was involved in the green chemistry, and it was another part for the manufacturing of chemicals on the industrial scale with the mantra—"*Think Green.*" Selectivity has been the vital concern of chemical engineers than conversion. Green technology studies alternate (solvent-free) media, reaction conditions, and energy

sources (Li & Trost, 2008). The most basic approach for pollution prevention is the design of chemical process and products that eliminate or reduce the generation and use of hazardous substances. In green chemistry, the need to produce services and goods that are environment-friendly and on which society depends is addressed. Plastics that biodegrade can be synthesized from plants, minimizing the number of waste lifesaving pharmaceuticals can be produced, and instead of traditional organic solvents, reactions can be run in water by applying green chemistry principles to chemical processes and products.

1.9 SUSTAINABILITY CONCEPTS

Sustainable global development has become a norm for environmental protection and global economic development since the start of the 21st century. The three fundamental aspects of sustainable development include environment, community, and economy. Therefore, it is essential to follow the subsequent steps to build a sustainable society.

- The natural step,
- Eco-efficiency,
- Pollution prevention,
- Eco-effectiveness,
- Design for environment,
- Cradle-to-cradle design,
- Industrial ecology,
- Environmental management, and
- Sustainable management systems.

1.10 RECENT DEVELOPMENTS IN GREEN TECHNOLOGY

Innovative and creative skills are being applied by scientists from all over the world to develop new synthetic methods, processes, reaction conditions, analytical tools, catalysts, etc., under the envelope of new green technology. Some of these areas are as follows:

A continuous apparatus and process convert the biomass into industrial fuels, chemicals, and animal feed. There is another process that converts biomass such as sewage sludge, municipal solid waste, agricultural residues,

tires, and plastic into useful products which include acetic acid, ethanol, and hydrogen.

- A method of semicontinuous culture of Texas genus plant for the mass production of taxol.
- Carboxylic acid production by the fermentation method.
- Using a supercritical fluid mobile, a method of partially oxidizing alcohol, such as esters or acids methanol to aldehydes, ethers.
- Using supercritical carbon dioxide, a process to manufacture a fluoropolymer.
- Production of a non-toxic solvent ethyl lactate derived from corn by an economical method.
- Worker and environment-friendly variety of organic solvents, for example bioethanol.
- To recover zinc and ferrous chloride from pickle liquor, a novel environment-friendly technology that has been in use.
- There is an increase in demand of nonionic surfactants. Alkyl glycoside is an innovative example which is made from saccharide. This product can be a replacement for alkyl aryl sulfonate anionic surfactants in shampoos.

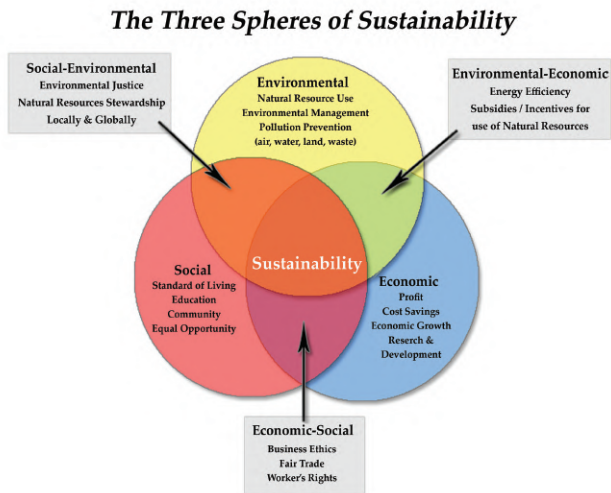

Figure. 8. Green chemistry is genuinely sustainable

[Source: http://projectwork001.blogspot.com/]

1.11 USE OF ALTERNATIVE CHEMICALS IN CHEMICAL AND RESEARCH INDUSTRY

From the experience of last five decades, it has been known that the majority of starting materials and raw chemicals not only from chemical industry but also from other main industries were goods of the petrochemical industry.

1.11.1 Renewable Raw Materials and Feedstocks

There is a need to change green chemical technology into renewable feedstocks. Lower toxicity and environmental impact are the second most desired property of the starting materials. Safety and health protection of the workers and the environment is the important priority. Changes in the direction of biological raw materials are suggested by the green chemistry (biogas, plant and animal waste, products from the fermentation of plant waste, etc.).

1.11.2 Use of Oleochemicals as Modern Biological Materials

Oils and fats (from animals and plants) as oleochemical raw materials can be considered as a new source of chemical feedstocks. There are some raw materials present in the market with many applications in lubricating oils, cosmetics, polymers, and other products.

1.11.2 Light-Aided Photochemical Reactions

In chemical processes, green technology emphasizes on the photochemical reactions. Light (visible and ultraviolet) can be main catalysts for many reactions which can replace many toxic metals in many reactions. Photochemistry, according to many scientists, has a huge potential in many research applications and innovation in the last years.

1.11.3 Photocatalytic synthesis with Titanium dioxide (TiO_2)

In recent years, there has been a lot of research on the use of TiO_2 dioxide for photocatalytic reactions at industrial scale under visible light. The waste products are shallow; energy use is minimized and yielded much higher than traditional reactions.

1.11.4 Decomposition of Toxic Chemicals and Photocatalytic oxidation Waste

In photocatalytic oxidations, TiO_2 and other metallic oxides (Fe_2+) can be used for the decomposition of waste and toxic chemical materials. Neutral chemicals with minimum toxicity can be produced by these decompositions, especially polychlorinated compounds, phenols, etc. Toxic industrial waste can be decomposed with the aid of light using a mixture Fe_2+/H_2O_2 (Fenton reagent).

1.11.5 Waste Biomass as Biomaterials, Chemical Feedstock, and Biofuels

There has been a remarkable advancement in the use of biomass for the production of various materials in the last decade. It was known for years that biomass from the agricultural processes was wasted. Many aspects and effectiveness of the biomass were examined by scientists. With the increase in the fossil fuel value, biomass is considered as a vital problem of sustainability.

1.11.6 Degradation of Biomass for Biodiesel and Biogas

Biofuel is the well-recognized use of biomass especially from landfill organic waste. Biomass can be used for the production of biodiesel through chemical and physical processes.

1.11.7 Biotransformation and Biocatalysis in the Chemical Industry

Green technology includes biocatalysis which has many applications and is considered environment- and energy-friendly. In the pharmaceutical and food industries, enzymes have been used for synthetic chemical routes with some rewards.

1.11.8 Sequestration or Capture of Carbon Dioxide

In chemical industries, green chemistry is implicated in the reduction of carbon dioxide. The phenomenon of the greenhouse effect and climate change due to CO_2 emissions is considered an important environmental problem.

1.12 NOVEL FABRICATION TECHNOLOGIES FOR THE SYNTHESIS OF CHEMICAL COMPOUNDS

In this section, some of the important changes in the manufacturing of the chemicals under green chemical engineering and alternative methods are discussed.

1.12.1 Ionic Liquids in Organic Synthesis

In organic synthesis, ionic liquids are used as alternative solvents in recent years. These substances are named as ionic melts, liquid electrolytes, fused salts, ionic glasses, or liquid salts. Ionic liquids have various applications as electrically conducting fluids and powerful solvents. For the future progress, they are believed to be good candidates that can give green credentials to their use and applications.

1.12.2 Organic Synthesis in Aqueous Medium

Water was considered as a medium and was avoided as a solvent for synthetic organic chemistry for many decades. For many synthetic methods, water is regarded as an excellent solvent. Diels–Alder organic synthesis is the most interesting example of water as a solvent.

1.12.3 Organic Fabrication in Polyfluorinated Phase

A two-phase system of solvents named as polyfluorinated is being used by chemists in these techniques which dissolve catalysts with a long aliphatic chain or hyper fluorinated alcylo. The organic solvent that is insoluble in the hyperfluorinated phase dissolves reagents. Heating up the mixture accelerates the reaction with an excellent yield of products.

1.12.4 Supercritical Water and Supercritical Carbon Dioxide

Any liquid substance at pressure and temperature above the critical point is supercritical fluid where distinct gas and liquid phases do not exist. It can dissolve materials like a liquid and can diffuse through solids like a gas. Moreover, a small change in temperature or pressure at close to the critical point results in a large change in density which allows many properties of the supercritical fluid to be “fine-tuned.”

1.12.5 Use of Microwave Processes for Organic Chemical Synthesis

For cooking and food warming, microwave furnaces are commonly used. They are being used in organic synthesis for many years, and their success in organic synthesis with "green" is well recognized. High yield without solvent, very low energy requirements, and low waste organic synthesis already have many applications and research papers on the topic.

1.12.6 The Use of Ultrasonic Waves for Chemical Synthesis

Advanced green techniques involve chemical reactions enhanced by ultrasound and sonic waves with excellent yield. Three classes of sonochemical reactions have been described: heterogeneous sonochemistry of liquid–liquid, homogeneous sonochemistry of liquids that extend beyond with the previous techniques, and sonocatalysis. The exploration of chemical improvement of reactions by ultrasound has been carried out and has valuable applications in materials chemistry, mixed phase synthesis, and biomedical uses.

1.13 MODERN TRENDS

New and alarming challenges in chemical engineering will be posted in 21st century: the necessity to apply new methodological approaches, increasing environmental considerations, and a change in the raw material base. However, this century will sneak into many other industries such as biotechnology, the pharmaceutical industry and electronic industry, and other sectors, mainly food production and agriculture.

Reinventing the use of materials is the challenge that sustainability of technological advancement is facing in a chemical industry. Green chemical technologies are essential to address these challenges. These technologies are, hence, environmentally advanced and cost-effective.

These green technologies are, hence, cost-effective, feasible, appropriate to climate, environmentally advanced, geographic, social, ecological, and economic conditions of the country. The development of new safe, environment-friendly, and non-toxic can be the only way to achieve this aim. Therefore, by investing in green technologies, CPI must encourage sustainable development and ensure improved adherence to health, safety, and environmental standards.

REFERENCES

1. Anastas, P. T. (1998). Green Chemistry; Anastas, P. T., Williamson, TC, Eds.
2. Anastas, P. T., Heine, L. G., & Williamson, T. C. (2000). Green chemical syntheses and processes: Introduction.
3. Anastas, P. T., & Kirchhoff, M. M. (2002). Origins, current status, and future challenges of green chemistry. *Accounts of Chemical Research, 35*(9), 686-694.
4. Anastas, P. T., & Kirchhoff, M. M. (2002). Origins, current status, and future challenges of green chemistry. *Accounts of Chemical Research, 35*(9), 686-694.
5. Anastas, P. T., & Kirchhoff, M. M. (2002). Origins, current status, and future challenges of green chemistry. *Accounts of Chemical Research, 35*(9), 686-694.
6. Anastas, P. T., & Zimmerman, J. B. (2003). Peer reviewed: Design through the 12 principles of green engineering. *Environmental Science and Technology, 37*(5), 94A-101A.
7. Aramendía, M. A., Borau, V., Jiménez, C., Marinas, A., Marinas, J. M., Ruiz, J. R., & Urbano, F. J. (2004). Magnesium-containing mixed oxides as basic catalysts: Base characterization by carbon dioxide TPD–MS and test reactions. *Journal of Molecular Catalysis A: Chemical, 218*(1), 81-90.
8. Arpentinier, P., Basile, F., Del Gallo, P., Fornasari, G., Gary, D., Rosetti, V., & Vaccari, A. (2005). Role of the hydrotalcite-type precursor on the properties of CPO catalysts. *Catalysis Today, 99*(1), 99-104.
9. Albrecht, M. A., Evans, C. W., & Raston, C. L. (2006). Green chemistry and the health implications of nanoparticles. *Green Chemistry, 8*(5), 417-432.
10. Anastas, P., & Eghbali, N. (2010). Green chemistry: Principles and practice. *Chemical Society Reviews, 39*(1), 301-312.
11. Butlin, J. (1989). *Our common future. By world commission on environment and development* (p. 383). London: Oxford University Press, 1987.
12. Borowiecki, T., Gołębiowski, A., & Skowroński, B. (1998). Nowe procesy katalityczne w produkcji gazu syntezowego i wodoru z węglowodorów. *Przemysł Chemiczny, 77*, 128-132.

13. Bozell, J. J. (2001). *Chemicals and materials from renewable resources.* Golden, CO: National Renewable Energy Laboratory.
14. Broering, J. M., Hill, E. M., Hallett, J. P., Liotta, C. L., Eckert, C. A., & Bommarius, A. S. (2006). Biocatalytic reaction and recycling by using CO_2-induced organic–aqueous tunable solvents. *Angewandte Chemie*, *118*(28), 4786-4789.
15. Ballini, R. (2009). *Eco-friendly synthesis of fine chemicals* (Vol. 3). Cambridge: Royal Society of Chemistry.
16. Biermann, U., Bornscheuer, U., Meier, M. A., Metzger, J. O., & Schäfer, H. J. (2011). Oils and fats as renewable raw materials in chemistry. *Angewandte Chemie International Edition*, *50*(17), 3854-3871.
17. Bednarek-Gejo, A., Mianowany, M., Skoczylas, P., & Głowacka, A. (2012). Świadomość ekologiczna studentów. *Hygeia Public Health*, *47*(2), 201-206.
18. Chum, H. L., & Overend, R. P. (2001). Biomass and renewable fuels. *Fuel Processing Technology*, *71*(1), 187-195.
19. Catani, R., Mandreoli, M., Rossini, S., & Vaccari, A. (2002). Mesoporous catalysts for the synthesis of clean diesel fuels by oligomerisation of olefins. *Catalysis Today*, *75*(1), 125-131.
20. Cavani, F., Centi, G., Perego, C., & Vaccari, A. (2005). Selectivity in catalytic oxidation: An issue or an opportunity for innovation? *Catalysis Today*, *99*(1), 1-3.
21. Charpentier, J. C. (2005). Process intensification by miniaturization. *Chemical engineering & technology*, *28*(3), 255-258.
22. Chen, H., Armand, M., Demailly, G., Dolhem, F., Poizot, P., & Tarascon, J. M. (2008). From biomass to a renewable LiXC6O6 organic electrode for sustainable Li-ion batteries. *ChemSusChem*, *1*(4), 348-355.
23. Cheng, H., & Gross, R. (2011). *Green polymer chemistry: Biocatalysis and biomaterials (ACS Symposium)*. American Chemical Society.
24. Dalton, A. J. (1998). *Safety, health and environmental hazards at the workplace*. Cengage Learning EMEA.
25. Degnan, T. F. (2000). Applications of zeolites in petroleum refining. *Topics in Catalysis*, *13*(4), 349-356.
26. Degnan, T. F. (2003). The implications of the fundamentals of shape selectivity for the development of catalysts for the petroleum and petrochemical industries. *Journal of Catalysis*, *216*(1), 32-46.

27. Dijkema, G. P. J., Ferrão, P., Herder, P. M., & Heitor, M. (2006). Trends and opportunities framing innovation for sustainability in the learning society. *Technological Forecasting and Social Change, 73*(3), 215-227.

28. Davood Abadi Farahani, M. H., Rabiee, H., Vatanpour, V., & Borghei, S. M. (2016). Fouling reduction of emulsion polyvinylchloride ultrafiltration membranes blended by PEG: The effect of additive concentration and coagulation bath temperature. *Desalination and Water Treatment, 57*(26), 11931-11944.

29. Elkington, J. (1994). Towards the sustainable corporation: Win-win-win business strategies for sustainable development. *California Management Review, 36*(2), 90-100.

30. Erdélyi, Z., Cserháti, C., Csik, A., Daróczi, L., Langer, G. A., Balogh, Z., & Erko, A. (2009). Nanoresolution interface studies in thin films by synchrotron x-ray diffraction and by using x-ray waveguide structure. *X□Ray Spectrometry, 38*(4), 338-342.

31. Fukui, T., Murakami, T., & Ichikawa, M. (1994). The behavior of ash components in the sludge melting process. *Water Science and Technology, 30*(8), 197-207.

32. Francisco, É. C., Franco, T. T., Zepka, L. Q., & Jacob-Lopes, E. (2015). From waste-to-energy: The process integration and intensification for bulk oil and biodiesel production by microalgae. *Journal of Environmental Chemical Engineering, 3*(1), 482-487.

33. Grubb, M. (1993). *The earth summit agreements: A guide and assessment; an analysis of the Rio'92 UN Conference on environment and development*. London: Earthscan and the Energy and Environmental Programme of the Royal Institute of International Affairs.

34. Gawlitza, P., Braun, S., Leson, A., Lipfert, S., & Nestler, M. (2007). Herstellung von Präzisionsschichten mittels Ionenstrahlsputtern. *Vakuum in Forschung und Praxis, 19*(2), 37-43.

35. Guillena, G., Ramón, D. J., & Yus, M. (2007). Alcohols as electrophiles in C–C bond-forming reactions: The hydrogen autotransfer process. *Angewandte Chemie International Edition, 46*(14), 2358-2364.

36. Houghton, J. T., Callander, B. A., & Varney, S. K. (1992). *Climate change 1992*. Cambridge University Press.

37. Hopwood, B., Mellor, M., & O'Brien, G. (2005). Sustainable development: Mapping different approaches. *Sustainable Development, 13*(1), 38-52.

38. Horváth, I. T., & Anastas, P. T. (2007). Innovations and green chemistry. *Chemical Reviews, 107*(6), 2169-2173.

39. Holmen, A. (2009). Direct conversion of methane to fuels and chemicals. *Catalysis Today, 142*(1), 2-8.

40. Hongbo, R., Yuancheng, Q., Chengwei, S., Yutie, B., & Lin, Z. (2010). Adsorption and desorption properties of hybrid aerogels derived form MPMS-SSO at 77 K. *Rare Metal Materials and Engineering, 39*, 475-478.

41. Irwin, A. (1995). *Citizen science: A study of people, expertise and sustainable development*. Psychology Press.

42. Ismagilov, Z. R., Matus, E. V., Kerzhentsev, M. A., Tsikoza, L. T., Ismagilov, I. Z., Dosumov, K. D., & Mustafin, A. G. (2011). Methane conversion to valuable chemicals over nanostructured Mo/ZSM-5 catalysts. *Petroleum Chemistry, 51*(3), 174-186.

43. Jena, H. M. (2009). *Hydrodynamics of gas-liquid-solid fluidized and semi-fluidized beds* (Doctoral dissertation). Retrieved from http://ethesis.nitrkl.ac.in/1560/

44. Keeble, B. R. (1988). The Brundtland report: 'Our common future'. *Medicine and War, 4*(1), 17-25.

45. Kioes, S., & Liebner, W. (2004). Methane—the promising career of a humble molecule. *Journal of Natural Gas Chemistry, 13*(2), 71-78.

46. Koros, W. J. (2004). Evolving beyond the thermal age of separation processes: Membranes can lead the way. *AIChE Journal, 50*(10), 2326-2334.

47. Koempel, H., Liebner, W., & Wagner, M. (2005). Lurgi's gas to chemicals (GTC): Advanced technologies for natural gas monetization. *Proceedings of the Gastech*.

48. Lélé, S. M. (1991). Sustainable development: A critical review. *World Development, 19*(6), 607-621.

49. Lunsford, J. H. (1995). The catalytic oxidative coupling of methane. *Angewandte Chemie International Edition, 34*(9), 970-980.

50. Lunsford, J. H. (2000). Catalytic conversion of methane to more useful chemicals and fuels: A challenge for the 21st century. *Catalysis Today, 63*(2), 165-174.

51. Levenspiel, O. (2005). What will come after petroleum? *Industrial & Engineering Chemistry Research, 44*(14), 5073-5078.

52. Liebner, W., & Koempel, H. (2005, January). Gas to propylene: Report on commercialisation by Lurgi. In *18th World Petroleum Congress*. World Petroleum Congress.

53. Lorenz, P., & Eck, J. (2005). Outlook: Metagenomics and industrial applications. *Nature Review Microbiology, 3*(6), 510.

54. Lorenz, P., & Zinke, H. (2005). White biotechnology: Differences in US and EU approaches? *Trends in Biotechnology, 23*(12), 570-574.

55. Lepoutre, J. (2008). *Proactive environmental strategies in small businesses: Resources, institutions and dynamic capabilities* (Doctoral dissertation, Ghent University). Retrieved from https://biblio.ugent.be/publication/4101123/file/4334820

56. Li, C. J., & Trost, B. M. (2008). Green chemistry for chemical synthesis. *Proceedings of the National Academy of Sciences, 105*(36), 13197-13202.

57. Meadows, D. H., Meadows, D. L., Randers, J., & Behrens, W. W. (1972). The limits to growth. *New York, 102*, 27.

58. Marcilly, C. (2003). Present status and future trends in catalysis for refining and petrochemicals. *Journal of Catalysis, 216*(1), 47-62.

59. McDonough, W., Braungart, M., Anastas, P. T., & Zimmerman, J. B. (2003). Peer reviewed: Applying the principles of green engineering to cradle-to-cradle design. *Environmental Science & Technology, 37*(23), 434A-441A.

60. Metzger, J. O. (2006). Production of liquid hydrocarbons from biomass. *Angewandte Chemie International Edition, 45*(5), 696-698.

61. Muda, A. A. B. (2014). *Synthesis of MoVTeNb oxide catalysts for propane oxidation to acrylic acid via microwave irradiation assisted slurry method*.

62. Nishikawa, G., Yanagawa, T., Morikawa, H., Sakata, E., & Kojima, Y. (2001). *Large Scale Urea Granulation Plants based on TEC Technology*. Japan: Toyo Engineering Corporation.

63. Noble, R. D., & Agrawal, R. (2005). Separations research needs for the 21st century. *Industrial & Engineering Chemistry Research, 44*(9), 2887-2892.

64. Nouralishahi, A., Pahlavanzadeh, H., & Daryan, J. T. (2008). Determination of optimal temperature profile in an OCM plug flow reactor for the maximizing of ethylene production. *Fuel Processing Technology, 89*(7), 667-677.

65. Paula, L., & Birrer, F. (2006). Including public perspectives in industrial biotechnology and the biobased economy. *Journal of Agricultural and Environmental Ethics, 19*(3), 253-267.

66. Polshettiwar, V., Nadagouda, M. N., & Varma, R. S. (2009). Microwave-assisted chemistry: A rapid and sustainable route to synthesis of organics and nanomaterials. *Australian Journal of Chemistry, 62*(1), 16-26.

67. Pace, V. (2012). 2-Methyltetrahydrofuran: A versatile eco-friendly alternative to THF in organometallic chemistry. *Australian Journal of Chemistry, 65*(3), 301-302.

68. Puchała, C. (2012). *International action on chemical threats reduction. Chemistry education in the light of the research* (pp. 111-113). Krakow: Pedagogical University.

69. Patil, K. D. (2013). Sustainable green chemical technology for developments in process industries. *Development, 27*, 30.

70. Pushparaj, H., Ganesh, M. A. N. I., Muthiahpillai, P., Velayutham, M., Yong-Ki, P. A. R. K., Choi, W. C., & Jang, H. T. (2013). Effects of crystallinity of ZSM-5 zeolite on para-selective tert-butylation of ethylbenzene. *Chinese Journal of Catalysis, 34*(2), 294-304.

71. Patil, K. D. (2014). Review of green chemical technologies for sustainable developments in chemical process industries. *Emerging Trends in Chemical Engineering, 1*(2), 8-14.

72. Renn, O. (2008). *White paper on risk governance: Toward an integrative framework. In global risk governance* (pp. 3-73). Netherlands: Springer.

73. Rahmani, F., Haghighi, M., Estifaee, P., & Rahimpour, M. R. (2012). A comparative study of two different membranes applied for auto-thermal methanol synthesis process. *Journal of Natural Gas Science and Engineering, 7*, 60-74.

74. Sheldon, R. A., & Dakka, J. (1994). Heterogeneous catalytic oxidations in the manufacture of fine chemicals. *Catalysis Today, 19*(2), 215-245.

75. Sheldon, R. A. (1996). Chirotechnology: Designing economic chiral syntheses. *Journal of Chemical Technology and Biotechnology, 67*(1), 1-14.

76. Sheldon, R. A. (1996). Selective catalytic synthesis of fine chemicals: Opportunities and trends. *Journal of Molecular Catalysis A: Chemical, 107*(1-3), 75-83.

77. Sheldon, R. A., Wallau, M., Arends, I. W., & Schuchardt, U. (1998).

Heterogeneous catalysts for liquid-phase oxidations: Philosophers' stones or Trojan horses? *Accounts of Chemical Research, 31*(8), 485-493.

78. Sheldon, R. A., & Downing, R. S. (1999). Heterogeneous catalytic transformations for environmentally friendly production. *Applied Catalysis A: General, 189*(2), 163-183.
79. Skutil, K., & Taniewski, M. (2006). Some technological aspects of methane aromatization (direct and via oxidative coupling). *Fuel Processing Technology, 87*(6), 511-521.
80. Sneddon, C., Howarth, R. B., & Norgaard, R. B. (2006). Sustainable development in a post-Brundtland world. *Ecological Economics, 57*(2), 253-268.
81. Sheldon, R. A. (2007). Enzyme immobilization: The quest for optimum performance. *Advanced Synthesis & Catalysis, 349*(8-9), 1289-1307.
82. Sheldon, R. A. (2007). The E factor: Fifteen years on. *Green Chemistry, 9*(12), 1273-1283.
83. Sheldon, R. A. (2008). E factors, green chemistry and catalysis: An odyssey. *Chemical Communications,* (29), 3352-3365.
84. Sharma, S. K. (2010). Green Chemistry for Environmental Sustainability. Series: Advancing Sustainability Through Green Chemistry and Engineering.
85. Soetaert, W., & Vandamme, E. J. (2010). Industrial biotechnology: Sustainable growth and economic success. John Wiley & Sons.
86. Sell, I., Ott, D., & Kralisch, D. (2014). Life cycle cost analysis as decision support tool in chemical process development. *ChemBioEng Reviews, 1*(1), 50-56.
87. Suraweera, N. S., Albert, A. A., Peretich, M. E., Abbott, J., Humble, J. R., Barnes, C. E., & Keffer, D. J. (2014). Methane and carbon dioxide adsorption and diffusion in amorphous, metal-decorated nanoporous silica. *Molecular Simulation, 40*(7-9), 618-633.
88. Shanmugam, K., & Donaldson, A. A. (2015). Extraction of EPA/DHA from 18/12EE fish oil using AgNO3 (aq): Composition, yield, and effects of solvent addition on interfacial tension and flow pattern in mini-fluidic systems. *Industrial & Engineering Chemistry Research, 54*(33), 8295-8301.Taniewski, M. (1999). *Przemysłowa synteza organiczna: Kierunki rozwoju.* Gliwice: Politechniki *Śląskiej*.

89. Taniewski, M. (2002). Alternative petrochemical technologies. *Przemysl Chemiczny*, *81*(11), 697-703.

90. Trost, B. M. (2002). On inventing reactions for atom economy. *Accounts of Chemical Research*, *35*(9), 695-705.

91. Taniewski, M. (2004). The Challenges And Recent Advances In C1chemistry And Technology. *Polish Journal of Applied Chemistry, 48*(1-2), 1-21.

92. Taniewski, M. (2005). Sustainable development in petrochemical industry. *Polish Journal of Applied Chemistry*, *49*(3), 183-194.

93. Taniewski, M. (2006). Sustainable chemical technologies—development trends and tools. *Chemical Engineering & Technology*, *29*(12), 1397-1403.

94. Taniewski, M. (2008). Sustainable chemical technologies in production of clean fuels from fossil fuels. *CLEAN—Soil, Air, Water*, *36*(4), 393-398.

95. Tang, W. L., & Zhao, H. (2009). Industrial biotechnology: Tools and applications. *Biotechnology Journal*, *4*(12), 1725-1739.

96. Taniewski, M. (2012). Chemistry of synthesis gas and carbon dioxide. The outline of contemporary opportunities. *Przemysl Chemiczny*, *91*(4), 492-498.

97. Van Hove, M. A. (2006). From surface science to nanotechnology. *Catalysis Today*, *113*(3), 133-140.

98. Wang, H., Deng, Z., Chu, W., & Yang, W. (2009). A new approach to achieving a pure M1 phase catalyst for the selective oxidation of propane. *Reaction Kinetics and Catalysis Letters*, *97*(2), 233-241.

99. White, A. (2009). *2nd summit on the future of corporation: Paper series on restoring the primacy of the Real Economy*. Retrieved August 24, from http://www.corporation2020.org/corporation2020/documents/Papers/2nd-Summit-Paper-Series.pdf

100. Wilson, M. P., & Schwarzman, M. R. (2009). Toward a new US chemicals policy: Rebuilding the foundation to advance new science, green chemistry, and environmental health. *Environmental Health Perspectives*, *117*(8), 1202.

101. Xu, Y., Bao, X., & Lin, L. (2003). Direct conversion of methane under nonoxidative conditions. *Journal of Catalysis*, *216*(1), 386-395.

102. Zhang, Z., Zhou, Y., Zhang, Y., Xiang, S., Zhou, S., & Sheng, X. (2014). Encapsulation of Au nanoparticles with well-crystallized anatase TiO_2 mesoporous hollow spheres for increased thermal stability. *RSC Advances*, *4*(14), 7313-7320

CHAPTER 2

MICROBIAL AND BIOCHEMICAL TECHNOLOGY

CONTENTS

2.1 INTRODUCTION

Microbes have developed various systems to store carbon for the duration of stress. In the natural environment of a cell, the carbon that has been stored can be used for growth purposes when there is a good supply of other nutrients. Storage of such other nutrients and carbon is pervasive throughout eukaryotic and prokaryotic domains of life. Such molecules having the ability to store carbon have great industrial significance. They can be utilized as value-added products, as either biofuels or biopolymers. Large quantities of cells are grown, and such compounds are harvested. These compounds served as a replacement for a petroleum-based product. Presently, generation of entire industries has been based on the production as well as utilization of these compounds. Our focus is on two bacteria that can be considered a paradigm of their respective specific carbon storage strategy. These two bacteria are *Rhodococcus opacus* and *Ralstonia eutropha*. *R. opacus* is considered model bacteria for high-yield triacylglycerol (TAG) used making for biofuels, whereas *R. eutropha* has been thoroughly studied as a producer of polyhydroxyalkanoate (bioplastic). Both species of these bacteria produce molecules for storage of carbon which, in turn, can potentially decrease our dependence on fossil-based petroleum. Nevertheless, in both cases, there are certain complications which need to be resolved before the development of effective schemes by employing these microorganisms. In this chapter, we have explored the current as well as previous works that were undertaken to address these challenges.

With the deterioration and significant diminishing of petroleum reserves, concerns have started to arise worldwide, especially because most of the largest reserves of oil are situated in unstable regions of the world. Products of petroleum are widely used for chemical and fuel needs, and it is therefore in our best interest to develop renewable, economical process to synthesize biobased fuels and various other required chemicals (e.g., plastics). Since polymers and fuels are carbon-based, we can count on microbes that are master of storage of carbon for this task. As mentioned earlier, bacteria can store carbon in different forms during periods of stress. Another important family of carbon storage molecules is the polyhydroxyalkanoates (PHA), which is popular for exhibiting characteristics of petroleum-based plastics (Madison & Huisman, 1999; Steinbüchel & Valentin, 1995). Another capability of bacteria is that they can store carbon in the form of triacylglycerols (TAGs) (Alvarez & Steinbüchel, 2002; Wältermann & Steinbüchel, 2005). Although this form of storing carbon is less popular, still it is gaining recognition

rapidly as a scheme of biofuel production. To compete with products of petroleum, production of bioplastics and biofuel must be made cost-effective and efficient. Even though several researchers in both industry and academia have produced industrial-scale PHA production methods or pilot plants, still the cost has remained high to develop products of the polymer as compared to the cost of developing plastics from petroleum products. In several such cases, recombinant *Escherichia coli* strain or *R. eutropha*, the model microbe for the biosynthesis of PHA, are employed. There is not much information on the production of the industrial TAG using bacteria, even though one microbe named as *R. opacus* strain PD630 has been identified as an efficient TAG-accumulating microbe. In this chapter, the state-of-the-art TAG and PHA production processes have been discussed, mainly how bacterial carbon storage molecules are turned into value-added products.

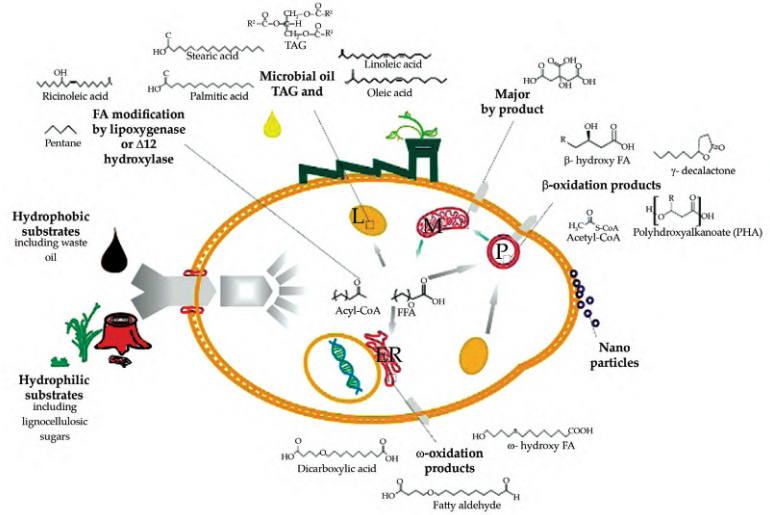

Figure 9. Applications of microbial and biochemical substances in consumable products

[Source: https://www.frontiersin.org/articles/10.3389/fenrg.2014.00021/full]

As the study of the production of the bacterial TAG is still in its initial phases, this chapter outlines some recent researches in support of the pursuit to find a cheap method for the production of the target molecule, with the aim of challenging the petroleum products.

2.2 POLYHYDROXYALKANOATES

Polyhydroxyalkanoates have many chemical and biochemical applications, which are discussed in subsequent sections:

2.2.1 Ecology of Important Storage Polyesters

Nutrient storage systems have progressed all the way through nature as a mechanism of stress survival. Prokaryotes can store carbon which can be later used in diverse forms, such as glycogen, triacylglycerols (TAGs), and polyhydroxyalkanoates (PHA) (Peoples & Sinskey, 1989; Preiss & Romeo, 1990; Alvarez, Mayer, Fabritius, & Steinbüchel, 1996). Microbes store carbon naturally when there is a short supply of other nutrients (i.e., unbalanced growth) and make use of such in carbon-sparse conditions. From the beginning of time, humans have made use of carbon stores of other organisms as food (e.g., starches and plant oils), cosmetics (palm kernel oil, coconut oil), fuel (whale oil), and various other applications. Recently, we are counting on microorganisms for the rapid production of carbon storage products for our personal use. One extensively studied example of carbon storage molecules turning into value-added products is the above-mentioned PHA.

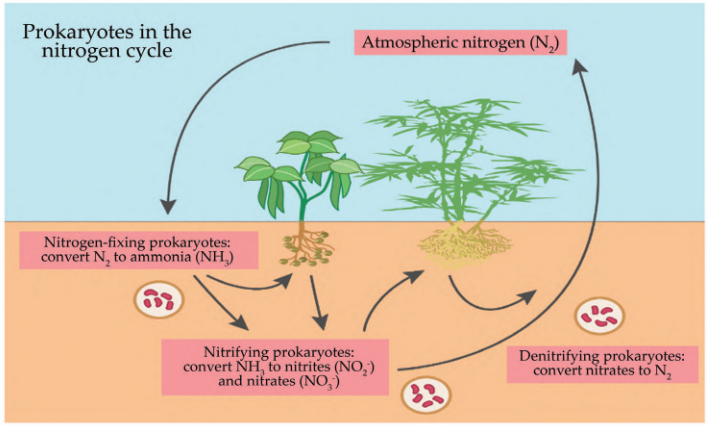

Figure 10. Schematic illustration of the nitrate production in plants by prokaryotes

[Source: https://www.khanacademy.org/science/biology/ecology/biogeochemical-cycles/a/the-nitrogen-cycle]

Various species of microbes have been characterized to express the production of enzymes of PHA (Bernd, 2003; Jendrossek, 2009). Stores of PHA that have been stored between cells help in the survival of the microbes during times when nutrients are sparse. In few cases, independent living bacteria responsible for the production of PHA can surpass producers of non-PHA for the similar niche (Kadouri, Jurkevitch, Okon, & Castro-Sowinski, 2005). PHA is polymerized by cells of microorganism and reserved for future use in thick, protein-covered inclusion bodies known as granules. There are two kinds of PHAs, based on the content of monomer: short-chain length, or SCL-PHA, which contains 4-carbon 3-hydroxybutyrate (3HB) and/or the 5-carbon 3-hydroxyvalerate (3HV) monomers. The second is medium-chain length, or MCL-PHA, which contains monomers having a length of chain greater than 6 carbons, including 3-hydroxyoctanoate (3HO, 8 carbons), 3-hydroxyhexanoate (3HHx, 6 carbons), and other monomers having much longer chain length than 3HHx. There are no less than two separate metabolic pathways for the biosynthesis of microbial PHA. For SCL-PHA such as polyhydroxybutyrate (PHB), two acetyl-CoA molecules are tied up to form acetoacetyl-CoA, and the acetoacetyl-CoA is condensed to form β-hydroxybutyryl-CoA. Afterward, the β-hydroxybutyryl-CoA molecule plays a role as a monomer substrate for the PHA synthesis, and hence, it is integrated into the nascent polymer chain with the help of a thioesterase reaction which takes place at the actual location of the enzyme, and the coenzyme A is released (Li, Chakraborty, & Stubbe, 2009). Figure 11 shows a schematic production of PHA and intermediates initiating with acetyl-CoA. The polymerization pathway that has been shown here is the representative of PHB production in the bacteria *R. eutropha* strain H16 by employing multiple carbon substrates. *R. eutropha* bacteria are freshwater and soil-dwelling bacteria; these bacteria have been considered the model microbe for the biosynthesis of PHA since it can generate up to 80% of dry weight of its cell as PHA for the duration of nitrogen limitation (York, Stubbe, & Sinskey, 2002). It is possible to produce monomers (used for the production of PHA) from intermediates of fatty acid β-oxidation. The breakdown of fatty acid via β-oxidation results in the production of 3-hydroxyacyl-CoA which can be utilized as a monomer for the production of MCL-PHA. Nonetheless, it cannot be used by the PHAS synthase as 3-hydroxyacyl-CoA, the β-oxidation intermediate, is in the (S) shape. The production of polymerizable (R)-3hydroxyacyl-CoA takes place by the conversion of enoyl-CoA using an (R)-specific enoyl-CoA hydratase, commonly known as PhaJ (Hisano et al., 2003; Tsuge, Hisano, Taguchi, &

Doi, 2003). For both MCL-PHA and SCL-PHA, cells produce and afterward store polymer in inclusion bodies present in between cells; these intracellular bodies are known as a granule and are surrounded by proteins (Figure 2). These proteins play several roles such as facilitating the metabolism of PHA, protecting the granule from coalescence, and breaking up the hydrophobic polymer from the flowing cytoplasm. Phasin (PhaP1) is certainly the most abundant protein present in the PHA granule. It has been named since it has a similar function as oleosins that border TAG inclusion bodies in plants (Potter, Madkour, Mayer, & Steinbüchel, 2002). It has been demonstrated that in *R. eutropha*, the PhaP1 phasin covers anywhere from 27 to 54% of the surface of PHA granule (Tian, Sinskey, & Stubbe, 2005; Gerngross, Reilly, Stubbe, Sinskey, & Peoples, 1993; Maehara, Taguchi, Nishiyama, Yamane, & Doi, 2002). Some of the other proteins that are associated with granule include the PhaC and PHA synthase, depolymerase enzymes, PhaZs, and the regulatory protein, PhaR (York et al., 2003; Yamada et al., 2007). Figure 2 shows the formation of PHA granule in *R. eutropha*. Lately, additional proteins have been discovered in *R. eutropha* which too are associated with granule (Pfeiffer & Jendrossek, 2011). This includes a granule-associated protein having dual function of binding to the nucleotide region of the cell (Pfeiffer et al., 2011). This recently discovered protein known as PhaM seems to have functional biology to the protein associated with the lipid body known as TadA from *R. opacus* (MacEachran, Prophete, & Sinskey, 2010). The relationship between various proteins, each one having a special function in the production cycle of PHA, proposes that the PHA granule is a complex organelle that permits the optimal carbon mobilization and sequestration, depending on the availability of a nutrient in the extracellular milieu.

2.2.2 Value-Added Products of Polyhydroxyalkanoates (PHA)

Long before, the earliest patents for the production of commercial PHA were granted to a company known as W. R. Grace and Company in the 1960s, and several persons have already acknowledged the business potential of these biopolymers. Numerous kinds of PHA biopolymer possess such mechanical and thermal properties that compete with those thermoplastics which are petroleum-based.

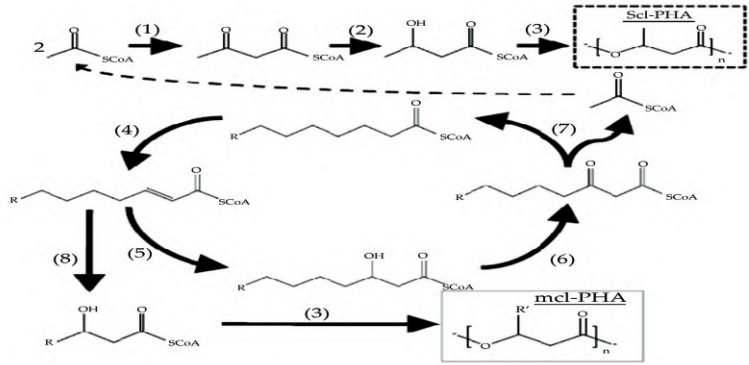

Figure 11. A schematic development of microbial PHA paths. Two molecules of acetyl-CoA are connected via β-ketothiolase for SCL-PHA. (1) To form acetoacetyl-CoA, which becomes concentrated by reductase of acetoacetyl-CoA. (2) To form 3-hydroxybutyryl-CoA (3HB-CoA). Enzyme PHA synthase is utilized for 3HB-CoA polymerization. (3) For the manufacturing of PHB (i.e., black dashed box). Acetyl-CoA for PHB biosynthesis can be produced using the fatty acid β-oxidation cycles (enzymes 4–7). Substrates for MCL-PHA synthesis can also be acquired from β-oxidation, using an (R)-specific enoyl-CoA hydratase. (8) The polymerization of hydroxyacyl-CoA molecules of medium chain length is facilitated by PHA synthase. (3) For the fabrication of MCL-PHA (gray box). These monomers of medium chain length can also be synthesized through biosynthesis of fatty acid. Enzyme designations: 2-enoyl-CoA hydratase (5), fatty acyl-CoA dehydrogenase (4), β-ketothiolase (7), and 3-hydroxyacyl-CoA dehydrogenase (6).

[Source: https://www.omicsonline.org/bacterial-carbon-storage-to-value-added-products-1948–5948. S3–002.php? aid=2836]

A summary of mechanical and thermal characteristics of several PHAs is presented in Table 1. In different applications, these PHAs can provide the role of substitute in place of petrochemical plastics. Presently, the world's largest industrial manufacturer of PHA is an American company named, Metabolix, and is based in Cambridge, MA, USA (www.metabolix.com). As per the joint venture between Metabolix and Archer Daniels Midland, the company will produce P(3HB-co-4HB), copolymer poly (3-hydroxybutyrateco-4-hydroxybutyrate) in large quantities from corn sugar using engineered bacterial strains. Other companies that produce PHA are operational all over the world, for example, Biocycle in Brazil and TianAn Biologic Materials in

China. Recently, a bioplastic production plant has been opened in Malaysia for the experimental purpose for the production of PHA from palm oil products by employing engineered *R. eutropha* (Budde et al., 2011).

Table 1. Mechanical and thermal characteristics of petrochemical polymers and PHA polymers

Polymer	T_m (°C)	T_g (°C)	Young's modulus (GPa)	Tensile strength (MPa)	Elongation to break (%)	Reference
P(HB-*co*-10 mol% HHx)	127	−1	nd[a]	21	400	(Doi, Kitamura, & Abe, 1995)
PHB	177	4	3.5	43	5	(Sudesh, Abe, & Doi, 2000)
P(HB-*co*-12 mol% HHx)	103	−2	0.5	10	130	(Wei & Shen, 2010)
P(4HB)	53	−48	0.15	104	1000	(Saito & Doi, 1994)
P(HB-*co*-15 mol% HHx)	115	0	nd[a]	23	760	(Doi et al., 1995)
Polystyrene	240	100	nd[a]	nd[a]	nd[a]	(Sudesh et al., 2000)
P(3HB-*co*-12 mol% 4HB)	124	−4	0.54	25	630	(Wei & Shen, 2010)
Polypropylene	176	−10	1.7	38	400	(Sudesh et al., 2000)
LDPE[-b]	130	−30	0.2	10	620	(Sudesh et al., 2000)

[a]nd = not determined in the indicated study, [b]low-density polyethylene

The question arises that what makes a biopolymer appropriate for production on an industrial scale. The PHA polymer must have valuable physical as well as thermal properties due to which it can replace petroleum-based plastics, for instance polypropylene. As mentioned in Table 1, the polyhydroxybutyrate (PHB) homopolymer is quite brittle and stiff and therefore can only be used for a limited range of applications. Copolymers of PHA exhibit excellent characteristics. The reason behind this is the

decrease in the crystallinity which results from the interactions between two different chain length monomers in the polymer (Anderson & Dawes, 1990; Anderson, Haywood, & Dawes, 1990; Brigham, Kurosawa, Rha, & Sinskey, 2011). Different copolymers such as P(3HB-co-3HV) (3HV = 3-hydroxyvalerate), P(3HB-co-4HB), and P(3HBco-3HHx) (3HHx = 3-hydroxyhexanoate) have been extensively studied for their prospective applications in various fields as a substitute for petrochemical polymers. These polymers are biodegradable, biobased, and biocompatible (Holmes, 1985; Philip, Keshavarz, & Roy, 2007; Chen, 2009). Every single type of copolymers is an attractive substitute for petroleum-based polymers and therefore has been under production in large quantities on a commercial scale.

2.2.3 Fermentative manufacturing of PHA polymers

Industrial-level production of PHAs needs many challenges to be overcome. Notably, high-cell-density development is a requirement to maximize the volumetric production of fermentation of microorganisms. In various cases, an *E. coli* strain is used for the biosynthesis of polymers (Wang & Lee, 1998; Choi, Lee, & Han, 1998; Choi, Lee, & Han, 1999; Choi & Lee, 1999). Since wild-type, *E. coli* cannot produce 3-hydroxyacyl-CoAs (3HA-CoA) de novo for the synthesis of the polymer, the pathway of PHA production should be supplied heterologously. Some benefits of employing a recombinant *E. coli* strain in the clued rapid rate of growth and the fact that biosynthesis of PHA is not restricted by the limitation of nutrient in a recombinant strain; therefore cell keeps producing PHA associated with growth. An *E. coli* strain exhibiting genes of PHA biosynthesis and overexhibiting FtsZ (a cell division protein) gathered PHB to a concentration of around 104 g/l in fed-batch conditions (Choi & Lee, 1999). *E. coli* exhibits production genes of PHA from Alcaligenes latus. The concentration of PHB >140 g/l was acquired in fed-batch culture using *E. coli*. The similar strain was employed in a fed-batch culture containing propionic acid feeding. P (HB-co-HV) was manufactured with a productivity greater than >2.8 g/l/hour (Wang & Lee, 1998). For the production of P (HB-co-HHx), recombinant *E. coli* has also been used with ultimate productivities of ~0.5 g PHA/l/hour (Park et al., 2002; Tian et al., 2005). An attractive species for the production of PHA on an industrial scale is *R. eutropha*. Bacteria are native producers of PHA; as a result, regulatory systems and the cellular machinery are already in suitable places for the production of large quantities of PHA (Wilde, 1962; Tsuge, Tanaka, & Ishizaki, 2001; Yang et al., 2010). Moreover, *R. eutropha* can

utilize an extensive array of carbon sources for polymer as well as growth biosynthesis including organic acids, sugars, fatty acids, CO_2, and plants (Kahar, Tsuge, Taguchi, & Doi, 2004; Brigham et al., 2010; Budde et al., 2011). Hence, it is possible to produce a polymer in large quantity and at competitive prices by making use of cost-effective feedstocks such as food processing and agricultural wastes, concentrated CO_2, and unrefined natural products (e.g., plant oils). In case of industrial polymer production, it is critical to get high production rate (i.e., space–time yield) of PHA (Ng, Ooi, Goh, Shenbagarathai, & Sudesh, 2010; Budde, Riedel, Willis, Rha, & Sinskey, 2011). Over the recent years, researchers have tried their best to enhance the yield of biomass along with an increase in the yield of PHA (Volova, Kalacheva, & Altukhova, 2000; Volova & Voinov, 2003; Riedel et al., 2012). Whereas for the production of TAG, culture carbon/nitrogen (C/N) ratios are vital to maximizing productivity, high productivity of PHA can be acquired from the limitation of phosphate or nitrogen (or another nutrient) in cultures. When *R. eutropha* was cultivated in fed-batch culture using steep corn liquor, it was observed that productivities of PHA were over 1.0 g/l/hour (Kim et al., 1994; Ryu Hahn, Chang, & Chang, 1997). For maximizing PHA production using *R. eutropha*, culture systems consisting of two stages have also been observed. The primary stage served as cell growth and thus produced maximum biomass, whereas the second stage consisted of accretion of PHB. The above-mentioned two cultures showed the maximum productivity of 1.2 g/l/hour with greater than 70% PHB per dry cell weight (Du, Chen, Yu, & Lun, 2001). Normally, nitrogen is responsible for restraining nutrient to trigger biosynthesis of polymer for the production of PHA in *R. eutropha* strains. High productivity has also been resulted by employing phosphate restriction, with productivity >1.5 g PHB/l/hour (Shang, Jiang, & Chang, 2003).

Despite the fact that high-productivity PHB production is a suitable method of demonstrating that *R. eutropha* can be employed for the efficient fermentation, still, PHA copolymer remains an ideal fermentation product due to their more suitable properties (see Table 1). Two researchers Anderson and Madden used an alternative feeding method by making use of propionic acid and sugar in *R. eutropha* fed-batch culture which resulted in the production of P (HB-co-HV) having productivity >1.5 g/l/hour. In this study, the ultimate 3HV content obtained was ~7.5 mol% (Madden, Anderson, & Asrar, 1998). P (HB-co-HHx) was formed using a strain of *R. eutropha* exhibiting a heterologous PHA synthase (obtained from *Aeromonas caviae*) with a productivity of merely above 1.0 g/l/hour. The sole carbon

source used in this case was soybean oil. The 3HHx fraction of the polymer, in this case, was around ~5 mol% (Riedel et al., 2012). Lately, a strain of *R. eutropha* was designed using a novel approach that expressed a PhaJ gene (from *Pseudomonas aeruginosa*) as well as heterologous PHA synthase (from *Rhodococcus aetherivorans*) for converting intermediates of fatty acid β-oxidation into (R)-3HACoA substrates for PHA biosynthesis. In fed-batch fermentations, the growth of this strain by employing palm oil as the only source of carbon and urea as the source of nitrogen ended in the biosynthesis of P (HB-co-HHx) with a productivity greater than 1.0 g/l/hour and a 3HHx content of around ~17 mol%. During this work, a comparison was made between PHA productivities of various feeding strategies with fed-batch fermentation as the ideal method of fermentation (Riedel et al., 2012). Some of the other high-density fermentations were also performed which resulted in the efficient production of P (HB-co-HHx). Using fatty acids as the only source of carbon, cultures of Aeromonas hydrophila produced P (HB-co-HHx) having the productivity of ~1.0 g/l/hour (Lee et al., 2000). Moreover, using A. hydrophila grown on glucose, large-scale (20,000 l) fermentations were accomplished with a P (HB-co-HHx) productivity slightly greater than 0.5 (Ryu et al., 1997). The productivity of around 0.8 g PHA/l/hour experimented in the production of MCL-PHA in the fed-batch culture of *Pseudomonas putida* which were grown on mixed sugars (Diniz, Taciro, Gomez, & da Cruz Pradella, 2004). On the other hand, the productivity of 2.0 was obtained with high-density *P. putida* cultures using the limitation of phosphate (Lee et al., 2000). The following table (Table 2) shows a summary of high-yield production of PHAs according to the latest studies.

Table 2. A summary of high-yield production of PHAs according to the latest surveys

Production organism	Polymer produced	Carbon source	Biomass yield (g/l)	PHA yield (g/l)	Productivity (g/l/hour)	Reference
Ralstonia eutropha	PHB	Glucose	208.0	139.0	3.1	(Shang, Jiang, & Chang 2003)
R. eutropha	PHB	Glucose	164.0	121.0	2.4	(Kim et al., 1994)
Escherichia coli	PHB	Glucose	194.1	141.6	4.6	(Choi, Lee, & Han, 1998)

R. eutropha	PHB	Corn steep liquor	281.0	232.0	3.1	(Ry et al., 1997)
Aeromonas hydrophila	P (HB-*co*-HHx)	Oleic acid	95.7	43.2	1.0	(Lee et al., 2000)
E. coli	PHB	Glucose	149.0	104.0	2.1	(Wang & Lee, 1998)
Aeromonas hydrophila	P (HB-*co*-HHx)	Glucose and lauric acid	50	25	0.5	(Ryu, Hahn, Chang, & Chang, 1997)
R. eutropha	P (HB-*co*-HV)	Glucose and propionic acid	84.0	65.5	1.6	(Madden, Anderson, & Asrar, 1998)
Pseudomonas putida	MCL-PHA	Sugar cane carbohydrates	50.0	31.5	0.8	(Diniz et al., 2004)
R. eutropha	P (HB-*co*-HHx)	Palm oil	140.0	104.0	1.1	(Riedel et al., 2012)
Pseudomonas putida	MCL-PHA	Oleic acid	141.0	72.6	1.9	(Lee et al., 2000)
E. coli	P (HB-*co*-HHx)	Dodecanoic acid	79.0	21.5	0.5	(Park, Ahn, Green, & Lee, 2001)

2.2.4 PHA Fabrication Challenges

Even though some researchers have shown scalable, robust PHA production in various systems, nevertheless, there are challenges need to be overcome. Most of the challenges are associated with the production of PHA in a cost-effective manner, so that the cost of the finished product may compete with petrochemical-based plastics. For this purpose, the first step is to make use of inexpensive and readily available feedstocks for carbon substrates in PHA and growth production. Carbon dioxide is easily available and therefore has been utilized as the only source of carbon for the production of PHA (Ishizaki, Tanaka, & Taga, 2001; Volova, Gitelson, Terskov, & Sidko, 1998). However, carbon dioxide needs to be concentrated on using it as carbon feedstock in an autotrophic fermentation, which presents a major challenge. Same is the case with fermentation parameters themselves, which also requires concentrated carbon dioxide (Dionisi et al., 2005; Cavalheiro, de Almeida, Grandfils, & Da Fonseca, 2009). Lately, research has been undertaken to investigate whether waste streams can be utilized as nutrient sources for the production of value-added products, for example, TAGs and PHA (Braunegg et al., 1999; Hassan et al., 2002 et al., 2009). A company named Hassan and his team has constructed a methodology for the production of PHA from organic acids which result from the absorption

of processing sludge from palm oil mill waste (Koller et al., 2005; Gouda, Omar, & Aouad, 2008). Production of the polymer has also been carried out from pure cultures by employing beet molasses, whey, waste glycerol, and jatropha oil (Page, Manchak, & Rudy, 1992; Wong & Lee, 1998).

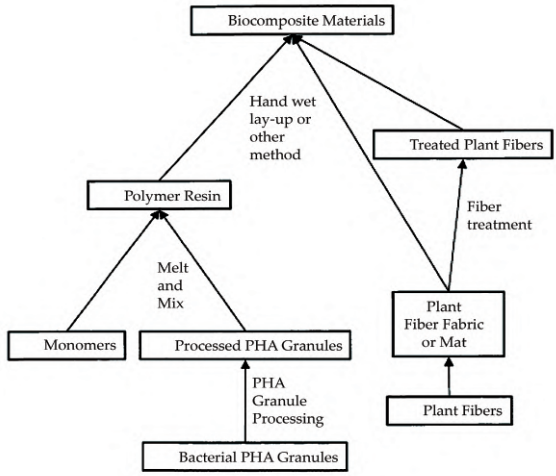

Figure. 12. Applications of PHA in manufacturing of various composite materials

[Source: https://www.google.com/patents/US7887893]

Extensive research has been carried out for the production of PHA using mixed cultures with different species of bacteria, and most of the times, strains have been obtained from the same waste stream (Dias et al., 2006; Salehizadeh, 2004). This method of production normally involves enriching of PHA-producing cultures of microorganisms as well as proliferating stable cultures before harvesting of the polymer. This method of enriching a mixed culture for PHA production can be achieved by a microaerophilic–aerobic system. This system is responsible for controlling the content of oxygen of the culture for the selection of such bacteria which accumulate PHA over those bacteria which accumulate "feast/famine" cycling (known as aerobic dynamic feeding) or glycogen (Beun, Paletta, Van Loosdrecht, & Heijnen, 2000; Satoh, Mino, & Matsuo, 1999). The selection of microorganisms that accumulate PHA is made by their capability to make use of a polymer as a nutrient (Majone, Massanisso, Carucci, Lindrea, & Tandoi, 1996). The main benefit of the mixed culture is that conditions of cultivation do not essentially have to be sanitized, which therefore will save costs of energy.

There is also no need for purifying feedstocks even though often acetate has been used as a source of carbon to enrich for bacteria producing PHA. Nonetheless, there are several challenges related to the production of mixed culture PHA such as the development of culture selection approaches toward higher yields of PHA and productivities (Serafim, Lemos, Albuquerque, & Reis, 2008). As there are some unknown or uncharacterized as well as wild-type microorganisms in the mixed culture, the resultant PHA produced (e.g., PHB) may not come out to be suitable for several applications; hence, the result of this process is dependent on the microbial input. Moreover, there exist some downstream challenges associated with the production of PHA on an industrial scale (Choi & Lee, 1999). The harvesting of biopolymer from cells exhibits challenges in the construction of an inexpensive production process. Several different chemicals have been investigated for the recovery of polymers (Dong & Sun, 2000). Among these chemicals include sodium hypochlorite, NaOH, methyl ethyl ketone (MEK), chloroform, ethyl acetate, methyl isobutyl ketone (MIBK), and aqueous detergent solutions (Ramsay, Berger, Voyer, Chavarie, & Ramsay, 1994; Kurdikar, Strauser, Solodar, Paster, & Asrar, 2000). For the recovery of PHA, ideal compounds are those that can be reused, can be recycled, and can easily be separated from aqueous solutions (Shang et al., 2003; Kim, Cho, Ryu, Lee, & Chang, 2003; Yang, Brigham, Willis, Rha, & Sinskey, 2011). From the above-mentioned list of chemicals, the most promising chemicals for the recovery of highly pure PHA from biomass are MIBK and MEK. Not all solvents will be able to recover all types of PHA successfully. For instance, MIBK is more suitable for those PHAs which contain longer-chain-length monomers, whereas it is less effective with PHB. Some other methods for recovery have been performed to extract PHA from biomass, including controlled autolysis, enzymatic digestion, and dissolved air flotation (Yasotha, Aroua, Ramachandran, & Tan, 2006; Van Hee, 2006; Martínez, García, García, & Prieto, 2011). However, it is not sure whether or not these alternative recovery approaches would be desirable in an industrial setting.

2.2.5 Overview of Polyhydroxyalkanoates

At present, in the market, PHAs are used as biodegradable, renewable alternative to conventional plastic. PHA has various uses in several industrial, household, as well as medical applications. Even though PHA, when produced in a large amount, is comparatively not very expensive, still its price is more than plastics which are made from petroleum. The cost of production of PHA can be reduced using several waste streams, such as

food processing waste, milling waste, agricultural waste, or even emissions of concentrated CO_2. This will help in making PHA a more economically viable polymer as compared to the conventional plastics. Additionally, to make the production of bioplastics a greener process, it is significant to employ environmentally friendly methods of polymer recovery from cells; for instance, using recyclable and non-halogenated solvents, we can make the production of bioplastics a greener process. Given that polyhydroxyalkanoates can be customized to show similar characteristics such as petroleum-based plastic, a more cost-effective and robust process of production is required to compete in the present market of plastics. In few cases, this kind, of course, is already in practice and thus helping in the advancement of the bioplastic industry on a global scale.

2.3 TRIACYLGLYCEROLS

Triacylglycerols (TAGs) are storage lipids possessing a non-polar and neutral nature. This particular nature permits them to be conveniently stored in anhydrous environments and the chief storage molecules of fatty acids for the synthesis of membrane lipids as well as energy utilization in living beings (Yen, Stone, Koliwad, Harris, & Farese, 2008). TAGs are the type of esters in which three fatty acid molecules are associated with glycerol. These fatty acids can be of all different kinds, all the same kind, or else merely two and may perhaps consist of unsaturated or saturated fatty acids. In naturally occurring TAGs, the lengths of a chain of the fatty acids mostly differ, but consist of 16 or 18 atoms of carbon. Naturally occurring fatty acids that are present in plants and animals are mostly composed of just even numbers of atoms of carbon, therefore exhibiting the path to their biosynthesis using the two-carbon building block acetyl-CoA (Murphy, 2001; Durrett, Benning, & Ohlrogge, 2008). On the other hand, bacteria can synthesize branched and odd chain fatty acids. The physicochemical characteristics of TAGs are mainly dependent on the length of the chain, nature of the fatty acids present, and to the extent to which their fatty acids are desaturated. TAGs have been employed in several versatile materials, for example, cosmetics, oleochemicals, and food applications; moreover, they are gaining more attention owing to their growing interest in alternative fuels (Lestari, Mäki-Arvela, Beltramini, Lu, & Murzin, 2009).

2.3.1 Triacylglycerols for Production of Biofuel

It is an acknowledged fact that the fatty acyl chains of TAGs are analogous

(chemically) to the aliphatic hydrocarbons that build up the bulk of molecules present in diesel and gasoline (Ryan, Dodge, & Callahan, 1984; Ali & Hanna, 1994). Around 120 years ago, when diesel engines were first invented, vegetable oil was used to run them. This vegetable oil was composed mainly of triacylglycerols. As with time, petroleum has become inexpensive as well as abundant. Therefore, the use of vegetable oil as a source of fuel has been sidelined, and the development of the diesel engine has been founded on the efficiency of petroleum-derived diesel fuel. However, with the sudden increase up to fourfold in the prices of petroleum, the interest in the production of biofuel has been reawakened globally.

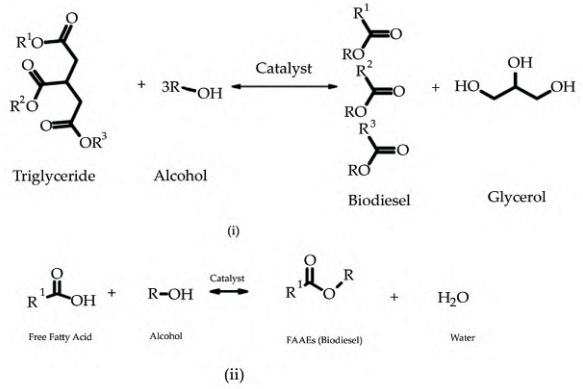

Figure 13. Production of biodiesel from triglyceride and alcohol

[Source: http://www.sciencedirect.com/science/article/pii/S246802571-6300164]

Since 1973, the main development in the production of biobased alternative fuel has been under progress in those countries which have no or minimal resources of internal petroleum (Manzanera, Molina-Muñoz, & González-López, 2008). Afterward, the price of oil rose steadily between 2003 and 2008. In 2003, one barrel of crude oil priced around $30 in the New York Mercantile Exchange which, in 2005, reached up to $60 and afterward peaked at $147 in 2008 (http://tfccharts.com/chart/QM/W). Therefore, variation in the cost of petroleum fuel, reducing reserves of petroleum, and increasing concerns about the impacts of enhancing levels of atmospheric carbon dioxide are intensifying the research on various renewable biofuels which can help in reducing our present usage of fossil fuels (Hill, Nelson, Tilman, Polasky, & Tiffany, 2006). For the last few years, significant efforts

have been made for the development of bioethanol as a substitute fuel (Jarboe, Grabar, Yomano, Shanmugan, & Ingram, 2007). Nonetheless, bioethanol has some restrictions, for example, high vapor pressure, corrosiveness, and low energy density which hinder its extensive utilization given the common infrastructure (Yan & Liao, 2009). One imaginable way out to this problem can be the exploitation of TAGs for producing lipid-based biofuels. Biofuels with different properties and compositions can be formed using different TAG-based bioprocesses. One such example is biodiesel which is developed by transesterification of TAGs with alcohol, commonly methanol. This takes place in the occurrence of an alkaline catalyst and hence creates monoalkyl esters of long-chain fatty acids, for instance, fatty acid ethyl esters (FAEEs) and fatty acid methyl esters (FAMEs). During the mid-1980s to early 2000s, most research carried out on the production of biodiesel has paid focus on vegetable oils from oleaginous plants (Ma & Hanna, 1999; Fjerbaek, Christensen, & Norddahl, 2009).

According to the recent research, the use of raw vegetable oils in diesel engines gives rise to several different problems such as injector coking, deposits, and piston ring sticking. These problems can be avoided or reduced by transesterification of vegetable oil to produce ethyl or methyl esters (Canakci & Van Gerpen, 2001; Azócar, Heipieper, & Navia, 2010). Majority of the biodiesel that is produced presently employs an extensive range of both edible and non-edible vegetable oils, frying oil, animal fats, and waste cooking oil. A more comprehensive review of the production of biodiesel is available in the literature (Knothe, 2010; Canakci & Sanli, 2008). The biodiesel offers several environmental benefits, such as the low amount of sulfur dioxide in emissions during burning and low levels of suspended particulate matter; hence, it is possible to use it in most diesel engines with slight or even no alteration. Few physical restrictions have been underlined when these molecules are utilized as the only source of fuel and not just as blend stock because of cold flow characteristics (Vasudevan & Briggs, 2008). Since the early 2000s, another type of biofuel, commonly termed as "renewable diesel," has been gaining much attention. This diesel is manufactured from TAGs, in the presence of a catalyst through a hydro-de-oxygenation reaction (Brigham et al., 2011; Schatz, Witkowski, & McCombie, 2012). The extended benefit of the process is the flexibility of its feedstock, which shows that renewable diesel can be treated using an extensive variety of feedstocks which contain TAG—animal fats, weedy plants, algae, oleaginous microorganisms, and waste oils (Clark, Luque, & Matharu, 2012). TAGs are converted to different products, for

example, gasoline, kerosene, diesel, and jet fuels, all containing paraffinic hydrocarbons. After that, the chain length of hydrocarbons is kept under control to deliver a distribution that is alike in nearly all aspects of commercially available petroleum-derived fuels (Meng et al., 2009; Brigham et al., 2011). Thus, in a nutshell, we can say that at present, energy-rich TAG molecules have appealed great attention for the development of high-quality and environmental-friendly lipid-based biofuels.

2.3.2 Triacylglycerol Synthesis in Bacteria

There is an extensive distribution of TAG biosynthesis in nature, and the existence of TAG in the form of reserve compounds is prevalent among animals, plants, fungi, and yeast. However, in contrast, they have not been considered as general storage compounds in bacteria. Both accumulations and biosynthesis of TAGs have been defined merely for a few bacteria which belong to the actinomycetes group, such as genera of Rhodococcus, Streptomyces, Mycobacterium, Nocardia, Gordonia, and Dietzia and, to a smaller extent, in some other bacteria, including Alcanivorax borkumensis and Acinetobacter baylyi. The existence of TAGs in the form of vacuoles in bacteria has been previously reported in Streptomyces and Mycobacterium in the 1940s to 1960s. Moreover, a systematic study on TAG formation at the time of growth has been reported in the 1990s with Streptomyces sp. (Olukoshi & Packter, 1994). TAGs are stored in the form of sphere-shaped lipid bodies such as intracellular insertions, with the quantity dependent on the corresponding species, growth phase, and cultural conditions. Normally, the main factor for the fabrication of TAGs is the quantity of nitrogen that is provided to the culture medium. The surplus carbon, which is accessible to the culture after exhaustion of nitrogen, is being absorbed by the cells and is directly converted into lipids owing to the oleaginous bacteria which possess the essential enzymes. The structures and compositions of TAG molecules of bacteria differ significantly depending on the cultural conditions (particularly carbon sources) as well as on bacterium. Manilla-Pérez, Lange, Luftmann, Robenek, & Steinbüchel (2011) published revolutionary work for the production of TAG in bacteria. For the past few years, many researchers are investigating the aspects of the biochemistry and the physiology of bacterial TAG accretion, as well as the molecular biology of the lipid inclusion (Kalscheuer et al., 2007; Kosa & Ragauskas, 2011; Santala et al., 2011).

2.3.3 Triacylglycerol Synthesis of Rhodococcus opacus PD630

Numerous species of bacteria do not accumulate considerable amounts of TAGs, and the content is normally around 20–40% of dry mass. In the domain of oleaginous bacteria, research carried out by Alvarez and coworkers has confirmed that *R. opacus* PD630 (DSMZ 44193), when grown on defined medium carrying olive oil, can accumulate TAGs which account for as high as 87% of the cell dry weight (CDW). A soil sample was obtained from a gas work plant in Germany, and then, strain was isolated from this sample as an oleaginous hydrocarbon-mortifying bacterium. They were able to grow this sample on long-chain-length gluconate, alkanes, acetate, propionate, fructose, phenylacetic acid and phenyldecane (among others) and could create an amazingly high quantity of TAGs intracellularly. This quantity was significantly more than the other bacteria at a time when the cells were cultured on analogous substrates under nitrogen-limiting conditions. According to a report, *R. opacus* PD630 when cultivated in fed-batch conditions on a medium which was composed of sugar beet molasses and sucrose achieved a cell density of about 37.4 g^{-1} CDW with the content of fatty acid reaching around 51.9% of the CDW. This observation further suggested that we can apply the fermentation on carbon sources from agricultural yield for the biotechnological fabrication of TAGs (Voss & Steinbüchel, 2001). To produce "second-generation biofuel technologies" in an appropriate manner and to further avoid the conflict of food and fuel, it is a must to develop lignocellulosic biomass as feedstocks for production of the TAG (Stein, 2007; Tollefson, 2008). Lignocellulosic biomass accepts cellulose which is a glucose polymer. Nevertheless, production of the TAG of *R. opacus* PD630 on glucose as a source of carbon had not been demonstrated up till recently. We found out that *R. opacus* PD630 has the unique ability to accumulate a lot of TAGs in batch cultivation which contains a high amount of glucose under defined circumstances (Kurosawa, Boccazzi, de Almeida, & Sinskey, 2010).

2.3.4 Fermentation of R. opacus PD630 by Higher Concentrations of Glucose

For maximization of volumetric productivity of microbial fermentation, cultivation of high cell density is vital (Riesenberg & Guthke, 1999). In this regard, the affluent execution of the fermentation is mainly dependent on the capability of the bacterial strain which is employed to deal with stress forced by high concentrations of sugar (Teixeira, Raposo, Palma, & Sá-Correia,

2010). The growth rate of *R. opacus* PD630 was examined in flask cultures on a distinct medium having initial concentrations of glucose around 200, 250, 300, and 350 g l^{-1} at preliminary inoculums of 1.0 OD660. The strain grew in good health on medium holding up to 300 g l^{-1} and reached a standstill phase after 48 hours on 200 g l^{-1}, 72 hours on 250 g l^{-1}, and 96 hours on 300 g l^{-1}. The growth was repressed at the maximum concentration of glucose of 350 g l^{-1}, as is shown in Figure 3. Therefore, *R. opacus* PD630 can prove to be an ideal candidate for industrial fermentations which require consumption of high concentrations of glucose, whereas our preface studies have demonstrated the existence of high concentrations of $(NH_4)_2SO_4$ in the media which consequences in a simultaneous reduction in the storage of TAG among the cells.

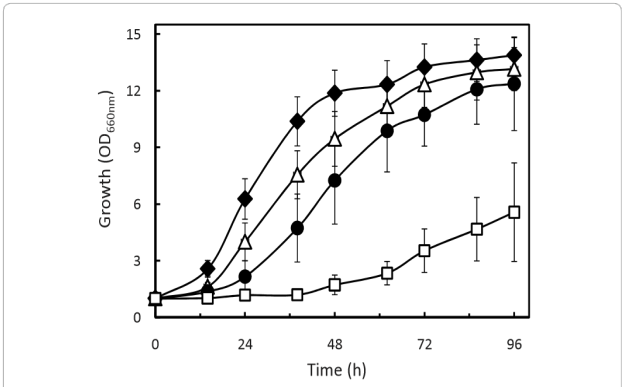

Figure 14. The growth of R. opacus PD630 from high concentrations of glucose concentrations in flask cultures. The concentrations of glucose tested in defined media containing 1.4 g l^{-1}

[Source: https://www.omicsonline.org/bacterial-carbon-storage-to-value-added-products-1948–5948. S3–002.php? aid=2836]

Various preceding reports have verified that storage of carbon in several bacteria is profoundly subjective to the ratio of carbon to nitrogen (C/N). The impacts of change in the C/N ratio on production of the TAG of *R. opacus* PD630 were observed by the amalgamation of several concentrations of $(NH_4)_2SO_4$ and glucose. The results were obtained by altering the quantity of $(NH_4)_2SO_4$ and glucose in the medium starting from 5 to 60 g l^{-1} and 0.3 to 2.8 g l^{-1}, respectively. As is shown in Figure 15, when the concentration of $(NH_4)_2SO_4$ was augmented from 0.3 to 1.4 g l^{-1} while having the concentrations of glucose from 20 to 40 g l^{-1}, the production of fatty acid

and CDW increased proportionally from 1.0–1.1 to 4.0–4.9 g l^{-1} and 1.9–2.2 to 7.8–9.2 g l^{-1}, respectively. This production concentration is equivalent to a cellular fatty acid concentration of 50–55% CDW.

In the meantime, when the concentration of $(NH_4)_2SO_4$ of the medium was further enlarged to 1.7 g l^{-1}, the content of the fatty acid and CDW decreased to 52–59 and 58–73%, respectively. After the measurement of the final pH of the culture, it was observed that increasing concentrations of $(NH_4)_2SO_4$ resulted in lowering the final pH. The broth supernatants of *R. opacus* PD630 cultivated in a particular medium which was composed of more than 1.7 g l^{-1} $(NH_4)_2SO_4$ had the concluding pH value of 4.2–4.8.

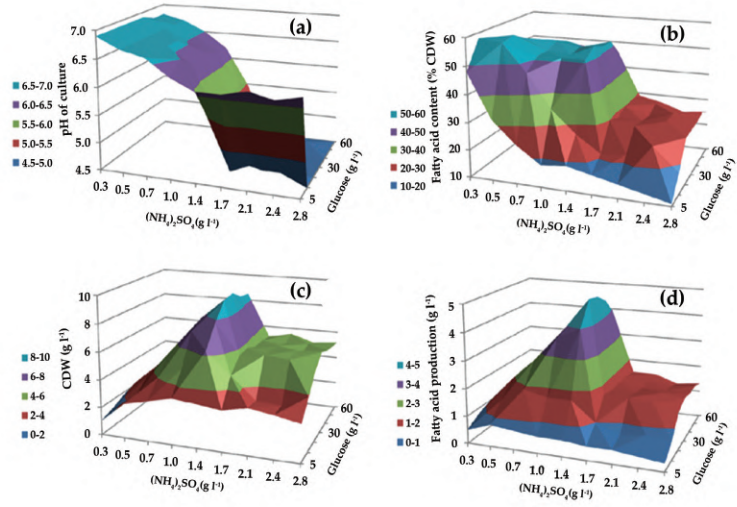

Figure 15. The effects of $(NH_4)_2SO_4$ and glucose concentrations on pH of the culture. (a) Representation of fatty acid content, (b) representation of CDW, and (c) representation of fatty acid creation (d) by R. opacus PD630 in flask culture

[Source: https://www.omicsonline.org/bacterial-carbon-storage-to-value-added-products-1948–5948. S3–002.php? aid=2836]

These results indicate that a decrease in pH represses growth and resultantly reduces production of lipid when *R. opacus* PD630 is cultivated under unrestrained pH cultivations. Under controlled pH conditions, batch fermentations permitted for the enhancement in the concentrations of $(NH_4)_2SO_4$ and glucose in the medium, which resulted in a remarkable increase in TAG production (Kurosawa et al., 2010). For maximizing the

production of fatty acids, the critical operational C/N ratio was optimized using a response surface procedure which was based on the Box–Wilson central composition design. The used design predicted that cultivation of *R. opacus* PD630 in a particularly defined medium having a C/N of 17.8 and comprising of 13.4 g l^{-1} $(NH_4)_2SO_4$ and 240 g l^{-1} glucose would lead to the highest production of 25.1 g l^{-1} of fatty acids (Figure 5). Cultivation of *R. opacus* PD630 in batch fermentations with the previously mentioned predicted favorable conditions resulted in the production of 25.2 g l^{-1} of fatty acids which correspond to around 38% of the cell dry weight after 147 hours of cultivation. The fatty acid piled up in the cells is mainly composed of oleic acid (25%), palmitic acid (28%), and cis-10-heptadecenoic acid (16%). These results show the high potential of *R. opacus* PD630 as a TAG producer for industrial production of lipid-based biofuels on starchy lignocellulosic biomass that is composed mainly of glucose polymers.

2.3.5 Fermentation of *R. opacus* PD630 on starchy lignocellulosic sugars

An investigation was carried out on the lipid accumulation and growth characteristics of *R. opacus* PD630 on saccharified solutions which were derived from corn silage. A company known as Sweetwater Energy Inc. (Rochester, NY, USA) provided the corn silage which was homogenized by acid treatment. The feedstock that was not digested was adjusted to a pH level of 5.0, and industrial enzymes comprising of 0.5 ml Celluclast and 2 ml Viscozyme L were appended into 100 ml of the suspension which contained the silage of 67 g l^{-1} in the form of the dried mass. The saccharification process was carried out with a rotational speed of 200 rpm and at 45°C. As is shown in Figure 6, after 72 hours of incubation, the resulted sugar of the hydrolysate comprised of 3.1 g l^{-1} xylose, 32.2 g l^{-1} glucose, 3.6 g l^{-1} other unidentified sugars, and 0.7 g l^{-1} arabinose. These results show that we can convert around 50% of the feedstock to monosaccharides. As it is common knowledge that there are large quantities of starch present in the feedstock, therefore around 0.5 ml of glucoamylase was mixed into 100 ml of the feedstock during a separate treatment. Afterward, incubation of the suspension was carried out at 45°C for 72 hours at 200 rpm (data not shown).

The HPLC statistics of the hydrolysate indicated that glucose is present as a major sugar with more than 96% selectivity. Considering that 28 g l^{-1} of glucose was identified in the supernatant when glucoamylase unaccompanied

was appended into the saccharified and feedstock suspension (67 g l^{-1}), it indicates that the feedstock contained around 35% starch.

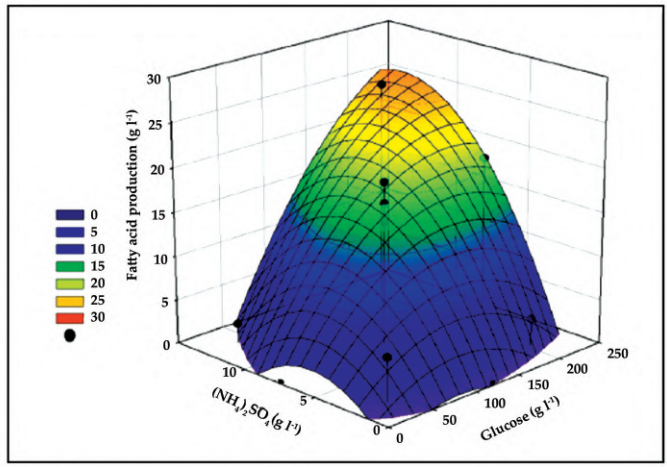

Figure. 16. The response surface curve showing the varying concentrations of $(NH_4)_2SO_4$ and glucose on fatty acid synthesis by R. opacus PD630

[Source: https://www.omicsonline.org/bacterial-carbon-storage-to-value-added-products-1948–5948. S3–002.php? aid=2836]

The impacts of application of the saccharified solution of corn silage on the progress of *R. opacus* PD630 were observed in flasks. Subjected to the required conditions, after 72 hours of incubation, the saccharified solution was synched with 7.2 pH with 1 M NaOH and either concentrated by freeze-drying or diluted with deionized water as shown in Figure 6. While examining the growth of the cell in the saccharified solution, application of a 100% stock intended for feeding leads to inhibition of growth. Therefore, researchers made use of 3:1 saccharified solution/water (designated "75%") or diluted stocks of 1:1 saccharified solution/water (designated "50%"). As depicted in Figure 7, the growth of PD630 started taking place in a particular medium which composed of 1 g l^{-1} $(NH_4)_2SO_4$ and 18 g l^{-1} glucose and in media which contained 75% (30 g l^{-1} of fermentable sugars) and 50% (20 g l^{-1} of fermentable sugars) levels of the saccharified solution after cultivation of 24 hours, whereas after cultivation of 72 hours, it started growing in undiluted solution (40 g l^{-1} of fermentable sugars). On the other hand, utilization of a concentrated solution (50 g l^{-1} of fermentable sugars) showed inhibition of growth on *R. opacus* PD630 (data not shown). These results proposed that

apparently, the hydrolysate of corn silage comprises of particular growth-restraining compounds, as *R. opacus* cells can grow by employing sugars as a source of carbon. Furthermore, a distinct difference was observed in the percentage of fatty acids present per CDW between the saccharified solution fermentation and the defined medium. The content of fatty acid in the fermentation of defined medium, which contained 1 g l^{-1} $(NH_4)_2SO_4$ and 18 g l^{-1} glucose, was higher than 50% of the CDW at the fixed phase of growth after cultivation of 96 hours. While in the fermentation of the 50% saccharified solution which consisted of 3.7 g l^{-1} other sugars and 16.1 g l^{-1} glucose, the content of fatty acid found was 34.3 (±4.0)% of CDW at the cultivation of 96 hours and reduced gradually after accomplishing the maximum accumulation of fatty acid. Hence, this result suggested that the C/N ratio of the solution got unbalanced using the saccharified solution, with an addition of nitrogen source above carbon source.

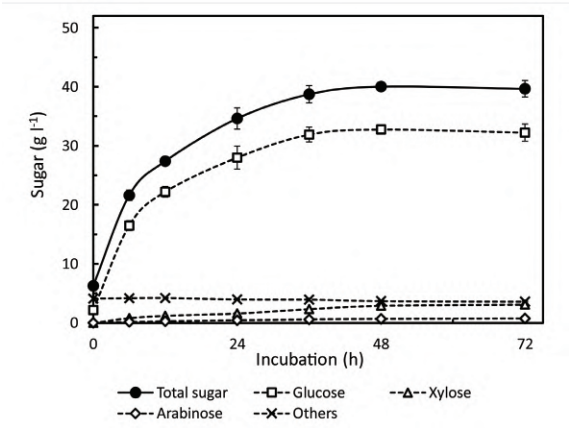

Figure 17. Saccharification of corn silage with industrial enzymes; the adjustment of homogenized feedstock (i.e., 67 g l^{-1} of dried material stuff) was carried out adjusted to the pH value of 5.0. The addition of Novozymes (0.5 ml Celluclast sand 2 ml Viscozyme L) into the suspension of 100 ml was carried out followed by the hydrolysis at 200 rpm at 45°C. The error bars show the standard deviations of the three (3) independent replicates.

[Source: https://www.omicsonline.org/bacterial-carbon-storage-to-value-added-products-1948–5948. S3–002.php? aid=2836]

Another important observation on lipid production was made by adding glucose by *R. opacus* PD630 cultivated on the saccharified solution in flasks. PD630 was cultivated on the 75% saccharified solution which was

appended with 10, 20, or 30 g l^{-1} of glucose, or without any of it, and the time duration of production of fatty acid was investigated in flask cultures. As is shown in Figure 8, fermentations that allow modifications such as adding extra glucose into the 75% solution comprising of 30 g l^{-1} of sugars caused a substantial increase in the production of fatty acid and the content of fatty acid of the CDW in comparison with the solution which lacked extra glucose. After cultivation of 120 hours, the production of fatty acid and the CDW of PD630 developed in the solution not containing any excess glucose were 4.4 (±0.7) and 14.2 (±1.3) g l^{-1}, which shows the fatty acid presence of 31.0 (±2.0)% CDW, respectively. On the other hand, the fatty acid production of 8.9 (±0.3) g l^{-1} and the CDW of 16.9 (±1.1) g l^{-1} correspond to the fatty acid presence of 52.7 (±2.1)% CDW, respectively. The content of fatty acid was observed to be maximum when around 20 g l^{-1} of glucose was supplemented into the solution. The amount of fatty acid in the solution appended with 20 g l^{-1} of glucose was equivalent to that of [55.0 (±3.0)% CDW] in a particularly defined medium comprising of 1 g l^{-1} $(NH_4)_2SO_4$ (Fig. 18) and 18 g l^{-1} glucose.

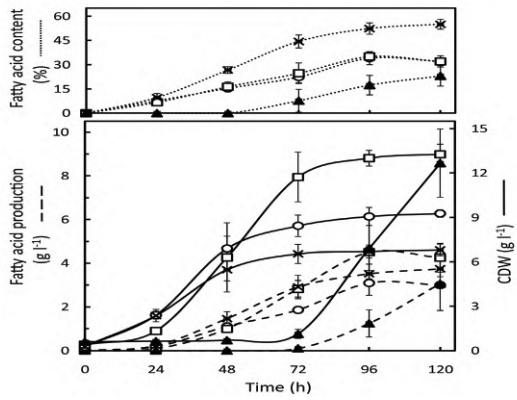

Fig. 18. Production and growth of lipids from R. opacus PD630 with different saccharified corn silage in flasks. The inoculation of the strain in the saccharified solution was around 100 (▲), 75 (□), and 50% (○). The solutions along with a defined media (x) comprising of 1 g l^{-1} $(NH_4)_2SO_4$ and 18 g l^{-1} glucose at an initial OD 660 of about 0.3. A diluted saccharified stock, having a dilution ratio of 3:1 with the addition of water, is categorized as 75%, while a diluted saccharified stock, having a dilution ratio of 1:1 with the addition of water, is categorized as 50%. The error bars show the standard deviations of the three (3) independent replicates.

[Source: https://www.omicsonline.org/bacterial-carbon-storage-to-value-added-products-1948–5948. S3–002.php? aid=2836]

Figure 19 demonstrates the morphology of lipid body of *R. opacus* PD630 cultivated in a 75% saccharified silage solution which was appended with approximately 20 g l^{-1} of glucose for a time duration of 120 hours in flask cultures.

R. opacus PD630 cultivated in the saccharified solution contains numerous small lipid bodies which more or less fill the entire cytoplasm of the cells. This behavior is quite similar to what has been observed in cells grown in a defined medium.

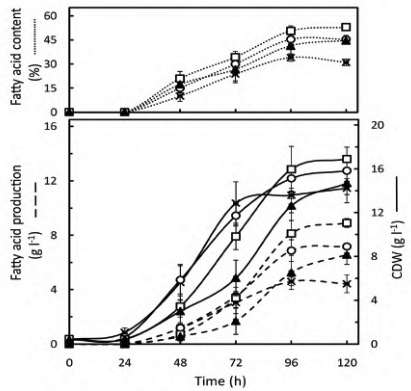

Figure 19. Effect of glucose addition on the production of lipid by R. opacus PD630 developed from the saccharified corn silage in flasks. The inoculation of the strain in the saccharified solution was around 75% solution appended with 30 (▲), 20 (□), or 10 g l^{-1} glucose at an initial OD 660 of about 0.3 without a medium (x). The error bars show the standard deviations of the three (3) independent replicates

[Source: https://www.omicsonline.org/bacterial-carbon-storage-to-value-added-products-1948–5948. S3–002.php? aid=2836]

These results showed that saccharified solution from corn silage comprises adequate nutrients for the production of TAGs by *R. opacus* PD630, even though the (C/N) ratio in the composition of the solution has been optimized for high production of lipids.

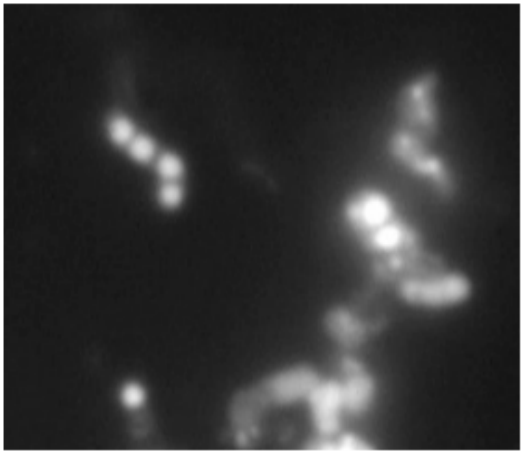

Figure. 20. Fluorescent image of stained cells of R. opacus PD630 tainted with the lipophilic fluorophore, that is, Nile Red. Cells were produced in a nominal medium inclosing a solution of saccharified corn silage for 120 hours in a flask culture**.**

[Source: https://www.omicsonline.org/bacterial-carbon-storage-to-value-added-products-1948–5948. S3–002.php? aid=2836]

2.4 OUTLOOKS OF BACTERIAL TAG FOR BIOFUELS

Several countries are now focusing on the development of sustainable and clean energy sources (Du, Li, Sun, Chen, & Liu, 2008). Among different achievable sources of renewable energy, ones that are of greatest interest include advanced liquid (lipid-based) fuels, for example, biojet fuel, and biodiesel. These cutting-edge fuels are expected to play a significant role in the future for the global energy infrastructure. TAGs are being used as pioneers for producing lipid-based biofuels, and presently, the major sources for TAG include animal fats, vegetable oils, and waste cooking oils. However, the biofuels that are manufactured from crop seeds have been under inspection due to fuel vs. food competition problem. Microalgae can produce a significant amount of TAG, and so recently, it has been started to consider it as an attractive alternative feedstock for lipid-based fuels. Studies have been carried out to produce TAG by microalgae by employing the best available cultivation procedures and strains; however, it has led

to lower production of TAG than the theoretical maximum (Radakovits, Jinkerson, Darzins, & Posewitz, 2010; Chen, Yeh, Aisyah, Lee, & Chang, 2011; Singh, Nigam, & Murphy, 2011). In spite of the positive effects which can be gained by the commercialization of TAG-based biofuels, the inadequate supply of bioresources for obtaining a TAG for the production of lipid-based biofuels represents major bottleneck at present. One alternative way for the production of TAGs is to use heterotrophic organisms which are known for producing TAGs from lignocellulose-derived sugars. Hence, now bacteria are thought as one of the more promising potential sources of TAG for the production of lipid-based biofuels. This is because they contain various favorable qualities such as ease of cultivability, fast rate of growth, and having the characteristic of being a renewable source of biomass (Li, Du, & Liu, 2008; Rude & Schirmer, 2009). While few bacteria are known to accumulate TAG, one of particular significance is *R. opacus* PD630. The intracellular lipid amount in these bacteria can reach to greater than 70% of the entire cellular dry weight in cells which are cultivated on olive oil or gluconate as the only sources of carbon under limited growth conditions. Since mid-1990s, research has been continuing on this particular strain (Alvarez, Alvarez, Kalscheuer, Wältermann, & Steinbüchel, 2008). Lately, experiments have shown that *R. opacus* PD630 has a suitable possibility for industrial fermentations. Research has been continued on a global level to accumulate TAGs in bacteria (Elbahloul & Steinbüchel, 2010; Haenisch, Wältermann, Robenek, & Steinbuechel, 2006). Even though apparently it seems feasible to modify the performance of bacteria for improving its TAG accumulation of lignocellulosic biomass and resultantly establishing an economical consolidated bioprocess; but various complications have negatively impacted the attainment of lower costs of production on a large scale (Hänisch, Wältermann, Robenek, & Steinbüchel, 2006).

Lignocellulose is a widely occurring but underutilized renewable feedstock. However, it is a compound containing rigid cellulose fibers which are implanted in a cross-linked matrix of hemicellulose and lignin that help in binding the fibers. To convert lignocellulosic biomass into TAGs, the hemicelluloses and celluloses are required to be fragmented into their corresponding monosaccharides so that bacteria may use them for lipid production and growth (Lennen & Pfleger, 2013; Galbe & Zacchi, 2007; Kumar, Barrett, Delwiche, & Stroeve, 2009). One of the main challenges that need to be overcome is to deal with the presence of cell growth inhibitors which are generated in the course of the treatment of lignocellulosic biomass

(Margeot, Hahn-Hagerdal, Edlund, Slade, & Monot, 2009; Parawira & Tekere, 2011). The existence of lignin in lignocellulosic hydrolysates causes the growth inhibition of *R. opacus*. Research has indicated that *R. opacus* PD630 can break down some compounds derived from lignin, while Figure 7 demonstrates that specific components containing a comparatively high amount, possibly lignin, existing in the lignocellulosic hydrolysate hinder the growth of cell (Plaggenborg et al., 2006). Higher initial concentrations of sugar in the medium are a result of maximizing the efficiency of the fermentation and the volumetric productivity which leads to a lower cost of the process. Presently, it is not easy to prepare greater than 200 g/l of a lignocellulose-derived sugar solution without the excess of growth inhibitors in an economical manner (Roche, Dibble, & Stickel, 2009). To improve the problem of inhibition, we can employ genetic engineering to afford augmented lignin tolerance to *R. opacus* PD630. A mixture of inhibitor-tolerant strains along with the preferred properties for the purification of lignocellulose hydrolysates will probably help in the improvement of lignocellulose-to-TAG production procedure.

As of now, bacterial TAG production is not economically feasible at industrial scale owing to its high costs of production as well as low productivity of the bioprocesses. To overcome these hindrances, we need to engineer highly productive strains and further optimize them for high oil production on lignocellulose-derived sugars. In a nutshell, our research shows that an engineered *R. opacus* strain can provide a significant contribution to the achievement of our ultimate goal of producing cost-effective and scalable advanced liquid biofuels.

REFERENCES

1. Ali, Y., & Hanna, M. A. (1994). Alternative diesel fuels from vegetable oils. *Bioresource Technology, 50*(2), 153-163.
2. Alvarez, A. F., Alvarez, H. M., Kalscheuer, R., Wältermann, M., & Steinbüchel, A. (2008). Cloning and characterization of a gene involved in triacylglycerol biosynthesis and identification of additional homologous genes in the oleaginous bacterium *Rhodococcus opacus* PD630. *Microbiology, 154*(8), 2327-2335.
3. Alvarez, H. M., Mayer, F., Fabritius, D., & Steinbüchel, A. (1996). Formation of intracytoplasmic lipid inclusions by *Rhodococcus opacus* strain PD630. *Archives of Microbiology, 165*(6), 377-386.
4. Alvarez, H., & Steinbüchel, A. (2002). Triacylglycerols in prokaryotic microorganisms. *Applied Microbiology and Biotechnology, 60*(4), 367-376.
5. Anderson, A. J., & Dawes, E. A. (1990). Occurrence, metabolism, metabolic role, and industrial uses of bacterial polyhydroxyalkanoates. *Microbiological Reviews, 54*(4), 450-472.
6. Anderson, A. J., Haywood, G. W., & Dawes, E. A. (1990). Biosynthesis and composition of bacterial poly (hydroxyalkanoates). *International Journal of Biological Macromolecules, 12*(2), 102-105.
7. Azócar, L., Heipieper, H. J., & Navia, R. (2010). Biotechnological processes for biodiesel production using alternative oils. *Applied Microbiology and Biotechnology, 88*(3), 621-636.
8. Bernd, H. A. (2003). Polyester synthases: Natural catalysts for plastics. *Biochemical Journal, 376*(1), 15-33.
9. Beun, J. J., Paletta, F., Van Loosdrecht, M. C., & Heijnen, J. J. (2000). Stoichiometry and kinetics of poly-b-hydroxybutyrate metabolism in aerobic, slow growing, activated sludge cultures. *Biotechnology and Bioengineering, 67*(4), 379-389.
10. Beun, J. J., Verhoef, E. V., Loosdrecht, M. V., & Heijnen, J. J. (2000). Stoichiometry and kinetics of poly-b-hydroxybutyrate metabolism under denitrifying conditions in activated sludge cultures. *Biotechnology and Bioengineering, 68*(5), 496-507.
11. Braunegg, G., Genser, K., Bona, R., Haage, G., Schellauf, F., & Winkler, E. (1999, October). Production of PHAs from agricultural waste material. In *Macromolecular Symposia* (Vol. 144, No. 1, pp. 375-383). WILEY-VCH Verlag GmbH & Co. KGaA.

12. Brigham, C. J., Budde, C. F., Holder, J. W., Zeng, Q., Mahan, A. E., Rha, C., & Sinskey, A. J. (2010). Elucidation of β-oxidation pathways in *Ralstonia eutropha* H16 by examination of global gene expression. *Journal of Bacteriology, 192*(20), 5454-5464.
13. Brigham, C. J., Kurosawa, K., Rha, C., & Sinskey, A. J. (2011). Bacterial carbon storage to value added products.
14. Budde, C. F., Riedel, S. L., Hübner, F., Risch, S., Popović, M. K., Rha, C., & Sinskey, A. J. (2011). Growth and polyhydroxybutyrate production by *Ralstonia eutropha* in emulsified plant oil medium. *Applied Microbiology and Biotechnology, 89*(5), 1611-1619.
15. Budde, C. F., Riedel, S. L., Willis, L. B., Rha, C., & Sinskey, A. J. (2011). Production of poly (3-hydroxybutyrate-co-3-hydroxyhexanoate) from plant oil by engineered *Ralstonia eutropha* strains. *Applied and Environmental Microbiology, 77*(9), 2847-2854.
16. Canakci, M., & Sanli, H. (2008). Biodiesel production from various feedstocks and their effects on the fuel properties. *Journal of Industrial Microbiology & Biotechnology, 35*(5), 431-441.
17. Canakci, M., & Van Gerpen, J. (2001). Biodiesel production from oils and fats with high free fatty acids. *Transactions of the ASAE, 44*(6), 1429.
18. Cavalheiro, J. M., de Almeida, M. C. M., Grandfils, C., & Da Fonseca, M. M. R. (2009). Poly (3-hydroxybutyrate) production by *Cupriavidus necator* using waste glycerol. *Process Biochemistry, 44*(5), 509-515.
19. Chen, C. Y., Yeh, K. L., Aisyah, R., Lee, D. J., & Chang, J. S. (2011). Cultivation, photobioreactor design and harvesting of microalgae for biodiesel production: a critical review. *Bioresource Technology*, *102*(1), 71-81.
20. Chen, G. Q. (2009). A microbial polyhydroxyalkanoates (PHA) based bio-and materials industry. *Chemical Society Reviews, 38*(8), 2434-2446.
21. Choi, J. I., & Lee, S. Y. (1999). Efficient and economical recovery of poly (3-hydroxybutyrate) from recombinant *Escherichia coli* by simple digestion with chemicals. *Biotechnology and Bioengineering, 62*(5), 546-553.
22. Choi, J. I., & Lee, S. Y. (1999). High-level production of poly (3-hydroxybutyrate-co-3-hydroxyvalerate) by fed-batch culture of recombinant *Escherichia coli*. *Applied and Environmental Microbiology*, *65*(10), 4363-4368.

23. Choi, J. I., Lee, S. Y., & Han, K. (1998). Cloning of the *Alcaligenes latus* polyhydroxyalkanoate biosynthesis genes and use of these genes for enhanced production of poly (3-hydroxybutyrate) in *Escherichia coli*. *Applied and Environmental Microbiology, 64*(12), 4897-4903.

24. Choi, J. I., Lee, S. Y., & Han, K. (1999). Cloning of the *Alcaligenes latus* polyhydroxyalkanoate biosynthesis genes and use of these genes for enhanced production of poly (3-hydroxybutyrate) in *Escherichia coli*. *Applied and Environmental Microbiology, 65*(3), 1361.

25. Clark, J. H., Luque, R., & Matharu, A. S. (2012). Green chemistry, biofuels, and biorefinery. *Annual Review of Chemical and Biomolecular Engineering, 3,* 183-207.

26. Dias, J. M., Lemos, P. C., Serafim, L. S., Oliveira, C., Eiroa, M., Albuquerque, M. G., & Reis, M. A. (2006). Recent advances in polyhydroxyalkanoate production by mixed aerobic cultures: From the substrate to the final product. *Macromolecular Bioscience, 6*(11), 885-906.

27. Diniz, S. C., Taciro, M. K., Gomez, J. G. C., & da Cruz Pradella, J. G. (2004). High-cell-density cultivation of *Pseudomonas putida* IPT 046 and medium-chains-length polyhydroxyalkanoate production from sugarcane carbohydrates. *Applied Biochemistry and Biotechnology, 119*(1), 51-69.

28. Dionisi, D., Carucci, G., Papini, M. P., Riccardi, C., Majone, M., & Carrasco, F. (2005). Olive oil mill effluents as a feedstock for production of biodegradable polymers. *Water Research, 39*(10), 2076-2084.

29. Doi, Y., Kitamura, S., & Abe, H. (1995). Microbial synthesis and characterization of poly (3-hydroxybutyrate-co-3-hydroxyhexanoate). *Macromolecules, 28*(14), 4822-4828.

30. Dong, Z., & Sun, X. (2000). A new method of recovering polyhydroxyalkanoate from *Azotobacter chroococcum*. *Chinese Science Bulletin, 45*(3), 252-256.

31. Du, G., Chen, J., Yu, J., & Lun, S. (2001). Continuous production of poly-3-hydroxybutyrate by *Ralstonia eutropha* in a two-stage culture system. *Journal of Biotechnology, 88*(1), 59-65.

32. Du, W., Li, W., Sun, T., Chen, X., & Liu, D. (2008). Perspectives for biotechnological production of biodiesel and impacts. *Applied Microbiology and Biotechnology, 79*(3), 331-337.

33. Durrett, T. P., Benning, C., & Ohlrogge, J. (2008). Plant triacylglycerols as feedstocks for the production of biofuels. *The Plant Journal, 54*(4),

593-607.

34. Elbahloul, Y., & Steinbüchel, A. (2010). Pilot-scale production of fatty acid ethyl esters by an engineered *Escherichia coli* strain harboring the p (Microdiesel) plasmid. *Applied and Environmental Microbiology*, *76*(13), 4560-4565.
35. Fjerbaek, L., Christensen, K. V., & Norddahl, B. (2009). A review of the current state of biodiesel production using enzymatic transesterification. *Biotechnology and Bioengineering*, *102*(5), 1298-1315.
36. Galbe, M., & Zacchi, G. (2007). Pretreatment of lignocellulosic materials for efficient bioethanol production. In *Biofuels* (pp. 41-65). Heidelberg, Berlin: Springer.
37. Gerngross, T. U., Reilly, P., Stubbe, J., Sinskey, A. J., & Peoples, O. P. (1993). Immunocytochemical analysis of poly-beta-hydroxybutyrate (PHB) synthase in *Alcaligenes eutrophus* H16: Localization of the synthase enzyme at the surface of PHB granules. *Journal of Bacteriology*, *175*(16), 5289-5293.
38. Gouda, M. K., Omar, S. H., & Aouad, L. M. (2008). Single cell oil production by *Gordonia* sp. DG using agro-industrial wastes. *World Journal of Microbiology and Biotechnology*, *24*(9), 1703.
39. Haenisch, J., Wältermann, M., Robenek, H., & Steinbuechel, A. (2006). The *Ralstonia eutropha* H16 phasin PhaP1 is targeted to intracellular triacylglycerol inclusions in *Rhodococcus opacus* PD630 and *Mycobacterium smegmatis* mc2155, and provides an anchor to target other proteins. *Microbiology*, *152*(11), 3271-3280.
40. Hänisch, J., Wältermann, M., Robenek, H., & Steinbüchel, A. (2006). Eukaryotic lipid body proteins in oleogenous actinomycetes and their targeting to intracellular triacylglycerol inclusions: Impact on models of lipid body biogenesis. *Applied and Environmental Microbiology*, *72*(10), 6743-6750.
41. Hassan, M. A., Nawata, O., Shirai, Y., Rahman, N. A. A., Yee, P. L., Ariff, A. B., & Karim, M. I. A. (2002). A proposal for zero emission from palm oil industry incorporating the production of polyhydroxyalkanoates from palm oil mill effluent. *Journal of Chemical Engineering of Japan*, *35*(1), 9-14.
42. Hill, J., Nelson, E., Tilman, D., Polasky, S., & Tiffany, D. (2006). Environmental, economic, and energetic costs and benefits of biodiesel and ethanol biofuels. *Proceedings of the National Academy of Sciences*, *103*(30), 11206-11210.

43. Hisano, T., Tsuge, T., Fukui, T., Iwata, T., Miki, K., & Doi, Y. (2003). Crystal structure of the (R)-specific enoyl-CoA hydratase from *Aeromonas caviae* involved in polyhydroxyalkanoate biosynthesis. *Journal of Biological Chemistry, 278*(1), 617-624.

44. Holmes, P. A. (1985). Applications of PHB-a microbially produced biodegradable thermoplastic. *Physics in Technology, 16*(1), 32.

45. Ishizaki, A., Tanaka, K., & Taga, N. (2001). Microbial production of poly-D-3-hydroxybutyrate from CO 2. *Applied Microbiology and Biotechnology, 57*(1), 6-12.

46. Jarboe, L. R., Grabar, T. B., Yomano, L. P., Shanmugan, K. T., & Ingram, L. O. (2007). Development of ethanologenic bacteria. In *Biofuels* (pp. 237-261). Heidelberg, Berlin: Springer.

47. Jendrossek, D. (2009). Polyhydroxyalkanoate granules are complex subcellular organelles (carbonosomes). *Journal of Bacteriology, 191*(10), 3195-3202.

48. Kadouri, D., Jurkevitch, E., Okon, Y., & Castro-Sowinski, S. (2005). Ecological and agricultural significance of bacterial polyhydroxyalkanoates. *Critical Reviews in Microbiology, 31*(2), 55-67.

49. Kahar, P., Tsuge, T., Taguchi, K., & Doi, Y. (2004). High yield production of polyhydroxyalkanoates from soybean oil by *Ralstonia eutropha* and its recombinant strain. *Polymer Degradation and Stability, 83*(1), 79-86.

50. Kalscheuer, R., Stöveken, T., Malkus, U., Reichelt, R., Golyshin, P. N., Sabirova, J. S., & Steinbüchel, A. (2007). Analysis of storage lipid accumulation in *Alcanivorax borkumensis*: Evidence for alternative triacylglycerol biosynthesis routes in bacteria. *Journal of Bacteriology, 189*(3), 918-928.

51. Kim, B. S., Lee, S. C., Lee, S. Y., Chang, H. N., Chang, Y. K., & Woo, S. I. (1994). Production of poly (3-hydroxybutyric acid) by fed-batch culture of *Alcaligenes eutrophus* with glucose concentration control. *Biotechnology and Bioengineering, 43*(9), 892-898.

52. Kim, M., Cho, K. S., Ryu, H. W., Lee, E. G., & Chang, Y. K. (2003). Recovery of poly (3-hydroxybutyrate) from high cell density culture of *Ralstonia eutropha* by direct addition of sodium dodecyl sulfate. *Biotechnology Letters, 25*(1), 55-59.

53. Knothe, G. (2010). Biodiesel and renewable diesel: A comparison. *Progress in Energy and Combustion Science, 36*(3), 364-373.

54. Koller, M., Bona, R., Braunegg, G., Hermann, C., Horvat, P., Kroutil, M., & Varila, P. (2005). Production of polyhydroxyalkanoates from

agricultural waste and surplus materials. *Biomacromolecules, 6*(2), 561-565.

55. Kosa, M., & Ragauskas, A. J. (2011). Lipids from heterotrophic microbes: Advances in metabolism research. *Trends in Biotechnology, 29*(2), 53-61.
56. Kumar, P., Barrett, D. M., Delwiche, M. J., & Stroeve, P. (2009). Methods for pretreatment of lignocellulosic biomass for efficient hydrolysis and biofuel production. *Industrial & Engineering Chemistry Research, 48*(8), 3713-3729.
57. Kurdikar, D. L., Strauser, F. E., Solodar, A. J., Paster, M. D., & Asrar, J. (2000). *U. S. patent no. 6,043,063*. Washington, DC: U. S. Patent and Trademark Office.
58. Kurosawa, K., Boccazzi, P., de Almeida, N. M., & Sinskey, A. J. (2010). High-cell-density batch fermentation of *Rhodococcus opacus* PD630 using a high glucose concentration for triacylglycerol production. *Journal of Biotechnology, 147*(3), 212-218.
59. Lee, S. H., Oh, D. H., Ahn, W. S., Lee, Y., Choi, J. I., & Lee, S. Y. (2000). Production of poly (3-hydroxybutyrate-co-3-hydroxyhexanoate) by high-cell-density cultivation of *Aeromonas hydrophila*. *Biotechnology and Bioengineering, 67*(2), 240-244.
60. Lee, S. Y., Wong, H. H., Choi, J. I., Lee, S. H., Lee, S. C., & Han, C. S. (2000). Production of medium-chain-length polyhydroxyalkanoates by high-cell-density cultivation of *Pseudomonas putida* under phosphorus limitation. *Biotechnology and Bioengineering, 68*(4), 466-470.
61. Lennen, R. M., & Pfleger, B. F. (2013). Microbial production of fatty acid-derived fuels and chemicals. *Current Opinion in Biotechnology, 24*(6), 1044-1053.
62. Lestari, S., Mäki-Arvela, P., Beltramini, J., Lu, G. Q., & Murzin, D. Y. (2009). Transforming triglycerides and fatty acids into biofuels. *ChemSusChem, 2*(12), 1109-1119.
63. Li, P., Chakraborty, S., & Stubbe, J. (2009). Detection of covalent and noncovalent intermediates in the polymerization reaction catalyzed by a C149S class III polyhydroxybutyrate synthase. *Biochemistry, 48*(39), 9202-9211.
64. Li, Q., Du, W., & Liu, D. (2008). Perspectives of microbial oils for biodiesel production. *Applied Microbiology and Biotechnology, 80*(5), 749-756.
65. Lim, J., Wang, Z. Y., Zhang, Q. Y., Teo, E. Y., Teoh, S. H., & Wen, F. (2011,

August). Blending of poly (3-hydroxybutyrate-co-3-hydroxyhexanoate) and polycaprolactone: Characterization and degradation studies. In *Defense Science Research Conference and Expo (DSR), 2011* (pp. 1-4). IEEE.

66. Ma, F., & Hanna, M. A. (1999). Biodiesel production: A review. *Bioresource Technology*, *70*(1), 1-15.
67. MacEachran, D. P., Prophete, M. E., & Sinskey, A. J. (2010). The *Rhodococcus opacus* PD630 heparin-binding hemagglutinin homolog TadA mediates lipid body formation. *Applied and Environmental Microbiology*, *76*(21), 7217-7225.
68. Madden, L. A., Anderson, A. J., & Asrar, J. (1998). Synthesis and characterization of poly (3-hydroxybutyrate) and poly (3-hydroxybutyrate-co-3-hydroxyvalerate) polymer mixtures produced in high-density fed-batch cultures of *Ralstonia eutropha* (*Alcaligenes eutrophus*). *Macromolecules*, *31*(17), 5660-5667.
69. Madison, L. L., & Huisman, G. W. (1999). Metabolic engineering of poly (3-hydroxyalkanoates): From DNA to plastic. *Microbiology and Molecular Biology Reviews*, *63*(1), 21-53.
70. Maehara, A., Taguchi, S., Nishiyama, T., Yamane, T., & Doi, Y. (2002). A repressor protein, PhaR, regulates polyhydroxyalkanoate (PHA) synthesis via its direct interaction with PHA. *Journal of Bacteriology*, *184*(14), 3992-4002.
71. Majone, M., Massanisso, P., Carucci, A., Lindrea, K., & Tandoi, V. (1996). Influence of storage on kinetic selection to control aerobic filamentous bulking. *Water Science and Technology*, *34*(5-6), 223-232.
72. Manilla-Pérez, E., Lange, A. B., Luftmann, H., Robenek, H., & Steinbüchel, A. (2011). Neutral lipid production in *Alcanivorax borkumensis* SK2 and other marine hydrocarbonoclastic bacteria. *European Journal of Lipid Science and Technology*, *113*(1), 8-17.
73. Manzanera, M., Molina-Muñoz, M. L., & González-López, J. (2008). Biodiesel: An alternative fuel. *Recent Patents on Biotechnology*, *2*(1), 25-34.
74. Marchetti, J. M., Miguel, V. U., & Errazu, A. F. (2007). Possible methods for biodiesel production. *Renewable and Sustainable Energy Reviews*, *11*(6), 1300-1311.
75. Margeot, A., Hahn-Hagerdal, B., Edlund, M., Slade, R., & Monot, F. (2009). New improvements for lignocellulosic ethanol. *Current Opinion in Biotechnology*, *20*(3), 372-380.

76. Martínez, V., García, P., García, J. L., & Prieto, M. A. (2011). Controlled autolysis facilitates the polyhydroxyalkanoate recovery in *Pseudomonas putida* KT2440. *Microbial Biotechnology, 4*(4), 533-547.

77. Meng, X., Yang, J., Xu, X., Zhang, L., Nie, Q., & Xian, M. (2009). Biodiesel production from oleaginous microorganisms. *Renewable Energy*, *34*(1), 1-5.

78. Murphy, D. J. (2001). The biogenesis and functions of lipid bodies in animals, plants and microorganisms. *Progress in Lipid Research*, *40*(5), 325-438.

79. Ng, K. S., Ooi, W. Y., Goh, L. K., Shenbagarathai, R., & Sudesh, K. (2010). Evaluation of jatropha oil to produce poly (3-hydroxybutyrate) by *Cupriavidus necator* H16. *Polymer Degradation and Stability*, *95*(8), 1365-1369.

80. Olukoshi, E. R., & Packter, N. M. (1994). Importance of stored triacylglycerols in *Streptomyces*: Possible carbon source for antibiotics. *Microbiology, 140*(4), 931-943.

81. Page, W. J., Manchak, J. A. N. E. T., & Rudy, B. R. E. N. T. (1992). Formation of poly (hydroxybutyrate-co-hydroxyvalerate) by *Azotobacter vinelandii* UWD. *Applied and Environmental Microbiology*, *58*(9), 2866-2873.

82. Parawira, W., & Tekere, M. (2011). Biotechnological strategies to overcome inhibitors in lignocellulose hydrolysates for ethanol production. *Critical Reviews in Biotechnology, 31*(1), 20-31.

83. Park, S. J., Ahn, W. S., Green, P. R., & Lee, S. Y. (2001). Production of poly (3-hydroxybutyrate-co-3-hydroxyhexanoate) by metabolically engineered *Escherichia coli* strains. *Biomacromolecules, 2*(1), 248-254.

84. Peoples, O. P., & Sinskey, A. J. (1989). Poly-beta-hydroxybutyrate (PHB) biosynthesis in *Alcaligenes eutrophus* H16. Identification and characterization of the PHB polymerase gene (PHBC). *Journal of Biological Chemistry*, *264*(26), 15298-15303.

85. Peoples, O. P., & Sinskey, A. J. (1989). Poly-beta-hydroxybutyrate biosynthesis in *Alcaligenes eutrophus* H16. Characterization of the genes encoding beta-ketothiolase and acetoacetyl-CoA reductase. *Journal of Biological Chemistry, 264*(26), 15293-15297.

86. Pfeiffer, D., & Jendrossek, D. (2011). Interaction between poly (3-hydroxybutyrate) granule-associated proteins as revealed by two-hybrid analysis and identification of a new phasin in *Ralstonia eutropha* H16. *Microbiology*, *157*(10), 2795-2807.

87. Pfeiffer, D., Wahl, A., & Jendrossek, D. (2011). Identification of a multifunctional protein, PhaM, that determines number, surface to volume ratio, subcellular localization and distribution to daughter cells of poly (3-hydroxybutyrate), PHB, granules in *Ralstonia eutropha* H16. *Molecular Microbiology, 82*(4), 936-951.

88. Philip, S., Keshavarz, T., & Roy, I. (2007). Polyhydroxyalkanoates: Biodegradable polymers with a range of applications. *Journal of Chemical Technology and Biotechnology, 82*(3), 233-247.

89. Plaggenborg, R., Overhage, J., Loos, A., Archer, J. A., Lessard, P., Sinskey, A. J., & Priefert, H. (2006). Potential of *Rhodococcus* strains for biotechnological vanillin production from ferulic acid and eugenol. *Applied Microbiology and Biotechnology, 72*(4), 745.

90. Pötter, M., Madkour, M. H., Mayer, F., & Steinbüchel, A. (2002). Regulation of phasin expression and polyhydroxyalkanoate (PHA) granule formation in *Ralstonia eutropha* H16. *Microbiology, 148*(8), 2413-2426.

91. Preiss, J., & Romeo, T. (1990). Physiology, biochemistry and genetics of bacterial glycogen synthesis. *Advances in Microbial Physiology, 30*, 183-238.

92. Radakovits, R., Jinkerson, R. E., Darzins, A., & Posewitz, M. C. (2010). Genetic engineering of algae for enhanced biofuel production. *Eukaryotic cell, 9*(4), 486-501.

93. Ramsay, J. A., Berger, E., Voyer, R., Chavarie, C., & Ramsay, B. A. (1994). Extraction of poly-3-hydroxybutyrate using chlorinated solvents. *Biotechnology Techniques, 8*(8), 589-594.

94. Riedel, S. L., Bader, J., Brigham, C. J., Budde, C. F., Yusof, Z. A. M., Rha, C., & Sinskey, A. J. (2012). Production of poly (3-hydroxybutyrate-co-3-hydroxyhexanoate) by *Ralstonia eutropha* in high cell density palm oil fermentations. *Biotechnology and Bioengineering, 109*(1), 74-83.

95. Riesenberg, D., & Guthke, R. (1999). High-cell-density cultivation of microorganisms. *Applied Microbiology and Biotechnology, 51*(4), 422-430.

96. Roche, C. M., Dibble, C. J., & Stickel, J. J. (2009). Laboratory-scale method for enzymatic saccharification of lignocellulosic biomass at high-solids loadings. *Biotechnology for Biofuels, 2*(1), 28.

97. Rude, M. A., & Schirmer, A. (2009). New microbial fuels: A biotech perspective. *Current Opinion in Microbiology, 12*(3), 274-281.

98. Ryan, T. W., Dodge, L. G., & Callahan, T. J. (1984). The effects of

vegetable oil properties on injection and combustion in two different diesel engines. *Journal of the American Oil Chemists Society*, *61*(10), 1610-1619.

99. Ryu, H. W., Hahn, S. K., Chang, Y. K., & Chang, H. N. (1997). Production of poly (3-hydroxybutyrate) by high cell density fed-batch culture of *Alcaligenes eutrophus* with phosphate limitation. *Biotechnology and Bioengineering*, *55*(1), 28-32.
100. Saito, Y., & Doi, Y. (1994). Microbial synthesis and properties of poly (3-hydroxybutyrate-co-4-hydroxybutyrate) in *Comamonas acidovorans*. *International Journal of Biological Macromolecules*, *16*(2), 99-104.
101. Salehizadeh, H., & Van Loosdrecht, M. C. M. (2004). Production of polyhydroxyalkanoates by mixed culture: Recent trends and biotechnological importance. *Biotechnology Advances*, *22*(3), 261-279.
102. Santala, S., Efimova, E., Kivinen, V., Larjo, A., Aho, T., Karp, M., & Santala, V. (2011). Improved triacylglycerol production in *Acinetobacter baylyi* ADP1 by metabolic engineering. *Microbial Cell Factories*, *10*(1), 36.
103. Satoh, H., Mino, T., & Matsuo, T. (1999). PHA production by activated sludge. *International Journal of Biological Macromolecules*, *25*(1), 105-109.
104. Schatz, M. C., Witkowski, J., & McCombie, W. R. (2012). Current challenges in de novo plant genome sequencing and assembly. *Genome Biology*, *13*(4), 243.
105. Serafim, L. S., Lemos, P. C., Albuquerque, M. G., & Reis, M. A. (2008). Strategies for PHA production by mixed cultures and renewable waste materials. *Applied Microbiology and Biotechnology*, *81*(4), 615-628.
106. Shang, L., Jiang, M., & Chang, H. N. (2003). Poly (3-hydroxybutyrate) synthesis in fed-batch culture of *Ralstonia eutropha* with phosphate limitation under different glucose concentrations. *Biotechnology Letters*, *25*(17), 1415-1419.
107. Shang, L., Jiang, M., & Chang, H. N. (2003). Poly (3-hydroxybutyrate) synthesis in fed-batch culture of *Ralstonia eutropha* with phosphate limitation under different glucose concentrations. *Biotechnology Letters*, *25*(17), 1415-1419.
108. Singh, A., Nigam, P. S., & Murphy, J. D. (2011). Mechanism and challenges in commercialisation of algal biofuels. *Bioresource Technology*, *102*(1), 26-34.
109. Stein, K. (2007). Food vs biofuel. *Journal of the American Dietetic*

Association, 107(11), 1870.

110. Steinbüchel, A., & Valentin, H. E. (1995). Diversity of bacterial polyhydroxyalkanoic acids. *FEMS Microbiology Letters, 128*(3), 219-228.
111. Sudesh, K., Abe, H., & Doi, Y. (2000). Synthesis, structure and properties of polyhydroxyalkanoates: Biological polyesters. *Progress in Polymer Science, 25*(10), 1503-1555.
112. Teixeira, M. C., Raposo, L. R., Palma, M., & Sá-Correia, I. (2010). Identification of genes required for maximal tolerance to high-glucose concentrations, as those present in industrial alcoholic fermentation media, through a chemogenomics approach. *OMICS A Journal of Integrative Biology, 14*(2), 201-210.
113. Tian, J., He, A., Lawrence, A. G., Liu, P., Watson, N., Sinskey, A. J., & Stubbe, J. (2005). Analysis of transient polyhydroxybutyrate production in *Wautersia eutropha* H16 by quantitative western analysis and transmission electron microscopy. *Journal of Bacteriology, 187*(11), 3825-3832.
114. Tian, J., Sinskey, A. J., & Stubbe, J. (2005). Kinetic studies of polyhydroxybutyrate granule formation in *Wautersia eutropha* H16 by transmission electron microscopy. *Journal of Bacteriology, 187*(11), 3814-3824.
115. Tollefson, J. (2008). Not your father's biofuels: If biofuels are to help the fight against climate change, they have to be made from more appropriate materials and in better ways. Jeff Tollefson asks what innovation can do to improve the outlook. *Nature, 451* (7181), 880-884.
116. Tsuge, T., Hisano, T., Taguchi, S., & Doi, Y. (2003). Alteration of chain length substrate specificity of *Aeromonas caviae* R-enantiomer-specific enoyl-coenzyme A hydratase through site-directed mutagenesis. *Applied and Environmental Microbiology, 69*(8), 4830-4836.
117. Tsuge, T., Tanaka, K., & Ishizaki, A. (2001). Development of a novel method for feeding a mixture of L-lactic acid and acetic acid in fed-batch culture of *Ralstonia eutropha* for poly-D-3-hydroxybutyrate production. *Journal of Bioscience and Bioengineering, 91*(6), 545-550.
118. Van Hee, P., Elumbaring, A. C., van der Lans, R. G., & Van der Wielen, L. A. (2006). Selective recovery of polyhydroxyalkanoate inclusion bodies from fermentation broth by dissolved-air flotation. *Journal of Colloid and Interface Science, 297*(2), 595-606.
119. Vasudevan, P. T., & Briggs, M. (2008). Biodiesel production—current

state of the art and challenges. *Journal of Industrial Microbiology & Biotechnology, 35*(5), 421.

120. Volova, T. G., & Voinov, N. A. (2003). Kinetic parameters of a culture of the hydrogen-oxidizing bacterium *Ralstonia eutropha* grown under conditions favoring polyhydroxybutyrate biosynthesis. *Applied Biochemistry and Microbiology, 39*(2), 166-170.
121. Volova, T. G., Kalacheva, G. S., & Altukhova, O. V. (2000). Autotrophic synthesis of polyalkanoates by *Alcaligenes eutrophus* in presence of carbon monoxide. *Mikrobiologiia, 70*(6), 745-752.
122. Volova, T., Gitelson, J., Terskov, I., & Sidko, F. (1998). Hydrogen bacteria as a potential regenerative LSS component and producer of ecologically clean degradable plastic. *Life Support & Biosphere Science: International Journal of Earth Space, 6*(3), 209-213.
123. Voss, I., & Steinbüchel, A. (2001). High cell density cultivation of *Rhodococcus opacus* for lipid production at a pilot-plant scale. *Applied Microbiology and Biotechnology, 55*(5), 547-555.
124. Wältermann, M., & Steinbüchel, A. (2005). Neutral lipid bodies in prokaryotes: Recent insights into structure, formation, and relationship to eukaryotic lipid depots. *Journal of Bacteriology, 187*(11), 3607-3619.
125. Wang, F., & Lee, S. Y. (1998). High cell density culture of metabolically engineered *Escherichia coli* for the production of poly (3-hydroxybutyrate) in a defined medium. *Biotechnology and Bioengineering, 58* (2-3), 325-328.
126. Wei, X., & Shen, C. Y. (2010). Transcriptional regulation of oct4 in human bone marrow mesenchymal stem cells. *Stem Cells and Development, 20*(3), 441-449.
127. Wilde, E. (1962). Unterschungen uber wachstum und speicherstoffsythese von 701 Hydrogenomonas. *Arch Mikrobiol, 43*(109), 702.
128. Wong, H. H., & Lee, S. Y. (1998). Poly-(3-hydroxybutyrate) production from whey by high-density cultivation of recombinant *Escherichia coli*. *Applied Microbiology and Biotechnology, 50*(1), 30-33.
129. Yamada, M., Yamashita, K., Wakuda, A., Ichimura, K., Maehara, A., Maeda, M., & Taguchi, S. (2007). Autoregulator protein PhaR for biosynthesis of polyhydroxybutyrate [P (3HB)] possibly has two separate domains that bind to the target DNA and P (3HB): Functional mapping of amino acid residues responsible for DNA binding. *Journal of Bacteriology, 189*(3), 1118-1127.
130. Yan, Y., & Liao, J. C. (2009). Engineering metabolic systems for

production of advanced fuels. *Journal of Industrial Microbiology & Biotechnology, 36*(4), 471-479.

131. Yang, Y. H., Brigham, C. J., Budde, C. F., Boccazzi, P., Willis, L. B., Hassan, M. A., & Sinskey, A. J. (2010). Optimization of growth media components for polyhydroxyalkanoate (PHA) production from organic acids by *Ralstonia eutropha*. *Applied Microbiology and Biotechnology, 87*(6), 2037-2045.
132. Yang, Y. H., Brigham, C., Willis, L., Rha, C., & Sinskey, A. (2011). Improved detergent-based recovery of polyhydroxyalkanoates (PHAs). *Biotechnology Letters, 33*(5), 937-942.
133. Yasotha, K., Aroua, M. K., Ramachandran, K. B., & Tan, I. K. P. (2006). Recovery of medium-chain-length polyhydroxyalkanoates (PHAs) through enzymatic digestion treatments and ultrafiltration. *Biochemical Engineering Journal, 30*(3), 260-268.
134. Yen, C. L. E., Stone, S. J., Koliwad, S., Harris, C., & Farese, R. V. (2008). Thematic review series: Glycerolipids. DGAT enzymes and triacylglycerol biosynthesis. *Journal of Lipid Research, 49*(11), 2283-2301.
135. York, G. M., Lupberger, J., Tian, J., Lawrence, A. G., Stubbe, J., & Sinskey, A. J. (2003). *Ralstonia eutropha* H16 encodes two and possibly three intracellular poly [d-(−)-3-hydroxybutyrate] depolymerase genes. *Journal of Bacteriology, 185*(13), 3788-3794.
136. York, G. M., Stubbe, J., & Sinskey, A. J. (2002). The *Ralstonia eutropha* PhaR protein couples synthesis of the PhaP phasin to the presence of polyhydroxybutyrate in cells and promotes polyhydroxybutyrate production. *Journal of Bacteriology, 184*(1), 59-66.

CHAPTER 3

INDUSTRIAL APPLICATIONS OF GREEN CHEMICAL TECHNOLOGIES

CONTENTS

3.1 INTRODUCTION

Green chemistry has been making an impact on our lives for around two decades now. Several popular organizations and companies that have embraced the discipline include BASF, the National Aeronautics and Space Administration, Nike, United Soybean Board, Pfizer, Hewlett-Packard, Eastman Chemical, the Environmental Protection Agency, Amgen, Bayer Material Science, Johnson & Johnson, DuPont, Codexis, and World Wildlife Fund. In the coming years, this widely spreading global market for green chemistry is expected to grow exponentially to around $98.5 billion by 2020. This emerging discipline has created hundreds of scientific papers. In more than 30 countries of every stable state, research network has been formed accompanying at least four innovative novel international scientific journals. Green chemistry is significant for reducing the quantity of chemical waste that is released into the water, air, and land. It has also procreated new fields of research such as an alternative energy science, green solvents, molecular self-assembly, biobased transformations and materials, molecular design for reduced hazard, and next-generation catalyst design. According to some industry reports, green chemistry is going to be the future of all chemistry.

3.2 HISTORY

Green chemistry has been built upon advances in such disciplines and fields that were present before the field's inception such as atom–economical synthesis, alternative solvents, catalysis, and degradable materials. Green chemistry was founded in the early 1990s. At that time, a widespread prevalent concern was about potential negative impacts of waste pollution, by-products, industrial chemicals in people's daily life, and chemical processes on the environment and human health. In the same decade (1990), the field of sustainability was created; moreover, Pollution Prevention Act of 1990 was passed in the same year, thereby marking a change in the regulatory policy of pollution control (Anastas, 2011).

In 1995, the Environmental Protection Agency (EPA) of the United States received huge support from the President Bill Clinton for the establishment of an annual awards program which highlights scientific innovations in the industry as well as academia that advanced green chemistry (Clark & Macquarrie, 2008). This gave rise to the annual Presidential Green Chemistry Challenge Awards. These awards have been a significant platform for the promotion of awareness and spreading knowledge about green chemistry

(Bowes, 2016). The University of Massachusetts at Boston, in 1997, initiated the field's first green chemistry Ph. D. program. In that same year, the Green Chemistry Institute (GCI) was founded in cooperation between a chemist Dennis Hjeresen and the EPA, Dr. Joe Breen, as an independent nonprofit organization comprising of staff which was devoted to working exclusively toward the expansion of green chemistry (Kim, Sung, Ryu, Kim, & Yoon, 2013).

John C. Warner and Paul Anastas coauthored the revolutionary book named Green Chemistry: Theory and Practice in 1998 (Anastas & Kirchhoff, 2002). In this book, "12 Principles of Green Chemistry" have been outlined, which stated the philosophy that helped in motivating industrial and academic scientists at that time and has been continuing to guide the green chemistry movement ever since. The green chemistry movement received a lift in 2005 when three scientists—Richard Schrock and Robert Grubbs of the United States and Yves Chauvin of France—won the Nobel Prize for chemistry for making the process of synthesizing carbon compounds simpler (Anastas & Warner, 2000; Vetenskapsakademien, 2005). Another milestone in green chemistry took place in 2008 when Arnold Schwarzenegger, governor of California, backed legislation to tighten limitations on toxic chemicals in household goods. In 2013, the state's Safer Consumer Products Law was implemented, and in 2014, an initial scrutiny of 164 chemicals was carried out (Rouhi, 2005).

3.3 ENVIRONMENTAL IMPACTS

According to the statistics collected by the EPA's Toxics Release Inventory (TRI), the quantity of chemical waste that is released into air, land, and water has reduced by almost 7% in between 2004 and 2013. According to these data, releases of several chemicals such as trichloroethylene, hydrochloric acid, and methyl isobutyl ketone have undergone a decrease of more than 60% during this period. The pharmaceutical industry is long known to have generated the most chemical waste per kilogram of product and thereby results in the production of complex molecules of high purity. According to the latest published reports, this production of chemical waste by the pharmaceutical industry has dropped by about half. An EPA analysis attributes much of this improvement to green chemistry and engineering practices (Porter & Van der Linde, 1995). Nonetheless, David J. C. Constable who is the present director of the Green Chemistry Institute has

stated that he believes the declines highlighted by EPA are still principally associated with changes in process and do not essentially specify that the core synthetic chemistry has altered significantly. Green chemistry can play a significant part in the designing of innovative chemicals; these chemicals can be used in place of ones that have been verified as problematic, as published in a recent report by the US National Research Council. Several chemical manufacturers, including DuPont, have now hired dedicated staff for an exploration of green chemistry and incorporating life cycle analysis to manufacturing processes and products. Such steps have been taken not just to prevent pollution, but also with the anticipation that those alterations can positively affect the companies' bottom lines (Kammerer, 2011).

A powerful promoter of green chemistry and sustainable innovation is the European Union's regulation on Registration, Evaluation, Authorization, and Restriction of Chemicals (REACH). REACH promotes the innovation of novel processes and materials by allowing potential exemptions from registration for up to five years for materials that are employed in research and development. Experts consider the authorization process of REACH as the primary instrument for the promotion of sustainable innovation and green chemistry, by providing aid in the phasing out of harmful chemicals and providing a substitute in the form of safe alternatives (Ritter, 2015).

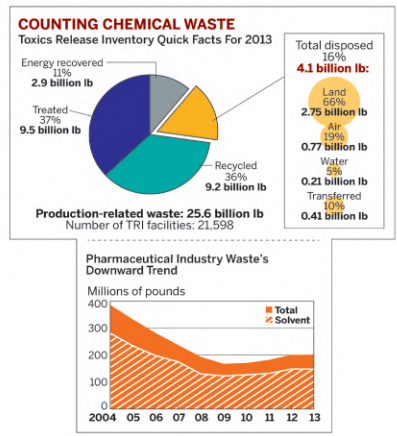

Figure 21. Detailed graphical representation of different wastes in 10 years from 2004 to 2013

[Source: https://www.acs.org/content/dam/acsorg/membership/acs/benefits/extra-insights/green-chemistry-applications.pdf]

In the United States, California has taken the initiative for the development of safe consumer products. According to this proposal, manufacturers may remove harmful chemicals from consumer products, either by reformulation with safer alternative chemicals or by eradicating harmful chemicals (DeVito, Keenan, & Lazarus, 2015; Kerton & Marriott, 2013). Although this law is currently applicable only within California, experts predict that it will affect manufacturing processes nationwide because of the state's significance to the broader US economy. Few experts believe that it can become a template for legislation in different places (Wilson & Schwarzman, 2009).

With the increase in the interest in green chemistry, the number of academic courses particularly designed for sustainable chemistry has also multiplied at both graduate and undergraduate levels. Prof. Terry Collins taught the first college-level course in green chemistry at Carnegie Mellon University in Pittsburgh, PA. More than 40 academic programs have now been enlisted on the ACS Web site that is offering green chemistry coursework in the United States and Puerto Rico (Hogue, 2015). Several institutes have offered classes which range from small four-year colleges to significant research universities (Manley, Anastas, & Cue, 2008). Few institutes in the United States that have launched green chemistry graduate programs include the University of Toledo (Ohio), Yale University, the University of California, Berkeley, and the University of Massachusetts. European universities with programs in green chemistry include the University of Copenhagen and the University of York (United Kingdom) (Kolopajlo, 2017).

3.4 GREEN CHEMISTRY APPLICATIONS

Green chemistry has an extensive range of applications in several industries including the pharmaceutical industry, as well as innovative methods that eradicate or reduce the utilization of solvents, or makes them safer for use and more efficient. Another significant impact of green chemistry is that it has inspired an increasing number of methods for the synthesis of chemicals from biological materials such as animal waste or plant matter instead of synthesizing them using conventional petroleum-based methods.

Green chemistry has played a significant role in providing alternative sources of energy and novel ways for the production of fuel cells, solar cells, and batteries for storage of energy. When self-assembling molecules make use of biobased plant materials, it is regarded as green chemistry. The key goal of green chemistry is to eliminate or lessen the production of

waste during the manufacturing of chemicals and its by-products. This goal has motivated the initiation of several green "next-generation" catalysts. Another significant development that is taking place in green chemistry is shifting toward the trend of redesigning chemical products to decrease their hazard.

3.5 GREENER PHARMACEUTICALS

Among different industries, the pharmaceutical industry was the first one to recognize the significance of green chemistry (Collins, 1995). Since 1996, various processes have been developed by or for the pharmaceutical industry, among which 11 have received Presidential Green Chemistry Award.

By 2005, all well-known drug companies had united with the American Chemical Society's Green Chemistry Institute for a round table. This institute aims at developing less polluting and more efficient processes. The US drug industry usage of chemicals was dropped almost to half in between 2004 and 2013. According to an analysis by the EPA, these reductions in the drug industry are mainly due to the usage of less organic solvents. Dichloromethane, dimethylformamide, methanol, acetonitrile, and toluene account for almost 75% of the industry's reduction. Pharmaceutical companies, too, are opting for less toxic reagents, decreasing reaction steps, and manufacturing improved catalysts (Cann, 1999).

Viagra, also commonly known as sildenafil citrate, is a bombastic drug that has been a "poster child" for quite long now for the green credentials of its producer, Pfizer (Sneddon, 2014). While preparing up for industrial manufacturing of Viagra, Pfizer's chemists developed a novel reaction strategy that helped in radically decreasing the quantity of solvent needed, cut out the chemicals tin chloride (an environmental contaminant) and hydrogen peroxide (hydrogen peroxide is considered a transportation and fire hazard), and hence resulted in the production of just a quarter of the waste as compared to the original process (Lasker, Mellor, Mullins, Nesmith, & Simcox, 2017). Researchers have also upgraded the method of developing Lipitor (atorvastatin) which is a well-known drug popular for its property of reducing blood cholesterol. The upgradation method involves using an enzyme that catalyzes chemical reactions taking place in water and thereby minimizes the requirement for potentially polluting organic solvents (Anastas & Beach, 2009). Some other popular drugs have been acknowledged by the EPA's green chemistry awards for decreasing the production of waste material by improving the methods of manufacturing.

A chemical company known as BASF now produces its yearly output of the painkiller named "ibuprofen" around 2 billion tablets—by employing a three-step process unlike previously used six-step method (Cernansky, 2015). Most of the atoms that are used during the synthesis procedure are derived from hydrocarbons. Unlike before, 70% of the used atoms make it into the concluding product compared with 40% before.

Another drug that is considered a leading drug for the treatment of high cholesterol is known as Zocor (simvastatin). The traditional method of manufacturing this drug involved multisteps involving large quantities of harmful reagents that resulted in producing a large quantity of toxic waste. The novel approach for the synthesis of this drug employs an engineered enzyme and an inexpensive feedstock that has been optimized by a biocatalysis company named Codexis (Ritter & Nike, 2014; Qian, Zhong, & Du, 2017). Moreover, Codexis worked in collaboration with Merck for the development of a greener route for the synthesis of sitagliptin, which is an active constituent in Januvia™ which is a treatment method for type 2 diabetes. As a result of this collaboration, an enzymatic process has been developed that decreases the amount of waste, improves safety and yield, and eradicates the requirement for a metal catalyst (Liveris, 2013).

Another prominent drug that now needs less production of waste is the chemotherapy drug paclitaxel (known as Taxol in the market). Originally, it was produced by extracting chemicals from the bark of a yew tree. This process previously made use of a lot of solvents in addition to killing the tree. Now, it is made by cultivating cells of the tree in a fermentation vat (Heddle et al., 1983).

3.6 GREEN SOLVENTS

According to the fifth principle of green chemistry, the use of auxiliary substances like solvents must be avoided whenever possible (Hupp & Poeppelmeier, 2005). Solvents are the main focus when using greening chemistry, due to their high volume usage and because normally they are volatile organic compounds (VOCs). The use of such compounds leads to high risks, producing a large amount of air pollution, waste, and other health distresses. To find a safer, more efficient substitute or removing solvents in total is one of the most impactful ways to affect the efficiency and safety of a product or process (Kirchhoff, 2005). Amid 1996 and 2014, a total of 22 Presidential Green Chemistry Awards have acknowledged methods

that decrease the use of traditional solvents, including greener, alternative solvents, and procedures that make use of water or carbon dioxide or just avoid using solvents altogether (Dunn, Galvin, & Hettenbach, 2004).

A currently industrial use example of a green solvent is used in the dying of fabric. Conventional methods of dying need large quantities of water, around 7 gallons for dyeing a T-shirt. Moreover, the process of dying is energy intensive as the dyed material needs to be dried. DyeCoo Textile Systems, which is Dutch start-up firm, recently developed an industrial-scale, dyeing process which is free of water as well as equipment that employs supercritical carbon dioxide. This supercritical carbon dioxide, when under pressure and at marginally higher temperature, functions just like a liquid.

During the recent years, manufacturers of spray cleaners, laundry detergents, and other cleaning products for the industry as well as in homes have been adding more green solvents to increase their performance, for both human health and environmental reasons. DuPont and Procter & Gamble have recently announced their plans to employ cellulosic ethanol which is derived from corncobs and stalks in cold water tide. DuPont is cultivating a plant in Iowa which helps in producing cellulosic ethanol. This will work as a replacement of ethanol which is derived from corn kernels. According to partners, by blending this cellulosic ethanol with cold water tide will repurpose more than 7000 tons of agricultural water per year, and this process will help in saving the amount of energy required for washing all the clothes of people in California homes for about a month (Patel, Joshi, & Panchal, 2012). DuPont also manufactures another biobased chemical known as 1, 3-propanediol. This chemical is sold as a stabilizer, a solvent, and an enzyme carrier.

Another green solvent developed with a similar aim is ethyl levulinate glycerol ketal. This solvent has been developed by the biobased chemicals start-up Segetis. The key role of this green solvent is to provide help in solubilizing fragrance oils as well as to keep stable the overall cleaning formulae, instead of dissolving grease or soil. Some other green solvents that were employed in method products include ethyl levulinate glycerol ketal, propanediol, methyl esters, and glycerin.

Another popular green cleaning solvent is known as butyl 3-hydroxybutyrate. The trade name of this solvent is Omnia. It was manufactured by Eastman Chemical. Eastman developed this new solvent by categorically going through a database of around 3000 molecules. These molecules had prospective potential as cleaning solvents. They were then

shaped into one using a combination of computer simulations and wet laboratory testing (Patel et al., 2012). A small company, named Elevance Renewable Sciences, Inc., transforms vegetable oils into special chemicals. The technology employed for this process is olefin metathesis technology which was invented by Robert H. Grubbs. This company has also been involved in the manufacturing of two green solvents. The company has manufactured a surfactant known as Steposol MET-10U, by working in partnership with the surfactants' manufacturer Stepan. This solvent has been used as a replacement for solvents including methylene chloride and n-methyl-pyrrolidone in paint strippers and adhesive removers. This surfactant can also be employed in industrial as well as household cleaners as an alternative of glycol ethers (Patel et al., 2012).

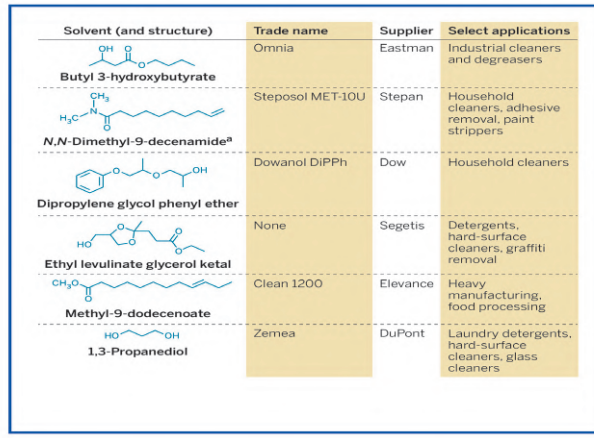

Solvent (and structure)	Trade name	Supplier	Select applications
Butyl 3-hydroxybutyrate	Omnia	Eastman	Industrial cleaners and degreasers
N,N-Dimethyl-9-decenamide[a]	Steposol MET-10U	Stepan	Household cleaners, adhesive removal, paint strippers
Dipropylene glycol phenyl ether	Dowanol DiPPh	Dow	Household cleaners
Ethyl levulinate glycerol ketal	None	Segetis	Detergents, hard-surface cleaners, graffiti removal
Methyl-9-dodecenoate	Clean 1200	Elevance	Heavy manufacturing, food processing
1,3-Propanediol	Zemea	DuPont	Laundry detergents, hard-surface cleaners, glass cleaners

Figure. 22. List of solvents and their applications in various industrial sectors

[Source: https://www.acs.org/content/dam/acsorg/membership/acs/benefits/extra-insights/green-chemistry-applications.pdf]

Elevance has also developed a degreasing, heavy-duty solvent called Elevance Clean 1200. This solvent is intentional to be used in food processing, manufacturing, and transportation maintenance of customers. It is intended to attract such companies which are looking for constituents that are thought to be low vapor pressure by California and have enough low vapor pressure or contain enough carbon atoms to be relieved from EPA's VOC designation. This solvent is being marketed as an alternative for d-limonene and aromatic hydrocarbons. Recently, a team of researchers at the University of Wisconsin Madison pronounced a capable biobased green

solvent (Beach, Cui, & Anastas, 2009). They employed mineral acid catalysts to be used as a solvent for converting cellulose and hemicellulose biomass into transportation fuels and high-value platform chemicals. The application of alkyl phenols as solvents, derived from lignin, in this procedure (taken place in a biphasic reactor) greatly reduced side reactions taking place in the aqueous phase and facilitated recycling of the mineral acid catalysts (Anastas, Bartlett, Kirchhoff, & Williamson, 2000).

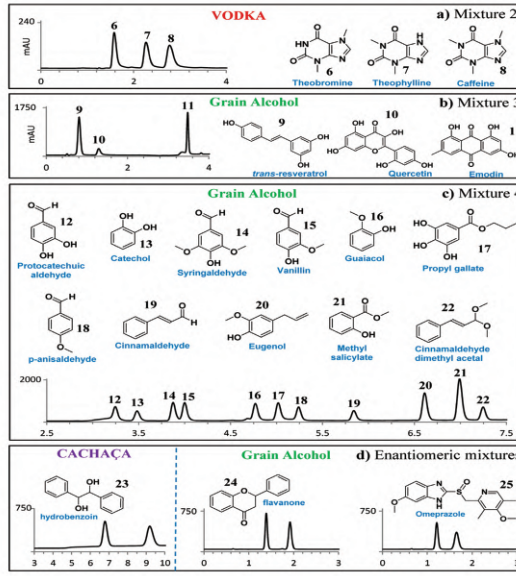

Figure. 23. Reverse-phase HPLC-UV investigation of various pharmaceutical and dietary compounds using traditional HPLC instrumentation with various spirit alcohol-based phases

[Source: https://www.acs.org/content/dam/acsorg/membership/acs/benefits/extra-insights/green-chemistry-applications.pdf]

For analytical chemists, a new method for avoiding solvents like acetonitrile in high-performance liquid chromatography (HPLC) might be their replacement with different distilled alcohols, such as vodka or rum, together with household products (Andraos & Dicks, 2012). A team of researchers from Merck Research Laboratories has carried out research which suggests that combination like this can serve as a sustainable and economical substitute for HPLC; moreover, in several cases, it can also lead to producing excellent analytical results (Dunn, 2012). Some of the

other green solvents that are now increasingly used are supercritical carbon dioxide, ionic liquids, and water (Yoon, Ischay, & Du, 2010).

3.7 BIOBASED TRANSFORMATIONS AND MATERIALS

Green chemical technology has played a significant part in developing an increasing number of alternative methods for the synthesis of chemicals which were conventionally made from renewable resources such as petroleum. Now, advances in process chemistry, genetics, biotechnology, and engineering are forming new and advance manufacturing concept for the conversion of renewable biomass into reliable products and fuels, commonly known as the biorefinery concepts (Li & Vederas, 2009).

During the period 1996–2014, 34 of technologies that were awarded Presidential Green Chemistry Award involved employing a renewable resource as an alternative to using petroleum or any other depleting resource (Tang, Bourne, Smith, & Poliakoff, 2008). These technologies had used an extensive variety of biological materials such as bacteria and other microorganisms, cellulose, algae, biomass, starch, oils from crops and several other plants, yeast, and sugar. Technologies like these have been established by various well-known companies including Cargill, Dow, Archer Daniels Midland, DuPont, Procter and Gamble, Eastman Chemical, Sherwin-Williams, as well as other smaller companies and academic researchers.

In 2003, DuPont's Sorona® polymer received a Presidential Green Chemistry Award. This polymer is an example of a commercially available biobased process. DuPont established the process, which makes use of a renewable cornstarch and genetically engineered microorganism in place of using petroleum to make economic textiles (Yanes, Gratz, Baldwin, Robison, & Stalcup, 2001). The Sorona polymer has various uses including its use in carpeting, apparel, and packaging. This biobased method is popular for using less energy, which in turn reduces emissions, and makes use of renewable resources unlike previously used traditional petrochemical processes (Cann, 1999).

Genomatica has developed a process which received the EPA's 2011 Presidential Green Chemistry Challenge Award for developing "greener synthetic pathways." Now, using this process, BASF is manufacturing

renewable 1, 4-butanediol (1, 4-BDO) on an industrial scale (Porter & Van der Linde, 1995). This biobased material is employed in the production of BASF's Ecoflex compostable polyester film. This film is afterward used together with calcium carbonate and cassava starch to make Ecovio® bags which are fully biodegradable. Biodegradable Products Institute has certified these bags. They can disintegrate into CO_2, water, and biomass in industrial composting processes.

Recently, a few innovations have taken place in the production of biobased chemicals. These innovations are a consequence of coupling biological and chemical processes (Azadi et al., 2012). A team of academic researchers has demonstrated in a recent study that an extensive variety of high-value products can be manufactured from a platform chemical which has not been previously explored. This chemical is known as triacetic acid lactone and is a 2-pyrone compound (Pandey & Kim, 2011). The synthesis of pyrone was carried out from glucose by employing a genetically modified *E. coli*, and a yeast species are known as Saccharomyces cerevisiae. The researchers were successful in producing 2, 4-pentanedione (also named as acetylacetone). It has numerous industrial applications such as in metal plating, in metal extraction, and as a fuel additive and. The researcher also further transformed it into dienoic acid. This acid is manufactured using petrochemical sources and can be utilized as feed as well as food additive owing to its capability to hinder the growth of several bacteria and mold. As per the reports, two other compounds produced by the team are γ-caprolactone and hexenoic acid. Hexenoic acid can be utilized as a flavoring agent. Y-caprolactone is used as a cosmetic ingredient and fragrance.

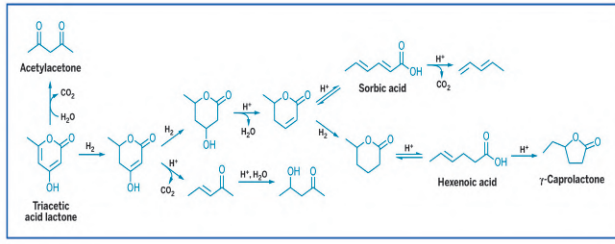

Figure 24. Synthesis of γ-caprolactone, sorbic acid, and hexenoic acid from acetylene and triacetic acid lactone

[Source: https://www.acs.org/content/dam/acsorg/membership/acs/benefits/extra-insights/green-chemistry-applications.pdf]

One more example is the procedure employed by Auckland, New Zealand-based LanzaTech. This process includes the conversion of gases containing carbon monoxide to ethanol and other chemicals using microbial fermentation. Since steel mills are known to produce CO-rich gas streams, LanzaTech has constructed an ethanol production demonstration plant producing 100,000-gallon-per-annum Shanghai at Baosteel which is the China's largest producer of steel. LanzaTech's microbes also can produce 2,3-butanediol, which can further be transformed into other compounds for instance, in 1,3-butadiene, which is a monomer utilized in the manufacturing of synthetic rubber (Azadi et al., 2012). Another US-based company named Coskata is commercializing hybrid chemical processing technology. Coskata manufactures syngas is a combination of mainly hydrogen and CO, using thermochemical gasification of biomass or some other solids or using catalytic remodeling of natural gas. Careful microbial fermentation of syngas results in yielding low molecular weight alcohols. Coskata controls a plant that can produce tens of thousands of gallons of ethanol per annum using wood chips.

As a result of new processes of synthesizing from biomass, a chemical known as the levulinic acid can be used extensively. A US-based company known as Segetis sells constituents for cleaning products and personal care which are based on levulinic ketals. This company controls a biobased levulinic acid pilot plant located in Minnesota. Two chemical firms have recently launched projects in Italy for the production of levulinic acid from biomass. According to the company, their technology will reduce price and turn a niche chemical into a striking new building block for products used in coatings, fuels, crop protection, and solvents. The traditional method of synthesizing levulinic acid involves its production from maleic anhydride which is an expensive method of production and therefore confines its use to low-volume applications for instance, in food additives and fragrances (Mahmood, Yuan, Schmidt, & Xu, 2015).

A California-based biotech company Solazyme engineers microalgae for producing much higher quantities of oil as compared to the 5–10% content of oil in wild algae. In 2014, this same company won a Presidential Green Chemistry Challenge Award. The products of this company include the industrial manufacturing of algal oils that have been engineered to be chemically analogous to products of palm oil such as the C_{12} and C_{10} fatty acids which are present in palm kernel oil (Giesbrecht & Greenfield, 1999). The company's oils are present in different products like in a laundry detergent from a company known as Ecover (Welch, Nowak, Joyce, &

Regalado, 2015). Few other firms that are well known for producing biobased chemicals are Myriant and Solazyme. Myriant is located in Massachusetts and produces biobased drop-in substitutes and replacements for an extensive variety of chemicals which are based on petroleum such as acrylic acid, which currently has several million dollar international market, and succinic acid, which is utilized in pharmaceuticals, pigments, and metal plating (Sheldon, 2005; Vemula & John, 2008).

3.8 ALTERNATIVE ENERGY SCIENCE

3.8.1 Solar Photovoltaics

A recent analysis has reported that solar photovoltaic technology is among one of the limited low-carbon, renewable resources which have both the technological maturity and the scalability to meet the ever-increasing worldwide demand for electricity (Manley et al., 2008). The utilization of solar photovoltaics has been increasing at an average of almost 43% per annum since 2000. In the past few years, clean energy experts have been very enthusiastic about the rise of two novel chemistry-driven solar technologies, namely quantum dots and perovskite solar cells.

Perovskite solar cells can be compared well with most of the conventional photovoltaic technologies since they offer good power outputs from inexpensive materials that are comparatively easy to process into working devices (Kirchhoff, 2003; Kidwai & Mohan, 2005). The appellation of perovskite is a nod to a mineral which was discovered long ago and was composed primarily of calcium titanate ($CaTiO_3$). Presently, scientists use this term loosely as a reference for a large class of materials that, similar to $CaTiO_3$, display ABX3 stoichiometry and adopt the crystal structure of perovskite. These days, a type of perovskites is getting much-increased thoughtfulness in the photovoltaics world. These perovskites are organometal trihalides, among which the most generally studied is $CH_3NH_3PbI_3$ (CH_3NH_3 is the A group in ABX3.) The main reason behind the increased enthusiasm is the latest steep rate of progress in perovskite solar cell performance (Kurian, 2005).

In the duration of just a few years, the efficiency of conversion of perovskite cells has jumped from merely a few percent in a forerunner version to greater than 20% in 2015. This is a breakthrough that took decades to reach in case of most other solar cells [53]. Most of the advancement in

this field has been reported in 2012 and 2013. The fast-paced advancement, which has not given away any signs of slowing, together with cost-effective materials and manufacturing methods, has encouraged some experts to state that perovskite solar cells are determined "to break the predominant paradigm" by combining exceptional performance and low cost (Kurian, 2005)

Perovskite solar cells can be formed by employing techniques of common wet chemistry. The simple process of fabrication of components of solar cell by means of liquid-phase chemical reactions as well as deposition of the materials by techniques such as spin coating and spraying thus making it imaginable for manufacturers of solar cell to ultimately replace sophisticated manufacturing apparatus and clean rooms presently used for the production of photovoltaic with easy benchtop processes (Kurian, 2005).

In 2009, a Japanese research uncovered some of the main features of perovskite solar cells. The research involved in the treatment of a film of TiO_2 with a solution comprising of PbI_2 and CH_3NH_3I. The researchers activated a self-assembly procedure that involved coating of the oxide with a layer of nanocrystals of $CH_3NH_3PbI_3$, which is one of the perovskite materials present at the center of recent research efforts. The group formed solar cells by inserting the perovskite-coated oxide films and an organic electrolyte solution making a sandwich of them in between conducting glass electrodes. They observed that the triiodide cell was able to readily generate an electric current having a conversion efficiency of around 3.8% (Harmsen, Hackmann, & Bos, 2014; Bruijnincx & Weckhuysen, 2013). After two years, a team from South Korean used a similar cell having optimized parameters to gain a conversion efficiency of almost 6.5% (Welch et al., 2015). Later on, another team discovered that certain improvements could be made by employing a compound of the polyaromatic ring in the spiro-bifluorene family identified as spiro-OMeTAD to gain 9.7% efficiency (Giaquinto & Samide, 2013). Using a replacement of TiO_2 led to an unexpected conversion efficiency of 10.9%.

In quick succession all the way through 2013, multiple series of research papers were published on a variety of journal Web sites, each stating a slightly different design of perovskite solar cell and each reporting improvements in conversion efficiency (Jacoby, 2012). The National Renewable Energy Laboratory is considered as the official verifier of the performance of solar cell all over the world. This laboratory has been verifying the performance of each improved version. Few researchers from the UK-published information in March 2015, about a new low-temperature procedure to make perovskite

solar cells in a way that they can be utilized in colorful, high-efficiency, see-through photovoltaic films that would be possible to plaster on walls or else laminate on windows (Manley et al., 2008; Wirth & Thiesse, 2014). Presently, minimum of two companies have assured to initiate the production of perovskite cells industrially; the companies include Australian company, Dyesol, and Oxford Photovoltaic of the U. K.

3.8.2 Quantum Dots

Quantum dots are nanocrystals composed of semiconductor materials that release a bright glow of a pure color upon excitation by an applied voltage or light (Chia, Schwartz, Shanks, & Dumesic, 2012). Several experts of alternative energy are enthusiastic about solar cells based on quantum dots for the reason that they have a theoretical conversion of 45%. This has been conceivable because when a quantum dot absorbs a single photon, it results in the production of more than one bound electron–hole pair, or exciton, hence doubling up the general conversion efficiency numbers that are visible in single-junction silicon cells (Jong, Higson, Walsh, & Wellisch, 2012). Till now, no one has come close to gain that type of efficiency; however, the rates have been improving continuously. For instance, in 2014, research teams testified that quantum dot solar cells that employ ternary $CuInS_2$ had gained the best record of 7.04% (along with the certified efficiency of 6.66%) (Scott, 2015).

Moreover, in 2014, few researchers from the Massachusetts Institute of Technology (MIT) developed a quantum-dot-based solar cell that transforms light into electricity with a conversion efficiency of 9% (Tullo, 2013). According to the MIT team, the technology can be created using a low-cost production method that assures to keep costs of manufacturing down. Lately, an innovative class of organometal halide perovskite-based semiconductors has arisen as a possible nominee for quantum dot solar cells (Anastas, Kirchhoff, & Williamson, 2001). These cells can make use of methyl ammonium lead iodide chloride ($CH_3NH_3PbI_2Cl$) perovskite. Few other quantum dot solar cells employ cadmium, encouraging some observers to interrogate whether it is accurate to call applications of the technology that make use of such metals “green” or “clean” (Scott, 2015).

3.8.3 Fuel Cells

The price of the fuel cells has dropped during the last decade; on the contrary, the vehicle range has increased; moreover, with time, engineers

have mastered the ability to work well in frigid weather conditions and perform under challenging conditions (Jean, Brown, Jaffe, Buonassisi, & Bulović, 2015). In the United States, this year, the first ever fuel cell car became available to produce electricity by the conversion of oxygen and hydrogen into the water.

For instance, with time, normal fuel cell operation begins to corrode and oxidizes the carbon material normally employed as catalyst supports, which leads to the degradation of catalyst and hence poor performance of the device. The study of metal nitrides has been carried out as alternative supports, but the side effect is that they are not always tolerant of the acidic conditions that are needed for some fuels. A team from Cornell University recently has reported that a titanium chromium nitride material seems able to solve this problem (Asif, Singh, & Alapatt, 2015). The researchers made use of palladium–silver nanoparticles that were supported by a highly porous $Ti_{0.5}Cr_{0.5}N$ network and found out that it can serve as a stable and an active catalyst system in alkaline and acidic media across the normal range of fuel cell voltages. Results of the test verified this material to be more durable and active as compared to the standard materials of carbon.

Few other research topics explored include how to store such hydrogen fuel which is required by fuel cells. Recently, another research group from Boston College created an H_2 storage molecule. This molecule does not decompose even at high temperatures such as reaching 150°C (Asif, 2017). A team of researchers has developed a new compound, namely bis-BN cyclohexane, which might prove suitable for such applications as backup generators that would stock energy for a longer period during the incident of a natural disaster.

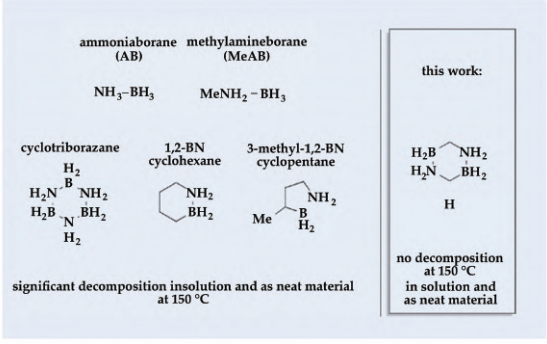

Figure 25. Thermal stability behavior of amine–borane-based hydrogen storage

[Source: https://www.acs.org/content/dam/acsorg/membership/acs/benefits/extra-insights/green-chemistry-applications.pdf]

3.8.4 Battery Power

The significance of sustainable energy technologies cannot be overlooked since they can let the best possible utilization of energy that is produced by renewable sources. An increasing tendency in both energy conversion and energy storage systems is to imitate nature and its extensive biodiversity (Loi & Hummelen, 2013). Few researchers have been working on the invention of new batteries by getting motivation from life chemistry, which gets power by chemical reactions that depend on membrane potential and ion flux. Recently, a team of researchers has identified a molecule having the formulae $Li_2C_6O_6$. This molecule can be synthesized from myoinositol, which is a renewable resource and inserts and deinserts lithium ions that are related to an energy density which is almost double than the amount that can be achieved with present day's lithium methyl carbonate ($LiNi_{1/3}$,$n_{1/3}Co_{1/3}O_2$) electrodes (Jacoby, 2014).

The main component of the battery is electrodes. Theoretically, batteries composed of lithium–sulfur electrodes can store four times more energy as compared to traditional lithium-ion batteries, hence promising longer run times for electronics as well as more miles for electric cars between charges. According to the research, industrialization in such batteries is within reach. A novel design scheme employing new materials such as graphene oxide with a sulfur coating seems promising for lengthening the life of the battery by conserving a high storage capacity (Jean et al., 2015). The battery was charged as well as discharged, or cycled, 1500 times, successfully exhibiting impressive performance. The initial storage capacity of this battery was 500 watt-hours per kilogram (Wh/kg) of battery material. In contrast, the storage capacity of traditional lithium-ion batteries was around 200 Wh/kg. The target of the US Department of Energy for batteries of the electric vehicle is 400 Wh/kg. After going through 1000 cycles, the storage capacity of this battery dropped down to around 300 Wh/kg which is still larger than traditional lithium-ion batteries (Kojima, Teshima, Shirai, & Miyasaka, 2009).

A team from Stanford University has described a novel approach that involves a new electrode material. According to the claim made by the team, this specific material holds promise for grid storage batteries that can work as long as 30 years without any sharp decline in their performance. This

new electrode material described by the team contains secondary hydrated potassium ions for carrying charge in between the two ends of the battery (Im, Lee, Lee, Park, & Park, 2011). The experiment was performed in the laboratory in which the iron- and copper-based nanoengineered material took 40,000 charge/discharge cycles at the same time maintaining around 80% storage capacity. On the contrary, the traditional lithium-ion batteries employed in consumer electronics degrade visibly after merely a few hundred cycles (Kim et al., 2012).

Some researchers have been carrying out research to find a substitute to be used in place of lithium because of the growing concern of the shortage of this element owing to the rapid growth of its demand worldwide. One option under consideration is sodium batteries (Kim et al., 2012). A sodium-ion battery has been developed by UK-based Faradion, which, according to him, is one-third cheaper as compared to lithium-ion batteries for the similar performance (Lee, Teuscher, Miyasaka, Murakami, & Snaith, 2012).

Some engineers at the University of Illinois have recently employed holograms, on a smaller scale. Holograms are the 3D interference configurations of various laser beams for the precise creation of porous blocks in light-curable polymers (Zhou et al., 2015). Afterward, the teams used these blocks as scaffolding for building electrodes that could be employed for microbatteries to power microelectronic devices, including medical implants, sensors, and radio frequency transmitters. The process of the hologram is compatible with traditional 2D photolithography, which is extensively utilized in the microelectronics industry (Piatkowski et al., 2016).

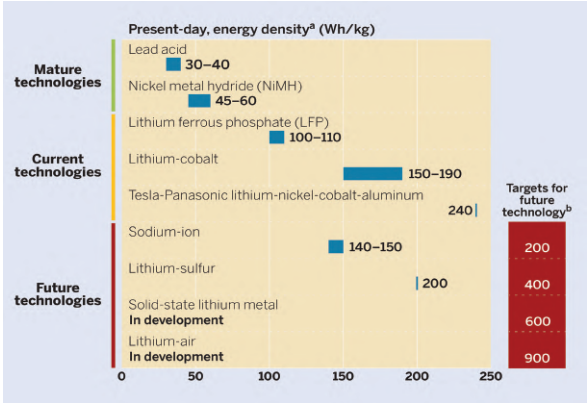

Figure 26. Characteristics of different generations of batteries

[Source: https://www.acs.org/content/dam/acsorg/membership/acs/benefits/extra-insights/green-chemistry-applications.pdf]

3.9 MOLECULAR SELF-ASSEMBLY

Molecular self-assembly is a method in which parts of molecules or molecules themselves suddenly form ordered combinations without needing any human intervention. The interactions that are involved are non-covalent, and the structures created resultantly are generally in equilibrium states or else in metastable states to be very least. The practice of molecular self-assembly is pervasive in materials science, chemistry, and biology (Weidman, Seitz, Stranks, & Tisdale, 2016). An evolving notion in molecular self-assembly implicates consuming formerly underutilized biobased plant materials (Moras, Strandberg, Suc, & Wilson, 1996). For instance, glycolipids created as industrial derivatives such as cashew nutshell liquid can undergo self-assembling for the production of soft nanomaterials including twisted/helical nanofibers, lipid nanotubes, liquid crystals, and low molecular weight gels.

Some scientists are also in the process of developing molecules that can spontaneously gather into simpler versions of the extracellular matrix that is surrounding several cells of the body to offer a medium of growth for cells, particularly for tissue engineering. The extracellular matrix consists of a complex web of biomolecules which includes sugar molecules and proteins that aids in intercellular communication, provides structure for tissues, and traps nutrients. The main focus of this field is on self-assembling peptides (Ahn et al., 2015).

In 2014, a team of researchers from Brandeis University developed a sugar-decorated molecule that can self-assemble into a hydrogel that imitates the extracellular matrix (Pan et al., 2014). Molecules that are found on the surface of stem cells, mostly sugars, interact with this extracellular matrix using methods that are critical to stemming cell development and differentiation. According to the researchers, the gel plays the role of encouraging mouse embryonic stem cells to propagate; moreover, it forces zygotes to progress into blastocysts, signifying that someday, the molecule could aid in the growth of human tissue in the laboratory. A main constituent of the hydrogel is glycoconjugate which is a carbohydrate molecule linked with a covalent bond to other molecules that researchers are reviewing to comprehend how it might stimulate the growth of stem cell and which proteins are involved (Ahn et al., 2015).

Scientists from Tufts University as well as another team of researchers from the same Brandeis laboratory mutually designed a peptide that combines and swaps cancer cells; this is done when its phosphate group is eradicated (Chuang, Brown, Bulović, & Bawendi, 2014). Peptides that are free from phosphate group have a hydrophobic and a hydrophilic end, which permits them to gather just like lipids in a cell membrane. The phosphate group contains negative charge which creates electrostatic repulsion among the molecules and inhibits the peptide from submerging the cancer cells. This on–off switch of phosphate is ideal for attacking cancer since some kinds of cancer cells overexpress alkaline phosphatase (an enzyme that is known to slash phosphates) (Ahn et al., 2015).

Another use of molecular self-assembly under investigation is making of artificial viruses from it. Artificial viruses could be used as structural materials as well as DNA-based drug delivery particles. A team of scholars at Wageningen University, in the Netherlands, has significantly progressed toward this aim with a viral coat protein. This protein self-assembles with DNA in such a manner that it impersonates the tobacco mosaic virus (Kamat, 2013). These investigators have demonstrated that these viruslike particles could go into cells and shield the DNA against degradation (Van Mierlo, Maggetto, & Lataire, 2006).

During the ACS National Meeting in 2015, in Denver, researchers reported forming a collection of light-releasing platinum–organic metal cages and metal cycles (Cui, Yang, & DiSalvo, 2014). Chemists at the University of Utah demonstrated how the selection of different combinations of organic linking groups as well as angular and linear metal complexes enables them to construct two- and three-dimensional molecules having versatile properties and eccentric geometries. Such molecules can prove valuable as building blocks for fibers and polymeric hydrogels, for optoelectronic chemical sensors, as therapeutics, and as bioprobes for visualization and monitoring of physiological processes. Another approach to green chemistry that involves self-assembling includes an approach established by a team of researchers from the University of Nottingham, in the United Kingdom. This approach involves self-assembling for fabrication of trimesic acid monolayer structures on extremely oriented pyrolytic graphite (Chen et al., 2014). An additional self-assembly technique, recently developed, permits chemists to develop polymeric structures on the scale having micrometer length. The resultant structures may perhaps eventually be employed for drug delivery applications and molecular electronics (Larcher & Tarascon, 2015).

3.10 NEXT-GENERATION CATALYST DESIGN

A total of 20 Presidential Green Chemistry Challenge Awards have acknowledged green catalysts (Song, Zhang, & Cairns, 2013). A current example is the technology that has been developed by Elevance, which employs a Nobel Prize-winning catalysis method for the production of green, high-performing, specialty chemicals at beneficial costs. In this catalyst technology, natural oils are broken down, and then, the fragments are recombined into innovative, high-performance green chemicals. These chemicals have the advantage of combining the benefits of both biobased chemicals and petrochemicals. As compared to petrochemical technology, this technology consumes considerably less amount of energy and lessens greenhouse gas emissions by almost 50%. Elevance is manufacturing specialty chemicals for various uses, such as in lubricants, cleaning products, personal care products, and candle waxes (Caims et al., 2014). Few of these chemicals are available commercially (Palomares et al., 2012).

One of the Dow Chemical's rewards is for a special green catalyst that decreases the environmental footprint linked with the production of propylene oxide which is one of the largest volume industrial chemicals produced in the world (Wessells, Huggins, & Cui, 2011). The process of hydrogen peroxide to propylene oxide (HPPO) was established in collaboration with BASF and works as a chemical building block for an extensive array of products such as de-icers, detergents, food additives, polyurethanes, and personal care products. As compared to the traditional technologies, this new process decreases the consumption of energy by 35 percent and the production of wastewater by almost 70–80 percent.

Another newly developed catalyst has the potential to be a more efficient and less expensive catalyst for cleaning of the exhaust of diesel engine (Buchholz et al., 2013). This catalyst has been developed by a team of researchers from China, the United States, and South Korea. The catalyst employs Mn mullite (Sm, Gd) Mn_2O_5—manganese mullite materials—which contain either gadolinium or samarium for the conversion of harmful diesel engine-exhaust product nitric oxide into the more gentle nitrous oxide (Scott, 2014).

Pharmaceutical companies Codexis and Merck have developed a new catalyst for the green synthesis of sitagliptin. Sitagliptin is an active constituent in the treatment of type 2 diabetes. Januvia™ may also be helpful in the development of other drugs. For instance, a recent clinical trial has demonstrated that it may aid patients suffering from acute coronary

syndrome (Ning et al., 2015). An example of a green catalyst that has the potential to lessen the environmental effects of the pharmaceutical industry is the powerful chain of tetra-amido macrocyclic ligand (TAML) catalysts which have been modeled on naturally existing peroxidase enzymes. This enzyme has been developed by Terry Collins of Carnegie Mellon University (Davenport, 2015). According to Collins, the use of this catalyst at a late stage in the process of sewage treatment would permit them to break down an extensive variety of chemical residues, such as those from Prozac, Lipitor, the contraceptive pill, Zoloft, and several more, before they enter the environment (Whitesides & Boncheva, 2002).

3.11 MOLECULAR DESIGN FOR REDUCED HAZARD

Some Presidential Green Chemistry Awards acknowledge non-toxic chemical products that are designed for use in an extensive variety of industries (Vemula & John, 2008). The Solberg Company won an award in 2014 for its halogen-free RE-HEALING foams that are to be used in fighting fires. Conventionally, fluorinated surfactants were used in firefighting; these surfactants are persistent chemicals and have the capability for producing environmental effects. The RE-HEALING firefighting foam concentrates employ a mixture of sugars and non-fluorinated surfactants. Extinguishing time, control, and burn back resistance are vital for the safety of firefighters in all places, and these new foams have exceptional performance in each of these qualities. These foams have also attained the full regulatory compliance with prevailing standards of fire protection (Ng et al., 2008).

Cargill, Inc. was esteemed, in 2013, for its Envirotemp™ FR3™ vegetable oil-based insulating fluid to be used in high-voltage transformers. Until the 1970s, polychlorinated biphenyls (PCBs) were employed in the insulating fluid required to make an available cooling mechanism for high-voltage electric transformers and to inhibit short-circuiting; however, after 1970, it was banned. After the banning of PCB, mineral oil befitted as the primary replacement. Unluckily, mineral oil is flammable and can prove to be deadly to fish. Cargill's transformer fluid based on vegetable oil is far less flammable, is less poisonous, provides higher performance, and has a significantly lower carbon footprint (Du et al., 2014). According to a life sequence assessment, a transformer that employs FR3™ fluid has inferior carbon footprint throughout the entire life span of a transformer,

with the highest reductions taking place in the raw materials, buildup, and transportation stages. The complete carbon footprint of an electric transformer is almost 55 times lesser when FR3™ fluid is used instead of using mineral oil. Additional benefits are high biodegradability and the fact that renewable resources are the basis of FR3™ fluids. Moreover, there has not been reported any fires or known explosions in the hundreds of thousands of transformers that are filled with FR3™ fluid ever since the product has launched. FR3™ fluid has received several industry validations as a less flammable fluid by both Factory Mutual Research Corporation and Underwriters Laboratory (UL) (Kuang et al., 2014). One such validation received is EPA's environmental technology verification and certification.

Faraday Technology, Inc. received a Presidential Green Chemistry Award for developing a chrome plating technology that employs trivalent chromium that is less poisonous as compared to hexavalent chromium, which is a known carcinogen. Applications of the process of Faraday's plating comprise of a high-performance chrome plating for several uses in commercial and military markets. This replacement can decrease lots of pounds of hexavalent chromium without having to compromise on performance (). Chrome coatings deliver suitable resistance to sliding wear and abrasives in heavy-duty machinery, specifically pneumatic tubing. The plating process mechanism of FARADAYIC® TriChrome retains the benefits of a functional chrome coating but greatly decreases the risks that are associated with the plating procedure by employing Cr (III). The newly developed technology is not difficult to install in chrome plating facilities due to the requirement of just new plating bath electrodes. Using Faraday's technology, we can eradicate around 13 million pounds of a waste of hexavalent chromium every year in the United States and almost around 300 million pounds worldwide.

Buckman International, Inc. received a green chemistry award, in 2012, for producing enzymes that reduce the requirement of energy and wood fiber for the manufacture of high-quality paperboard and paper. The conventional method of making strong paper needed expensive wood pulp, chemical additives as well as energy-intensive treatment. These enzymes developed by Buckman's Maximyze® can achieve the same objective by the modification of the cellulose present in wood to enhance the amount of "fibrils" that help in binding the wood fibers to each other, hence improving the quality and strength of the paper—without having to use additional energy or chemicals. Moreover, Buckman's process permits making of paper using less wood fiber and higher proportions of recycled paper which enables a single plant to

save around $1 million each year (Kuang et al., 2014). Maximyze increases the strength to reduce the weight of the paper product or to replace some of the wood fiber with a mineral filler-like calcium carbonate. Maximyze treatment also makes use of less steam since the paper drains at a fast speed (increasing the rate of production) and expends less amount of electricity for refining. Such treatment is less lethal than presently used alternatives and is therefore safer to handle, transport, manufacture, and practice than prevalent chemical treatments employed for the production of paper.

REFERENCES

1. Ahn, N., Son, D. Y., Jang, I. H., Kang, S. M., Choi, M., & Park, N. G. (2015). Highly reproducible perovskite solar cells with average efficiency of 18.3% and best efficiency of 19.7% fabricated via Lewis base adduct of lead (II) iodide. *Journal of the American Chemical Society, 137*(27), 8696-8699.
2. Anastas, P. (2011, June 27). Twenty years of green chemistry. *Chemical and Engineering NEWS, 89*(26), 62-65.
3. Anastas, P. T., & Beach, E. S. (2009). Changing the course of chemistry.
4. Anastas, P. T., & Kirchhoff, M. M. (2002). Origins, current status, and future challenges of green chemistry. *Accounts of Chemical Research, 35*(9), 686-694.
5. Anastas, P. T., & Warner, J. C. (2000). *Green chemistry: theory and practice*. Oxford University Press.
6. Anastas, P. T., Bartlett, L. B., Kirchhoff, M. M., & Williamson, T. C. (2000). The role of catalysis in the design, development, and implementation of green chemistry. *Catalysis Today, 55*(1), 11-22.
7. Anastas, P. T., Kirchhoff, M. M., & Williamson, T. C. (2001). Catalysis as a foundational pillar of green chemistry. *Applied Catalysis A: General, 221*(1), 3-13.
8. Andraos, J., & Dicks, A. P. (2012). Green chemistry teaching in higher education: A review of effective practices. *Chemistry Education Research and Practice, 13*(2), 69-79.
9. Asif, A. A. (2017). *Manufacturing of photovoltaic devices, power electronics and batteries for local direct current power based nanogrid* (Doctoral dissertation, Clemson University). Retrieved from https://tigerprints.clemson.edu/cgi/viewcontent.cgi?article=2878&context=all_dissertations
10. Asif, A. A., Singh, R., & Alapatt, G. F. (2015). Technical and economic assessment of perovskite solar cells for large scale manufacturing. *Journal of Renewable and Sustainable Energy, 7*(4), 043120.
11. Azadi, P., Carrasquillo-Flores, R., Pagán-Torres, Y. J., Gürbüz, E. I., Farnood, R., & Dumesic, J. A. (2012). Catalytic conversion of biomass using solvents derived from lignin. *Green Chemistry, 14*(6), 1573-1576.
12. Beach, E. S., Cui, Z., & Anastas, P. T. (2009). Green Chemistry: A

design framework for sustainability. *Energy & Environmental Science*, *2*(10), 1038-1049.

13. Bowes, D. R. (2016.). Stock Market Volatility and presidential election uncertainty: Evidence from political futures markets. In *2016 International Academic Business Conference New Orleans, LA 2016 International Education Conference*.
14. Bruijnincx, P. C., & Weckhuysen, B. M. (2013). Shale gas revolution: An opportunity for the production of biobased chemicals. *Angewandte Chemie International Edition*, *52*(46), 11980-11987.
15. Buchholz, D., Moretti, A., Kloepsch, R., Nowak, S., Siozios, V., Winter, M., & Passerini, S. (2013). Toward Na-ion batteries synthesis and characterization of a novel high capacity Na ion intercalation material. *Chemistry of Materials*, *25*(2), 142-148.
16. Cairns, E. J., Song, M. K., & Zhang, Y. (2014). *U. S. Patent Application No. 14/899,997*.
17. Cann, M. C. (1999). Bringing state-of-the-art, applied, novel, green chemistry to the classroom by employing the Presidential Green Chemistry Challenge Awards. *Journal of Chemical Education*, *76*(12), 1639.
18. Cernansky, R. (2015). Chemistry: Green refill. *Nature*, *519*(7543), 379-380.
19. Chen, G., Zakharov, L. N., Bowden, M. E., Karkamkar, A. J., Whittemore, S. M., Garner III, E. B., & Liu, S. Y. (2014). Bis-BN cyclohexane: A remarkably kinetically stable chemical hydrogen storage material. *Journal of the American Chemical Society*, *137*(1), 134-137.
20. Chen, H., Armand, M., Demailly, G., Dolhem, F., Poizot, P., & Tarascon, J. M. (2008). From biomass to a renewable LiXC6O6 organic electrode for sustainable Li-ion batteries. *ChemSusChem*, *1*(4), 348-355.
21. Chia, M., Schwartz, T. J., Shanks, B. H., & Dumesic, J. A. (2012). Triacetic acid lactone as a potential biorenewable platform chemical. *Green Chemistry*, *14*(7), 1850-1853.
22. Chuang, C. H. M., Brown, P. R., Bulović, V., & Bawendi, M. G. (2014). Improved performance and stability in quantum dot solar cells through band alignment engineering. *Nature Materials*, *13*(8), 796.
23. Clark, J. H., & Macquarrie, D. J. (2008). *Handbook of green chemistry and technology*. John Wiley & Sons.

24. Collins, T. J. (1995). Introducing green chemistry in teaching and research. *Journal of Chemical Education, 72*(11), 965.

25. Cui, Z., Yang, M., & DiSalvo, F. J. (2014). Mesoporous Ti0.5Cr0.5N supported PdAg nanoalloy as highly active and stable catalysts for the electro-oxidation of formic acid and methanol. *ACS Nano, 8*(6), 6106-6113.

26. Davenport, M. (2015). Holograms help to power up microbatteries. *Chemical & Engineering News, 93*(20), 7.

27. DeVito, S. C., Keenan, C., & Lazarus, D. (2015). Can pollutant release and transfer registers (PRTRs) be used to assess implementation and effectiveness of green chemistry practices? A case study involving the toxics release inventory (TRI) and pharmaceutical manufacturers. *Green Chemistry, 17*(5), 2679-2692.

28. Du, X., Zhou, J., Guvench, O., Sangiorgi, F. O., Li, X., Zhou, N., & Xu, B. (2014). Supramolecular assemblies of a conjugate of nucleobase, amino acids, and saccharide act as agonists for proliferation of embryonic stem cells and development of zygotes. *Bioconjugate Chemistry, 25*(6), 1031-1035.

29. Dunn, P. J. (2012). The importance of green chemistry in process research and development. *Chemical Society Reviews, 41*(4), 1452-1461.

30. Dunn, P. J., Galvin, S., & Hettenbach, K. (2004). The development of an environmentally benign synthesis of sildenafil citrate (Viagra™) and its assessment by Green Chemistry metrics. *Green Chemistry, 6*(1), 43-48.

31. Giaquinto, J. R., & Samide, M. J. (2013). Cleaning and recycling mobile phase for chromatographic separations. *ACS Sustainable Chemistry & Engineering, 1*(10), 1225-1230.

32. Giesbrecht, N., & Greenfield, T. K. (1999). Public opinions on alcohol policy issues: A comparison of American and Canadian surveys. *Addiction, 94*(4), 521-531.

33. Harmsen, P. F., Hackmann, M. M., & Bos, H. L. (2014). Green building blocks for bio-based plastics. *Biofuels, Bioproducts and Biorefining, 8*(3), 306-324.

34. Heddle, J. A., Hite, M., Kirkhart, B., Mavournin, K., MacGregor, J. T., Newell, G. W., & Salamone, M. F. (1983). The induction of micronuclei

as a measure of genotoxicity: A report of the US Environmental Protection Agency Gene-Tox Program. *Mutation Research/Reviews in Genetic Toxicology, 123*(1), 61-118.

35. Hogue, C. (2014). California targets products. *Chemical & Engineering News, 92*(12), 6.
36. Hupp, J. T., & Poeppelmeier, K. R. (2005). Better living through nanopore chemistry. *Science, 309*(5743), 2008-2009.
37. Im, J. H., Lee, C. R., Lee, J. W., Park, S. W., & Park, N. G. (2011). 6.5% efficient perovskite quantum-dot-sensitized solar cell. *Nanoscale, 3*(10), 4088-4093.
38. Jacoby, M. (2012). Teaming up for biobased chemicals. *Chemical & Engineering News, 90*(32), 37-38.
39. Jacoby, M. (2014). Tapping solar power with perovskites. *Chemical & Engineering News, 92*(8), 10.
40. Jean, J., Brown, P. R., Jaffe, R. L., Buonassisi, T., & Bulović, V. (2015). Pathways for solar photovoltaics. *Energy & Environmental Science, 8*(4), 1200-1219.
41. Jeon, N. J., Noh, J. H., Yang, W. S., Kim, Y. C., Ryu, S., Seo, J., & Seok, S. I. (2015). Compositional engineering of perovskite materials for high-performance solar cells. *Nature, 517*(7535), 476.
42. Jong, E., Higson, A., Walsh, P., & Wellisch, M. (2012). Product developments in the bio-based chemicals arena. *Biofuels, Bioproducts and Biorefining, 6*(6), 606-624.
43. Kamat, P. V. (2013). Quantum dot solar cells. The next big thing in photovoltaics. *The Journal of Physical Chemistry Letters, 4*(6), 908-918.
44. Kammerer, F. (2011). *Green Chemistry Hazard Traits,* Chapter 54 (Modified text of proposed regulations, Division 4.5, Title 22, California Code of Regulations). Sacramento, California: The Rubber Manufacturers Association.
45. Kerton, F. M., & Marriott, R. (2013). *Alternative solvents for green chemistry* (No. 20). Royal Society of Chemistry.
46. Kidwai, M., & Mohan, R. (2005). Green chemistry: An innovative technology. *Foundations of Chemistry, 7*(3), 269-287.
47. Kim, B. R., Sung, G. H., Ryu, K. E., Kim, J. J., & Yoon, Y. J. (2013). Rapid

and ecofriendly esterification of alcohols with 2-acylpyridazinones. *Bulletin of the Korean Chemical Society, 34*(11), 3410-3414.

48. Kim, H. S., Lee, C. R., Im, J. H., Lee, K. B., Moehl, T., Marchioro, A., & Grätzel, M. (2012). Lead iodide perovskite sensitized all-solid-state submicron thin film mesoscopic solar cell with efficiency exceeding 9%. *Scientific Reports, 2,* 591.
49. Kirchhoff, M. M. (2003). Promoting green engineering through green chemistry. *Environmental science & Technology, 37* (23), 5349-–5353.
50. Kirchhoff, M. M. (2005). Promoting sustainability through green chemistry. *Resources, Conservation and recycling, 44*(3), 237-243.
51. Kojima, A., Teshima, K., Shirai, Y., & Miyasaka, T. (2009). Organometal halide perovskites as visible-light sensitizers for photovoltaic cells. *Journal of the American Chemical Society, 131*(17), 6050-6051.
52. Kolopajlo, L. (2017). Green Chemistry Pedagogy. *Physical Sciences Reviews, 2*(2), 17.
53. Kuang, Y., Shi, J., Li, J., Yuan, D., Alberti, K. A., Xu, Q., & Xu, B. (2014). Pericellular hydrogel/nanonets inhibit cancer cells. *Angewandte Chemie International Edition, 53*(31), 8104-8107.
54. Kurian, J. V. (2005). A new polymer platform for the future—Sorona® from corn derived 1, 3-propanediol. *Journal of Polymers and the Environment, 13*(2), 159-167.
55. Larcher, D., & Tarascon, J. M. (2015). Towards greener and more sustainable batteries for electrical energy storage. *Nature Chemistry, 7*(1), 19-29.
56. Lasker, G. A., Mellor, K. E., Mullins, M. L., Nesmith, S. M., & Simcox, N. J. (2017). Social and environmental justice in the chemistry classroom. *Journal of Chemical Education, 94*(8), 983-987.
57. Lee, M. M., Teuscher, J., Miyasaka, T., Murakami, T. N., & Snaith, H. J. (2012). Efficient hybrid solar cells based on meso-superstructured organometal halide perovskites. *Science, 338*(6107), 643-647.
58. Li, J. W. H., & Vederas, J. C. (2009). Drug discovery and natural products: End of an era or an endless frontier? *Science, 325*(5937), 161-165.
59. Liveris, A. N. (2013). Building the future. *Chemical & Engineering News, 91*(26), 3.
60. Loi, M. A., & Hummelen, J. C. (2013). Hybrid solar cells: Perovskites under the sun. *Nature Materials, 12*(12), 1087.

61. Mahmood, N., Yuan, Z., Schmidt, J., & Xu, C. C. (2015). Hydrolytic depolymerization of hydrolysis lignin: Effects of catalysts and solvents. *Bioresource Technology, 190,* 416-419.

62. Manley, J. B., Anastas, P. T., & Cue, B. W. (2008). Frontiers in Green Chemistry: Meeting the grand challenges for sustainability in R&D and manufacturing. *Journal of Cleaner Production, 16*(6), 743-750.

63. Moras, J. D., Strandberg, B., Suc, D., & Wilson, K. (1996). Semiconductor clusters, nanocrystals, and quantum dots. *Science, 271*, 933.

64. Ng, B. C., Yu, M., Gopal, A., Rome, L. H., Monbouquette, H. G., & Tolbert, S. H. (2008). Encapsulation of semiconducting polymers in vault protein cages. *Nano Letters, 8*(10), 3503-3509.

65. Ning, H., Pikul, J. H., Zhang, R., Li, X., Xu, S., Wang, J., & Braun, P. V. (2015). Holographic patterning of high-performance on-chip 3D lithium-ion microbatteries. *Proceedings of the National Academy of Sciences, 112*(21), 6573-6578.

66. Palomares, V., Serras, P., Villaluenga, I., Hueso, K. B., Carretero-González, J., & Rojo, T. (2012). Na-ion batteries, recent advances and present challenges to become low cost energy storage systems. *Energy & Environmental Science, 5*(3), 5884-5901.

67. Pan, Z., Mora-Seró, I., Shen, Q., Zhang, H., Li, Y., Zhao, K., & Bisquert, J. (2014). High-efficiency "green" quantum dot solar cells. *Journal of the American Chemical Society, 136*(25), 9203-9210.

68. Pandey, M. P., & Kim, C. S. (2011). Lignin depolymerization and conversion: A review of thermochemical methods. *Chemical Engineering & Technology, 34*(1), 29-41.

69. Patel, P. V., Joshi, N., & Panchal, D. P. (2012). Process for preparation of 5-(2-ethoxy-5-((4-methylpiperazin-1-yl) sulfonyl) phenyl)-3-isobutyl-1-methyl-1H-pyrazolo[4,3-d] pyrimidin-7(6H)-one (sildenafil citrate impurity). *Indian Patent Application No. IN 2012MU02516 A, 20140606,* 29.

70. Piatkowski, P., Cohen, B., Ponseca Jr, C. S., Salado, M., Kazim, S., Ahmad, S., & Douhal, A. (2016). Unraveling charge carriers generation, diffusion, and recombination in formamidinium lead triiodide perovskite polycrystalline thin film. *Journal of Physical Chemistry Letter, 7*(1), 204-210.

71. Porter, M. E., & Van der Linde, C. (1995). Green and competitive:

Ending the stalemate. *Harvard Business Review*, *73*(5), 120-134.

72. Qian, F., Zhong, W., & Du, W. (2017). Fundamental theories and key technologies for smart and optimal manufacturing in the process industry. *Engineering*, *3*(2), 154-160.
73. Ritter, S. K. (2015). EPA analysis suggests green success. *Chemical & Engineering News*, *93*(5), 32-33. Dorman, D. C., Beckman, E. J., Beak, P., Cura, J. J., Fairbrother, A., Greene, N., & Quint, J. B. (2014). A framework to guide selection of chemical alternatives.
74. Ritter, S. K., & Nike, B. A. S. F. (2014). Seeing the Green Side of Innovation. *Chemical & Engineering News*, *92*(26), 24-28.
75. Rouhi, M. (2005). Olefin metathesis gets Nobel nod.
76. Scott, A. (2014). Chemistry's electric opportunity. *Chemical & Engineering News*, *92*(28), 11-15.
77. Scott, A. (2015). Making Palm Oil Sustainable. *Chemical & Engineering News*, *93*(9), 19-21.
78. Sheldon, R. A. (2005). Green solvents for sustainable organic synthesis: state of the art. *Green Chemistry*, *7*(5), 267-278.
79. Sneddon, H. (2014). Embedding sustainable practices into pharmaceutical R&D: What are the challenges? *Future Medicinal Chemistry*, *6*(12), 1373-1376.
80. Song, M. K., Zhang, Y., & Cairns, E. J. (2013). A long-life, high-rate lithium/sulfur cell: A multifaceted approach to enhancing cell performance. *Nano Letters*, *13*(12), 5891-5899.
81. Tang, S. Y., Bourne, R. A., Smith, R. L., & Poliakoff, M. (2008). The 24 principles of green engineering and green chemistry: "Improvements productively." *Green Chemistry*, *10*(3), 268-269.
82. Tullo, A. H. (2013). Sustainable acrylic acid. *Chemical & Engineering News*, *91*(46), 18-19.
83. Van Mierlo, J., Maggetto, G., & Lataire, P. (2006). Which energy source for road transport in the future? A comparison of battery, hybrid and fuel cell vehicles. *Energy Conversion and Management*, *47*(17), 2748-2760.
84. Vemula, P. K., & John, G. (2008). Crops: A green approach toward self-assembled soft materials. *Accounts of Chemical Research*, *41*(6),

769-782.

85. Vetenskapsakademien, K. (2005). The Nobel Prize in Chemistry 2005. *Press release, Nobelprize.org*.
86. Weidman, M. C., Seitz, M., Stranks, S. D., & Tisdale, W. A. (2016). Highly tunable colloidal perovskite nanoplatelets through variable cation, metal, and halide composition. *ACS Nano*, *10*(8), 7830-7839.
87. Welch, C. J., Nowak, T., Joyce, L. A., & Regalado, E. L. (2015). Cocktail chromatography: Enabling the migration of HPLC to nonlaboratory environments. *ACS Sustainable Chemistry & Engineering*, *3*(5), 1000-1009.
88. Wessells, C. D., Huggins, R. A., & Cui, Y. (2011). Copper hexacyanoferrate battery electrodes with long cycle life and high power. *Nature Communications*, *2*, 550.
89. Whitesides, G. M., & Boncheva, M. (2002). Beyond molecules: Self-assembly of mesoscopic and macroscopic components. *Proceedings of the National Academy of Sciences*, *99*(8), 4769-4774.
90. Wilson, M. P., & Schwarzman, M. R. (2009). Toward a new US chemicals policy: Rebuilding the foundation to advance new science, green chemistry, and environmental health. *Environmental Health Perspectives*, *117*(8), 1202.
91. Wirth, M., & Thiesse, F. (2014). Shapeways and the 3D printing revolution.
92. Yanes, E. G., Gratz, S. R., Baldwin, M. J., Robison, S. E., & Stalcup, A. M. (2001). Capillary electrophoretic application of 1-alkyl-3-methylimidazolium-based ionic liquids. *Analytical Chemistry*, *73*(16), 3838-3844.
93. Yoon, T. P., Ischay, M. A., & Du, J. (2010). Visible light photocatalysis as a greener approach to photochemical synthesis. *Nature Chemistry*, *2*(7), 527-532.
94. Zhou, Y., Yang, M., Wu, W., Vasiliev, A. L., Zhu, K., & Padture, N. P. (2015). Room-temperature crystallization of hybrid-perovskite thin films via solvent–solvent extraction for high-performance solar cells. *Journal of Materials Chemistry A*, *3*(15), 8178-8184.

CHAPTER 4

CHEMICAL SYNTHESIS ROUTES AND CHARACTERIZATION OF GALLIUM OXIDE-BASED NANOSTRUCTURES

CONTENTS

4.1 INTRODUCTION

Micro- to nanosized gallium oxide can be synthesized with and without the use of surfactant at low temperatures through various synthesis techniques involving hydrothermal routes. Rodlike structures of GaOOH crystals having an average width of 1.5 µm and length of approximately 2.5 µm can be manufactured from Ga and OH with an initial molar ratio of 1:3. Calcination of GaOOH at 900°C yields gallium oxide (â-Ga_2O_3) with morphological features similar to GaOOH. Ga and OH with an initial molar ratio of 1:5 can yield 65-nm-long nanotubes of ç-Ga_2O_3 with external and internal diameters of about 3 and 0.8 3 nm. These oxides of gallium can be synthesized directly in a solution using hydrothermal treatments at 100°C. The suitable combination of transmission electron microscopy (TEM), X-ray diffraction (XRD), N_2 adsorption, energy-dispersive spectroscopy (EDS), and small-area electron diffraction (SAED) can be used to characterize the oxide micro- or nanostructures synthesized via a chemical route. Nonionic and cationic surfactants are typically used for the synthesis of gallium oxide nanostructures. Fabrication of inorganic nanostructured materials has gained an immense importance in nanotechnology and materials science over the last decade due to its wide-spread applications in adsorption, catalysis, ceramics, fluorescence materials, optical materials, and electrochemistry (Planeix et al., 1994; Fendler & Maldrum, 1995; Lakshmi, Patrissi, & Martin, 1997).

Gallium oxide (Ga_2O_3), typically called gallia, is a ceramic with the high melting point of approximately 1900°C (Patrissi & Martin, 1999; Li, Patrissi, Che, & Martin, 2000; Sides, Li, Patrissi, Scrosati, & Martin, 2002; Gowtham, Costales, & Pandey, 2006). Similar to aluminum oxide, gallium oxide can crystallize and form the polymorphs (R, ç, and â). Ga_2O_3 typically exists as an insulator at ambient temperature and pressure condition with an energy (band) gap of about 4.9 eV. However, Ga_2O_3 is a semiconductor at elevated temperatures, typically above 800°C (Sharma & Sunkara, 2002; Mazeina et al., 2009; Sinha et al., 2009; Samala, 2012). Oxygen vacancies in Ga_2O_3 convert it into an N-type semiconductor when it is calcinated in reducing environments (Tippins, 1965; Harwig & Kellendonk, 1978; Binet & Gourier, 1998; Liang et al., 2001).

Phosphorus, gas sensors, and catalysts have been extensively prepared using Ga_2O_3 (Ogita, Saika, Nakanishi, & Hatanaka, 1999; Ogita, Higo, Nakanishi, & Hatanaka, 2001; Tas et al., 2000; Weh, Frank, Fleischer, & Meixner, 2001). Presently, Ga_2O_3 is also being used to manufacture the solid

electrolytes of superior conductivity (Nakagawa et al., 2001; Petre, Auroux, Gelin, Caldararu, & Ionescu, 2001; Xu, Zheng, Hua, Yue, & Gao, 2006; Ishihara, Matsuda, & Takita, 1994; Ishihara, Matsuda, & Takita 1995). One-dimensional (1D) gallium oxide, due to its large surface area, has also been of great importance for the synthesis of nanostructures such as nanotubes, nanowires, and nanoribbons for catalysts and sensor applications. The upcoming generation of optoelectronic and sensing devices can be a potential domain for the use of 1D gallium oxide nanostructures (Dai, You, Duan, Lian, & Qin, 2004; Xiang, Cao, Guo, & Zhu, 2003; Jung, Joo, & Min, 2007).

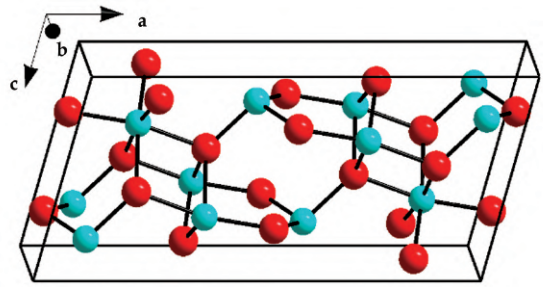

Figure 27. A typical crystal structure of gallium oxide crystal lattice

[Source: https://en.wikipedia.org/wiki/Gallium (III)_oxide]

4.2 SIGNIFICANCE OF SOFT CHEMISTRY ROUTE

Numerous fabrication techniques have been investigated to develop one-dimensional (1D) nanostructures of gallium oxide. Some common fabrication methods include thermal evaporation, chemical vapor deposition, thermal annealing, arc discharge, laser ablation, carbothermal reduction, microwave plasma, oxidation of milling gallium nitride, and catalyst-assisted routes (Kim, Kim, & Lee, 2004; Zhou et al., 2006 et al., 2007;). However, most of the fabrication techniques (discussed above) require high operating temperatures, typically about 1300°C and even above 1600°C (Hu, Li, Meng, Lee, & Lee, 2002; Choi et al., 2000; Huang, Yeh, & Ho, 2004; Gao, Bando, Sato, Zhang, & Gao, 2006). These synthesis routes also implicate complicated procedures, incorporating expensive elements as catalysts which may result in lower purification efficiencies, ultimately influencing

the characteristics of the target material. Recently, the fabrication of 1D nanostructures using via soft chemical routes at lower temperatures is drawing great attention due to the clear benefits, such as energy efficiency, environmental friendliness, and economics (Zhu, Yang, Zhou, & Zhang, 2006; Blom, Mihailetchi, Koster, & Markov, 2007; Chun et al., 2003). Similar to the synthesis of aluminum oxide, the essential precursor for the synthesis of gallium oxide is gallium oxide hydroxide (GaOOH) (Zhang et al., 1999; Gundiah, Govindaraj, & Rao, 2002; Kim et al., 2002).

Presently, a limited number of synthesis routes are used for the fabrication of 1D Ga_2O_3 or GaOOH nanostructures. Sato and Nakamura (1982) investigated the precipitation of GaOOH in a chemical solution formulated by blending gallium chloride with various alkalis such as Na_2CO_3, NaOH, KOH, $NaHCO_3$, and NH_4OH. Hamada, Bando, & Kudo (1986) investigated the creation of monodispersed GaOOH nanoparticles with an average diameter of 100 nanometers in the presence of sulfates by hydrolysis reactions at high temperatures. Avivi, Mastai, Hodes, & Gedanken (1999) developed cylindrical-layered scroll-like crystals of GaOOH with a trace amount of metallic gallium enclosed inside through a sonochemical reaction. Tas, Majewski, & Aldinger (2002) produced spindle-like single crystals of GaOOH and quadrilateral prisms by instigating the forced hydrolysis of Ga^{3+} in the presence of decomposed urea and pure water. The calcination process results in the loss of morphological features in spindles, whereas the morphology of quadrilateral prisms is maintained.

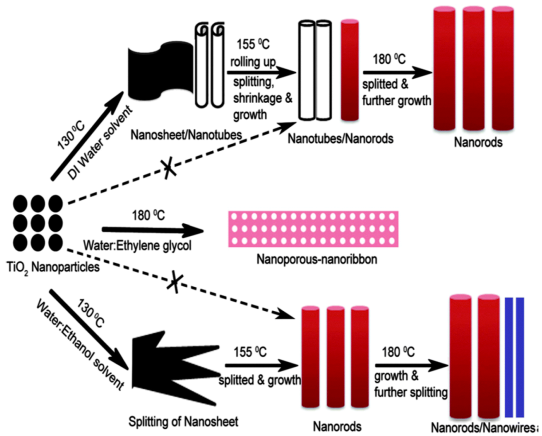

Figure 28. Schematic illustration of 1D nanostructure synthesis via various chemical routes using different solvents

[Source: http://pubs.rsc.org/en/content/articlelanding/2014/cs/c3cs60219b/unauth]

Cheng and Samulski (2001) synthesized â- and ç-Ga_2O_3 nanotubes by dipping Al_2O_3 membranes in an amorphous sol of $Ga_2O_3âH_2O$, followed by dehydrating and induction heating at 500°C. Patra et al. (2006) synthesized GaOOH rods of sub-micrometer size by refluxing the aqueous solution of NH_4OH and $Ga(NO_3)_3$ in a microwave furnace. Zhang, Wu, Hu, & Shi (2007) fabricated nanorods of GaOOH through a large-scale hydrothermal process using $GaCl_3$-H_2O-NaOH solution with controlled pH conditions (Liu, Qiu, Zhao, Zhang, & Yi, 2007). Ristic, Popović, & Musić (2005) investigated the use of the solgel technique in the fabrication of gallium oxide and gallium oxyhydroxide by the hydrolysis of $GaCl_3$ and gallium isopropoxide in the presence of aqueous tetramethylammonium hydroxide solution. In the recent past, Liu et al. (2007) synthesized nanorods of Ga_2O_3 by the conversion of hydrothermally produced GaOOH nanorods using NaN_3 and Ga_2O_3 as precursors. Zhang et al. (2007) explored a green hydrothermal route (performed at 200°C) for the production of GaOOH nanorods using water and Ga_2O_3 starting materials in the absence of a surfactant. It has been observed that gallium oxide hydroxide or gallium oxide nanostructures fabricated through non-hydrothermal methods are beltlike or threadlike which are much smaller in width and longer in length than those developed through hydrothermal routes. The morphology of GaOOH or Ga_2O_3 reported via the hydrothermal route is spindle-like or rodlike crystal having a width of 100 nanometers with a small surface area to volume ratio.

The objective of the research on the synthesis of Ga_2O_3 is to investigate the effect of experimental methods on the properties of gallium oxide-based nanomaterials. Zhao, Frost, & Martens (2007) prepared micro- to nanosized gallium oxide particles under different experimental conditions using the soft chemical route. For comparison purposes, both cationic and nonionic surfactants were employed to get a comprehensive understanding of the gallium oxide growth. Excitingly, it was reported that the nanotubes of Ga_2O_3 with a width of 3 nanometers could be materialized using a low-temperature hydrothermal process. The report by Zhao et al. (2007) is considered the pioneer for the synthesis of gallium oxide via a soft chemical route at lower temperatures without calcination reactions (Zhan, Bando, Hu, & Golberg, 2004; Graham, Sharma, Sunkara, & Davis, 2003; Knez et al., 2006).

4.3 EXPERIMENTAL METHODS

Analytical-grade $Ga(NO_3)_3$, HNO_3, and NaOH are employed as precursors to synthesize the precipitates of gallium hydrate. Cationic surfactants (N-cetyl-N, N, N-trimethylammonium bromide-CTAAB and $C_{19}H_{42}NBr$) and nonionic surfactants (polyethylene oxide-PEO, C_{12}-$14H_{25}$-29O (CH_2CH_2O)7H, and Tergitol 15-S-7) are typically used in the synthesis process. Two fabrication routes are explained in this chapter. The detailed experimental route followed by Zhao et al. (2007) is discussed in the appending text.

About 0.012 mol of $Ga(NO_3)_3$ was mixed in pure water to develop a solution (A) with a molar ratio of water to metal ion of 100:1 and heated to 80°C. 1.5 molar NaOH was gradually added into the solution (A) dropwise. Around 0.036 mols (three times the quantity of $Ga(NO_3)_3$) of NaOH was, collectively, used to create a precipitate. The chemical mixture was then airtight and put in a shaking bath at a shaking rate of 100 rpm at a temperature of 80°C for 2 hours. The resultant precipitate was obtained by centrifugation process and washed with the pure water many times to ensure the removal of sodium nitrate. The final (washed) precipitates were divided into three equal parts, followed by mixing of two parts with CTAB and PEO separately. However, no surfactant was incorporated in the remaining (third) part.

Table 3. Lattice parameters for various samples prepared before and after calculations

Sample ID	lattice parameter (Å)	Error	Value
precipitate	*a*	0.00243	9.820
	b	0.00073	2.975
	c	0.00141	4.565
P1-PEO	*a*	0.00104	9.812
	b	0.00032	2.974
	c	0.0006	4.572
P1-CTAB	*a*	0.00118	9.812
	b	0.00047	2.973
	c	0.00078	4.568
P1-None	*a*	0.0015	9.810
	b	0.00047	2.974
	c	0.00078	4.566

P1-PEO-c	*a*	0.00459	12.228
	b	0.00113	3.035
	c	0.00264	5.803
P1-CTAB-c	*a*	0.00308	12.243
	b	0.00042	3.035
	c	0.00098	5.810
P1-None-c	*a*	0.00432	12.254
	b	0.00084	3.035
	c	0.00158	5.803

The molar ratio of Ga to surfactant is 1: 0.4, while the amounts of added PEO and CTAB were equal. Samples were vigorously stirred for 2 hours at room temperature. After stirring, the specimens were treated hydrothermally at 100°C for 48 hours. The specimens were then splashed with ultrapure water many times and dehydrated in the air at about 80°C. The calcination of dried solids was carried out for 2 hours at 900°C. The dehydrating temperature was increased from the room temperature at a constant rate of 2.5°C/min. The end products prepared with and without the addition of surfactants (CTAB, PEO) before and after calcination were termed as P1-PEO, P1-None, P1-CTAB, P1-PEO-c, P1-None-c, and P1-CTAB-c, respectively.

Table 4. Crystallite size calculations, peak positions and HWHM for specimens manufactured through procedure

Sample name	***H, K, L***	**Size (nm)**	**Peak position (Deg)**	**HWHM (Rad)**
Precipitate	400	56.9	36.576	0.0026
	200	47.7	39.393	0.0031
P1-PEO	400	53.3	36.571	0.0027
	200	43.2	39.394	0.0034
P1-CTAB	400	58.6	36.590	0.0025
	200	36.2	39.467	0.0041
P1-None	400	54.1	36.584	0.0027
	200	34.3	39.456	0.0043
P1-PEO-c	400	22.0	30.058	0.0065

P1-CTAB-c	400	19.2	30.098	0.0075
P1-None-c	400	22.7	30.064	0.0063

The alternate synthesis route (procedure 2) does not involve the preparation of gallium hydrate (precursor) at the initial stage. However, clear solutions were synthesized in three different containers by mixing 0.015 molar $NaNO_3$ in 10 ml water and 0.003 molar gallium nitrate solution in 10 ml water at ambient room temperatures. The resultant transparent solution was sealed, followed by constant stirring at a rate of 100 rpm for 2 hours at 80°C. The first two containers were added with 0.0025 mol CTAB and PEO, respectively, while the third container was kept intact. After the addition of surfactants, the solutions were provided with 5 ml ultrapure water, followed by constant stirring for 30 minutes to ensure the uniformity of the solution. Analytical-grade HNO_3 was added to the solution in each container to form a white precipitate with a pH value of 9.5. Each container was sealed and stored in the autoclaves, followed by hydrothermal treatment at 100°C for 48 hours. The final products prepared with surfactants (CTAB and PEO) and without surfactants were categorized as P2-CTAB, P2-None, and P2-PEO, respectively. Finally, the resultant specimens were characterized using several advanced techniques (Zhao & Frost, 2008).

A transmission electron microscope (Philips CM 200) is used at 200 KV to examine the morphology of gallium oxide specimens. Energy-dispersive X-ray (EDX) analysis using the transmission electron microscope was carried out using Oxford Instruments Link microanalysis system. X-ray diffraction (XRD) analysis was carried out using an X-ray diffractometer (PANalytical X'Pert PRO) with a copper X-ray tube, operating at 35 mA and 45 kV (Zhao et al., 2007)

4.4 CHARACTERIZATION OF GALLIUM OXIDE

Different characterization methods are employed to investigate physical, chemical, morphological, and crystallographic properties of gallium oxide. Some common characterization techniques and their functionalities are discussed in the subsequent text.

4.4.1 Surface Properties, Morphology, and Phase

Figure 29 illustrates the XRD graph with patterns of different specimens synthesized through procedure 1. XRD pattern of pure CTAB is also incorporated in Figure 3 as a reference entity. PEO surfactant is liquid at

room temperature; therefore, no XRD peaks are shown in Figure 29. The precipitate specimen quoted in Figure 3 was synthesized through procedure 1 before hydrothermal treatment, followed by 2 hours of aging.

It was observed that the synthesis of GaOOH in place of Ga-$(OH)_3$ was desirable in a pH range of 6–8 (Carrot et al., 1987). The molar ratio of NaOH to $Ga(NO_3)_3$ used for reactions in procedure 1 is 3:1, in which the pH of the colloidal precipitates after reactions was closer to neutral. It is quite evident from Figure 29 that all the peaks in the diffraction pattern of the precipitate sample can be allotted to orthorhombic GaOOH. These results are congruent with the experimental results obtained by Zhang et al. (1999).

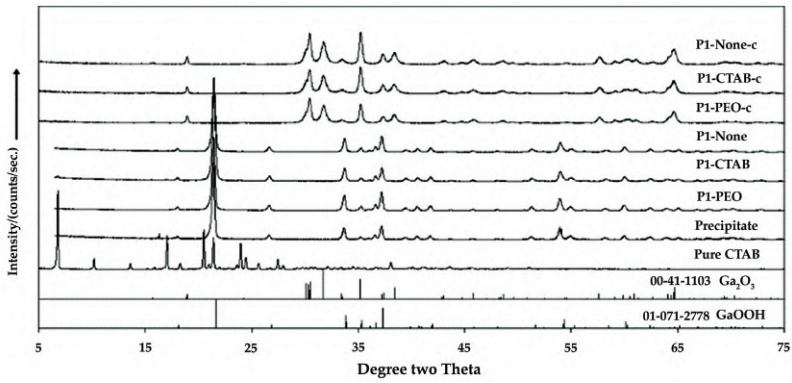

Figure 29. XRD patterns of the specimens prepared through procedure 1 prior and postcalcination

[Source: http://pubs.acs.org/doi/abs/10.1021/jp075575y]

It can be observed from the XRD patterns that all the specimens before and after hydrothermal treatment (with and without surfactant) at 100°C for 48 hours are pure and well-crystallized phases of GaOOH. The above indication suggests the absence of any phase transformation during the growth process of GaOOH crystals. As compared to the precipitate sample, the increment in peak sharpness was not observed for other samples after 48 hours of hydrothermal treatment. It was obvious from the observation that there was a negligible change in specimens' crystallinity during the process of hydrothermal treatment. XRD peaks of the specimens after calcination can be allocated to monoclinic â-Ga_2O_3, that is, JCPDS card 00–041–1103. The XRD peaks from the corresponding GaOOH were not observed, which indicate the complete transformation of the GaOOH phase into â-Ga_2O_3 after calcination (Kaneko, Ishii, & Ruike, 1992).

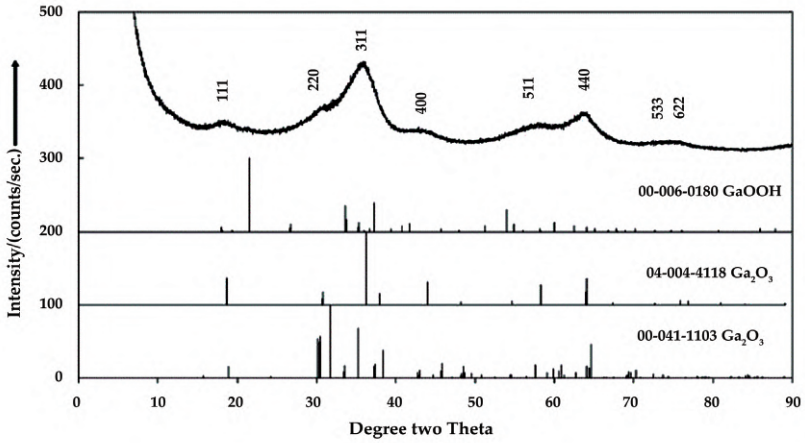

Figure 30. XRD patterns of specimens synthesized by PEO through procedure 2

Source: http://pubs.acs.org/doi/abs/10.1021/jp075575y]

XRD analysis was used to characterize the general crystal structure of the manufactured specimen via procedure 2. XRD patterns of all the specimens fabricated with and without the use of surfactants are similar. Figure 30 illustrates the XRD pattern of specimen formulated with PEO surfactant. It was reported that GaOOH phases were attained by low-temperature (180°C) hydrothermal treatment. However, Ga_2O_3 is prepared at high temperatures, that is, 500°C. All the specimens developed by Zhao et al. (2007) were treated at fairly low temperatures (<100°C). It is quite evident from Figure 30 that the diffraction pattern peaks cannot be indexed to gallium oxide hydroxide. The overall broad diffraction pattern indicates the presence of small-sized particles in the resultant specimen. It can be noticeably observed that all the diffraction peaks in Figure 30 can be allotted to cubic gallium oxide (ç-Ga_2O_3) instead of monolithic solid gallium oxide (â-Ga_2O_3), that is, JCPDS card 04–004–4118 instead of JCPDS card 00–041–1103.

4.4.2 Determination of pH

The molar ratio of NaOH to $Ga(NO_3)_3$ for procedure 2 reactions is 5:1, that is, there is an abundant amount of alkali in the reaction. In this study, the solution of sodium hydroxide was gently dropped into an aqueous solution of gallium nitrate with an initial pH value of around 1.8–1.9 (Barret et al., 1951; Voegtlin et al., 1997). A transparent solution, with the pH ≤ 10 and

pH ≤ 3, was formulated in the system containing $Ga(NO_3)_3$-H_2O-NaOH. The pH of the system is slightly different from the clear solution of the system containing $GaCl_3$-H_2O-NaOH with pH ≤ 9 and pH ≤ 4 (Joyner et al., 1951). In primary stages, gallium existed as soluble salts (e.g., $Ga(OH)_2NO_3$ and $Ga(OH)(NO_3)_3$) with pH ≤3. The system became turbid soon after the appearance of a fluffy precipitate accompanied by a pH change from 3 to 10. The gallium compound starts converting into a deprotonated acid of gallium due to a gradual increase in pH value over 10. In this experiment, the complete mixing aqueous $Ga(NO_3)_3$ solution and the NaOH solution result in the formation of a clear solution. No precipitate or solid product was witnessed after the aging of a clear solution for 2 hours, which was also observed for the system containing $GaCl_3$-H_2O-NaOH at a pH of 9 (Basaldella, Tara, Armenta, Patino-Iglesias, & Castellón, 2006).

4.4.3 Characteristics of Crystal Structure

Lattice parameters of the specimens (synthesized through procedure 1 pre- and postcalcination) before hydrothermal treatment and after aging process were calculated by utilizing XRD pattern data (Table 1). As compared to the precipitate specimen, the lattice parameters *c* increased, and *a* decreased after hydrothermal treatment of the other specimens. However, the lattice parameter *b* remained constant during the hydrothermal treatment. A minimal difference was observed in the lattice parameters *c* and *a* between specimens synthesized before calcination with and without the use of surfactants after hydrothermal treatment. It was reported that P1-PEO specimen possesses the highest lattice parameter *c*. On the other hand, the samples prepared after calcination with and without the use of surfactants also exhibited disparities in lattice parameters *c* and *a*. Parameter *a* particularly showed a comparatively large difference in its value. A minimum effect was observed for parameter *b* due to the addition of surfactant (Fernandez et al., 2004).

Table 5 exhibits the peak position, crystallite sizes, and half-width half-maximum of specimens synthesized through procedure 1 before and after calcination. The size of crystallites along *c* and crystallographic directions in precipitate specimen before hydrothermal treatment and after aging process are 47.7 and 56.9 nm, respectively. After 48 hours of hydrothermal treatment, the size of crystallites in specimens manufactured with and without the use of surfactants fluctuates from 34.3 to 43.2 nm alongside the crystallographic direction *c* and from 53.3 to 58.6 nm alongside the crystallographic direction *a*. It was observed that a specimen synthesized with CTAB surfactant contains a larger size of crystallites before calcination

reactions and smaller size of crystallites after calcination reactions along the crystallographic direction *a,* while the other two specimens, synthesized with PEO surfactant and without the use of surfactant, did not show such kind of dilation in the lattice parameters (Aaritalo, Piispanen, Rosling, & Areva, 2011).

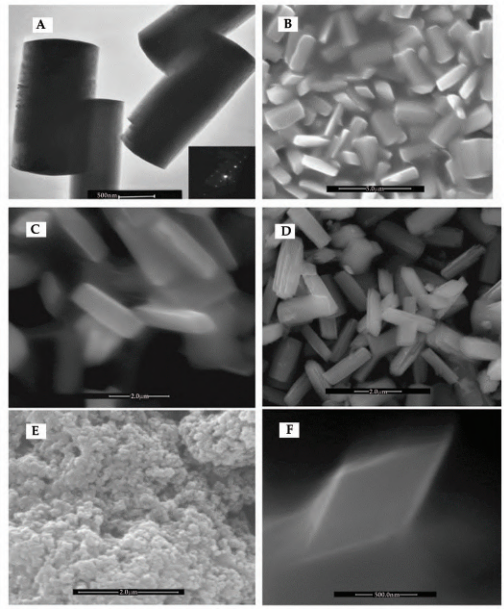

Figure 31. Morphological characteristics of specimens synthesized by procedure 1: (A) Transmission electron microscopic image of P1-PEO specimen. (B) Scanning electron microscopic (SEM) image of P1-PEO specimen. (C) SEM micrograph of precipitate samples with 2 hours of aging. (D) Specimen during constant shaking and stirring. (E) SEM micrograph of a precipitate specimen taken after the reaction and before aging process. (F) SEM image of the GaOOH crystal section at the end. [The scale bar in parts F and A is 500 nm, part B 5 μm, and parts C, D, and E 2 μm].

[Source: http://pubs.acs.org/doi/abs/10.1021/jp075575y]

The formation of spindle-like, rodlike, and zeppelin-like GaOOH nanoparticles under various conditions has been reported in some of the previous studies. In the current work by Zhao et al. (2007), the morphological characterization of the resultant specimens synthesized through procedure 1 was carried out by SEM and TEM. Figure 31(A, B) illustrates the typical SEM and TEM images of a specimen synthesized with PEO surfactant after

hydrothermal treatment before calcination reactions. It is quite obvious from Figure 31A that the resultant crystals of gallium oxide hydroxide in P1-PEO specimen are rodlike containing a smooth surface. The corresponding diffraction spectra of GaOOH single crystal have been shown in the inset. There was no evidence of fluffy aggregates in the specimens after 48 hours of hydrothermal treatment manufactured from procedure 1 with and without the use of surfactant. Figure 31 (B, F) depicts the rhombus cross section of the resultant GaOOH rods. The lengths of the quadrilateral rods manufactured with PEO surfactant ranged between 2.16 and 3.09 μm, with an average value of 2.56 μm. On the contrary, the average length values of a specimen synthesized with CTAB surfactant and without any surfactant are typically 2.52 and 2.54 μm, respectively. The average width of the quadrilateral prisms produced with CTAB and PEO and without the use of surfactant is 1.55, 1.53, and 1.56 μm, respectively. It is estimated that the overall morphological features of the specimens produced through procedure 1 (with and without the use of surfactant) must be similar (Yokoi, Yoshitake, & Tatsumi, 2004).

Figure 31C exhibits the morphological features of a precipitate specimen obtained after 2 hours of aging with a constant shaking before the hydrothermal treatments. The whole precipitate specimen is a quadrilateral prism with smooth surfaces. The width of the specimen ranges between 0.89 and 1.67 μm with an average value of 1.32 μm that is approximately 15% lesser than that of specimens obtained after 48 hours of hydrothermal treatment. On the other hand, the length of the quadrilateral prism in the precipitate specimen ranges between 2.05 and 2.63 µm, with a mean value of 2.40 µm, which is around 5% lesser than that of specimens obtained after 48 hours of hydrothermal treatment. The growth process of GaOOH was studied by taking out a specimen after the addition of NaOH solution in the aqueous solution of $Ga(NO_3)_3$ under the constant stirring at 80°C (before thermal aging). Figure 31E shows the morphology of this specimen. It can be observed that the specimen taken out before the aging process is a structureless aggregate with no ordered quadrilateral rods. The above data propose that the growth of GaOOH crystals from a colloidal precipitate to quadrilateral prism primarily occurred during the aging process. Conversely, a rapid crystal growth can occur during the 2 hours of stirred aging to produce natural gallium oxide hydroxide crystals (quadrilateral prisms). The specimens were compared by keeping all the synthesis parameters same except the use of stirring in place of shaking during the aging process. It was observed that the resultant crystals of GaOOH possessed layered structured

after aging and before hydrothermal treatment, which indicates the effect of vigorous stirring on the growth of GaOOH crystals.

A similar crystallographic phenomenon was also witnessed in an experiment on Ga-doped AlOOH with the Ga content of around 20%. The formation of layered GaOOH structure in the initial stage is unclear because of the constant stirring. It is quite probable that the stirring caused the regularly shaped quadrilateral prism to get damaged, ultimately resulting in the creation of the layered structure of gallium oxide hydroxide (GaOOH) crystals. A trace amount of comparatively smaller nanorods making flowerlike or cross-shaped structures was also witnessed in this specimen. The fragmented layered crystals of GaOOH retained their morphological features after 48 hours of hydrothermal treatment. The following conclusions can be drawn from the above observations:

- The rapid crystal growth occurred for GaOOH during the 2 hours of aging process.
- The crystals of GaOOH were created by consuming the structureless aggregate of nanoparticles.
- The formation of comparatively larger crystal resulted in the slowing of growth rates (Eklund, Bäckman, Idman, Norström, & Rosenholm, 2000; Klaysri, Tubchareon, & Praserthdam, 2017).

4.4.4 Absorption and Desorption Properties

Figure 32 demonstrates the morphological features of Ga_2O_3 specimens produced from procedure 1 with and without the use of the surfactants. The morphological characteristics of GaOOH can be reserved after calcination process, irrespective of the surfactant type and quantity.

It is quite a challenging job to demonstrate the morphological differences among specimens synthesized with CTAB and PEO just through SEM analysis. N_2 adsorption/desorption studies, cumulative pore volume, pore size distribution, and *t*-plot analysis studies were performed to measure the porosities and surface areas of the resultant samples. It is a well-established fact that the porosity of the solids strongly influences the absorption characteristics. If the material is mesoporous, the capillary-type condensation reactions will take place in each pore after the approaching the relative pressure to a certain value which is associated with the pore radius by the Kelvin equation, ultimately resulting in a type IV isotherm (Abou-El-Sherbini et al., 2010).

Figure 33 illustrates the adsorption/desorption isothermal curves for specimens synthesized through procedure 1 after calcination reactions. All these isothermal curves can be indexed as type IV isotherm due to the presence of the mesoporous structure. The presence of micropores and mesopores was indicated by three isotherms forming hysteresis loops of type H3, which do not show any restrictive adsorption at high P/P0. Sinha et al. (2009) reported that aggregates of platelike particles instigate the type H3 loop which is usually associated with slitlike pores. The rodlike morphological features present in the resultant $\hat{a}$-Ga_2O_3 result in slitlike as reported by Sinha et al. (2009). Monolayer–multilayer adsorption can be observed in the initial portion of the isotherms which contain the same adsorption and desorption curves.

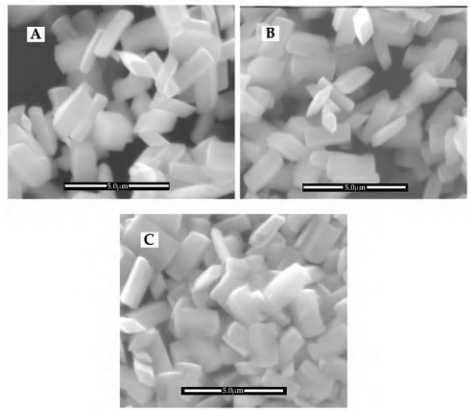

Figure 32. SEM micrographs of specimens. (A) Synthesized without the use of surfactant. (B) Synthesized with PEO and (C) synthesized with CTAB through procedure 1 after calculations.

[Source: http://pubs.acs.org/doi/abs/10.1021/jp075575y]

The extraordinary small adsorption of nitrogen at low P/P0 indicates the low porosity content in all the three samples. It is quite obvious from Figure 7 that specimens synthesized with surfactant (P1-PEO-c) and without surfactant (P1-None-c) exhibit similar hysteresis effects near superposition which is an indication of the lower absorption. The graph indicates the predominance of capillary condensation specimens P1-None-c and P1-PEO-c. The isothermal curve for a specimen manufactured with surfactant P1-CTAB-c exhibited a comparatively lower hysteresis effect that is considered from P1-None-c and of P1-PEO-c. The diameter of the

filling pore is associated with the P/P0 location of the reflection points. It was observed that the steeper gas uptake sites for P1-PEO-c, P1-CTAB, and P1-None-c are 0.8, 0.9, and 0.8, respectively. The positioning results indicate that the crystal texture in samples P1-PEO-c and P1-None-c would be different from the texture of sample P1-CTAB-c. The *t-plot* analysis discloses significant information regarding the structure of pores. The *t*-plot for microporous materials is described by two linear regions. The first region symbolizes the layer-by-layer adsorption of gas in the mesopores, while the second region is linked with monolayer coverage and micropore filling (De Witte, Vercruysse, Aernouts, Verwimp, & Uytterhoeven, 1996).

The linear part of the *t*-plot signifies the microporosity, while the residual portion at greater thickness region relates to pores of slit shape between the crystal layers (Pierre, 1998). Figure 34 displays the *t*-plots of specimens P1-None-c, P1-CTAB-c, and P1-PEO-c. It was reported by Kraout and Pierre (2007) that the *t*-plot would exhibit an upward deviation originating at a relative pressure which instigates the filling of the pores. Figure 6 displays the porosity profile of the three types of specimens. It can be observed that specimens P1-None-c and P1-PEO-c exhibit comparatively higher microporosity and mesoporosity than specimen P1-CTAB-c. The t-plot uptake was spanned over a lower thickness region for specimens P1-None-c and P1-PEO-c as compared to specimen P1-CTAB-c. The relative pressure is directly proportional to the thickness. Therefore, the t-plot analysis showed that the overall pore sizes in specimens fabricated with CTAB are unusually larger than those in specimens P1-None-c and P1-PEO-c. This result is consistent with the extraordinarily smaller hysteresis effects shown in Figure 30. The pore size distribution of specimens P1-PEO-c, P1-None-c, and P1-CTAB-c is shown in Figure 35. The pore sizes concentrated in 2–30 nm range and the overall distribution curve for pore size of specimens P1-None-c and P1-PEO-c are approximately similar. The highest volume of the pore was noted at 15 nm pore diameter for both samples P1-None-c and P1-PEO-c. On the contrary, the specimens synthesized from CTAB surfactant exhibit extraordinary broad pore distribution curve as compared to the specimens synthesized with PEO and without surfactant. Most of the pores present in P1-CTAB-c possess a wide range of diameters (typically between 10 and 70 nm). The highest volume of the pore was witnessed for the pores having a diameter between 20 and 30 nm (Schramm, Rinderer, Tessadri, & Duelli, 2010; Pierre & Rigacci, 2011).

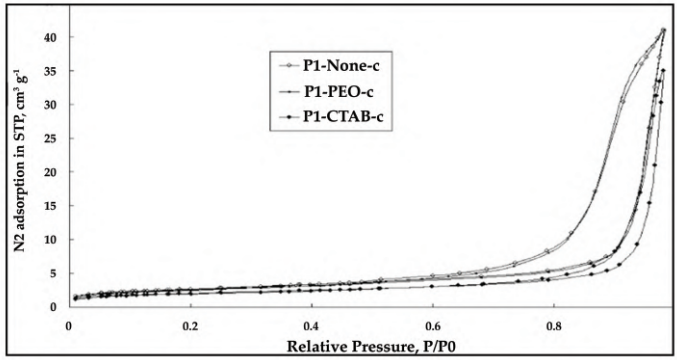

Figure 33. Nitrogen adsorption and desorption isotherms for specimens produced through procedure 1 after calculations

[Source: http://pubs.acs.org/doi/abs/10.1021/jp075575y]

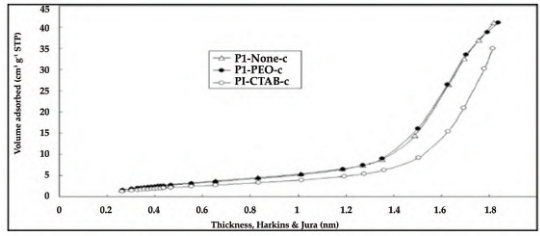

Figure 34. t-plot of specimens synthesized through procedure 1 after calculations

[Source: http://pubs.acs.org/doi/abs/10.1021/jp075575y]

Table 5. Pore volume (Vp), pore diameter, and BET-specific surface area (SBET) for samples fabricated via procedure 1 after calcination

Sample ID	S_{BET}, $m^2 g^{-1}$	V_P, [a] $cm^3 g^{-1}$	**mean *D*, nm**	
			BET[b]	**BJH**[c]
P1-PEO-c	9.09	16.16	27.9	15.7
P1-CTAB-c	7.11	7.38	30.5	29.1
P1-None-c	9.46	15.87	26.8	16.0

Vp[a]= Cumulative adsorption volume of pores ranging from 1.7 to 300 nm diameter.

BET[b]= Average adsorption diameter of the pore (4*V*/*A* by BET).

BJH[c]= BJH (Barrett–Joyner–Halenda) average desorption diameter of pore (4*V*/*A*)].

S_{BET} (BET-specific surface area), pore diameter, and V_p (pore volume) of specimens fabricated with and without the use of surfactant through procedure 1 are illustrated in Table 6.

BET-specific surface areas for specimens fabricated without surfactants and with surfactants (CTAB and PEO) through procedure 1 after calcination reactions are, respectively, 7.11, 9.09, and 9.46 $m^2âg^{-1}$. It was observed that specimens manufactured with surfactants contained lower surface areas as compared to the specimens synthesized without surfactants. Particularly, sample P1-CTAB-c exhibited 25% reduction in the surface area as compared to the specimen P-None-c. The surface areas of samples P1-None-c and P1-PEO-c are entirely congruent.

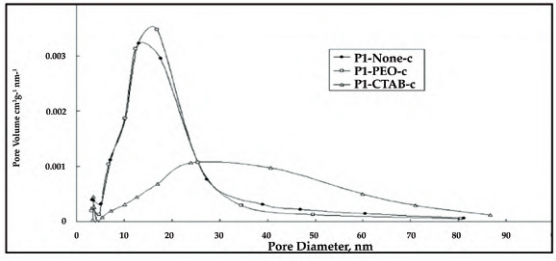

Figure 35. The distribution of pore size in specimens synthesized through procedure 1 after calculations

[Source: http://pubs.acs.org/doi/abs/10.1021/jp075575y]

Considerably lower pore volumes were observed for the specimens fabricated with CTAB surfactant (7.38 $cm^3âg^{-1}$). On the other hand, the specimens P1-None-c (15.87 $cm^3âg^{-1}$) and P1-PEO-c (16.16 $cm^3âg^{-1}$) exhibited higher pore volumes.

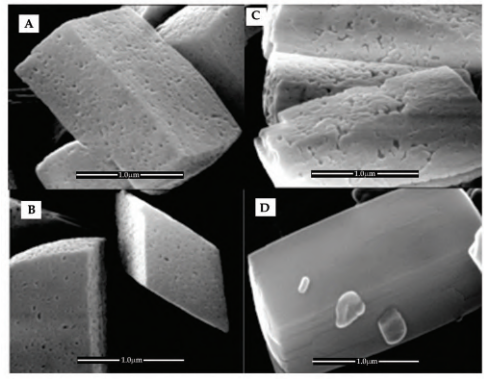

Figure 36. A SEM micrograph was taken at high magnification exhibiting the detailed morphological feature of (A) specimen P1-None-c, (B) specimen P1-PEO-c, (C) specimen P1-CTAB-c, and (D) specimen P1-CTAB.

[Source: http://pubs.acs.org/doi/abs/10.1021/jp075575y]

The morphological features of the specimens manufactured with and without the use of surfactants via procedure 2 are exhibited in Figure 36. It is quite obvious that amorphous aggregates are abundantly present in specimens P2-None, P2-CTAB-c, and P2-PEO. Approximately 69-nm-long nanotubes and CTAB with external and internal diameters of around 3.0 and 0.8 nm were produced in all these three specimens. The XRD results presented in Figure 29 are consistent with the above-mentioned TEM results.

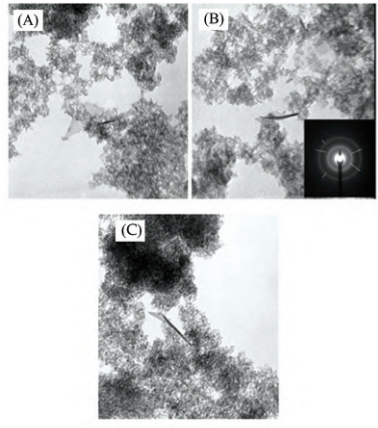

Figure 37. TEM image of the specimens synthesized (A) without any surfactant, (B) with PEO surfactant, and (C) with CTAB surfactant

[Source: http://pubs.acs.org/doi/abs/10.1021/jp075575y]

It was observed that a trace amount of nanotubes was produced in the specimen manufactured without a surfactant. The total length of the nanotubes produced in the specimen manufactured without a surfactant was extraordinary smaller than those produced in specimens fabricated with surfactants. A clear difference that can be observed from TEM images for specimens manufactured with CTAB and PEO is the formation of lesser nanotubes in the former (CTAB-based specimen) than in the latter (PEO-based specimen).

REFERENCES

1. Aaritalo, V., Piispanen, M., Rosling, A., & Areva, S. (2011). Silicon releasing sol–gel TiO_2–SiO_2 30/70 films. *Thin Solid Films, 519*(22), 7845-7849.
2. Abou-El-Sherbini, K. S., Pape, C., Rienetz, O., Schiel, D., Stosch, R., Weidler, P. G., & Höll, W. H. (2010). Stabilization of n-aminopropyl silica gel against hydrolysis by blocking silanol groups with TiO_2 or ZrO_2. *Journal of Sol-Gel Science and Technology, 53*(3), 587-597.
3. Avivi, S., Mastai, Y., Hodes, G., & Gedanken, A. (1999). Sonochemical hydrolysis of Ga3+ ions: Synthesis of scroll-like cylindrical nanoparticles of gallium oxide hydroxide. *Journal of the American Chemical Society, 121*(17), 4196-4199.
4. Barrett, E. P., Joyner, L. G., & Halenda, P. P. (1951). The determination of pore volume and area distributions in porous substances. I. Computations from nitrogen isotherms. *Journal of the American Chemical Society, 73*(1), 373-380.
5. Basaldella, E. I., Tara, J. C., Armenta, G. A., Patino-Iglesias, M. E., & Castellón, E. R. (2006). Propane/propylene separation by selective olefin adsorption on Cu/SBA-15 mesoporous silica. *Journal of Sol-Gel Science and Technology, 37*(2), 141-146.
6. Binet, L., & Gourier, D. (1998). Origin of the blue luminescence of β-Ga_2O_3. *Journal of Physics and Chemistry of Solids, 59*(8), 1241-1249.
7. Blom, P. W., Mihailetchi, V. D., Koster, L. J. A., & Markov, D. E. (2007). Device physics of polymer: Fullerene bulk heterojunction solar cells. *Advanced Materials, 19*(12), 1551-1566.
8. Calabrese, M. A., & Wagner, N. J. (2017). New insights from Rheo-small-angle neutron scattering. In *Wormlike Micelles* (pp. 193-235). Royal Society of Chemistry.
9. Carrott, P. J. M., Roberts, R. A., & Sing, K. S. W. (1987). Adsorption of nitrogen by porous and non-porous carbons. *Carbon, 25*(1), 59-68.
10. Cerveau, G., Corriu, R. J., Framery, E., & Lerouge, F. (2004). Auto-organization of nanostructured organic−inorganic hybrid xerogels prepared by sol−gel processing: The case of a “twisted” allenic precursor. *Chemistry of Materials, 16*(20), 3794-3799.
11. Charlton, I. D. (1999). New insights into micellar structural evolution

and interaction using voltammetric methods.

12. Cheng, B., & Samulski, E. T. (2001). Fabrication and characterization of nanotubular semiconductor oxides In_2O_3 and Ga_2O_3. *Journal of Materials Chemistry*, *11*(12), 2901-2902.
13. Chevalier, Y., & Zemb, T. (1990). The structure of micelles and microemulsions. *Reports on Progress in Physics*, *53*(3), 279.
14. Choi, Y. C., Kim, W. S., Park, Y. S., Lee, S. M., Bae, D. J., Lee, Y. H., & Kim, J. M. (2000). Catalytic growth of β-Ga_2O_3 nanowires by arc discharge. *Advanced Materials*, *12*(10), 746-750.
15. Chun, H. J., Choi, Y. S., Bae, S. Y., Seo, H. W., Hong, S. J., Park, J., & Yang, H. (2003). Controlled structure of gallium oxide nanowires. *The Journal of Physical Chemistry B*, *107*(34), 9042-9046.
16. Clausen, T. M., Vinson, P. K., Minter, J. R., Davis, H. T., Talmon, Y., & Miller, W. G. (1992). Viscoelastic micellar solutions: Microscopy and rheology. *The Journal of Physical Chemistry*, *96*(1), 474-484.
17. Cummins, P. G., Penfold, J., & Staples, E. (1992). A study of the structure of mixed cationic/nonionic micelles by small-angle neutron scattering spectrometry. *Langmuir*, *8*(1), 31-35.
18. Cummins, P. G., Staples, E., Penfold, J., & Heenan, R. K. (1989). The geometry of micelles of the poly (oxyethylene) nonionic surfactants C16E6 and C16E8 in the presence of electrolyte. *Langmuir*, *5*(5), 1195-1199.
19. Cummins, P. O., Hayter, J. B., Penfold, J., & Staples, E. (1987). A small-angle neutron scattering investigation of shear-aligned hexaethyleneglycolmonohexadecylether (C16E6) micelles as a function of temperature. *Chemical Physics Letters*, *138*(5), 436-440.
20. Dai, L., You, L. P., Duan, X. F., Lian, W. C., & Qin, G. G. (2004). Synthesis of Ga_2O_3 chains with closely spaced knots connected by nanowires. *Journal of Crystal Growth*, *267*(3), 538-542.
21. De Witte, B., Vercruysse, K., Aernouts, K., Verwimp, P., & Uytterhoeven, J. B. (1996). N2-adsorption on amorphous aluminosilicates: Application of the kelvin equation and the T-plot analysis for mixed micro-mesoporous materials. *Journal of Porous Materials*, *2*(4), 307-313.
22. Eklund, T., Bäckman, J., Idman, P., Norström, A. E. E., & Rosenholm, J. B. (2000). Investigation of the adsorption of mono- and bifunctional silanes from toluene onto porous silica particles and from aqueous

solution onto E-glass fibers. *Silanes and other coupling agents, 2*, 55.

23. Fendler, J. H., & Meldrum, F. C. (1995). The colloid chemical approach to nanostructured materials. *Advanced Materials, 7*(7), 607-632.
24. Fernandez, E., Sanchez, P., Panizza, M., Sanchez, V., Gallardo-Amores, J. M., Busca, G., & Resini, C. (2004). Influence of the Ga3+ doping in the textural and structural properties of the Mn and Al oxides. *Boletin de la Sociedad Espanola de Ceramica y Vidrio, 43*(2), 132-134.
25. Gao, Y. H., Bando, Y., Sato, T., Zhang, Y. F., & Gao, X. Q. (2002). Synthesis, Raman scattering and defects of β-Ga 2 O 3 nanorods. *Applied Physics Letters, 81*(12), 2267-2269.
26. Gowtham, S., Costales, A., & Pandey, R. (2006). Theoretical study of sequential oxidation of clusters of gallium oxide: Ga_3O_n (n: 4–8). *Chemical Physics Letters, 431*(4), 358-363.
27. Graham, U. M., Sharma, S., Sunkara, M. K., & Davis, B. H. (2003). Nanoweb Formation: 2D self-assembly of semiconductor gallium oxide nanowires/nanotubes. *Advanced Functional Materials, 13*(7), 576-581.
28. Gundiah, G., Govindaraj, A., & Rao, C. N. R. (2002). Nanowires, nanobelts and related nanostructures of Ga_2O_3. *Chemical Physics Letters, 351*(3), 189-194.
29. Hamada, S., Bando, K., & Kudo, Y. (1986). The formation process of hydrous gallium (III) oxide particles obtained by hydrolysis at elevated temperatures. *Bulletin of the Chemical Society of Japan, 59*(7), 2063-2069.
30. Harwig, T., & Kellendonk, F. (1978). Some observations on the photoluminescence of doped β-galliumsesquioxide. *Journal of Solid State Chemistry, 24*(3-4), 255-263.
31. Hu, J. Q., Li, Q., Meng, X. M., Lee, C. S., & Lee, S. T. (2002). Synthesis of β-Ga_2O_3 nanowires by laser ablation. *The Journal of Physical Chemistry B, 106*(37), 9536-9539.
32. Huang, C. C., Yeh, C. S., & Ho, C. J. (2004). Laser ablation synthesis of spindle-like gallium oxide hydroxide nanoparticles with the presence of cationic cetyltrimethylammonium bromide. *The Journal of Physical Chemistry B, 108*(16), 4940-4945.
33. Ishihara, T., Matsuda, H., & Takita, Y. (1994). Doped $LaGaO_3$ perovskite type oxide as a new oxide ionic conductor. *Journal of the*

American Chemical Society, *116*(9), 3801-3803.

34. Ishihara, T., Matsuda, H., & Takita, Y. (1995). Effects of rare earth cations doped for La site on the oxide ionic conductivity of $LaGaO_3$-based perovskite type oxide. *Solid State Ionics*, *79*, 147-151.
35. Jung, W. S., Joo, H. U., & Min, B. K. (2007). Growth of β-gallium oxide nanostructures by the thermal annealing of compacted gallium nitride powder. *Physica E: Low-dimensional Systems and Nanostructures*, *36*(2), 226-230.
36. Kaneko, K., Ishii, C., & Ruike, M. (1992). Origin of superhigh surface area and microcrystalline graphitic structures of activated carbons. *Carbon*, *30*(7), 1075-1088.
37. Kim, B. C., Sun, K. T., Park, K. S., Im, K. J., Noh, T., Sung, M. Y., & Park, S. S. (2002). β-Ga 2 O 3 nanowires synthesized from milled GaN powders. *Applied Physics Letters*, *80*(3), 479-481.
38. Kim, N. H., Kim, H. W., & Lee, C. (2004). Amorphous gallium oxide nanowires synthesized by metalorganic chemical vapor deposition. *Materials Science and Engineering: B*, *111*(2), 131-134.
39. Klaysri, R., Tubchareon, T., & Praserthdam, P. (2017). One-step synthesis of amine-functionalized TiO_2 surface for photocatalytic decolorization under visible light irradiation. *Journal of Industrial and Engineering Chemistry*, *45*, 229-236.
40. Knez, M., Scholz, R., Nielsch, K., Pippel, E., Hesse, D., Zacharias, M., & Gösele, U. (2006). Monocrystalline spinel nanotube fabrication based on the Kirkendall effect. *Nature Materials*, *5*(8), 627.
41. Lakshmi, B. B., Patrissi, C. J., & Martin, C. R. (1997). Sol−gel template synthesis of semiconductor oxide micro-and nanostructures. *Chemistry of Materials*, *9*(11), 2544-2550.
42. Li, N., Patrissi, C. J., Che, G., & Martin, C. R. (2000). Rate capabilities of nanostructured $LiMn_2O_4$ electrodes in aqueous electrolyte. *Journal of the Electrochemical Society*, *147*(6), 2044-2049.
43. Liang, C. H., Meng, G. W., Wang, G. Z., Wang, Y. W., Zhang, L. D., & Zhang, S. Y. (2001). Catalytic synthesis and photoluminescence of β-Ga_2O_3 nanowires. *Applied Physics Letters*, *78*(21), 3202-3204.
44. Lin, Z., Cai, J. J., Scriven, L. E., & Davis, H. T. (1994). Spherical-to-wormlike micelle transition in CTAB solutions. *The Journal of Physical Chemistry*, *98*(23), 5984-5993.
45. Lin, Z., Scriven, L. E., & Davis, H. T. (1992). Cryogenic electron

microscopy of rodlike or wormlike micelles in aqueous solutions of nonionic surfactant hexaethylene glycol monohexadecyl ether. *Langmuir*, *8*(9), 2200-2205.

46. Liu, X., Qiu, G., Zhao, Y., Zhang, N., & Yi, R. (2007). Gallium oxide nanorods by the conversion of gallium oxide hydroxide nanorods. *Journal of Alloys and Compounds*, *439*(1), 275-278.
47. Mazeina, L., Picard, Y. N., Maximenko, S. I., Perkins, F. K., Glaser, E. R., Twigg, M. E., & Prokes, S. M. (2009). Growth of Sn-Doped β-Ga_2O_3 nanowires and Ga_2O_3–SnO_2 heterostructures for gas sensing applications. *Crystal Growth & Design*, *9*(10), 4471-4479.
48. Nakagawa, K., Kajita, C., Okumura, K., Ikenaga, N. O., Nishitani-Gamo, M., Ando, T., & Suzuki, T. (2001). Role of carbon dioxide in the dehydrogenation of ethane over gallium-loaded catalysts. *Journal of Catalysis*, *203*(1), 87-93.
49. Ogita, M., Higo, K., Nakanishi, Y., & Hatanaka, Y. (2001). Ga_2O_3 thin film for oxygen sensor at high temperature. *Applied Surface Science*, *175*, 721-725.
50. Ogita, M., Saika, N., Nakanishi, Y., & Hatanaka, Y. (1999). Ga_2O_3 thin films for high-temperature gas sensors. *Applied Surface Science*, *142*(1), 188-191.
51. Patrissi, C. J., & Martin, C. R. (1999). Sol-gel-based template synthesis and Li-insertion rate performance of nanostructured vanadium pentoxide. *Journal of the Electrochemical Society*, *146*(9), 3176-3180.
52. Petre, A. L., Auroux, A., Gelin, P., Caldararu, M., & Ionescu, N. I. (2001). Acid–base properties of supported gallium oxide catalysts. *Thermochimica Acta*, *379*(1), 177-185.
53. Pierre, A. C. (1998). The chemistry of precursors solutions. In *Introduction to sol-gel processing* (pp. 11-89). US: Springer.
54. Pierre, A. C. (2007). Sol–gel technology. *Kirk-Othmer Encyclopedia of Chemical Technology*.
55. Pierre, A. C., & Rigacci, A. (2011). SiO_2 aerogels. In *Aerogels handbook* (pp. 21-45). New York: Springer.
56. Planeix, J. M., Coustel, N., Coq, B., Brotons, V., Kumbhar, P. S., Dutartre, R., & Ajayan, P. M. (1994). Application of carbon nanotubes as supports in heterogeneous catalysis. *Journal of the American Chemical Society*, *116*(17), 7935-7936.
57. Ristić, M., Popović, S., & Musić, S. (2005). Application of sol–gel

method in the synthesis of gallium (III)-oxide. *Materials Letters, 59*(10), 1227-1233.

58. Samala, S. K. (2012). *Structure, morphology and optical properties of nanocrystalline gallium oxide thin films*. The University of Texas at El Paso.
59. Sato, T., & Nakamura, T. (1982). Studies of the crystallisation of gallium hydroxide precipitated from hydrochloric acid solutions by various alkalis. *Journal of Chemical Technology and Biotechnology, 32*(3), 469-475.
60. Schramm, C., Rinderer, B., Tessadri, R., & Duelli, H. (2010). Synthesis and characterization of an aliphatic monoimide-bridged polysilsesquioxane by the sol–gel route. *Journal of Sol-Gel Science and Technology, 53*(3), 579-586.
61. Sharma, S., & Sunkara, M. K. (2002). Direct synthesis of gallium oxide tubes, nanowires, and nanopaintbrushes. *Journal of the American Chemical Society, 124*(41), 12288-12293.
62. Sides, C. R., Li, N., Patrissi, C. J., Scrosati, B., & Martin, C. R. (2002). Nanoscale materials for lithium-ion batteries. *Mrs Bulletin, 27*(8), 604-607.
63. Sinha, G., Datta, A., Panda, S. K., Chavan, P. G., More, M. A., Joag, D. S., & Patra, A. (2009). Self-catalytic growth and field-emission properties of Ga_2O_3 nanowires. *Journal of Physics D: Applied Physics, 42*(18), 185409.
64. Taş, A. C., Majewski, P. J., & Aldinger, F. (2002). Synthesis of gallium oxide hydroxide crystals in aqueous solutions with or without urea and their calcination behavior. *Journal of the American Ceramic Society, 85*(6), 1421-1429.
65. Tippins, H. H. (1965). Optical absorption and photoconductivity in the band edge of β−Ga_2O_3. *Physical Review, 140*(1A), A316.
66. Voegtlin, A. C., Matijasic, A., Patarin, J., Sauerland, C., Grillet, Y., & Huve, L. (1997). Room-temperature synthesis of silicate mesoporous MCM-41-type materials: Influence of the synthesis pH on the porosity of the materials obtained. *Microporous Materials, 10*(1), 137-147.
67. Voutsas, E. C., Flores, M. V., Spiliotis, N., Bell, G., Halling, P. J., & Tassios, D. P. (2001). Prediction of critical micelle concentrations of nonionic surfactants in aqueous and nonaqueous solvents with UNIFAC. *Industrial & Engineering Chemistry Research, 40*(10), 2362-2366.

68. Weh, T., Frank, J., Fleischer, M., & Meixner, H. (2001). On the mechanism of hydrogen sensing with SiO_2 modificated high temperature Ga_2O_3 sensors. *Sensors and Actuators B: Chemical, 78*(1), 202-207.

69. Xiang, X., Cao, C. B., Guo, Y. J., & Zhu, H. S. (2003). A simple method to synthesize gallium oxide nanosheets and nanobelts. *Chemical Physics Letters, 378*(5), 660-664.

70. Xu, B., Zheng, B., Hua, W., Yue, Y., & Gao, Z. (2006). Support effect in dehydrogenation of propane in the presence of CO_2 over supported gallium oxide catalysts. *Journal of Catalysis, 239*(2), 470-477.

71. Yokoi, T., Yoshitake, H., & Tatsumi, T. (2004). Synthesis of mesoporous silica by using anionic surfactant. *Studies in Surface Science and Catalysis, 154*, 519-527.

72. Zhan, J., Bando, Y., Hu, J., & Golberg, D. (2004). Bulk synthesis of single-crystalline magnesium oxide nanotubes. *Inorganic Chemistry, 43*(8), 2462-2464.

73. Zhang, H. Z., Kong, Y. C., Wang, Y. Z., Du, X., Bai, Z. G., Wang, J. J., & Feng, S. Q. (1999). Ga_2O_3 nanowires prepared by physical evaporation. *Solid State Communications, 109*(11), 677-682.

74. Zhang, Y. C., Wu, X., Hu, X. Y., & Shi, Q. F. (2007). A green hydrothermal route to GaOOH nanorods. *Materials Letters, 61*(7), 1497-1499.

75. Zhao, Y., & Frost, R. L. (2008). Synthesis and surface characterization of yttrium doped boehmite nanofibers. *Journal of Colloid and Interface Science, 326*(1), 289-299.

76. Zhao, Y., Frost, R. L., & Martens, W. N. (2007). Gallium-doped boehmite nanotubes and nanoribbons. A TEM, EDX, XRD, BET, and TG study. *The Journal of Physical Chemistry C, 111*(14), 5313-5324.

77. Zhao, Y., Frost, R. L., & Martens, W. N. (2007). Synthesis and characterization of gallium oxide nanostructures via a soft-chemistry route. *The Journal of Physical Chemistry C, 111*(44), 16290-16299.

78. Zhou, W. M., Yang, B., Yang, Z. X., Zhu, F., Yan, L. J., & Zhang, Y. F. (2006). Large-scale synthesis and characterization of SiC nanowires by high-frequency induction heating. *Applied Surface Science, 252*(14), 5143-5148.

79. Zhu, F., Yang, Z., Zhou, W., & Zhang, Y. (2006). Synthesis of β-Ga_2O_3 nanowires through microwave plasma chemical vapor deposition. *Applied Surface Science, 252*(22), 7930-7933.

CHAPTER 5

CHEMICAL ROUTES IN THE PREPARATION OF NANOMATERIALS VIA SOL-GEL PROCESS

CONTENTS

5.1 INTRODUCTION

This chapter accounts for the discussion related to the application of the solgel process for the synthesis of novel materials with nanostructures. This chapter contains detailed presentation regarding the processing of metallic, ferroelectric, semiconducting, and scintillating nanoparticles incorporated in a variety of oxide matrices. Various nanosynthesis methods for nanoporous oxides and inorganic–organic nanohybrids are also addressed in the subsequent sections.

The rising interest in nanomaterials requires the development and commercialization of processing methods which account for the tailoring of particular features at nanometer scales. One major technique employed for engineering such nanostructures deals with the chemical exploitation of building blocks at nanolevels. Traditional processing approaches for ceramics involve grinding, heating, and pressing microsized powders. Therefore, it is quite challenging to produce nanostructures with traditional fabrication methods. However, the following are the examples of nanostructure development which involve traditional synthesis routes.

- Nanocrystallites' growth from the glass melts.
- Synthesis of metallic and semiconducting nanocrystallites through a technique called "striking a glass."
- Formation of partially stabilized zirconia (ZrO_2)-containing metastable nanoparticles and tetragonal ZrO_2 in a cubic matrix.

The advent of low-temperature chemical synthesis processes (e.g., solgel) has provided a reliable alternative to develop novel material structures. Recently, numerous low-temperature processing methods have emerged with novel processing strategies. Controlled chemical reactions taking place at room temperature can be employed to synthesize nanomaterials with customized properties. The size, mobility, and compositions of the resultant molecules can be maneuvered by controlling different parameters. Therefore, the solgel method presents an excellent prospect to design and develop novel nanomaterials with tailor-made characteristics. This chapter contains the detailed information regarding several solgel techniques which have been effectively utilized to engineer nanostructure ceramics or glasses. Some of the solgel processes utilize the characteristics of versatile and complex condensation and hydrolysis reactions, while others make use of the nanoporosity (present in the gels) as a host for a variety of inorganic clusters or molecules. The chemical states and system chemistry play

an important role in controlling the resulting nanostructures. Examples of chemically produced products include nanoporous silica, metallic, ferroelectric, semiconductor, and oxide nanocrystallites and nanohybrids (organic/inorganic).

5.2 NANOPOROUS OXIDE GELS

Chemical synthesis of ceramics and other hybrid compounds is usually carried out by the solgel process (Henry & Sanchez, 1988; Brinker & Scherer, 1990; Hench & West, 1990). Solgel process has been extensively employed in the processing and engineering of various oxides in the form of fibers, coatings, and bulk compounds. The synthesis of silica from liquid silicon organic–metal precursors is possibly the oldest and most explored solgel technique. A solgel process involves hydrolysis and condensation reactions in the presence of an organic–metal precursor, for example, tetraethoxysilane, dissolved in a suitable solvent (i.e., ethanol) with or without the utilization of a catalyst. A gel is formed as a result of chemical reactions which lead to an increase in viscosity of the solution. A typical ceramic gel consists of Si–O–Si covalent bonds which form a network containing reaction products. The removal of reaction products via evaporation results in the formation of a nanoporous structure. Pore size, interconnectivity, and distribution are affected by process parameters which are listed below:

- The amount and type of solvent,
- Nature of the catalyst,
- Process temperature, and
- The presence and configuration of template molecules.

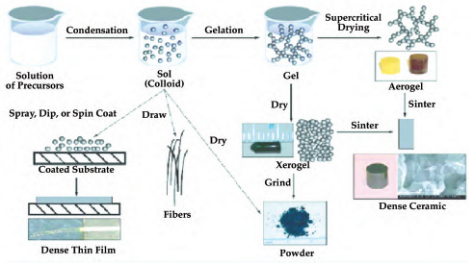

Figure 38. Synthesis route of a typical solgel process

[Source: https://www.researchgate.net/publication/290797153_Sol-gel_Based_Materials_for_Biomedical_Applications/figures? lo=1]

The porous gels produced by solgel method constitute an incredibly fascinating class of nanomaterials. The structure of nanoporous materials can be tailored for orientation, size, connectivity, or arrangement and investigated for various applications, for example, sensors, chromatography columns, low dielectric materials, catalyst support, or controlled reactant release.
Klein and Woodman (1996) investigated various solgel methods which can be utilized to synthesize silica. Additionally, the effect of different process parameters on the properties of gels has also been discussed in the study. The interconnected pores in the gels can be soaked and functionalized with an organic dye or molecules. This new material is considered the "backbone" of the chromatographic industry. The nanoporosity of the gels produced from solgel processes can also be engineered for different novel functionalities. For instance, tetramethylammonium silicate or TMAS can be used to manufacture materials with low dielectric constant. TMAS is a structuring agent which is typically used in the synthesis of zeolite. Previously, silica films with approximately 50% porosity and uniform distribution of pore size (i.e., average pore size= 40 Å) have been fabricated, resulting in a customized material having a dielectric constant of 2.5 (Kim, Du, Bhandarkar, & Johnson, 2002).

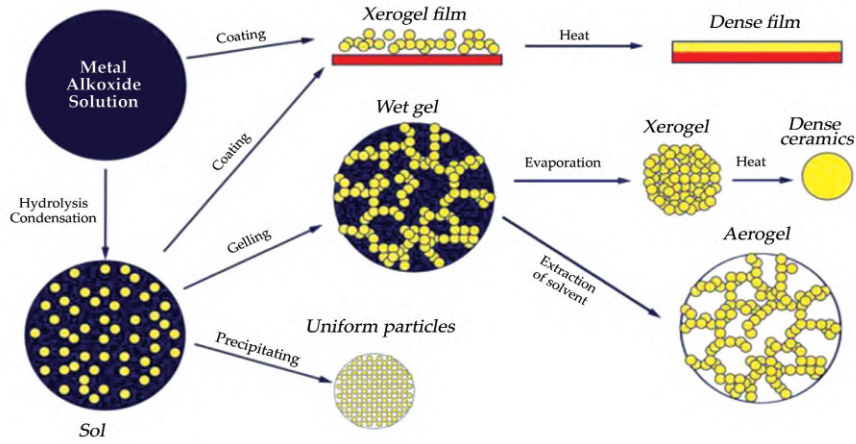

Figure 39. Common applications of solgel process

[Source: https://www.gelest.com/applications/sol-gel-applications/]

Currently, template molecules are being used to engineer nanoporous materials for various applications (Lu, 1998). The use of surfactant micelles

as pore-producing agents has resulted in the formation of nanoporous dielectric films having uniform pore sizes (typically 5-nm-thick films). Surfactants and tetraethoxysilane (TEOS) are usually blended in an aqueous–acidic environment. During the spin-coating process, the solvent is rapidly removed which results in the formation of micellar aggregates from the surfactant molecules. The removal of surfactant results in the formation of an extremely porous SiO_2 film, with controlled pore size and porosity. Proper application of dehydroxylation treatments results in the formation of a stable thin film with low dielectric constants, that is, 1.8–2.2 (Baskaran et al., 2001).

Presently, scientists are exploiting the use of self-assembling molecules for the synthesis of nanoporous and mesoporous materials from solgel processes. It is quite possible to facilitate mass transfer in catalysis or adsorption by confining one- or more dimensional parameters of mesoporous silica, ultimately forming a well-ordered nanoporous structure. Shan, Wang, Zhang, & Tang (2005) obtained nanoporous silica flakes using a TEOS-based chemical solution consisting of 24-nm pores. The flakes showed excellent characteristics in adsorbing biomolecules (Shan, 2005). Various nanoporous oxide-based gels have been synthesized using self-assembling molecules. Mesoporous silica with inconsistent architecture and pore size has been developed from block copolymers using one block of polyelectrolyte as a template. Connectivity and pore size are defined by the structural architecture of the block copolymer mesophases or micelles; that is, the resultant network of silica gel is a replica of the original self-assembling structure. Different aggregate structures with spherical pores (10–50 nm) are usually obtained depending on the salt content and relative block lengths of the copolymers in the reaction mixture. The resultant structures can also attain more complex architectures which include rattles, that is, the multilamellar vesicles (Kramer, Förster, Göltner, & Antonietti, 1998; Göltner, Berton, Krämer, & Antonietti, 1998; Göltner, Berton, Krämer, & Antonietti, 1999). Chemical fabrication routes present a great potential to fabricate complex and original material structures. For instance, Schlottig, Textor, Georgi, & Roewer (1999) used the mixture of ethanol, tetraethoxysilane, HCl, and water added in different molar ratios to develop the arrays of closed silica nanotubes. Pores in alumina (Al_2O_3) membrane were filled by employing both dip- and spin-coating techniques. Nanotubes were obtained after the partial removal of Al_2O_3 from the coated membrane (Schlottig et al., 1999).

5.3 NANO ORGANIC–INORGANIC HYBRID MATERIALS (POLYMERS, PROTEINS, AND DYES) IN GELS

As illustrated above, it is evident that the derivative of solgel route is a nanostructured gel which exhibits porosities in the range of nanometers. In several cases, the gel porosity is developed around an organic–template molecule, that is, surfactants. On the other hand, the porosity can also develop as a result of the evaporation reactions. In all the cases, one of the major benefits of the solgel process is the ability of the organic and inorganic ingredients to coexist in the same matrix at lower processing temperatures. In conventional ceramic processing, the coexistence of organic and inorganic phases is barred by the extremely high temperatures necessary for processing the oxide matrices. The organic constituents present (either adsorbed or chemically bonded) in the oxide gels play an important role in enhancing the functionality of structures at the nanoscale. Previously, the inorganic–organic hybrids were considered a kind of nanocomposites which were nearly impossible to engineer. However, nowadays, it is conveniently feasible to engineer these nanocomposites. The organic matrices can be positioned within the inorganic matrices using one of two methods: It is either soaked into the porous and dry gels or mixed into the solution containing solgel. In the first method, the organic constituent may be physically adsorbed onto the surface of the pore or chemically attached to the structural backbone. In the second method, the organic constituent is typically adsorbed on the pore surface (Sanchez & Ribot, 1994).

The organic dye molecules can be conveniently supplemented with a solgel aqueous solution. This phenomenon was primarily reported by Avnir et al. (1988) for the addition of rhodamine 6G dye to an alcoholic solution of TEOS. The dye molecules are evenly dispersed in the alcoholic TEOS solution. The gelation process results in trapping of the dye molecules that get in the porous oxide-based gel matrix. The trapping of dye molecules is followed by the formation of a nanomaterial (organic/inorganic). The intention of the experiment conducted by Anvir et al. (1988) was to develop lasers from organic dyes. The organic dyes were observed to be stable in the oxide matrices. On the other hand, it was established that the stability of several laser dyes was altered by atmospheric conditions, which emphasizes on the functionalities of the porosities in these nanomaterials (Lin, Bescher, Mackenzie, Dai, & Stafsudd, 1992; L'Espérance & Chronister, 1993; Salomons, 1998). To date, various organic dyes have been blended with a

solgel solution to develop a range of dyed glasses customized for various commercial applications (Reisfeld, 2002; Seker, Meeker, Kuech, & Ellis, 2000). Several other organic compounds have also been employed to enhance the sensing characteristics of dyes (Bescher & Mackenzie, 1998).

Schmidt (1985) observed that the oxide structure could be tailored by modifying polymeric chains. He suggested a name, "ormocers," for the materials containing organically customized ceramics. An alternate name often utilized for these kinds of materials (particularly organically tailored silicates) is known as "ormosils." Both of the above-mentioned terms will be utilized interchangeably in this chapter. The pioneering work of Schmidt (1985) laid the basis for the evolution of hybrid (organic–inorganic) composites. Covalent bonds between inorganic and organic constituents of the composites may/may not exist. Figure illustrates the typical examples of the nanostructural hybrid materials which can be materialized. Cracking and shrinkage can be prevented by adding a DCCA (drying control chemical additive) such as oxalic acid or formamide (Orcel & Hench, 1984; Uchida, Ishiyama, Kato, & Uematsu, 1994). Iler, Hench, & Ulrich (1986) investigated the effects of increasing dye amounts in a solgel solution. It was found that a lot of organics dissolved in a solgel solution of tetraethoxysilane (TMOS) or TEOS significantly reduced the average pore diameter and ultimately the pore size (Aksay & Schilling, 1984; Barringer, Jubb, Fegley, Pober, & Bowen, 1984).

The cubic silsesquioxane-based nanocomposites constitute a novel class of nanomaterials (Sellinger & Laine, 1996). The smallest imaginable nanopore in SiO_2 is perhaps the central vacant space in the silica cube, consisting of eight silica atoms, also known as the H8T8 unit. This unique crystal structure is rarely found in traditionally processed silica or glass. However, the derivatives of the H8T8 unit in silsesquioxanes have gained immense interest recently. These systems present the benefit of a very obvious characterization of the organic and inorganic nanophases. The inorganic phase usually consists of a rigid and distinct silica core (Novak & Davies, 1991). Eight organic entities (groups) can be attached to the vertices of the cages, connecting the cores to each other. The organic groups can have varying chemical composition and length. It is quite possible to fabricate nanohybrid networks which contain the interpenetration of organic network and oxides (Bonilla, Martínez, Mendoza, & Widmaier, 2006; Ellsworth & Novak, 1991; 1993). Such materials present the ability to develop the organic or inorganic networks independently, and the covalent

bonds are absent between them. However, there may be a need to develop nanomaterials with strong interatomic bonds between different phases (organic and inorganic). For instance, strong covalent bonds exist in PDMS (SiO_2–polydimethylsiloxane) system which has been researched extensively by numerous scientists.

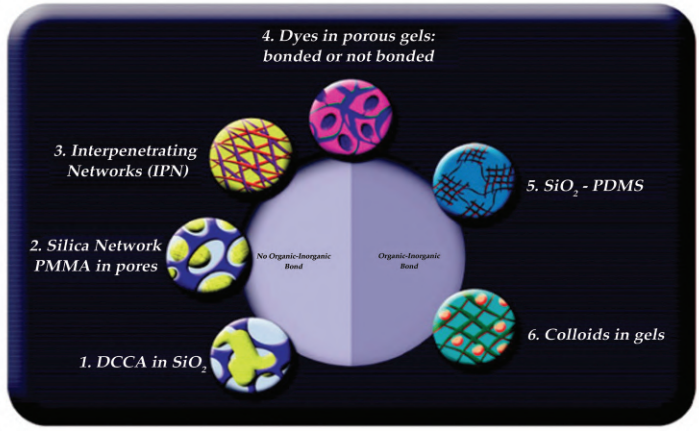

Figure 40. Different solgel-derived nanostructures for organic–inorganic hybrids

[Source: http://pubs.acs.org/doi/abs/10.1021/ar7000149]

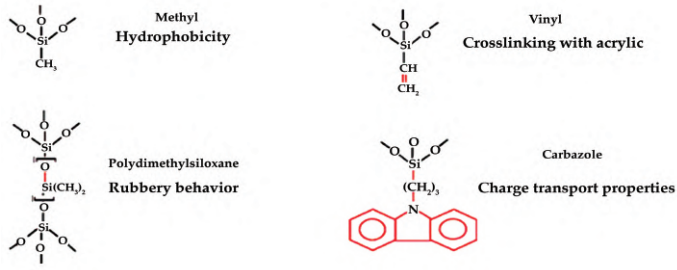

Figure 41. Different kinds of organic entities which may be attached to backbones of oxide in type II hybrids

[Source: http://pubs.acs.org/doi/abs/10.1021/ar7000149]

The primary feature of PDMS is the presence of Si-O-Si chains which can be linked to organic or inorganic phases during the solgel process. The

excellent compatibility between TEOS and the silanol-terminated PDMS has made these materials very fascinating for numerous scientists and researchers (Wilkes et al., 1985; Teowee et al., 1996; Figueira, Silva, & Pereira, 2005). A typical kind of reaction present in type II hybrids involves the cross-linking of organic and inorganic phases. The compatibility between TEOS and PDMS can be observed in the following reaction between a silicic acid molecule and PDMS chain (Wang, 2012).

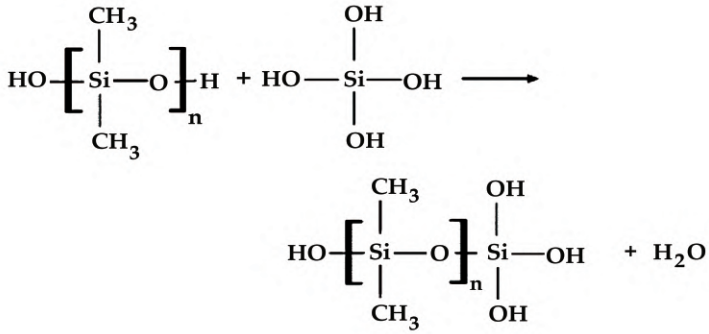

Figure 42. Cross-linking reaction between organic and inorganic constituents

[Source: http://pubs.acs.org/doi/abs/10.1021/ar7000149]

5.4 BENEFITS AND APPLICATIONS OF HYBRID NANOMATERIALS

The benefits of the above-mentioned system include the correspondence between the siloxane structure and silica network and the stability of PDMS at higher temperatures as compared to various other elastomeric compounds. The structure and characteristics of the pores can vary based on the solution conditions which include basic or acidic catalysis. The material can exist as either rubbery or glassy state depending on the organic constituent's weight fraction. The properties, structure, and prospective applications of the above-mentioned organic–inorganic hybrids are illustrated in the subsequent text (Latella, Ignat, Barbé, Cassidy, & Bartlett, 2003; Latella, Ignat, Barbe, Cassidy, & Li, 2004; Mackenzie & Bescher, 2003).

Various biological entities, such as enzymes or proteins, have been integrated with oxide matrices, especially silica-based matrices. The "nanocages" derived from oxides can accommodate the proteins along with the provision of protection mechanisms from external attacks (Zink

et al., 1994; Toselli, Marini, Fabbri, Messori, & Pilati, 2007). A variety of biological nanosensors have been developed by employing the nanocage approach. Some examples of the molecules that can be employed for the synthesis of hybrids are displayed in Figure 43.

A schematic illustration of different organic–inorganic hybrid materials is demonstrated in Figure 2. These hybrid nanocomposites can be categorized into two broad groups as reported by Sanchez and Ribot (1994). It can be deduced that the organic and inorganic entities are either bonded covalently or not bonded at all. Structure 1 corresponds to the DCCA–SiO_2-based nanohybrid material which contains trapped DCCA in the pores.

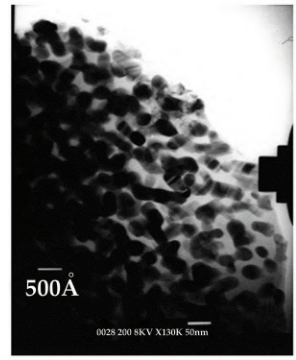

Figure. 43. Lu_2SiO_5 nanoparticles present in an optically transparent silica matrix

[Source: http://pubs.acs.org/doi/abs/10.1021/ar7000149]

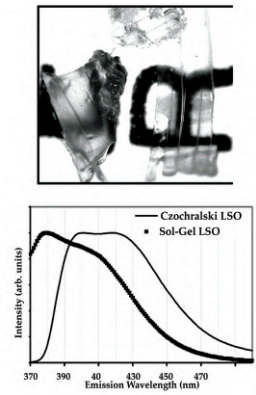

Figure. 44. (Top) Solgel-derived, optically transparent scintillators of Lu_2SiO_5–SiO_2. (Bottom) Distribution of wavelengths of light scintillation from LSO crystals excited with 356 nm (wavelength) of light at ambient temperatures.

The doublet structure related to the Ce^{+3} ion transitions from the 5d energy level to the 4f ground state is typically washed out at room temperatures but can still exist in the spectra.

[Source: http://pubs.acs.org/doi/abs/10.1021/ar7000149]

Structure 2 corresponds to the case of silica and polymethyl methacrylate (SiO_2–PMMA) which contains *in situ*-polymerized PMMA within the interlinked pores of the inorganic silica network (Pope, Asami, & Mackenzie, 1989). Structure 3 displays the organic and inorganic interpenetrating (IPN) networks (Ellsworth et al., 1991). Structure 4 contains organic molecules or dyes which are either bonded covalently to the inorganic network or not bonded at all. Structure 5 shows covalently bonded SiO_2 and PDMS. The material can exist in either rubbery or hard state depending on the weight fraction of PDMS (Bescher & Mackenzie, 1997; 2001; 2003). Structure 6 displays the inorganic colloids (e.g., silica) bonded covalently to gel.

5.5 NANOCRYSTALLITES ACQUIRED VIA CONTROLLED CRYSTALLIZATION OF GEL

Traditional glass ceramic materials have been recognized for several years. They are usually acquired by the formation of glass melt, followed by quenching and heating to produce a crystalline phase in the glass matrix. A transparent glass ceramic can be developed by keeping the particle size below the wavelength of light (Xu et al., 1997; Reisfield, 2004; Del Monte, Xu, Mackenzie, Claflin, & Lucovsky, 1998). Numerous material products including optical filters, telescopes, materials with zero coefficient of thermal expansion, and cooking ware have been fabricated through this process. In many cases, the crystallite size is kept in nanometer ranges to attain the desired characteristics (Nogami, Kojima, & Nagasaka, 1992; Li & Nogami, 1993; Chia, Kao, Xu, & Mackenzie, 1997). The solgel method presents an efficient substitute to this high-temperature procedure because various gels of amorphous oxides can now be produced at room temperature. This technology offers the prospect of growing nanocrystallites within a matrix containing organic phases. Numerous examples of the nanomaterials synthesized from the controlled crystallization of gels are discussed in the subsequent sections.

5.5.1 Scintillating Nanoparticles

Scintillators are typically grown as transparent, large single crystals. The most promising scintillator known as cerium-doped LSO (lutetium orthosilicate) was discovered almost five decades ago. It demonstrates a unique combination of essential properties for γ-ray and X-ray spectroscopy, that is, high density, large light yield, and fast decay.

However, the practical utilization of LSO is obstructed by difficulties associated with its synthesis of single crystals by the Czochralski process. Recently, the solgel process has successfully been employed to develop lutetium silicate scintillators. The most demanding concern is keeping the polycrystalline materials transparent in the visible range of the electromagnetic spectrum of light. The transparent scintillators are attained by keeping the LSO crystal's size below the wavelength of the visible spectrum of light. It is essential to control the nucleation and growth to maintain the size in nanometer range for the scintillating material phases. The growth process is typically based on the hydrolysis reaction of lutetium alkoxides (Bescher et al., 2000; Ivanczyck et al., 2000). There are two fundamental ways to control the sizes of Lu_2SiO_5-based nanocrystallites, that is, the maintenance of the Lu/Si ratio at lower values and the restriction of the heat treatment temperatures. Experiments have shown that appropriate firing and drying of lutetium silicate crystals can instigate the growth of lutetium silicate crystals in a silica matrix. Moreover, the careful control of the manufacturing process results in the development of a thin nanomaterial. The average particle size for Lu_2SiO_5 was about 200 Å. Γ-Ray spectral response and light decay measurement provide information about the morphology and nature of the polycrystalline nanomaterials synthesized by a solgel process. The characteristics of the crystals produced from the solgel process are comparable to that of the traditional LSO single crystals.

5.5.2 Ferroelectric Nanoparticles in Inorganic Gel

Several ferroelectric oxides have been developed by the solgel method (Mackenzie & Xu, 1997). Numerous scientists and researchers have studied the growth mechanisms of ferroelectric nanocrystallite phases from gels. The local ordering of the ferroelectric oxide materials has been observed with increasing temperature, starting with the development of nanosized clusters at lower temperatures. Such nanoclusters are known as "ferrous" and can display ferroelectric characteristics despite their small sizes. A theoretical model illustrating the behavior of the "ordered nanoclusters" was developed

by Xu et al. (1997). The ferroelectric crystals of $BaTiO_3$ and $LiNbO_3$ have been synthesized in an amorphous matrix of silica by the solgel method. Such particles also increase in number and size with increasing the temperature. Nicely grown $BaTiO_3$ nanocrystallites have been, reportedly, obtained after heat treatment at 800°C for 2 hours. Local ordering of microstructure is typically observed for $LiNbO_3$ at lower temperatures, that is, 200°C (Fig. 45). The minimum reported size of these ordered phases is in the order of 3 nanometers. P–E loops and ferroelectric properties can be witnessed in small crystals of $LiNbO_3$ and $BaTiO_3$.

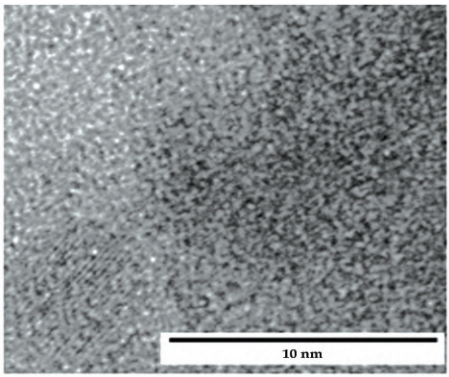

Figure 45. Nanoparticles of $BaTiO_3$ in the silica (SiO_2) matrix heat-treated at 800°C for 2 hours

[Source: http://pubs.acs.org/doi/abs/10.1021/ar7000149]

5.5.3 In Ormosils

As stated in the previous text, it is now possible to grow oxide phases in organically modified matrices at lower processing temperatures by employing the solgel process. The growth of $LiNbO_3$ crystals has been investigated in an ormosil matrix consisting of a covalently bonded organic molecule with high hyperpolarizability, for example, TDP (triethoxysilyl propyl dinitrophenylamine). $LiNbO_3$ errors can be observed at lower temperatures (about 200°C) below the breakdown temperature of the organic phase (Fig. 46). Various interactions take place between organic and inorganic constituents. For instance, a strong bathochromic redshift can be observed after the formation of ferrous due to the exposure of a TDP molecule to the solution of barium titanium alkoxide. Currently, other prospective organic/inorganic reactions are also being investigated. Ferroelectric properties of

novel hybrid compounds of organic/inorganic phases have been investigated by various researchers till date (Bescher, Xu, & Mackenzie, 1997; Bescher, Xu, & Mackenzie, 2001). An ideal structure of such nanohybrid materials is shown in Figure 47.

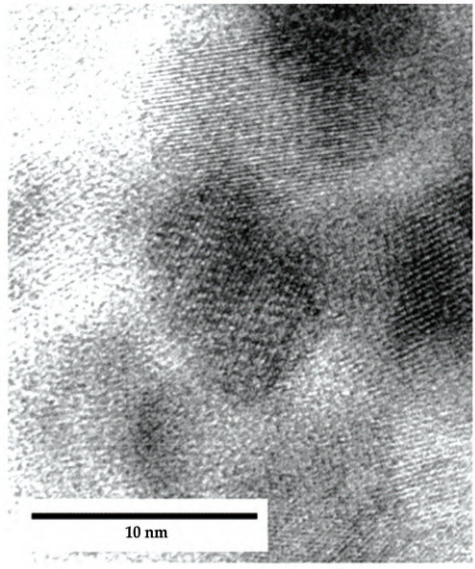

Figure 46. Nanoparticles of $LiNbO_3$ in the silica matrix heat-treated at 200°C for 2 hours

[Source: http://pubs.acs.org/doi/abs/10.1021/ar7000149]

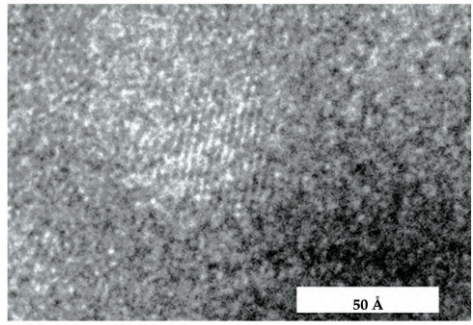

Figure 47. The nanoparticle of $LiNbO_3$ in a SiO_2–TDP ormosil heat-treated at 200°C for 2 hours.

[Source: http://pubs.acs.org/doi/abs/10.1021/ar7000149]

5.6 SEMICONDUCTING NANOPARTICLES

Semiconducting nanoparticle materials are often grown in optically transparent matrix materials for numerous nonlinear optical applications. Table 6 demonstrates the Bohr radii of different several semiconductor materials. Quantum confinement can be observed if the particles possess the smaller radii than the Bohr radii of the electron–hole pairs, usually lesser than 200 Å.

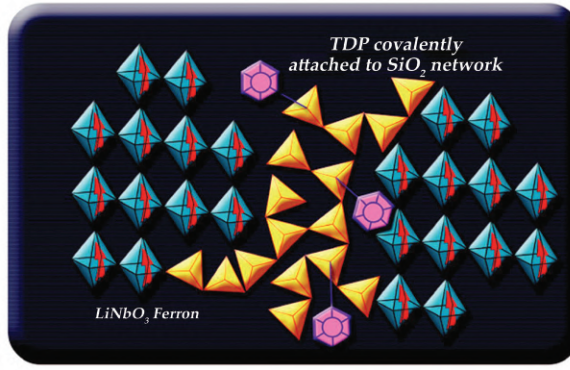

Figure 48. Schematic of a $LiNbO_3$–TDP ferroelectric ormosil nanocomposite material

[Source: http://pubs.acs.org/doi/abs/10.1021/ar7000149]

Table .6. Bohr radii of various semiconductors

Semiconductor	E_g **(eV)**	r_B **(Å)**
CdSe	1.7	53
CdS	2.5	28
GaAs	1.4	124
CdTe	1.5	75
PbS	0.41	180

The solgel synthesis approach has been effectively utilized to fabricate various types of nanomaterials. A typical solgel process involves the gelation of suitable precursors, followed by heat treatment of the gel in a reducing or sulfating environment to produce the semiconducting phases.

Many researchers have carried out the synthesis and behavioral analysis of different CdS-doped ceramics (e.g., sodium borosilicate glass and ORMOSIL glass) produced from various precursor systems such as boron ethoxide, sodium acetate, TEOS, TMOS, and PDMS. The introduction of cadmium was carried out in the form of the two distinct solutions which include cadmium nitrate and cadmium acetate, respectively. Dried H_2S gas (up to 20 wt.%) was impinged on the film to form crystals of CdS. APTES (3-aminopropyltriethoxysilane) was also incorporated into both of the solutions to offer improved control of the particle sizes and particle size distributions. Specimens treated with APTES contained smaller particles of crystals with a narrow size distribution (i.e., 0.9 nm standard deviation, 2.8 nm average size). APTES assisted in linking of the dopants to the silica networks of the ceramic glass, consequently avoiding the salt precipitation during the drying phase of solgel drying process. Various alternate and more difficult processing routes are also possible. The values of approximately 10–6–10–8 esu were noticed in these synthesized materials. Production of the channel waveguides was carried out by the exchange of ions in the sodium borosilicate glass. Moreover, the broadcast of pulses (110 fs long) resulted in spectral modulation and narrowing of the input pulse (Xu et al., 1997). Various other semiconducting quantum dots including CdTe, SbSI, or PbS have been effectively grown in oxide matrix using similar solgel techniques (Chia et al., 1997; Xu et al., 1999; Del Monte et al., 1998; Del Monte, Xu, & Mackenzie, 2000).

5.7 METALLIC NANOPARTICLES

Similar to semiconducting ceramic nanoparticles, the nanoparticles of metals can offer fascinating optical properties in oxide matrices. The metallic nanoparticles embedded in glass matrix have developed for centuries via traditional processing routes. However, the solgel technique offers an efficient and more versatile alternative approach. The solgel technique for the synthesis of metallic nanoparticles involves the heating of the gel in a reducing environment. The host matrices are typically inorganic gels or organic–inorganic hybrids.

5.7.1 In Inorganic Gels

Several nanoparticles of metals have been prepared in solgel-derived matrix materials. For instance, solgel films of silica are prepared by dipping method from acid-catalyzed solutions of TEOS doped with Pt, Au, Pd, and Ag

metal colloids. The precipitation temperatures for various metallic species depend on their physical properties, that is, 1000°C for Pd, 800°C for Pt, 600°C for Ag, and 200°C for Au (Renteria & Campero, 1998; Innocenzi & Kozuka, 1994; Innocenzi, Kozuka, & Sakka, 1994). Nanoparticles of silver metal are also synthesized in silica by the introduction of $AgNO_3$ in the solgel solution. The silver ions are thermodynamically reduced in the air at approximately 800°C, resulting in the formation of an intense yellow film. The nanoparticles of metallic silver are observed by XRD and TEM (transmission electron microscopy). The nanoparticles of silver usually have approximately 10 nm diameter. Silver colloid-doped gels have also exhibited thermochromic effects (Zhao, Hasebe, Sakagami, & Osaka, 1997).

5.7.2 In Ormosils

Innocenzi and Kozuka (1994) developed thin-film methyltriethoxysilane-derived gels consisting of Ag nanoparticles. The average size of the silver particles was approximately 10 nm. Other metallic elements (e.g., Pt and Au) can also be utilized to dope ormosil matrices available in both thin films and bulk forms. The major benefit of an ormosil matrix is its capability to assist in the fabrication of crack-free, large samples. Similar to the inorganic matrices, the metallic clusters are integrated into the ormosil matrices by the dissolution of metallic salts into the precursor solution before gelation.

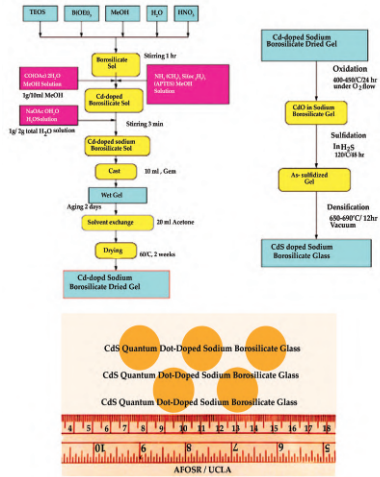

Figure 49. Synthesis route for CdS-doped borosilicate ceramic glass

[Source: http://pubs.acs.org/doi/abs/10.1021/ar7000149]

Ormosil matrices often do not require high temperatures for the reduction of the metallic ions. However, the reduction of metals is achieved by UV radiation. The correspondence between the volume fraction, particle size, and resonance absorption position of the colloidal metallic particles has been investigated by many scientists. Tseng, Li, Takada, Lechner, & Mackenzie (1992) performed X-ray analysis to observe the crystal structure of the metal particles. It was discovered that metallic nanoparticles possessed a crystalline structure (FCC). Transmission electron microscopy was employed to examine the particle sizes and their distribution (White, Harbison, & Nelson, 1983; White, Harbison, & Nelson, 1984; Ashlock, Mukamal, & White, 1985).

5.8 COLLOIDAL OXIDE PARTICLES

Organic polymers are typically soft and flexible, which need some additional processing to improve their mechanical characteristics. The properties of organic polymers can be improved by the addition of colloidal oxide nanoparticles, which enhance the elastic modulus of the polymers. The use of silica colloidal particles to reinforce the siloxanes has gained vital importance, lately. Numerous publications and patents are available on the above-mentioned topic regarding the synthesis of nanocomposites (Kang et al., 2005; January 1982). A considerable number of patents are available on novel materials for abrasion-resistant thin-film coatings on organic ophthalmic lenses. Tintable or UV-curable abrasion-resistant coatings can also be developed through the solgel process. Various colloidal particles (e.g., SiO_2, TiO_2, Al_2O_3, and ZrO_2) have also been used as dopants in siloxane matrices (Guest, Preus, & Lewis, 1991; Guest, Preus, & Lewis, 1992). The deposition of thick-film coating can be facilitated by the presence of colloidal SiO_2 particles (up to 300 μm) in gels (Otaki, 1997; Barrow & Olding, 2003). Colloids have been reported to restrict the cracking induced during the drying stage of a silica gel synthesis. Solgel can also produce coatings on large bulk components (Buissette, Moreau, Gacoin, Le Mercier, & Boilot, 2004; Costa et al., 2006).

Extensive research is being carried out to synthesize core–shell structure containing different kinds of nanoparticle materials. The core material can consist of semiconducting phase, and the shell material may contain metallic phases or vice versa. On the other hand, a shell may be manufactured from a semiconductor, metal, or a polymer and the core may be produced from an oxide, a dye, or a polymer.

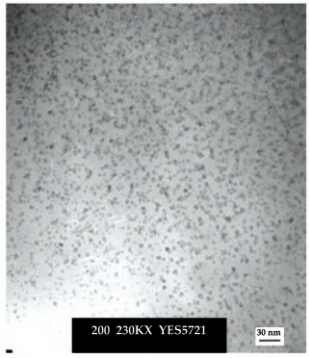

Figure 50. Nanoparticles of CdS present in borosilicate glass

[Source: http://pubs.acs.org/doi/abs/10.1021/ar7000149]

There are numerous potential ways of maneuvering the structure of these nanoparticle materials. Solgel methods are preferably suitable for the production of such nanoarchitectures.

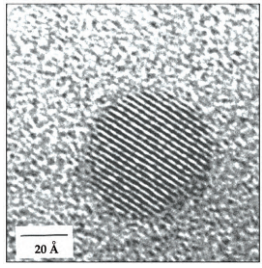

Figure 51. The nanoparticle of CdTe in a solgel-derived matrix of borosilicate (5 wt.% CdTe, treated at 500°C for 4 hours).

[Source: http://pubs.acs.org/doi/abs/10.1021/ar7000149]

For instance, the nanoparticles can be developed by reverse microemulsion process. In a few cases, a passivation film (e.g., aminosilane amorphous layer) is in connection with the core (Bhatia, Brinker, Gupta, & Singh, 2000; Castro & Barbera-Guillem, 2000). The optical features of such core–shell architectures are of enormous significance. For instance, luminescent nanocrystals can be used for various applications such as transparent light-emitting diodes (LEDs). Buissette et al. (2004) investigate the growth mechanisms of lanthanide-doped phosphate and vanadate nanoparticles via colloidal synthesis route, with less than 10 nm average particle sizes. Improvement in the luminescent characteristics of

the nanocrystals can be attained through the exploitation of a core/shell architecture grown at the amorphous shell of SiO_2 or a crystalline shell of La phosphate. $Al_2O_3/FeNi_3$ shell–core nanocomposites containing individual nanoparticles of $FeNi_3$ coated with Al_2O_3 thin layer are synthesized by a customized solgel process. The magnetic characteristics of such nanoarchitectures can also be investigated (Liu et al., 2005; 2006; Stoeck, 2012). The metal oxide precursors and amphiphilic organic polymers can be used to manufacture reactive nanoparticles of core–shell structure. The polymer-coated nanoparticles of Al_2O_3 are typically produced by nucleation reactions, followed by the formation of a core–shell structure. Nanoparticles produced using 10 wt.% Al $(OiPr)_3$ resulted in the formation of films with an average diameter of the core–shell nanoparticles as 45 nm with the glass transition temperature (Tg) of 27°C (above the Tg of the matrix). Many other core–shell systems have also been explored (Huignard et al., 2001; See, Mullins, Mills, & Heiden, 2005). Superficially modified amorphous oxides of metallic nanoparticles of zirconium, tantalum, titanium, vanadium, and yttrium have been produced using these common precursors in microemulsion-based solgel processes. The production of nanoparticles with diameters lower than 200 nm has been carried out by various researchers (Holzinger et al., 2003; Zhao, Ni, Kruczynski, Zhang, & Xiao, 2004). This core–shell fabrication approach has been effective in the synthesis of novel and intricate semiconductor nanoarchitectures. The dispersion of colloidal nanocrystals of CdSe/ZnS core–shell structure with a narrow size distribution was carried out in a hybrid sol obtained from the hydrolysis of 3-glycidoxypropyltrimethoxysilane and TEOS (Epifani, Leo, Lomascolo, Vasanelli, & Manna, 2003). Burns, Ow, and Wiesner (2006) reported the incorporation of multiple molecules of tetramethylrhodamine isothiocyanate dye into monodispersed and uniform nanoparticles (25 nm diameter) of silica core–shell (Ow et al., 2005; Larson et al., 2008). The resultant structure has reportedly shown a significant enhancement in the stability and brightness of the organic dye molecules. These core–shell particles are commonly known as “nanobio C-dots.” The interaction in core–shell structures plays an important role in the improvement of dye properties through an increment in the rigidity of the dye. Several mechanisms have been reported, which assist in the designing of the core–shell architectures for a variety of “nanobio” applications. Currently, extensive work is being carried out in this exciting area of research which will possibly yield various novel nanostructures with extraordinary properties.

REFERENCES

1. Aksay, I. A., & Schilling, C. H. (1984). Colloidal filtration route to uniform microstructures. In *Ultrastructure Processing of Ceramics, Glasses, and Composites*(p. 439).
2. Ashlock, L. T., Mukamal, H., & White, W. H. (1985).*U.S. Patent No. 4,500,669*. Washington, DC: U.S. Patent and Trademark Office.
3. Barringer, E., Jubb, N., Fegley, B., Pober, R. L., & Bowen, H. K. (1984). Processing monosized powders. In *Ultrastructure Processing of Ceramics, Glasses and Composites* (pp. 315–333).
4. Barrow, M., & Olding, T. (2003).*U.S. Patent Application No. 10/601,364*.
5. Baskaran, S., Liu, J., Li, X., Fryxell, G. E., Kohler, N., Coyle, C. A., & Dunham, G. (2001). Molecular templated sol-gel synthesis of nanoporous dielectric films. *Ceramic Transactions, 123*, 39-48.
6. Bescher, E. P., Xu, Y., & Mackenzie, J. D. (1997, October). Ferroelectric-glass nanocomposites. In *Proceedings of the SPIE-The International Society for Optical Engineering* (Vol. 3136, pp. 397-406).
7. Bescher, E., & Mackenzie, J. D. (1998). Hybrid organic-inorganic sensors. *Materials Science and Engineering: C, 6*(2–3), 145-154.
8. Bescher, E., Robson, S. R., Mackenzie, J. D., Patt, B., Iwanczyk, J., & Hoffman, E. J. (2000). New lutetium silicate scintillators. *Journal of Sol-Gel Science and Technology, 19*(1), 325-328.
9. Bescher, E., Xu, Y., & Mackenzie, J. D. (2001). New low temperature multiphase ferroelectric films. *Journal of Applied Physics, 89*(11), 6341-6348.
10. Bhatia, R. B., Brinker, C. J., Gupta, A. K., & Singh, A. K. (2000). Aqueous sol−gel process for protein encapsulation. *Chemistry of Materials, 12*(8), 2434-2441.
11. Bonilla, G., Martínez, M., Mendoza, A. M., & Widmaier, J. M. (2006). Ternary interpenetrating networks of polyurethane-poly (methyl methacrylate)-silica: preparation by the sol–gel process and characterization of films. *European Polymer Journal,42*(11), 2977-2986.
12. Borosilicates, S. (2009). Use of a drying control chemical additive (DCCA) in the sol-gel processing of soda silicate and soda borosilicates. In *8th Annual Conference on Composites and Advanced Ceramic*

Materials: Ceramic Engineering and Science Proceedings (Vol. 5, No. 7–8, p. 546). John Wiley & Sons.

13. Brinker, C. J., & Scherer, G. W. (2013). *Sol-gel science: the physics and chemistry of sol-gel processing*. Academic press.
14. Buissette, V., Moreau, M., Gacoin, T., Le Mercier, T., & Boilot, J. P. (2004). Highly luminescent composite films from core-shell oxide nanocrystals. *MRS Online Proceedings Library Archive, 846*.
15. Burns, A., Ow, H., & Wiesner, U. (2006). Fluorescent core–shell silica nanoparticles: towards "Lab on a Particle" architectures for nanobiotechnology. *Chemical Society Reviews, 35*(11), 1028-1042.
16. Castro, S. L., & Barbera-Guillem, E. (2000).*U.S. Patent No. 6,114,038*. Washington, DC: U.S. Patent and Trademark Office.
17. Chia, C., Kao, Y. H., Xu, Y., & Mackenzie, J. D. (1997, October). Cadmium telluride quantum dot-doped glass by the sol-gel technique. In *Proceedings of the SPIE-The International Society for Optical Engineering* (Vol. 3136, pp. 337-347).
18. Del Monte, F., Xu, Y., & Mackenzie, J. D. (2000). Preparation and characterization of PbS quantum dots doped ormocers. *Journal of Sol-Gel Science and Technology, 17*(1), 37-45.
19. Del Monte, F., Xu, Y., Mackenzie, J. D., Claflin, B., & Lucovsky, G. (1998). Controlling the particle size of quantum dots incorporated in hybrid materials. *MRS Online Proceedings Library Archive, 519*.
20. Ellsworth, M. W., & Novak, B. M. (1991). Mutually interpenetrating inorganic-organic networks. New routes into nonshrinking sol-gel composite materials. *Journal of the American Chemical Society, 113*(7), 2756-2758.
21. Ellsworth, M. W., & Novak, B. M. (1993). "Inverse" organic-inorganic composite materials. 3. High glass content "nonshrinking" sol-gel composites via poly (silicic acid esters). *Chemistry of Materials, 5*(6), 839-844.
22. Epifani, M., Leo, G., Lomascolo, M., Vasanelli, L., & Manna, L. (2003). Sol-gel synthesis of hybrid organic-inorganic monoliths doped with colloidal CdSe/ZnS core-shell nanocrystals. *Journal of sol-gel science and technology, 26*(1), 441-446.
23. Figueira, R. B., Silva, C. J., & Pereira, E. V. (2015). Organic–inorganic hybrid sol–gel coatings for metal corrosion protection: a review of recent progress. *Journal of Coatings Technology and Research, 12*(1),

1-35.

24. Göltner, C. G., Berton, B., Krämer, E., & Antonietti, M. (1998). Nanoporous silica from amphiphilic block copolymer (ABC) aggregates: control over correlation and architecture of cylindrical pores. *Chemical Communications*, (21), 2287-2288.
25. Göltner, C. G., Berton, B., Krämer, E., & Antonietti, M. (1999). Nanoporous silicas by casting the aggregates of amphiphilic block copolymers: the transition from cylinders to lamellae and vesicles. *Advanced Materials*,*11*(5), 395–398.
26. Guest, A. M., Preus, M. W., & Lewis, W. (1991).*U.S. Patent No. 5,013,608*. Washington, DC: U.S. Patent and Trademark Office.
27. Guest, A. M., Preus, M. W., & Lewis, W. (1992).*U.S. Patent No. 5,102,695*. Washington, DC: U.S. Patent and Trademark Office.
28. Hench, L. L., & West, J. K. (1990). The sol-gel process. *Chemical Reviews*,*90*(1), 33-72.
29. Henry, M., & Sanchez, C. (1988). Sol-gel chemistry of transition metal oxides. *Progress in Solid State Chemistry*,*18*(4), 259-341.
30. Holzinger, D., & Kickelbick, G. (2003). Preparation of amorphous metal-oxide-core polymer-shell nanoparticles via a microemulsion-based sol−gel approach. *Chemistry of Materials*, *15*(26), 4944-4948.
31. Huignard, A., Gacoin, T., Chaput, F., Boilot, J. P., Aschehoug, P., & Viana, B. (2001). Synthesis and luminescence properties of colloidal lanthanide doped YVO 4. *MRS Online Proceedings Library Archive*, *667*.
32. Iler, R. K., Hench, L. L., & Ulrich, D. R. (1986). *Science of ceramic chemical processing*. New York: Wiley.
33. Innocenzi, P., & Kozuka, H. (1994). Methyltriethoxysilane-derived sol-gel coatings doped with silver metal particles. *Journal of Sol-Gel Science and Technology*, *3*(3), 229-233.
34. Innocenzi, P., Kozuka, H., & Sakka, S. (1994). Preparation of coating films doped with gold metal particles from methyltriethoxysilane-tetraethoxysilane solutions. *Journal of Sol-Gel Science and Technology*, *1*(3), 305-318.
35. Iwanczyk, J. S., Patt, B. E., Tull, C. R., MacDonald, L. R., Bescher, E., Robson, S. R., & Hoffman, E. J. (2000). New LSO based scintillators. *IEEE Transactions on Nuclear Science*, *47*(6), 1781-1786.

36. January, J. R. (1982).*U.S. Patent No. 4,355,135*. Washington, DC: U.S. Patent and Trademark Office.

37. Kang, D. P., Park, H. Y., Ahn, M. S., Myung, I. H., Lee, T. J., Choi, J. H., & Kim, H. J. (2005). Properties of sol-gel materials synthesized from colloidal silica and alkoxy silanes. *Polymer Korea, 29*(3), 242-247.

38. Kim, D. Y., Du, H., Bhandarkar, S., & Johnson, D. W. (2002). Sol-gel processing of low dielectric constant nanoporous silica thin films. In *Materials research society symposium proceedings 1999* (Vol. 703, pp. 147-152). Warrendale, PA: Materials Research Society.

39. Klein, L. C., & Woodmann, R. H. (1996). Porous silica by the sol-gel process. In*Key engineering materials* (Vol. 115, pp. 109-124). Trans Tech Publications.

40. Krämer, E., Förster, S., Göltner, C., & Antonietti, M. (1998). Synthesis of nanoporous silica with new pore morphologies by templating the assemblies of ionic block copolymers.*Langmuir,14*(8), 2027-2031.

41. Larson, D. R., Ow, H., Vishwasrao, H. D., Heikal, A. A., Wiesner, U., & Webb, W. W. (2008). Silica nanoparticle architecture determines radiative properties of encapsulated fluorophores. *Chemistry of Materials, 20*(8), 2677-2684.

42. Latella, B. A., Ignat, M., Barbé, C. J., Cassidy, D. J., & Bartlett, J. R. (2003). Adhesion behaviour of organically-modified silicate coatings on stainless steel. *Journal of Sol-Gel Science and Technology, 26*(1), 765-770.

43. Latella, B. A., Ignat, M., Barbe, C. J., Cassidy, D. J., & Li, H. (2004). Cracking and decohesion of sol-gel hybrid coatings on metallic substrates. *Journal of Sol-Gel Science And Technology, 31*(1–3), 143-149.

44. L'Espérance, D., & Chronister, E. L. (1993). Rotational dynamics of quinizarin in silicate and aluminosilicate solutions, gels, and glasses. *Chemical Physics Letters,201*(1–4), 229-235.

45. Li, G., & Nogami, M. (1993). Formation of quantum-size PbTe microcrystals in sol-gel derived silica and borosilicate glasses. *Journal of Sol-Gel Science and Technology, 1*(1), 79-83.

46. Lin, H. T., Bescher, E., Mackenzie, J. D., Dai, H., & Stafsudd, O. M. (1992). Preparation and properties of laser dye-ORMOSIL composites. *Journal of Materials Science,27*(20), 5523-5528.

47. Liu, W., Zhong, W., Jiang, H. Y., Tang, N. J., Wu, X. L., & Du, W. Y. (2005). Synthesis and magnetic properties of FeNi3/Al2O3 core-shell nanocomposites. *The European Physical Journal B-Condensed Matter and Complex Systems, 46*(4), 471-474.

48. Liu, W., Zhong, W., Jiang, H., Tang, N., Wu, X., & Du, Y. (2006). Highly stable alumina-coated iron nanocomposites synthesized by wet chemistry method. *Surface and Coatings Technology, 200*(16), 5170-5174.

49. Lu, Y. (1998).*Nanoporous silica based on sol-gel processing and templating approaches*(Doctoral dissertation, University of New Mexico).

50. Mackenzie, J. D., & Bescher, E. (2003). Some factors governing the coating of organic polymers by sol-gel derived hybrid materials. *Journal of Sol-Gel Science and Technology, 27*(1), 7-14.

51. Mackenzie, J. D., & Bescher, E. P. (1998). Structures, properties and potential applications of ormosils. *Journal of Sol-Gel Science and Technology, 13*(1), 371-377.

52. Mackenzie, J. D., & Xu, Y. (1997). Ferroelectric materials by the sol-gel method. *Journal of Sol-Gel Science and Technology, 8*(1–3), 673-679.

53. Mackenzie, J. D., Chung, Y. J., & Hu, Y. (1992). Rubbery ormosils and their applications. *Journal of Non-Crystalline Solids,147,* 271-279.

54. Nogami, M., Kojima, I., & Nagasaka, K. (1992). Microcrystalline-CdTe-doped silica glasses: sol-gel preparation and quantum confinement effect. In *San Diego'92* (pp. 557-564). International Society for Optics and Photonics.

55. Novak, B. M., & Davies, C. (1991). "Inverse" organic-inorganic composite materials. 2. Free-radical routes into nonshrinking sol-gel composites. *Macromolecules, 24*(19), 5481–5483.

56. Otaki, S. (1997).*U.S. Patent No. 5,693,259*. Washington, DC: U.S. Patent and Trademark Office.

57. Ow, H., Larson, D. R., Srivastava, M., Baird, B. A., Webb, W. W., & Wiesner, U. (2005). Bright and stable core− shell fluorescent silica nanoparticles. *Nano Letters, 5*(1), 113-117.

58. Pope, E. J. A., Asami, M., & Mackenzie, J. D. (1989). Transparent silica gel–PMMA composites. *Journal of Materials Research, 4*(4), 1018-1026.

59. Reisfeld, R. (2002). Fluorescent dyes in sol-gel glasses. *Journal of Fluorescence,12*(3-4), 317-325.

60. Reisfeld, R. (2004). Doped sol-gel coatings. In *Sol-Gel Technologies for Glass Producers and Users*(pp. 307–311). US: Springer.

61. Renteria, V. M., & Campero, A. (1998). Thermochromic properties of silver colloids embedded in SiO2 gels. *Journal of Sol-Gel Science and Technology, 13*(1–3), 663-666.

62. Salomons, E. (1988). Monte Carlo simulation of hydrogen diffusion in metal and alloys.*Journal of Physics C: Solid State Physics,21*(35), 5953.

63. Sanchez, C., & Ribot, F. (1994). Design of hybrid organic-inorganic materials synthesized via sol-gel chemistry. *New Journal of Chemistry,18*(10), 1007-1047.

64. Schlottig, F., Textor, M., Georgi, U., & Roewer, G. (1999). Template synthesis of SiO2 nanostructures. *Journal of Materials Science Letters,18*(8), 599–601.

65. Schmidt, H. (1985). New type of non-crystalline solids between inorganic and organic materials. *Journal of Non-Crystalline Solids,73*(1), 681-691.

66. See, K. H., Mullins, M. E., Mills, O. P., & Heiden, P. A. (2005). A reactive core–shell nanoparticle approach to prepare hybrid nanocomposites: effects of processing variables. *Nanotechnology, 16*(9), 1950.

67. Seker, F., Meeker, K., Kuech, T. F., & Ellis, A. B. (2000). Surface chemistry of prototypical bulk II−VI and III−V semiconductors and implications for chemical sensing. *Chemical Reviews,100*(7), 2505-2536.

68. Sellinger, A., & Laine, R. M. (1996). Silsesquioxanes as synthetic platforms. Thermally curable and photocurable inorganic/organic hybrids. *Macromolecules, 29*(6), 2327-2330.

69. Shan, W., Wang, B., Zhang, Y., & Tang, Y. (2005). Fabrication of lotus-leaf-like nanoporous silica flakes with controlled thickness. *Chemical Communications,* (14), 1877-1879.

70. Stoeck, A. (2012). Synthese und Charakterisierung lumineszenter, transparenter Dünnfilme und deren Anwendung in Gasentladungslampen.

71. Teowee, G., McCarthy, K. C., Baertlein, C. D., Boulton, J. M., Motakef, S., Bukowski, T. J., & Uhlmann, D. R. (1996). Dielectric properties of organic-inorganic hybrids: PDMS-based systems. *MRS*

Online Proceedings Library Archive, 435.

72. Toselli, M., Marini, M., Fabbri, P., Messori, M., & Pilati, F. (2007). Sol–gel derived hybrid coatings for the improvement of scratch resistance of polyethylene. *Journal of Sol-Gel Science and Technology, 43*(1), 73-83.
73. Tseng, J. Y., Li, C. Y., Takada, T., Lechner, C., & Mackenzie, J. D. (1992, December). Optical properties of metal-cluster-doped ORMOSIL nanocomposites. In *Proceedings of the SPIE-The International Society for Optical Engineering* (Vol. 1758, p. 612).
74. Uchida, N., Ishiyama, N., Kato, Z., & Uematsu, K. (1994). Chemical effects of DCCA to the sol-gel reaction process. *Journal of Materials Science,29*(19), 5188-5192.
75. Wang, X. (2012).*Polyester based hybrid organic coatings* (Doctoral dissertation, The University of Akron).
76. White, W. H., Harbison, W. C., & Nelson, G. L. (1983).*U.S. Patent No. 4,390,373*. Washington, DC: U.S. Patent and Trademark Office.
77. White, W. H., Harbison, W. C., & Nelson, G. L. (1984).*U.S. Patent No. 4,442,168*. Washington, DC: U.S. Patent and Trademark Office.
78. Wilkes, G. L. (1985). "Ceramers" hybrid materials incorporating polymeric/oligomeric species into inorganic glasses utilizing a sol-gel approach. *Polymer Preprints, 26*, 300-301.
79. Xu, Y., & Mackenzie, J. D. (1999). A theoretical explanation for ferroelectric-like properties of amorphous $Pb(Zr_xTi_{1-x})O_3$ and $BaTiO_3$. *Journal of Non-Crystalline Solids, 246*(1), 136-149.
80. Xu, Y., Kao, Y. H., Chia, C., Mackenzie, J. D., Honkanen, S., & Peyghambarian, N. (1997). Optical waveguide based on CdS quantum-dot-doped sodium borosilicate glass fabricated by the sol-gel technique. In *Proceedings of the Optical Science, Engineering and Instrumentation'97* (pp. 326–336). International Society for Optics and Photonics.
81. Xu, Y., Monte, F. D., Mackenzie, J. D., Namjoshi, K., Muggli, P., & Joshi, C. (1999). Nanocomposite of semiconducting ferroelectric antimony sulphoiodide dots-doped glasses. *Ferroelectrics, 230*(1), 11-20.
82. Zhao, Y., Ni, C., Kruczynski, D., Zhang, X., & Xiao, J. Q. (2004). Exchange-Coupled Soft Magnetic FeNi−SiO2 Nanocomposite.*The Journal of Physical Chemistry B, 108*(12), 3691-3693.

83. Zhao, Z. H., Hasebe, K., Sakagami, Y., & Osaka, T. (1997). The inhibitory capability of decorative plated coatings for the growth of bacteria. *Bulletin of the Chemical Society of Japan, 70*(7), 1631-1637.

84. Zink, J. I., Yamanaka, S. A., Ellerby, L. M., Valentine, J. S., Nishida, F., & Dunn, B. (1994). Biomolecular materials based on sol-gel encapsulated proteins. *Journal of Sol-Gel Science and Technology, 2*(1), 791-795.

CHAPTER 6

THE ROLE OF CHEMICAL SYNTHESIS IN THE SUSTAINABILITY OF ORGANIC DYE-SENSITIZED SOLAR CELLS

CONTENTS

6.1 INTRODUCTION

The production of an efficient and novel π-extended D-A-π-A natural sensitizer (G3, η = 8.64%) intended for solar cells that are dye-sensitized has been achieved by the application of the green chemistry pillars. It aims at overriding conventional routes that involved organometallic intermediates with novel synthetic strategies for reduction in the production of waste material as well as reducing dye production costs. Research has shown that complex target sensitizer can be exclusively obtained through direct arylation reactions. Comparison of green metrics with that of a conventional synthetic pathway indicates that the novel approach, without a doubt, has a lower impact on the environment regarding generated wastes and chemical procedures. This, in turn, stresses on the significance of the synergy among the synthetic plan and the molecular design in the framework of ecological friendly routes to support the sustainable development of third-generation photovoltaic. Moreover, an investigation was also carried out to inspect the stability of the G3-based photovoltaic devices in aging tests on devices having large area which demonstrated the excellent potential of the planned structure for all practical applications that involve organic dye interfaces/ inorganic semiconductor (Ooyama et al., 2011; Ooyama & Harim, 2012; 2013).

Constant research has been ongoing to find the potential alternative to the commercially available photovoltaic technologies. One major attraction for this purpose is dye-sensitized solar cells (DSSCs) which have been a focus of attention due to various aspects such as ease of fabrication, their high efficiencies of conversion from light to energy, their distinctive peculiarity in terms of coloration and transparency, which enables the design of proficient, vibrant smart panels, and devices also amenable to building integration (Yen, Chou, Chen, Hsu, & Lin, 2012; Liang & Chen, 2013; Zhang, Yang, Numata, & Han, 2013). The typical configuration of a DSSC is composed of a counterelectrode, a photoanode (normally a duly dye-sensitized semiconducting film made of mesoporous titania material), and an electrolyte that contain a redox couple (O'regan & Grätzel, 1991; Mishra, Fischer, & Bäuerle, 2009; Zeng et al., 2010). A major portion of the research on DSSC has its focus on the dye, which is responsible for the harvesting of photons as well as assisting the injection of an electron into the titania conduction band (Ogura et al., 2009; Yum, Baranoff, Wenger, Nazeeruddin, & Grätzel, 2011; Fan et al., 2011). Nevertheless, the selection of the sensitizer greatly influences not just the efficiency of the device

but also most of the environmental factors and price associated with the production of technology (Zardetto et al., 2013; Fakharuddin, Jose, Brown, Fabregat-Santiago, & Bisquert, 2014; Matteocci et al., 2016). As a result, with particular reference to the sensitizer, even though it is permissible that fundamental research on DSSCs should focus to struggle for the accomplishment of higher and higher efficiencies, part of this research must also be directed toward minimizing the environmental effect that is related to the production of DSSCs.

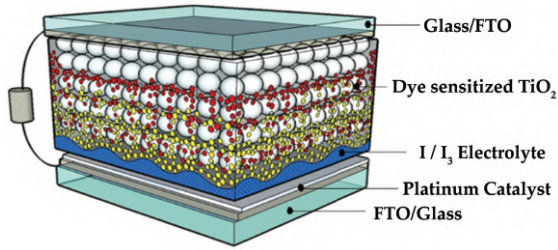

Figure 52. Typical configuration of a dye-sensitized solar cell (DSSC)

[Source: https://schanze.chem.ufl.edu/research/dye-sensitized-solar-cells/]

Sensitizers that are fully organic have shown great potential in both amenabilities to optimization and design flexibility regarding performances of devices (Hagfeldt, Boschloo, Sun, Kloo, & Pettersson, 2010; Yella et al., 2011; Mishra et al., 2009). From the environmental point of view, application of organic dyes calls off the requirement of restoring to rarely occurring heavy metals such as ruthenium or exceptionally toxic ones like lead (a constituting element of solar cells based on perovskite material and presently currently in the "spotlight" due to their high efficiency) for the environmental impacts that involve both production and postlife disposal (Gao, Grätzel, & Nazeeruddin, 2014; Green, Ho-Baillie, & Snaith, 2014; Sum & Mathews, 2014).

Among various proposed molecular architectures, synthesis of an extensive number of organic dyes has been carried out as per the D-π-A concept, by putting in fitting conjugation an electron-withdrawing group (A) and an electron-donating group (D) having the ability to bind to the titania through an appropriate π-spacer (π), the former being the primary focus of current structural tailoring intended for expansion of the light-harvesting range (Wu et al., 2012; Yen et al., 2012; Wu & Zhu, 2013). From the point of view of synthetic chemistry, the downside of the D-π-A concept is associated

with the asymmetric structure of the sensitizers, which inevitably leads to a high number of synthetic steps needed for obtaining the target molecule (He, Wu, Zhu, & Zhang, 2014; Xiao, Zhang, He, & Zhang, 2014; Xing, Chen, Jia, Jiang, & Yang, 2017).

Simultaneously, it is important to recognize that the main concern for the market breakthrough of DSSC will be to bridge the gap that exists between research of the fundamental materials and their scalability. In fact, customary laboratory practice puts a higher strain on the environment; furthermore, it is not always possible to transfer it to an industrial scale. The assurance of environmental sustainability is important since the key challenges in environmental science are not merely associated with exploitation of renewable energy sources but also for assessment, monitoring, and minimization of the effect related to the chemistry of materials behind a green technology (Burke & Lipomi, 2013 Osedach, Andrew, & Bulović, 2013; Po et al., 2014). For that reason, novel methods followed for organic synthesis of highly capable organic sensitizers that help maximizing sustainability (mainly in terms of amount of waste) are incredibly desirable, being potentially open to scalability without causing any severe impact on the environment (Zhang, Kang, Barlow, & Marder, 2012; 2013; He, Wu, C. Z., Qing, F. L., & Zhang, 2014).

In this regard, synthetic protocols that are based on the activation of C−H bond for constructing a π-conjugated scaffold can be considered the superior tool for reducing the number of synthetic steps, since they allow evading the preparation of organometallic intermediates that are required for the conventional cross-coupling methods (Schipper & Fagnou, 2011; Berrouard et al., 2012; Mercier & Leclerc, 2013). The rarity of examples that employ functioning of C−H bond for synthesizing organic sensitizers may be linked to the fact that few restrictions of the existing C−H activation protocols (such as the low selectivity in the presence of two or more active bonds) appear to form an undefeatable obstacle when applied to the assemblage of the complicated asymmetric structures of D-π-A organic sensitizers (Kang et al., 2014; Chai et al., 2015; Joly et al., 2015).

The main idea underlying this work is to exhibit that the roadmap directed toward highly capable dyes can be escorted with an appropriate plan of cleaner synthetic methodologies (Feng et al., 2013; Qian, Gao, Zhu, Lu, & Zheng, 2015). This work focuses on the application of the principles of green biotechnology about the production of reduced waste material and

the utilization of hazardous reactants (Double, 2014; Jiang, Fan, Lu, Zhou, & Wang, 2014; Li et al., 2014; Echeverry et al., 2015). On these grounds, in continuation with our studies on the function of a π-bridge extension in benzothiadiazole-based D-A-π-A sensitizers, a novel dye has been conceived (known as G3, Fig. 53) by the application of the simplest obtainable aromatic units (benzothiadiazole, thiophene, benzene) to call for an optimum DSSC work cycle (Grisorio et al., 2014; Liu et al., 2014; Roiati et al., 2015).

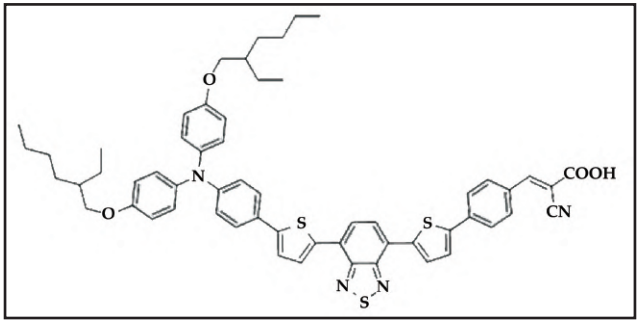

Figure 53. Chemical structure of the target sensitizer (G3)

[Source: http://pubs.acs.org/doi/abs/10.1021/acssuschemeng.5b00108]

Accordingly, a sustainable approach was applied to a large extent from the initial stage of the molecular design of the dye (Agosta et al., 2014; Shibayama, Ozawa, Abe, Ooyama, & Arakawa, 2014). This is because the implementation of further complex structures would have needed extra synthetic steps, inescapably leading to the higher production of waste material and increased costs (Krebs & Jørgensen, 2013). For the very first time, a comparison has been made between two synthetic protocols: a conventional approach that utilizes organometallic intermediates (used to validate the hypothesis on potentialities and efficacy of the dye) and secondly, an appropriately optimized course that is exclusively grounded on direct arylation reactions. The green metrics (yields on the whole, EcoScale parameter, E-factor) and the estimated price per gram of these two synthetic protocols have been calculated providing guiding principles that, if applied as good practice, will reduce the cost and the environmental impact associated with the production of the "green" technologies using organic materials (Po et al., 2014; Po, Bianchi, Carbonera, & Pellegrino 2015).

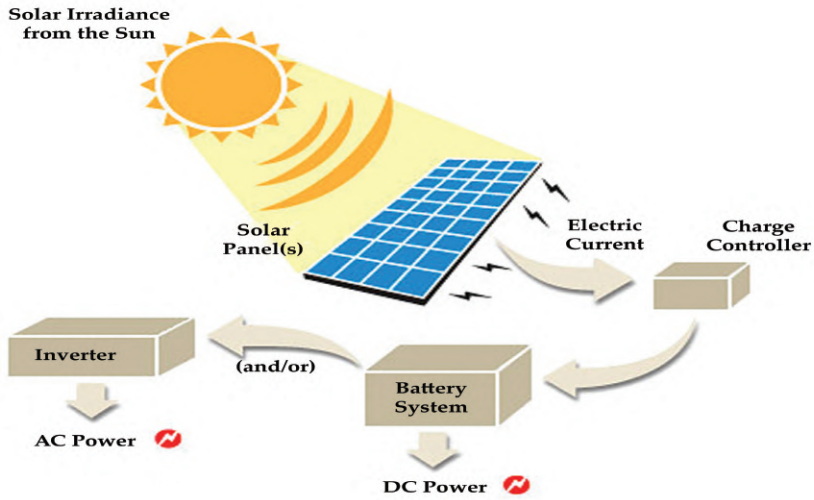

Figure 54. Typical working principle of a solar cell

[Source: https://saferenvironment.wordpress.com/2009/02/02/solar-power-%E2%80%93-sustainable-green-energy-to-protect-our-economy-and-environment/]

While DSSCs carry on exhibiting expected competitive prices about those of the conventional silicon-based solar technologies, at the same time, the stability of the device is put at severe risk when organic sensitizers are employed as light harvesters. The stability of ruthenium-based devices was anticipated to be around 25 years under Southern European ambient conditions using accelerated aging tests (Sheldon, 2007; 2010). As a result, once the environmental impact related to its costs and synthesis was evaluated, we deem it valuable to study the stability of the G3 sensitizer in an attractive DSSC application by employing transparent thin TiO_2 layers (Van Aken, Strekowski, & Patiny, 2006; Patel et al., 2012). In the case of cells containing G3, the drop in efficiency (15%) after 1000 hours of aging at 85°C of large area devices was observed to be extremely lower as compared to ruthenium-based devices.

6.2 SOLAR CELL SYNTHESIS AND ENVIRONMENTAL ASPECTS

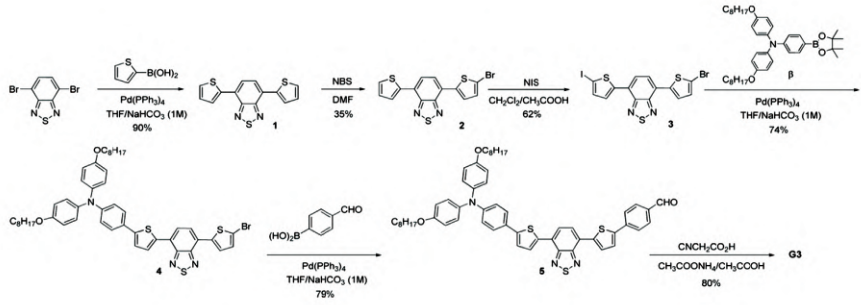

The plan of the first approach for the synthesis of G3 included using conventional Pd-catalyzed Suzuki cross-coupling steps (Route A), as explained in Scheme 1 (Kato et al., 2009; Harikisun & Desilvestro, 2011). The realization of the benzothiadiazole comprising of chromophore started from the commercially offered 4, 7-dibromo benzothiadiazole, which was delivered to a Suzuki cross-coupling having thiophene-2-aryl boronic acid resulting in the corresponding diphenyl derivative 1. The reaction between 1 and an equimolar quantity of N-bromosuccinimide (NBS) resulted in the corresponding bromo derivative 2; afterward, bromo derivative 2 was halogenated by reacting it with N-iodosuccinimide (NIS), which yielded compound 3. To bind together the electron group and the chromophore, a Suzuki coupling was carried out between 3 and the suitable triarylamine boronic ester β which led to the formation of intermediate 4, which, due to the halogen effect, is yet endowed with the bromide leaving the group. Following that, a Suzuki cross-coupling between 4-formyl-phenylboronic acid and 4 made it possible for us to acquire the aldehyde-functionalized precursor 5, which, in the end, was converted into the target molecule G3 as a result of a Knoevenagel reaction with cyano-acetic acid. After that, the acquired sensitizer was completely characterized via elemental analysis, NMR, UV−vis as well as by electrospray ionization high-resolution mass spectrometry (ESI-HRMS) that clearly confirmed its structure.

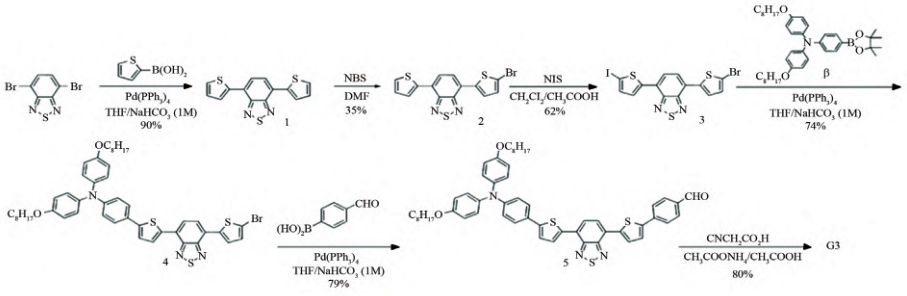

Figure 55. Synthetic sequence (Scheme 1) followed for obtaining G3 through a conventional approach (Route A)

[Source: http://pubs.acs.org/doi/abs/10.1021/acssuschemeng.5b00108]

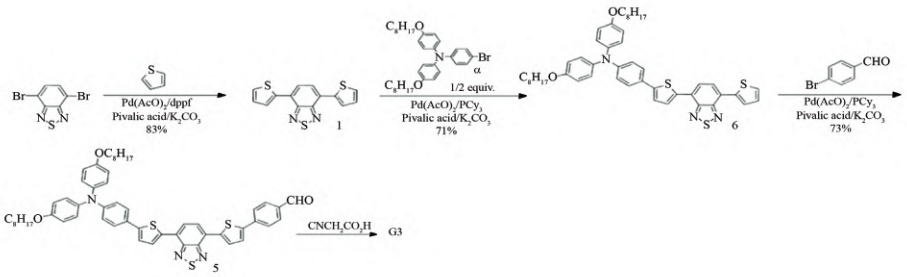

Figure 56. Synthetic sequence (Scheme 2) followed for obtaining G3 through C−H direct arylation (Route B)

[Source: http://pubs.acs.org/doi/abs/10.1021/acssuschemeng.5b00108]

Subsequently, we felt motivated to investigate terms for a synthetic scale-up of the material, as well as exploring the environmental problems associated with its synthesis. Within this perspective, our investigation initiated by selecting E-factor, overall yields, and an EcoScale parameter related to the preparation of G3 to assess the sustainability of the first approach (Route A) from the waste generation, chemical, and safety point of view, respectively. Particularly, the high E-factor (15815.19 g/g) unable to get along with the large-scale production of the dye verified the requirement for sustainable and alternative approaches.

The simplest method for lessening the environmental effects of a chemical synthesis is reducing the total number of the synthetic steps. To pursue this goal for achieving G3, the most appropriate considered method

is the setting up of a synthetic sequence based entirely on direct arylation reactions (Scheme 2) avoiding all metalation steps.

Table 7. Tuning of the reaction conditions for obtaining 1 through direct arylation

Sr. No.	Solvent	Ligand	Thiophene Equiv[a]	Yield (%) [B]
1	toluene	t-Bu_3P	1.0	traces
2	toluene	t-Bu_3P	5.0	8
3	toluene	t-Bu_3P	10.0	14
4	DMF	t-Bu_3P	10.0	traces
5	DMSO	t-Bu_3P	10.0	traces
6	thiophene	t-Bu_3P	20.8	35
7	thiophene	Cy_3P	20.8	38
8	thiophene	Ph_3P	20.8	47
9	thiophene	dppe	20.8	78
10	thiophene	dppf	20.8	83

a=per bromine atom; b=isolated yields by crystallization or chromatography.

On this basis, we embarked in the unique synthesis of the chromophore 1 initiating from 4,7-dibromobenzothiadiazole and triggering the C−H bonds on the thiophene by making use of Pd $(AcO)_2$ as a source of palladium, pivalic acid (30% mol/mol with regard to atoms of bromine) as a proton shuttle, K_2CO_3 (1.5 equiv. with regard to bromine atoms) as the base, and tri (t-butyl) phosphane (2.0 equiv. with regard to Pd) as the ligand (Cannavale et al., 2011; 2014; Matsidik et al., 2014; Matsidik, Komber, & Sommer, 2015). The preliminary screening of reaction conditions (as mentioned in Table 7) involved the relative amount of thiophene and the solvent. In the first attempts, to get better yields of the reaction, the impact of excess thiophene (Sr. No. 1−3) was assessed in toluene as the solvent. Unluckily, under such conditions, the reaction was barely selective, most likely for the reason that after arylation of the initially activated 2-position of the thiophene unit, the thiophene 5-position of the formed intermediate turns into more reactive.

While we increase the polarity of the reaction medium (Table 7: Nos. 4 and 5), it did not improve the reaction selectivity. It is thus logical to presume that the acidity of the thiophene α-proton within thiophene–benzothiadiazole segment (and in its higher homologues) is stronger as

compared to the acidity of the α-protons within isolated thiophene, owing to the existence of a strong electron withdrawing unit in the former (X. Wang, & M. Wang, 2014; Wang, Wang, & Wang, 2015).

6.3 ACS SUSTAINABLE CHEMISTRY AND ENGINEERING

Apparently, thiophene is not much prone toward the hydrogen abstraction step required for the direct arylation and is liable for the limited selectivity of the reaction under such conditions. On the other hand, if the reaction takes place within thiophene taken as the solvent (11.4 ml for each gram of dibromobenzothiadiazole, 20.8 equiv. for each bromine atom, No. 6), the yield of the reaction is increased to almost 35%. The strong, surplus thiophene reduced the side reactions by mass action, which led to an increase in the selectivity of the process, whereas the moderate yield appears to be connected with deactivation of the catalyst, which hindered a complete conversion of the substrate (Zhang et al., 2013; He et al., 2014). Consequently, the succeeding efforts made with an aim to improve the reaction course were directed at the exploration for a more robust catalytic system by conveniently varying the phosphine ligand. From the screening of the ligand (entries 6−10), it was obvious that aryl phosphanes are more performing as compared to aliphatic ones. In addition to this, apparently bidentate ligands (dppe and dppf) proved to be the most suitable for this reaction. The reaction that was carried out in the company of dppf as the ligand permitted us to obtain 1 in 83% isolated yield.

Particular attention was given to the optimization of workup procedure to reduce the waste load derived from the reaction, that is, the removal of the excess solvent (thiophene) was carried out by the distillation process. Additionally, the product was easily isolated by precipitation reaction involving a minimum quantity of ethanol/water mixture, followed by the formation of crystals from ethanol. The convenient isolation of the product was carried out due to the excellent solubility of K_2CO_3, pivalic acid and KBr by-products. The purification step was facilitated by the non-existence of organic by-products resulting from side reactions. Interestingly, the excess thiophene was recovered by distillation, followed by efficient recycling for further synthesis of 1 via activation of the C−H bond. The above-mentioned purification process resulted in the attainment of the same parameters for purity and yield of the target compound, that is, G3. The calculation of the E-factor for this particular step of Route B (specifically the attainment of

the building block 1) provided a value of 83.53 g/g, which is roughly one-sixth of the value, obtained for Route A (478.57 g/g). The above practice represents a great progress regarding waste creation for the attainment of the same product. In this framework, it is essential to note that the calculation of E-factor for the attainment of 1 in Route A is undervalued. This is because of the reason that this calculation does not consider the use of formerly dried and distilled solvents (e.g., toluene, DMSO, or DMF), which unavoidably leads to further production of waste. The above-mentioned process provides an added value to the direct arylation process proposed in Route B. The behavior of 1 under direct arylation was also investigated thoroughly to evaluate the environmental sustainability of asymmetric structure assemblies via subsequent activations of C−H bonds.

As illustrated in Scheme 2, binding of the donor-containing triarylamine group with benzothiadiazole-based chromophore takes place by the reaction of the bromo derivative α with 1 using the standardized catalytic system of Pd (AcO) 2/PCy3, to guarantee the attainment of soluble reaction products. The molar ratio (1/α) was varied to carry out the screening (Table 8). Differently from the other substrates containing two identical C−H-activated positions thus far explored in direct monoarylations (thiophene or bithiophene), Unlike formerly investigated cases, the present case depicts that the utilization of 2.0 equivalent of 1 with reference to α is adequate to guarantee a satisfactory yield (i.e., 71% with reference to the limiting reactant). The results illustrated in Table 2 demonstrate that the reactivity of the C−H bonds in 1 is analogous with that in 6, due to the use of 1.0 equivalent of 1 concerning α (entry 1) which led to a virtual statistical distribution of products.

Table 8. Product distribution of the reactions between α and 1 via direct arylation routes

entry	equiv[a]	recovered 1 (%)	monosub product (%)[c]	disub product (%)[c]
1	1.0	19	42	18
2	1.5	71[b]	59	11
3	2.0	80[b]	71	traces

[a]Equiv of 1 with respect to α. [b]Calculated with respect to the used excess. [c]Isolated yields with respect to the limiting reactant (α).

6.4 COMPARISON OF DIFFERENT SYNTHESIS APPROACHES

The uses of 2.0 equivalent of 1 with reference to α make an appropriate compromise between yield minimization and maximization during the waste production originating from the utilization of excess reagents (the relative waste load associated with the synthesis of 1). These experimental conditions (particularly the excess amounts of the powdery substance 1) do not impede the purification procedures. Amazingly, most of the one amount (80%) can be recovered, and only small amounts of the disubstituted product are formed. The utilization of a surplus of 1 leads to an increment in the E-factor during the reaction steps. It is well documented that the increase of E-factor improves the sustainability of the projected Route B for large-scale potential applications. Moreover, the above procedure can also be employed for the synthesis of a wide range of structures at laboratory scale. The path toward the fabrication of G3 via direct arylation procedures was further followed by improving the reactive behavior of the asymmetric substance 6 in the 4-bromobenzaldehyde environment along with the presence of aldehyde precursor 5. It has been reported that the yield of the reaction involving the Pd (AcO) 2/PCy3 catalytic systems approaches 73%. The synthetic Route B has also been evaluated for calculation of green metrics for G3. The calculation results were compared with the ones obtained from the conventional method, that is, Route A. It is obvious from the repeated results that the overall yield obtained with Route B is significantly higher than that obtained with Route A, representing the lesser number of synthetic steps. A preliminary deliberation has to be made regarding the environmental concerns associated with two different synthetic routes.

Table 9. Cost summary and green metric of the two processes for the attainment of the final sensitizer G3

entry	Route A (traditional approach)	Route B (C-H activation)
overall yield (%)	1.7	10.7
E-factor (g/g)	15815.19	7706.91
EcoScale parameter	-161.2	-82.7
cost (€/g)	1117.14	505.45

The comparison of E-factor values attained for various approaches using a variety of raw materials must be made carefully. Usually, the projected step-by-step assembling of the target molecules in Route A does not follow the comparison step. On the other hand, commercially available, 4-formyl-phenylboronic acid and thiophene-2-aryl boronic acid necessitate further manufacturing steps to be synthesized. Route A initiates the synthesis procedure by consuming the suitable raw materials (which are directly utilized as reactants in the case of Route B); consequently, escalating the waste burden linked with Route A. At the same instance, in the case of activation reactions associated with C−H, an appropriate blend of chemicals has to be employed to create the catalytic system, which differs from the conventional Pd (PPh3) 4 used in Suzuki cross-couplings. Almost every commercial reactant possesses an environmental impact, which cannot be exploited by calculating the E-factor of the individual reaction steps.

It can be predicted that the cost analysis of a fine chemical substance can prove helpful for a comparative assessment of the environmental impacts linked to the chemical compound. This is because of the reason that the sale price of a chemical compound is also determined by the percentage of the waste burden present in the overall weight (Anderson, 2012; Butter et al., 2006). Considering the waste content of the chemical compounds, it is quite possible to obtain lower prices of the published catalogs by negotiation. However, the cost estimation of all intermediate compounds is established by the presently available prices of the raw materials. On the above-mentioned basis, the projected per-gram cost of G3 was evaluated for Route A (approx. 1117.14 €/g). The projected cost is enormously high for a fine chemical compound with prospective large-scale applications. On the contrary, the expected per-gram cost of G3 for Route B was approximately 505.45 €/g, exhibiting a huge improvement (Table 3). Although the higher costs do not directly influence the environment, the manufacturing choices resulting in a considerable cut-down in cost are essential in the view of achieving competitiveness to the solar cell technology (Osedach et al., 2013; Hendsbee, Macaulay, & Welch, 2014). Immense benefits can also be obtained concerning waste production due to diminished E-factor calculation in Route B, that is, 7706.91 g/g, which is half of the calculation obtained for Route A. An additional key tool for the assessment of environmental impact of a process is the estimation of the EcoScale parameter. The evaluation of EcoScale parameter incorporates issues such as hazards and toxicity associated with the use of solvents, reagents, process setup, purification procedures, and prices. A higher value of EcoScale factor represents a better

method. The values acquired for Routes A and B. Low values are attained for Route A and Route B (−82.7 and −161.2 for Routes B and A, respectively), due to the higher number of manufacturing steps. However, it is evident that Route B is exceptionally favorable concerning the traditional approach due to the presence of C−H activation pathway.

6.5 DEVICE STABILITY AND PHOTOVOLTAIC PROPERTIES

The photovoltaic potentials of G3 devices have been evaluated by developing a series of liquid electrolyte dye-sensitized solar cells. The power conversion efficiency of G3 (i.e., $\eta = 8.64\%$) can be recognized as extraordinarily high. This is because power conversion efficiency of G3 is higher than that of the cells constructed from the ruthenium-based dye (N719) with the average laboratory-scale efficiency of around 8.3% (commonly recognized as a reference value in DSSCs). The higher conversion efficiencies of G3-based solar cells have motivated the scientists and researchers to explore this area of active devices.

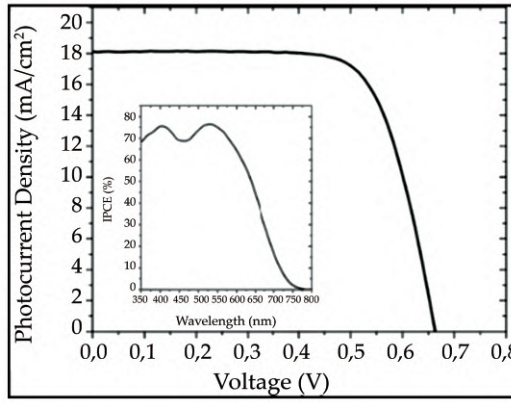

Figure 57. Relationship between photocurrent density and voltage (curve of a G3-based solar cell device under 1.0 sun illumination (VOC = 0.663 V, JSC = 18.11 mA/cm^2, FF = 0.72).

[Source: http://pubs.acs.org/doi/abs/10.1021/acssuschemeng.5b00108]

To evaluate the high efficiency of G3-based solar cells, the performances of transparent DSSC prototypes with a large area have been investigated repeatedly before and after the aging test (at 85°C for 1000 hours in variable

ambient conditions), followed by the comparison of the results with the N719-based standard.

6.5.1 Effect of Aging Process

Before the aging process, short-circuit current (JSC) and open-circuit voltage (VOC) were analogous to both cells prepared by Grisorio et al. (2015). The values of JSC and VOC were independent of the used dye (N719 or G3). However, the N719-based solar cells exhibited a superior fill factor (FF) resulting in slightly higher increasing efficiencies (Fig. 58A). The N719-based solar cell exhibited an efficiency drop of about 59% after undergoing aging for 1000 hours (Leonardi, Penna, Brown, Di Carlo, & Reale., 2010; Heo, Jun, Y., & Park, 2013). On the other hand, the decrement in the efficiency of the G3 device was approximately 15% (Fig. 58B).

Interpretation of the above data necessitates considering that the diffusion of water is only possible during a prolonged aging process in the dearth of any humidity control system at a constant aging temperature. The above-illustrated situation presents the detailed information on the long-term stability of a particular dye.

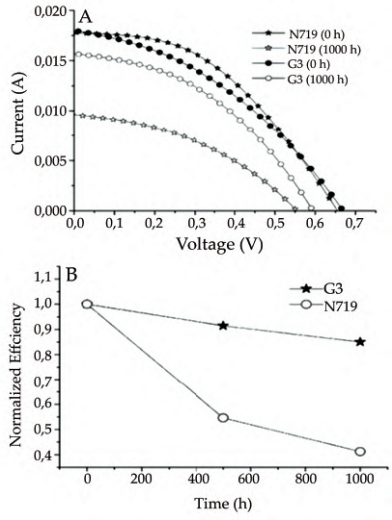

Figure 58. (A) I−V characteristics for the two different dyes before and after aging at 85°C for 1000 hours (potential scan direction was from high to low voltage). (B) Graph showing the relationship between efficiency decay and time during aging.

[Source: http://pubs.acs.org/doi/abs/10.1021/acssuschemeng.5b00108]

6.5.2 Effect of Aqueous Media on Electrochemical Properties of the DSSCs

It can be stated that G3-based devices are comparatively less sensitive to aqueous media as compared to N719-based devices. This behavior can be illustrated by the trends in the values of circuit resistance tabulated in Table 10, acquired by electrochemical impedance spectroscopy (EIS, Fig. 59).

Table 10. Fitting Data from EIS Plots

Parameters	**N719**		**G3**	
Time (hours)	0	0	1000	1000
Rrec (ohm)	1.72	0.71	0.59	1.34
Rct (ohm × cm^2)	8.77	9.53	9.60	14.06
Rd (ohm)	2.24	2.05	2.55	3.82

Rct: charge transfer resistance at the platinum layer. Rd: diffusion resistance of the redox pair in the electrolyte. Rrec: recombination resistance at the dye/TiO_2−electrolyte interface

The values given in Table 10 are stringently associated with each other, and their deviation with time is considered to be dependent on three major reasons which are listed below.

- Electrolyte bleaching (lessening the concentration of I_3^- in the electrolyte).
- Decrease in catalytic activity of Pt-based counterelectrode.
- Detachment of the dye from the TiO_2 surface.

The decrease in the recombination resistance (Rrec) suggests an increment in the recombination rate of the injected mobile electrons onto the surface of TiO_2. The mobile electrons instigate the presence of the oxidized state of the redox couple in the electrolyte system due to dye detachment from the photoanode (Heo et al., 2013). It can be logically assumed that the above-mentioned drawback is caused due to the hydrolysis reaction in the presence of the titanium carboxylate bonding between TiO_2 and the dye surface, triggered by the traces of water (Li et al., 2014; 2015). On the other hand, a sharp decrement in Rrec and Isc is observed for N719. This observation can be associated with two distinct effects caused by the

interaction of water with the dye and TiO_2, that is, dye modification and dye detachment from the surface of TiO_2 (Nguyen, Ta, & Lund, 2007; Nguyen, Degn, R., Nguyen, H. T., & Lund 2009; Nguyen, Andersen, Skou, & Lund 2010).

To further validate the water effect, the increment in the diffusion resistance (Rd) in both cases was observed after the aging process ((Papageorgiou, Maier, & Grätzel, 1997; Nour-Mohammadi, Nguyen, Boschloo, & Lund, 2007). This increment can be caused due to the bleaching of the electrolyte with time, as already illustrated in the literature (Hauch & Georg, 2001; Asghar et al., 2012; Mastroianni et al., 2014). Bleaching of the electrolyte can be caused by the formation of iodate in the aqueous medium (Macht et al., 2002; Jung, Yoo, Lim, Lee, & Kim, 2009; Modestino & Haussener, 2015).

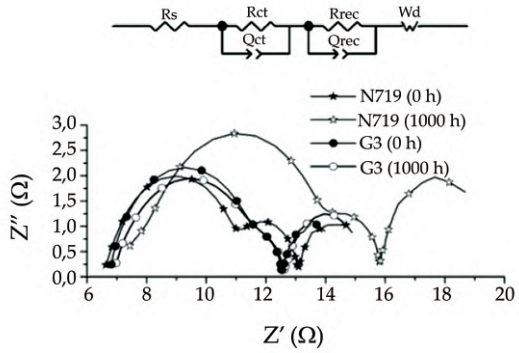

Figure 59. Nyquist graphs for cells consisting of N719 and G3. Equivalent circuit employed for curve fitting of the impedance data: Rct/Qct charge transfer, capacitance, and Rs series resistance at the surface of platinum (semicircle at high frequency); capacitance and Rrec/Qrec recombination resistance at the dye/titania–electrolyte interface (i.e., semicircle at intermediate frequency); semicircle at low frequency represents Wd diffusion

[Source: http://pubs.acs.org/doi/abs/10.1021/acssuschemeng.5b00108]

REFERENCES

1. Agosta, R., Grisorio, R., De Marco, L., Romanazzi, G., Suranna, G. P., Gigli, G., & Manca, M. (2014). An engineered co-sensitization system for highly efficient dye solar cells. *Chemical Communications, 50*(67), 9451-9453.
2. Anderson, N. G. (2012). *Practical process research and development: a guide for organic chemists*. Academic Press.
3. Asghar, M. I., Miettunen, K., Mastroianni, S., Halme, J., Vahlman, H., & Lund, P. (2012). In situ image processing method to investigate performance and stability of dye solar cells. *Solar Energy, 86*(1), 331-338.
4. Berrouard, P., Najari, A., Pron, A., Gendron, D., Morin, P. O., Pouliot, J. R., & Leclerc, M. (2012). Synthesis of 5-Alkyl [3, 4-c] thienopyrrole-4, 6-dione-based polymers by direct heteroarylation. *Angewandte Chemie International Edition, 51*(9), 2068-2071.
5. Burke, D. J., & Lipomi, D. J. (2013). Green chemistry for organic solar cells. *Energy & Environmental Science, 6*(7), 2053-2066.
6. Butters, M., Catterick, D., Craig, A., Curzons, A., Dale, D., Gillmore, A., & White, W. (2006). Critical assessment of pharmaceutical processes a rationale for changing the synthetic route. *Chemical Reviews, 106*(7), 3002–3027.
7. Cannavale, A., Manca, M., De Marco, L., Grisorio, R., Carallo, S., Suranna, G. P., & Gigli, G. (2014). Photovoltachromic device with a micropatterned bifunctional counter electrode.*ACS Applied Materials and Interfaces, 6*(4), 2415-2422.
8. Cannavale, A., Manca, M., Malara, F., De Marco, L., Cingolani, R., & Gigli, G. (2011). Highly efficient smart photovoltachromic devices with tailored electrolyte composition. *Energy & Environmental Science, 4*(7), 2567-2574.
9. Chai, Q., Li, W., Liu, J., Geng, Z., Tian, H., & Zhu, W. H. (2015). Rational molecular engineering of cyclopentadithiophene-bridged DA-π-A sensitizers combining high photovoltaic efficiency with rapid dye adsorption. *Scientific Reports, 5*, srep11330.
10. Double, D. (2014). π-A branched organic dye isomers for dye-sensitized solar cells Jiang, Shenghui; Fan, Suhua; Lu, Xuefeng; Zhou, Gang; Wang, Zhong-Sheng. *Journal of Materials Chemistry A: Materials for Energy and Sustainability, 2*(40), 17153-17164.

11. Echeverry, C. A., Cotta, R., Castro, E., Ortiz, A., Echegoyen, L., & Insuasty, B. (2015). New organic dyes with high IPCE values containing two triphenylamine units as co-donors for efficient dye-sensitized solar cells. *RSC Advances, 5*(75), 60823-60830.
12. Fakharuddin, A., Jose, R., Brown, T. M., Fabregat-Santiago, F., & Bisquert, J. (2014). A perspective on the production of dye-sensitized solar modules. *Energy & Environmental Science, 7*(12), 3952-3981.
13. Fan, S. Q., Kim, C., Fang, B., Liao, K. X., Yang, G. J., Li, C. J., & Ko, J. (2011). Improved efficiency of over 10% in dye-sensitized solar cells with a ruthenium complex and an organic dye heterogeneously positioning on a single TiO2 electrode. *The Journal of Physical Chemistry C, 115*(15), 7747-7754.
14. Feng, Q., Zhang, Q., Lu, X., Wang, H., Zhou, G., & Wang, Z. S. (2013). Facile and selective synthesis of oligothiophene-based sensitizer isomers: an approach toward efficient dye-sensitized solar cells. *ACS Applied Materials & Interfaces, 5*(18), 8982-8990.
15. Gao, P., Grätzel, M., & Nazeeruddin, M. K. (2014). Organohalide lead perovskites for photovoltaic applications. *Energy & Environmental Science, 7*(8), 2448-2463.
16. Green, M. A., Ho-Baillie, A., & Snaith, H. J. (2014). The emergence of perovskite solar cells. *Nature Photonics, 8*(7), 506-514.
17. Grisorio, R., De Marco, L., Agosta, R., Iacobellis, R., Giannuzzi, R., Manca, M., & Suranna, G. P. (2014). Enhancing dye-sensitized solar cell performances by molecular engineering: highly efficient π-extended organic sensitizers. *ChemSusChem, 7*(9), 2659-2669.
18. Hagfeldt, A., Boschloo, G., Sun, L., Kloo, L., & Pettersson, H. (2010). Dye-sensitized solar cells. *Chemical Reviews, 110*(11), 6595-6663.
19. Harikisun, R., & Desilvestro, H. (2011). Long-term stability of dye solar cells. *Solar Energy, 85*(6), 1179-1188.
20. Hauch, A., & Georg, A. (2001). Diffusion in the electrolyte and charge-transfer reaction at the platinum electrode in dye-sensitized solar cells. *Electrochimica Acta, 46*(22), 3457-3466.
21. He, C. Y., Wu, C. Z., Qing, F. L., & Zhang, X. (2014). Direct (Het) arylation of fluorinated benzothiadiazoles and benzotriazole with (Het) aryl iodides. *The Journal of Organic Chemistry, 79*(4), 1712-1718.
22. He, C. Y., Wu, C. Z., Zhu, Y. L., & Zhang, X. (2014). Selective thienylation of fluorinated benzothiadiazoles and benzotriazoles for

organic photovoltaics. *Chemical Science, 5*(4), 1317-1321.

23. Hendsbee, A. D., Macaulay, C. M., & Welch, G. C. (2014). Synthesis of an H-aggregated thiophene–phthalimide based small molecule via microwave assisted direct arylation coupling reactions. *Dyes and Pigments, 102*, 204-209.
24. Heo, N., Jun, Y., & Park, J. H. (2013). Dye molecules in electrolytes: new approach for suppression of dye-desorption in dye-sensitized solar cells. *Scientific Reports, 3*.
25. Jiang, S., Fan, S., Lu, X., Zhou, G., & Wang, Z. S. (2014). Double D–π–A branched organic dye isomers for dye-sensitized solar cells. *Journal of Materials Chemistry A, 2*(40), 17153-17164.
26. Joly, D., Pelleja, L., Narbey, S., Oswald, F., Meyer, T., Kervella, Y., & Demadrille, R. (2015). Metal-free organic sensitizers with narrow absorption in the visible for solar cells exceeding 10% efficiency. *Energy & Environmental Science, 8*(7), 2010-2018.
27. Jung, Y. S., Yoo, B., Lim, M. K., Lee, S. Y., & Kim, K. J. (2009). Effect of Triton X-100 in water-added electrolytes on the performance of dye-sensitized solar cells. *Electrochimica Acta, 54*(26), 6286-6291.
28. Kang, X., Zhang, J., O'Neil, D., Rojas, A. J., Chen, W., Szymanski, P., & El-Sayed, M. A. (2014). Effect of molecular structure perturbations on the performance of the D–A−π–A dye sensitized solar cells. *Chemistry of Materials, 26*(15), 4486-4493.
29. Kang, X., Zhang, J., Rojas, A. J., O'Neil, D., Szymanski, P., Marder, S. R., & El-Sayed, M. A. (2014). Deposition of loosely bound organic D–A–π–A′ dyes on sensitized TiO 2 film: a possible strategy to suppress charge recombination and enhance power conversion efficiency in dye-sensitized solar cells. *Journal of Materials Chemistry A, 2*(29), 11229-11234.
30. Kato, N., Takeda, Y., Higuchi, K., Takeichi, A., Sudo, E., Tanaka, H., & Toyoda, T. (2009). Degradation analysis of dye-sensitized solar cell module after long-term stability test under outdoor working condition. *Solar Energy Materials and Solar Cells, 93*(6), 893-897.
31. Krebs, F. C., & Jørgensen, M. (2013). Polymer and organic solar cells viewed as thin film technologies: What it will take for them to become a success outside academia. *Solar Energy Materials and Solar Cells, 119*, 73-76.
32. Leonardi, E., Penna, S., Brown, T. M., Di Carlo, A., & Reale, A. (2010).

Stability of dye-sensitized solar cells under light soaking test. *Journal of Non-Crystalline Solids, 356*(37), 2049-2052.

33. Li, H., Wu, Y., Geng, Z., Liu, J., Xu, D., & Zhu, W. (2014). Co-sensitization of benzoxadiazole based D–A–π–A featured sensitizers: compensating light-harvesting and retarding charge recombination. *Journal of Materials Chemistry A, 2*(35), 14649-14657.
34. Li, X., Cui, S., Wang, D., Zhou, Y., Zhou, H., Hu, Y., & Tian, H. (2014). New organic donor–acceptor–π–acceptor sensitizers for efficient dye-sensitized solar cells and photocatalytic hydrogen evolution under visible-light irradiation. *ChemSusChem, 7*(10), 2879-2888.
35. Li, X., Zhou, Y., Chen, J., Yang, J., Zheng, Z., Wu, W., & Tian, H. (2015). Stacked graphene platelet nanofibers dispersed in the liquid electrolyte of highly efficient cobalt-mediator-based dye-sensitized solar cells. *Chemical Communications, 51*(51), 10349-10352.
36. Liang, M., & Chen, J. (2013). Arylamine organic dyes for dye-sensitized solar cells. *Chemical Society Reviews, 42*(8), 3453-3488.
37. Liu, D. S., Ding, W. L., Zhu, K. L., Geng, Z. Y., Wang, D. M., & Zhao, X. L. (2014). The master factors influencing the efficiency of D–A–π–A configurated organic sensitizers in dye-sensitized solar cell via theoretically characterization: design and verification. *Dyes and Pigments, 105,* 192-201.
38. Macht, B., Turrion, M., Barkschat, A., Salvador, P., Ellmer, K., & Tributsch, H. (2002). Patterns of efficiency and degradation in dye sensitization solar cells measured with imaging techniques. *Solar Energy Materials and Solar Cells, 73*(2), 163-173.
39. Mastroianni, S., Asghar, I., Miettunen, K., Halme, J., Lanuti, A., Brown, T. M., & Lund, P. (2014). Effect of electrolyte bleaching on the stability and performance of dye solar cells. *Physical Chemistry Chemical Physics, 16*(13), 6092-6100.
40. Matsidik, R., Komber, H., & Sommer, M. (2015). Rational use of aromatic solvents for direct arylation polycondensation: C–H reactivity versus solvent quality. *ACS Macro Letters, 4*(12), 1346-1350.
41. Matsidik, R., Martin, J., Schmidt, S., Obermayer, J., Lombeck, F., Nübling, F., & Sommer, M. (2014). C–H Arylation of unsubstituted furan and thiophene with acceptor bromides: access to donor–acceptor–donor-type building blocks for organic electronics. *The Journal of Organic Chemistry, 80*(2), 980-987.

42. Matteocci, F., Cinà, L., Di Giacomo, F., Razza, S., Palma, A. L., Guidobaldi, A., & Di Carlo, A. (2016). High efficiency photovoltaic module based on mesoscopic organometal halide perovskite. *Progress in Photovoltaics: Research and Applications, 24*(4), 436-445.

43. Mercier, L. G., & Leclerc, M. (2013). Direct (hetero) arylation: a new tool for polymer chemists. *Accounts of Chemical Research, 46*(7), 1597-1605.

44. Mishra, A., Fischer, M. K., & Bäuerle, P. (2009). Metal-free organic dyes for dye-sensitized solar cells: from structure: property relationships to design rules. *Angewandte Chemie International Edition, 48*(14), 2474-2499.

45. Modestino, M. A., & Haussener, S. (2015). An integrated device view on photo-electrochemical solar-hydrogen generation. *Annual Review of Chemical and Biomolecular Engineering, 6*, 13-34.

46. Nguyen, H. T., Ta, H. M., & Lund, T. (2007). Thermal thiocyanate ligand substitution kinetics of the solar cell dye N719 by acetonitrile, 3-methoxypropionitrile, and 4-tert-butylpyridine. *Solar Energy Materials and Solar Cells, 91*(20), 1934-1942.

47. Nguyen, P. T., Andersen, A. R., Skou, E. M., & Lund, T. (2010). Dye stability and performances of dye-sensitized solar cells with different nitrogen additives at elevated temperatures—can sterically hindered pyridines prevent dye degradation? *Solar Energy Materials and Solar Cells, 94*(10), 1582-1590.

48. Nguyen, P. T., Degn, R., Nguyen, H. T., & Lund, T. (2009). Thiocyanate ligand substitution kinetics of the solar cell dye Z-907 by 3-methoxypropionitrile and 4-tert-butylpyridine at elevated temperatures. *Solar Energy Materials and Solar Cells, 93*(11), 1939-1945.

49. Nour-Mohammadi, F., Nguyen, H. T., Boschloo, G., & Lund, T. (2007). An investigation of the photosubstitution reaction between N719-dyed nanocrystalline TiO 2 particles and 4-tert-butylpyridine. *Journal of Photochemistry and Photobiology A: Chemistry, 187*(2), 348-355.

50. Ogura, R. Y., Nakane, S., Morooka, M., Orihashi, M., Suzuki, Y., & Noda, K. (2009). High-performance dye-sensitized solar cell with a multiple dye system. *Applied Physics Letters, 94*(7), 54.

51. Ooyama, Y., & Harima, Y. (2012). Photophysical and electrochemical properties, and molecular structures of organic dyes for dye-sensitized

solar cells. *ChemPhysChem, 13*(18), 4032-4080.

52. Ooyama, Y., & Harima, Y. (2013). Corrigendum: photophysical and electrochemical properties, and molecular structures of organic dyes for dye-sensitized solar cells. *ChemPhysChem,14*(5), 871-871.
53. Ooyama, Y., Nagano, T., Inoue, S., Imae, I., Komaguchi, K., Ohshita, J., & Harima, Y. (2011). Dye-sensitized solar cells based on donor-π-acceptor fluorescent dyes with a pyridine ring as an electron-withdrawing-injecting anchoring group. *Chemistry-A European Journal, 17*(52), 14837-14843.
54. O'regan, B., & Grätzel, M. (1991). A low-cost, high-efficiency solar cell based on dye-sensitized colloidal TiO_2 films. *Nature, 353*(6346), 737-740.
55. Osedach, T. P., Andrew, T. L., & Bulović, V. (2013). Effect of synthetic accessibility on the commercial viability of organic photovoltaics. *Energy & Environmental Science, 6*(3), 711-718.
56. Papageorgiou, N., Maier, W. F., & Grätzel, M. (1997). An iodine/triiodide reduction electrocatalyst for aqueous and organic media. *Journal of the Electrochemical Society, 144*(3), 876-884.
57. Patel, P. V., Joshi, N., & Panchal, D. P. (2012). Process for preparation of 5-(2-ethoxy-5-((4-methylpiperazin-1-yl) sulfonyl) phenyl)-3-isobutyl-1-methyl-1H-pyrazolo [4, 3-d] pyrimidin-7(6H)-one (sildenafil citrate impurity). *Indian Patent Application No. IN 2012MU02516 A, 20140606*, 29.
58. Po, R., Bernardi, A., Calabrese, A., Carbonera, C., Corso, G., & Pellegrino, A. (2014). From lab to fab: how must the polymer solar cell materials design change?—an industrial perspective. *Energy & Environmental Science, 7*(3), 925-943.
59. Po, R., Bianchi, G., Carbonera, C., & Pellegrino, A. (2015). "All That Glisters Is Not Gold": an analysis of the synthetic complexity of efficient polymer donors for polymer solar cells. *Macromolecules, 48*(3), 453-461.
60. Qian, X., Gao, H. H., Zhu, Y. Z., Lu, L., & Zheng, J. Y. (2015). Biindole-based double D–π–A branched organic dyes for efficient dye-sensitized solar cells. *RSC Advances, 5*(6), 4368-4375.
61. Qian, X., Gao, H. H., Zhu, Y. Z., Pan, B., & Zheng, J. Y. (2015). Tetraindole-based saddle-shaped organic dyes for efficient dye-

sensitized solar cells. *Dyes and Pigments, 121*, 152-158.

62. Rodriguez, C. A., Modestino, M. A., Psaltis, D., & Moser, C. (2014). Design and cost considerations for practical solar-hydrogen generators. *Energy & Environmental Science, 7*(12), 3828-3835.
63. Roiati, V., Giannuzzi, R., Lerario, G., Marco, L. D., Agosta, R., Iacobellis, R., & Gigli, G. (2015). Beneficial role of a bulky donor moiety in π-extended organic dyes for mesoscopic TiO2 sensitized solar cells. *The Journal of Physical Chemistry C, 119*(13), 6956-6965.
64. Schipper, D. J., & Fagnou, K. (2011). Direct arylation as a synthetic tool for the synthesis of thiophene-based organic electronic materials. *Chemistry of Materials, 23*(6), 1594-1600.
65. Sheldon, R. (2010). Introduction to green chemistry, organic synthesis and pharmaceuticals. *Green Chemistry in the Pharmaceutical Industry,* 1–20.
66. Sheldon, R. A. (2007). The E factor: fifteen years on. *Green Chemistry, 9*(12), 1273-1283.
67. Shibayama, N., Ozawa, H., Abe, M., Ooyama, Y., & Arakawa, H. (2014). A new cosensitization method using the Lewis acid sites of a TiO 2 photoelectrode for dye-sensitized solar cells. *Chemical Communications, 50*(48), 6398-6401.
68. Sum, T. C., & Mathews, N. (2014). Advancements in perovskite solar cells: photophysics behind the photovoltaics. *Energy & Environmental Science, 7*(8), 2518-2534.
69. Van Aken, K., Strekowski, L., & Patiny, L. (2006). EcoScale, a semi-quantitative tool to select an organic preparation based on economic and ecological parameters. *Beilstein Journal of Organic Chemistry, 2*(1), 3.
70. Wang, X., & Wang, M. (2014). Synthesis of donor–acceptor conjugated polymers based on benzo [1, 2-b: 4, 5-b′] dithiophene and 2, 1, 3-benzothiadiazole via direct arylation polycondensation: towards efficient C–H activation in nonpolar solvents. *Polymer Chemistry, 5*(19), 5784-5792.
71. Wang, X., Wang, K., & Wang, M. (2015). Synthesis of conjugated polymers via an exclusive direct-arylation coupling reaction: a facile and straightforward way to synthesize thiophene-flanked benzothiadiazole derivatives and their copolymers. *Polymer Chemistry, 6*(10), 1846-1855.

72. Wu, Y., & Zhu, W. (2013). Organic sensitizers from D–π–A to D–A–π–A: effect of the internal electron-withdrawing units on molecular absorption, energy levels and photovoltaic performances *Chemical Society Reviews, 42*(5), 2039-2058.

73. Wu, Y., Marszalek, M., Zakeeruddin, S. M., Zhang, Q., Tian, H., Grätzel, M., & Zhu, W. (2012). High-conversion-efficiency organic dye-sensitized solar cells: molecular engineering on D–A–π-A featured organic indoline dyes. *Energy & Environmental Science, 5*(8), 8261-8272.

74. Xiao, Y. L., Zhang, B., He, C. Y., & Zhang, X. (2014). Direct olefination of fluorinated benzothiadiazoles: a new entry to optoelectronic materials. *Chemistry-A European Journal, 20*(16), 4532-4536.

75. Xing, H., Chen, L., Jia, Y., Jiang, Z., & Yang, Z. (2017). Fe 2 O 3-catalyzed pummerer rearrangement of acyl chlorides and sulfoxides: facile synthesis of alkylthiomethyl ester. *Tetrahedron Letters, 58*(23), 2199-2202.

76. Yella, A., Lee, H. W., Tsao, H. N., Yi, C., Chandiran, A. K., Nazeeruddin, M. K., …& Grätzel, M. (2011). Porphyrin-sensitized solar cells with cobalt (II/III)–based redox electrolyte exceed 12 percent efficiency. *Science, 334*(6056), 629-634.

77. Yen, Y. S., Chou, H. H., Chen, Y. C., Hsu, C. Y., & Lin, J. T. (2012). Recent developments in molecule-based organic materials for dye-sensitized solar cells. *Journal of Materials Chemistry, 22*(18), 8734-8747.

78. Yum, J. H., Baranoff, E., Wenger, S., Nazeeruddin, M. K., & Grätzel, M. (2011). Panchromatic engineering for dye-sensitized solar cells. *Energy & Environmental Science, 4*(3), 842-857.

79. Zardetto, V., Di Giacomo, F., Garcia-Alonso, D., Keuning, W., Creatore, M., Mazzuca, C., & Brown, T. M. (2013). Fully plastic dye solar cell devices by low-temperature UV-irradiation of both the mesoporous TiO2 photo-and platinized counter-electrodes. *Advanced Energy Materials, 3*(10), 1292-1298.

80. Zeng, W., Cao, Y., Bai, Y., Wang, Y., Shi, Y., Zhang, M., & Wang, P. (2010). Efficient dye-sensitized solar cells with an organic photosensitizer featuring orderly conjugated ethylenedioxythiophene and dithienosilole blocks. *Chemistry of Materials, 22*(5), 1915-1925.

81. Zhang, J., Chen, W., Rojas, A. J., Jucov, E. V., Timofeeva, T. V., Parker,

T. C., & Marder, S. R. (2013). Controllable direct arylation: fast route to symmetrical and unsymmetrical 4, 7-diaryl-5, 6-difluoro-2, 1, 3-benzothiadiazole derivatives for organic optoelectronic materials. *Journal of the American Chemical Society, 135*(44), 16376-16379.

82. Zhang, J., Kang, D. Y., Barlow, S., & Marder, S. R. (2012). Transition metal-catalyzed C–H activation as a route to structurally diverse di (arylthiophenyl)-diketopyrrolopyrroles. *Journal of Materials Chemistry, 22*(40), 21392-21394.
83. Zhang, S., Yang, X., Numata, Y., & Han, L. (2013). Highly efficient dye-sensitized solar cells: progress and future challenges. *Energy & Environmental Science*, *6*(5), 1443-1464.

CHAPTER 7

MODERN APPLICATIONS OF CHEMICAL LOOPING PROCESSES AND TECHNOLOGIES

CONTENTS

7.1 INTRODUCTION

As has been discussed in the former chapters, the chemical looping procedure of type I employs a metal oxide/metal particle having specifically designed support and promoters that can endure numerous oxidation/reduction cycles while sustaining a high oxygen-carrying capacity. The oxidized form of these particles has the capability of reacting with several types of carbonaceous fuels, including biomass, hydrocarbons, coal, wax, and syngas, after which the particles are reduced down to their metallic form. Particles at the reduced stage are possible to oxidize into original state by CO_2, O_2, air, or steam (Blockstein & Shockley, 2006; Park, Gupta, Li, Sridhar, & Fan, 2010). Therefore, these contrived chemical looping particles permit the effective transformation of several carbonaceous fuels into CO_2, heat, syngas, H_2, or any other combination of these products (Satyapal, Petrovic, Thomas, Read, & Ordaz, 2006; Satyapal, Petrovic, Read, Thomas, & Ordaz 2007). Such particles can also be employed for the production of electricity, steam, chemicals, or liquid as well as gaseous fuels. Moreover, due to the presence of support and promoter, the reaction rate of the particle can significantly faster than metal oxide/metal in its pure form. Additionally, as already discussed in previous chapters, the oxidation/reduction process taking place in two different reactors also offers an incorporated CO_2 separation feature (Carpetis, 1980; 1982).

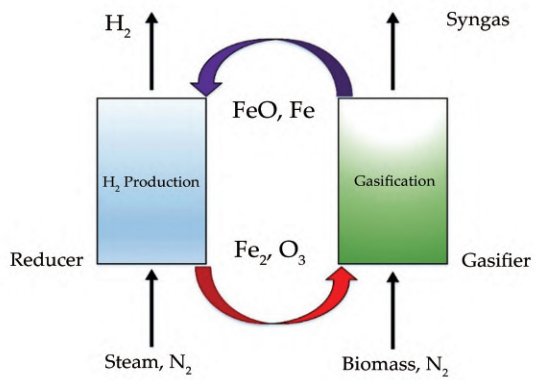

Figure 60. Typical example of a chemical looping process involving gasification and hydrogen production

[Source: https://www.aiche.org/academy/videos/conference-presentations/chemical-looping-gasification-and-hydrogen-clgh-process-solid-biomass-dual-fluidized-bed-system]

The type II chemical looping procedure employs metal carbonate/metal oxide particles for capturing sulfur, CO_2, and halide impurities concurrently over various cycles while preserving a high capture capability (0.5 g CO_2 captured for each gram of metal oxide). The particles of metal oxide can capture sulfur, CO_2, and halide impurities from fuel gas streams and fuel gas that are produced from an extensive variety of feedstocks, such as natural gas, coal, and biomass to manufacture a mixture of solids that is mostly composed of the metal carbonate (Chambers, Park, Baker, & Rodriguez, 1998; Park, Tan, Hidalgo, Baker, & Rodriguez, 1998). The calcination of metal carbonate can be carried out for the production of a sequestration-ready CO_2 stream. This chemical looping procedure incorporated with a gasification system can produce hydrogen, electricity, chemicals, as well as liquid fuel; moreover, using a combustion system, the production of electricity can be carried out with a very low CO_2 footprint (DeLuchi, 1989; Das, 1990).

The high flexibility and efficiency of such chemical looping procedures permit an extensive range of novel applications for this technology (Pant & Gupta, 2009; Al-Ghamdi et al., 2012). Some of these applications include carbon dioxide capture, onboard hydrogen production, direct solid fuel cell, solid oxide fuel cell, tar sand digestion, improved steam methane reforming, chemical looping with oxygen uncoupling, and liquid fuel production, all of these have been discussed in this chapter.

7.2 HYDROGEN STORAGE AND ONBOARD HYDROGEN PRODUCTION

Since hydrogen is a significant source of clean energy for several potential future projects, therefore, several technologies of hydrogen production, including the chemical looping process, are presently under development (Michel, Fieseler, Meyer, & Theiβen, 1998; Newson et al., 1998). We aim to develop both economically and technically feasible methods of generating hydrogen for large-scale production. One major issue associated with the application of hydrogen as a pollutant-free, carbon-free energy carrier is the storage of hydrogen (Verbetsky, Malyshenko, Mitrokhin, Solovei, & Shmal'ko, 1998; Scherer, Newson, & Wokaun, 1999). Particularly, one important potential application of hydrogen is its use as the transportation fuel of the future, since it does not lead to emissions of CO_2 which are responsible for global warming (Malyshenko et al., 2000; Crabtree Dresselhaus, & Buchanan, 2004; Crabtree, & Dresselha, 2005). Except if

hydrogen is employed in an energy conversion system that is stationary, it needs to be transported to another site, generated onboard a vehicle or generated in a distributed generation system. But, economically, storage of hydrogen or its generation onboard a vehicle at a high density (both gravimetric and volumetric) is a challenge itself (Gao & Krishnamurthy, 2008; Park et al., 2010). Hence, during the recent years, the development of hydrogen storage materials having high capacity has been one of the main areas for energy research. The main factors that need to be deliberated for the development of onboard hydrogen generation systems and hydrogen storage are as follows: hydrogen cost, capacity, hydrogen charging/discharging rates, durability, fuel quality, operability, the environment, health, and safety (Dillon et al., 2004; Gupta, 2008).

7.2.1 Compressed Hydrogen Gas and Liquefied Hydrogen

Two simplest methods that can be used for storing hydrogen are in liquefied form and as a compressed gas. At present, commercially available high-pressure tanks can store hydrogen gas at 680 atm (10,000 psi) or 340 atm (5000 psi). The specific volume of hydrogen at 340 atm is 42 l/kg. Therefore, for a tank that contains 5 kg of hydrogen, this is parallel to a volume of almost 210 l, without counting in the volume of the walls of the tank (Burke & Gardiner, 2005).

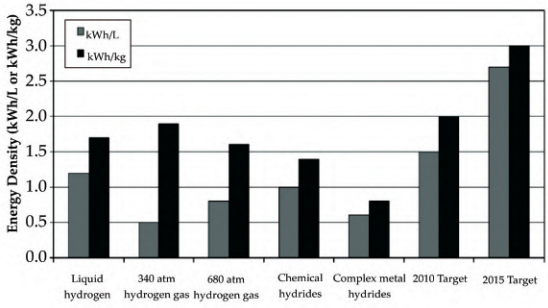

Figure 61. Volumetric and gravimetric energy densities of different hydrogen storage

[http://onlinelibrary.wiley.com/doi/10.1002/9780470872888.ch6/summary]

Even though the hydrogen is stockpiled in its pure form, the gravimetric fuel capability of high-pressure tanks is nearly 5 wt.% when the total weight of the tank is factored in (for instance, 86.3 kg for 4.7 kg of fuel at 204 atm).

This amount is considerably smaller as compared to traditionally used liquid fuels (Fig. 61). The results of an experiment carried out demonstrated the volumetric and gravimetric energy densities of hydrogen gas compressed at 680 and 340 atm; these values are still significantly lower than the target set by the DOE FreedomCAR Partnership. Bearing in mind the non-ideal performance of hydrogen gas at elevated pressure, the rise in pressure above 680 atm would not significantly increase the content of energy of this storage possibility. For instance, if we double the pressure from 680 to 1360 atm, it would just raise the density of volumetric hydrogen gas by 30%. However, higher pressure needs a significantly large increase in compression power. According to the estimation, 8.5% content of the energy of the hydrogen, at 340 atm, would get consumed in compression (Amold & Wolf, 2005). Unlike traditional tanks used for liquid fuels, which can be built in several different dimensions and shapes to utilize the offered space best, high-pressure tanks employed for storage of hydrogen can only be cylindrical. This also restricts the application of compressed gas as an option for hydrogen storage. Nonetheless, presently, compressed hydrogen gas is considered a mature selection for vehicular applications; moreover, advance research is continuing to reduce cost as well as lowering tank weight design (Aceves, Martinez-Frias, & Garcia-Villazana, 2000; Aceves, Martinez-Frias, & Espinosa-Loza 2002; Aceves, Berry, Martinez-Frias, & Espinosa-Loza, 2006).

Another procedure for storing pure hydrogen is its storage in the liquefied form. According to the phase diagram of hydrogen, it occurs in the liquid form at below—253°C. The density of liquid hydrogen is much higher as compared to compressed hydrogen having a specific volume of 14 l/kg, which greatly decreases the size of the onboard tank of fuel. The key problems connected with using liquefied hydrogen are the energy necessities for liquefaction purpose and the inactivity period. The average consumption of energy in the course of liquefaction of hydrogen is around 30% of the LHV (LHV is an abbreviation of the lower heating value of hydrogen). This value is quite greater than the energy for compression of hydrogen to 340–680 atm. The period of inactivity involves the steady warming up of hydrogen in the storing container as well as its succeeding boil-off.

According to the research, if a tank contains 4.6 kg of fuel, then nearly 4% of the hydrogen will be boiled off each day. Therefore, special cryogenic tanks containing excellent insulation are being manufactured to overcome the inactivity issues (Escribano Sanz, 2014). Particularly, a multilayer

vacuum insulation, a vessel of high pressure, furnished with an outer wrap composed of composite material and lined with aluminum, and an outer vacuum vessel, has been comprehensively tested and afterward implemented in a demonstration vehicle. Depending on the required driving distance, this vehicle can be fueled with either liquid hydrogen or compressed hydrogen gas (Park et al., 2010).

A relatively new idea is hybrid hydrogen tank comprising of a typical compressed hydrogen tank which, to some extent, is filled with reversible low-temperature hydrogen absorbing alloys (Heung & Wicks, 1999). Typical examples of reversible hydrides such as FeTi and LaNi can store hydrogen having volumetric densities of around 6.7–7.7 l/kg at 100°C; this value is quite a few times greater than compressed hydrogen concerning volumetric density (Bogdanović & Schwickardi, 2001). Owing to its high volumetric energy density, such joint storage choice can permit more compact storage of hydrogen without having to sacrifice the benefits of a compressed hydrogen system.

Liquefied, compressed, and hybrid tanks offer the major benefit of instantly delivering pure hydrogen at high rates; on the other hand, other systems that involve physisorption or chemisorption of hydrogen need a significant temperature swing for the regeneration of hydrogen on demand. Refueling too is comparatively fast and simple since no chemical reactions take place during the refilling of liquefied and compressed tanks (Heung, 2003).

7.2.2 Metal Hydrides

Storage of metal hydride-based hydrogen is not a new technology. It has been widely researched in the course of the past 30 years. Metal hydrides stockpile hydrogen chemically in the form of a crystalline structure that can pack more hydrogen into the provided volume than liquid hydrogen. The revocable equilibrium reaction that involves storage of hydrogen, as well as its regeneration, can be written as follows:

MHN, solid + Heat ↔ M solid +(*n*2) H2

Nevertheless, as hydrogen is very light as compared to the other metals that are usually quite heavy, therefore, storage of hydrogen for each unit weight is not as high as compared to the other metals. Hydrides that involve hydrogen light elements such as N, Be, B, Li, Na, Al, and Mg usually have adequate hydrogen storage for each unit weight, whereas, practically, the binding energy is quite strong for the binary hydrides of these elements.

A high value of binding energy ensures that the hydride will discharge hydrogen only at high temperatures (Bowman, Hwang, Ahn, & Vajo, 2004). For instance, MgH_2, which is one of the minimum stable binary hydrides amid the light metals, has a hypothetical hydrogen capability of around 7.6 wt.%; however, its equilibrium hydrogen pressure merely reaches 1 atm at around 300°C (Li, Jena, Araujo, & Ahuja, 2004).

AlH_3 is a solid covalently bonded with 10.1 wt.% hypothetical hydrogen storage that in actual is thermodynamically not stable at room temperature (Bruster, Dobbins, Tittsworth, & Anton, 2004). Since it is not stable at room temperature, it can release hydrogen at temperatures less than 100°C. There is no known process at present that could produce AlH_3 in an efficient manner or on a large scale, and hence, this reutilizing of Al into AlH_3 would have to be completed offsite. Several other hydrides demonstrate high capabilities of hydrogen and might have other advantageous characteristics (Schüth, Bogdanović, & Felderhoff, 2004). Nevertheless, they have the similar disadvantage as AlH_3 in the aspect that there is no acknowledged method of recharging the spent "fuel" in an efficient manner or on a large scale. On the other hand, present examples of a few known hydride reactions consist of hydrolysis of MgH_2 with water for producing hydrogen and $Mg(OH)_2$, as well as catalytic hydrolysis of $NaBH_4$ (that can be stored in the form of a 25% solution in water) for producing hydrogen and aqueous $NaBO_2$ as can be seen in the following chemical reaction (Araújo, Ahuja, Osorio Guillén, & Jena, 2005):

$$NaBH_4 + 2H_2O_2 \rightarrow NaBO_2 + 4H_2$$

Such kinds of hydrides might still discover specialty applications where economics are not the main factor to consider; however, currently, they are not appropriate for mobile applications. However, if an effective and simple process for restoration of any of such compounds was established, in reality, they could fulfill the requirements for both gravimetric and volumetric energy density (Garberoglio, Skoulidas, & Johnson, 2005).

A hydride that can both release and regenerate hydrogen under mild conditions is known as a reversible hydride. Such hydrides normally have equilibrium hydrogen pressures of around 1 atm at slight temperatures (approximately 0–60°C). With the help of these proper catalysts, these hydrides can be created using their metal alloys at high pressure and room temperature and will discharge hydrogen at 1–2 atm at elevated temperatures (still not greater than 100°C). Primary reversible metal hydrides contain transition metal alloys, for example, MNi_5H_6 and $FeTiH_2$, after upon that

M can be several transition metals (Manovic & Anthony, 2008). Excitingly enough, the former compound is already used in Ni–MH rechargeable batteries that are used in several digital cameras as well as other electronics. Unluckily, such alloys normally have only 1–2 wt.% hydrogen, and hence, they are not appropriate for mobile applications (Rosi et al., 2003; Rowsell, Millward, Park, & Yaghi, 2004).

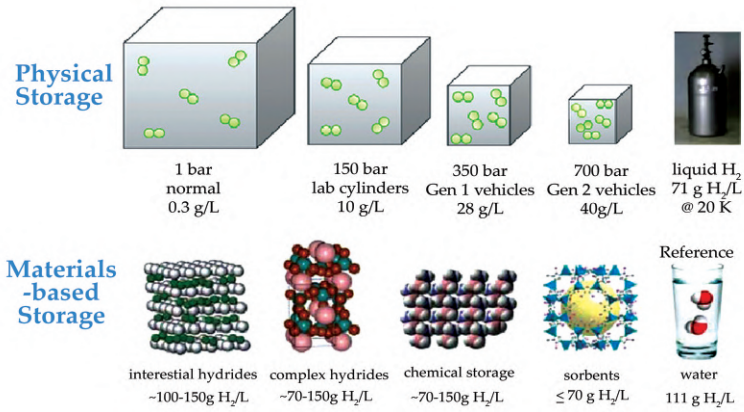

Figure 62. A comprehensive comparison of metal-based and material-based storage systems

[https://www.researchgate.net/figure/274016408_fig1_Figure-1-Compressed-hydrogen-vs-materials-based-hydrogen-storage-2-Re-organized-from]

Since long, sodium alanate ($NaAlH_4$) was thought out to be in the same class as $NaBH_4$ and other irretrievable hydrides in spite of having an equilibrium hydrogen pressure of approximately 1 atm at a temperature reaching 30°C. In 1997, this concept was changed when Schwickardi and Bogdanovic reported based on their experimentation and research that it is possible to regenerate $NaAlH_4$ under moderately mild conditions when it is doped with particular transition metals (Wang et al., 2010; Wang, Ramkumar, Wong, & Fan, 2012). Till now, the best results have been gathered by employing Ti as the dopant. Usual conditions for Ti-catalyzed rehydrogenation are the temperature of around 100°C and an atmospheric pressure of 100 atm. Balance is necessary to achieve among the kinetics, which becomes more promising as the temperature is increased, and the thermodynamics, which becomes less promising with the rise in the temperature (Jin & Ishida, 2004; Lu, Hughes, & Anthony, 2008). Theoretically, the capacity of hydrogen storage of NaAlH4 is around 5.5 wt.%. Additionally, it has a reversible

hydrogen storage capacity of approximately 5 wt.% (Jung et al., 2006; Sun, Lim, & Grace, 2008).

Other methodologies that are worth mentioning, however, are not yet fully developed and include destabilized mixtures of various hydrides as well as lithium imide/lithium amide systems. The hydrogenation of lithium imide to lithium amide can be carried out with 6.5 wt.% reversible storage at almost 250°C (Fennell, Pacciani, Dennis, Davidson, & Hayhurst, 2007; Li, Yang, & Yang, 2007). In addition to the requirement of comparatively high temperature, this system also has another problem, which is producing a small quantity of ammonia, which is responsible for poisoning the polymer electrolyte membrane (PEM) fuel cells. The formation of destabilized mixtures of hydrides takes place by mixing a stable, high-capacity hydride with such a compound that can form a stable intermediate with the dehydrogenated form of the hydride. An example of such mixture is a blend of $LiBH_4$ and MgH_2, which has been testified to have a reversible storage capacity of 9 wt.%; however, it can only be achieved with slow kinetics and at a high temperature (Li & Yang, 2006; Chrissafis, 2007). This specific blend has been able to achieve a high capacity owing to fairly high hydrogen capacities of both components. More research in the future can result in the production of more destabilized mixtures holding more advantageous thermodynamics and kinetics (Dillon et al., 2004; Grasa & Abanades, 2006).

7.2.3 Carbon Nanotubes and Graphite Nanofibers

Upon initially published reports of carbon nanotubes (CNTs), significant excitement was created among researchers and scientists as according to these reports, carbon nanotubes contain high storage capacities (Gupta, Tiwari, & Srivastava, 2004; Fan & Gupta, 2006). A researcher named, Dillon et al., carried out his initial research on the storage capability of CNTs. Scientists studied the adsorption mechanism of hydrogen on soot that enclosed 0.1–0.2 wt.% single-walled nanotubes (SWNTs) and further extrapolated their data for determining a hydrogen storage ability of 5–10 wt.%. Based on his theoretical calculations, another researcher, Lee et al., predicted a hydrogen storage ability of almost 14 wt.% in SWNTs (Lee et al., 2004). Multiwalled nanotube (MWNT) capacity was observed to fluctuate from 2.7 wt.% to around 7.7 wt.% (Taerakul et al., 2007; Fan, Ramkumar, Wang, & Statnick, 2008).

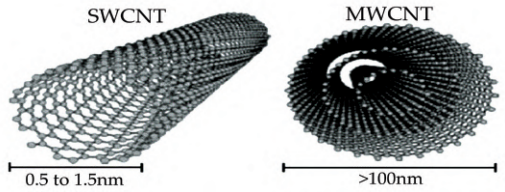

Figure 63. A typical view of single-wall carbon nanotubes and multiwall carbon nanotubes

[Source: https://www.quora.com/What-is-the-difference-between-single-walled-and-multi-walled-carbon-nanotubes]

Recently, more studies have been carried out. However, they have failed to achieve the results foretold by Lee et al. (2004). Two other researchers, Wang and Iqbal, conducted a research and found absorption of hydrogen to be 2.5–3.2 wt.% for SWNTs that were charged electrochemically. With desorption taking place at 70°C, reversible hydrogen storage was achieved at 1.5 wt.%. Further research conducted by Dillon et al. (2004) on hydrogen adsorption on MWNTs revealed that despite the fact that no hydrogen was absorbed by iron nanoparticles or fresh MWNTs under near-ambient settings, MWNTs that had considerable quantities of nanoparticles of iron were able to stock 0.035 wt.% hydrogen (White, Strazisar, Granite, Hoffman, & Pennline, 2003; Fan & Jadhav, 2002).

They drew out the conclusion that the characteristics of adsorption must result from an interaction between the iron nanoparticles and the MWNTs. Some other studies have also confirmed that the existence of metal nanoparticles is required for absorption of hydrogen in both MWNTs and SWNTs. Studies undertaken most recently have observed absorption in the range of 1–4 wt.% for SWNTs and even lower for MWNTs (Wang & Iqbal, 2004; Lee, Verdooren, Caram, & Sircar, 2007).

Nanofibers constructed from graphite and known as GNFs are a nanostructured formula of carbon comprising of layers of graphite that are fashioned into fibers. The discrete layers of graphite can be perpendicular (platelet), parallel (tubular), or at an angle (herringbone) to the fiber axis. The diameter and length of such individual GNFs can alter depending on several factors, but normal values include diameters of 250 nm and lengths of around 50 μm. GNFs can be constructed through various processes. However, the most common processes of their construction are catalytic graphitization of electrospun polymer fibers, usually poly (vinylidene fluoride) and thermal

decomposition of hydrocarbons, usually ethylene; acetylene; or benzene (Ahn et al., 1998; Escribano Sanz, 2014).

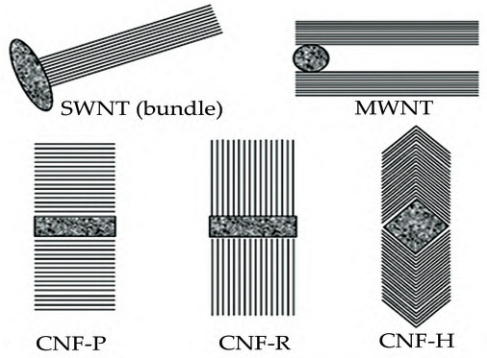

Figure 64. Single-wall and multiwall CNTs along with carbon nanofibers (CNFs), that is, platelet-like CNF-P, ribbon-like CNF-R, and herringbone CNF–H

[Source: http://pubs.rsc.org/en/content/articlehtml/2010/ay/b9ay00312f]

In 1998, the first research was published on the usage of GNFs for storage of hydrogen. Preliminary research was carried out by Chambers et al. (1998). Chambers et al. acquired hydrogen adsorption altering from 11 wt.% for tubular GNFs to almost 67 wt.% for herringbone GNFs. Following that, hydrogen desorption was observed to be as high as 58 wt.% (Bowman Jr et al., 1998; Park et al., 2010).

Adsorption phenomenon took place at pressures varying from 44 to 112 atm and at room temperature. On the other hand, desorption phenomenon took place at atmospheric pressure and room temperature. A researcher named, Ahn et al. (1998), researched GNFs and few other kinds of activated carbon and observed quite lower storage capabilities at 77 K (−196°C) and room temperature. GNFs were observed to absorb almost the equal quantity of hydrogen as can be absorbed by the other forms of activated carbon, with the best-absorbing capability being ~ 1 wt.% at 77 K for GNFs. Another researcher, Fan et al. (1999), stated a hydrogen storage capacity of around 10–13 wt.% for GNFs in his report. Recently, research has been conducted by Gupta et al. (2004), who has found a hydrogen storage capacity of approximately 17 wt.% for GNFs developed through the thermal decomposition of acetylene on Pd sheets. Another example is a researcher named Hong et al. (2007) who formed GNFs by using electrospun poly

(vinylidene fluoride) nanofibers and observed a storage capability of 0.11–0.18 wt.% (Garcia-Labiano, Adánez, de Diego, Gayán, & Abad, 2006; Escribano Sanz, 2014).

7.3 CHEMICAL LOOPING GASIFICATION INTEGRATED WITH FUEL CELLS

The flexibility and high efficacies to produce preferred products, together with the incorporated environmental advantages regarding eagerly sequestrable stream of CO_2, make chemical looping gasification of coal an appealing methodology for energy management and conversion (Kronberger, Lyngfelt, Löffler, & Hofbauer, 2005; Fan, Li, Zeng, & Sridhar, 2016). As discussed previously, the process of coal-direct chemical looping (CDCL) is appealing since it can convert as maximum as 80% of the coal thermal energy into hydrogen. Now, schemes of energy conversion are proposed to efficiently extract chemical energy from the fuels by the integration of the fuel cell with chemical looping.

7.3.1 Chemical Looping Gasification Integrated with Solid Oxide Fuel Cells

Figure 65 demonstrates a scheme of electricity generation. In this method, a chemical looping gasification system has been strategically combined with industrially available solid oxide fuel cells (SOFC) to minimize the loss of energy (Chuang, 2005).

In the configuration shown below, the hydrogen-rich gas is produced as a result of the chemical looping oxidizer. This gas is then directly introduced to the anode side of SOFC for the generation of power. The exhaust of the anode of SOFC is a lean hydrogen gas and contains a substantial quantity of steam which is recycled again to the chemical looping oxidizer for generating hydrogen (Chuang, Mirzababaei, & Rismanchian, 2014).

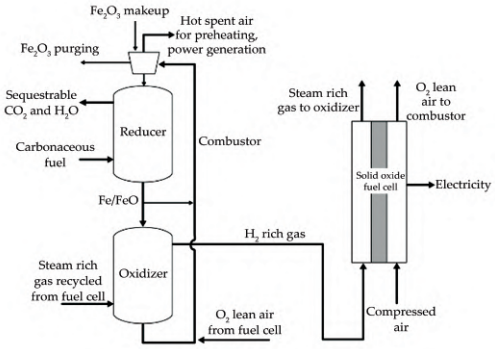

Figure 65. Chemical looping gasification combined with a solid oxide fuel cell.

[Source: http://onlinelibrary.wiley.com/doi/10.1002/9780470872888.ch6/summary]

Table 11. Coal to electricity configurations and efficiencies of process

Process configuration	**Conventional IGCC**	**CDCL—combined cycle**	**C D C L — SOFC**
Efficiency (%HHV)	30–35	47–53	64–71
CO_2 capture rate (%)	90	100	100

As is shown in Figure 65, a closed loop is formed between the SOFC anode and the chemical looping oxidizer using the circulation of the gaseous mixture of H_2 and steam. The mixture of H_2 and steam basically acts as a "working fluid" for the generation of power. Even though some exclusion, recompression, and makeup may be essential for the working fluid, the most amount of the steam will not be condensed and is circulated in the closed loop. As a result, condensation, as well as reheating of steam, is a step that is responsible for considerable loss of energy in the traditional process of power generation, which can be minimized (Ruff, Ebert, & Stephan, 1929; Rydén & Lyngfelt, 2006). The amalgamation of the SOFC anode and the chemical looping oxidizer also cuts down the requirement for a gas turbine, which is needed in a typical SOFC combined cycle system. To increase the efficiency of the process, the configuration of chemical looping combustor can be carried out in a manner that the oxygen-l may exhaust air from the cathode of SOFC which is then utilized for the combustion of Fe_3O_4 to Fe_2O_3. As a consequence of this, the production of the high-grade heat is improved and the compression work for the air is decreased. In Table 11, a

comparison has been made between the efficiencies of the traditional IGCC process, the CDCL integrated with SOFC, and the CDCL combined cycle. As is illustrated in the table, the CDCL–SOFC method has the capability of doubling up the proficiency of state-of-the-art methods of power generation (Riedel et al., 1999; Riedel, Schaub, Jun, & Lee, 2001; Rydén, Lyngfelt, & Mattisson, 2006). The substantial improvement in efficiency of energy conversion results from the innovative scheme of energy integration between the SOFC and chemical looping.

7.3.2 Direct Solid Fuel Cells

A more advanced method of generating electricity involves the integration of a direct solid fuel cell and a chemical looping reducer (Zhang, Jacobs, Sparks, Dry, & Davis, 2002). By the modification of the electrochemical oxidation of sustained Fe to Fe_2O_3, electricity is generated, and hence, a system can be developed by the integration of a direct solid fuel cell and a chemical looping reducer. This system has been illustrated in Figure 66.

In this method, we feed reduced metal particles directly to a solid oxide fuel cell that can process solids directly. At first, particles get reduced down in the fuel reactor and afterward introduced to the fuel cell for reaction with air or oxygen at 500–1000°C for producing electricity. After that, the oxidized particles are reprocessed back to the fuel reactor to be concentrated again. It is necessary for the particles to have conductive properties for the duration when the metal is in both the reduced and the oxidized states (Dorner, Hardy, Williams, & Willauer, 2010).

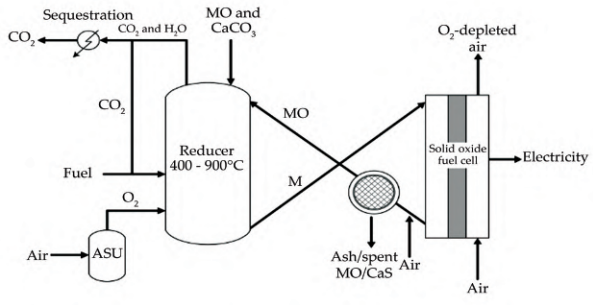

Figure 66. Application of direct solid oxide fuel cell for chemical looping

[Source: http://onlinelibrary.wiley.com/doi/10.1002/9780470872888.ch6/summary]

Two universities, namely the University of Akron, headed by S. S. C. Chuang, and the Ohio State University, headed by L. S. Fan, are in the process of making chemical looping solid oxide fuel cell systems. At UA, the initial study of the solid oxide fuel cell has been carried out, which states that the reduced iron (Fe) on Fe–Ti–O may function as a fuel, generating 45 mA/cm ^{2} at 0.4 V and at temperature of 800°C (Kronberger et al., 2004; 2005). The resulting composite material, that is, oxidized Fe–Ti–O, continued to be in the form of the powder and did not stick to the surface of anode of the fuel cell (Scott, Dennis, Hayhurst, & Brown, 2006; Arjmand, Azad, Leion, Lyngfelt, & Mattisson, 2011). The results indicate that a fuel cell integrated with chemical looping can be a possible tactic for generating electricity and an approximately pure stream of CO_2 from coal (Patel, Hildebrandt, Glasser, & Hausberger, 2007; Hildebrandt, Glasser, Hausberger, Patel, & Glasser, 2009).

The step for generating electricity from Fe on Fe–Ti–O consists of the following reactions:

Cathodic $O_2 + 4e^- \rightarrow 2O^{2-}$

Anodic $2Fe + 3O^{2-} \rightarrow Fe\ O_{23} + 6e^-$

The complete reaction parallels with an ideal cell potential (that being open-circuit voltage) of 0.996 V at temperature of 800°C. The complete reaction is stated in the equation below:

$2Fe + 32O_2 \rightarrow Fe\ O_{23} \Delta G = 384$ kJ mol

The observation of the generation of electricity from the Fe–Ti–O composite points out that the O^{2-} can reach the reduced Fe for carrying out the anodic reaction (Leion, Mattisson, & Lyngfelt, 2007; Leion, Mattisson, & Lyngfelt, 2009; Mattisson, Leion, & Lyngfelt, 2009). As this is one of the first efforts at employing solid metal in place of the fuel for the fuel cell, the results seem encouraging. Moreover, this concept of the direct solid fuel cell can be stretched out to additional types of oxygen carriers, for example, Cu and Ni (Garcia-Labiano, de Diego, Adánez, Abad, & Gayán, 2004; 2006). Table 12 makes a comparison of the ideal cell potentials by employing these metals in place of fuels. Fe/Fe_2O_3 is the type of oxygen carrier that provides the highest ideal cell potential. CuO has not been included, as it is unstable at 800°C; hence, it will not be effectual for coal chemical looping. Observation of the anodic reaction indicates the requirement to construct such a pathway that will help the electrochemical oxidation of supported Fe (Hallberg, Rydén, Mattisson, & Lyngfelt, 2014; Ströhle, Orth, & Epple, 2014).

Table 12. The ideal cell potentials (open-circuit voltage)

Reactions	***n***	**700°C**	**800°C**		**900°C**		
		ΔG (kJ) E (V)	ΔG (kJ)	E (V)	ΔG (kJ)	E (V)	
$2Ni + O_2 \rightarrow 2NiO$	4	310	0.803	290	0.751	270	0.699
$4Cu + O_2 \rightarrow 2Cu_2O$	4	220	0.570	200	0.518	180	0.466
$4/3Fe + O_2 \rightarrow 2/3Fe_2O_3$	4	407	1.053	384	0.996	363	0.941
$2Fe + O_2 \rightarrow 2FeO$	4	405	1.049	390	1.010	370	0.958
$3/2Fe + O_2 \rightarrow 1/2Fe_3O_4$	4	405	1.049	390	1.010	370	0.958

In contrast to the chemical looping–SOFC system which has been discussed in previous sections, the scheme of the direct solid fuel cell has proved to be more challenging as it involves the comparatively immature direct solid fuel cell technology. The following problems need to be addressed for the fruitful development of this direct solid fuel cell technology (Pröll, Schmid, Pfeifer, & Hofbauer, 2010; Tong et al., 2013).

i. The efficacy of the direct solid fuel cell technology for the generation of electricity by employing the supported Fe as a fuel.
ii. The efficiency of the supported Fe_2O_3 formed from the fuel cell for reacting with coal in the chemical looping method.

Overall, the evaluation of the capability of integrating a fuel cell with the process of chemical looping for the generation of electric power should be continued in more detail.

REFERENCES

1. Aceves, S. M., Berry, G. D., Martinez-Frias, J., & Espinosa-Loza, F. (2006). Vehicular storage of hydrogen in insulated pressure vessels. *International Journal of Hydrogen Energy, 31*(15), 2274-2283.
2. Aceves, S. M., Martinez-Frias, J., & Espinosa-Loza, F. (2002). *Certification testing and demonstration of insulated pressure vessels for vehicular hydrogen storage* (No. UCRL-JC-148495). Lawrence Livermore National Laboratory (LLNL), Livermore, CA.
3. Aceves, S. M., Martinez-Frias, J., & Garcia-Villazana, O. (2000). Analytical and experimental evaluation of insulated pressure vessels for cryogenic hydrogen storage. *International Journal of Hydrogen Energy, 25*(11), 1075-1085.
4. Ahn, C. C., Ye, Y., Ratnakumar, B. V., Witham, C., Bowman Jr, R. C., & Fultz, B. (1998). Hydrogen desorption and adsorption measurements on graphite nanofibers. *Applied Physics Letters, 73*(23), 3378-3380.
5. Al-Ghamdi, A. A., Shalaan, E., Al-Hazmi, F. S., Faidah, A. S., Al-Heniti, S., & Husain, M. (2012). Adsorption sites of hydrogen atom on pure and Mg-doped multi-walled carbon nanotubes. *Journal of Nanomaterials, 2012*, 89.
6. Araújo, C. M., Ahuja, R., Osorio Guillén, J. M., & Jena, P. (2005). Role of titanium in hydrogen desorption in crystalline sodium alanate. *Applied Physics Letters, 86*(25), 251913.
7. Arjmand, M., Azad, A. M., Leion, H., Lyngfelt, A., & Mattisson, T. (2011). Prospects of Al_2O_3 and $MgAl_2O_4$-supported CuO oxygen carriers in chemical-looping combustion (CLC) and chemical-looping with oxygen uncoupling (CLOU). *Energy & Fuels, 25*(11), 5493-5502.
8. Arnold, G., & Wolf, J. (2005). Liquid hydrogen for automotive application next generation fuel for FC and ICE vehicles. *Teion Kogaku (Journal of Cryogenics and Superconductivity Society of Japan), 40*(6), 221-230.
9. Blockstein, D. E., & Shockley, M. A. (2006). *National Council for Science and the Environment. 2006. Energy for a Sustainable and Secure Future: A Report of the Sixth National Conference on Science.* Washington, DC: Policy and the Environment.
10. Bogdanović, B., & Schwickardi, M. (2001). Ti-doped $NaAlH_4$ as a hydrogen-storage material–preparation by Ti-catalyzed hydrogenation of aluminum powder in conjunction with sodium hydride. *Applied Physics A: Materials Science & Processing, 72*(2), 221-223.
11. Bowman Jr, R. C., Ahn, C., Ye, Y., Ratnakumar, B., Witham, C., &

Fultz, B. (1998). Hydrogen desorption and adsorption measurements on graphite nanofibers. *Applied Physics Letters, 73*(23), 3378.

12. Bowman, R. C., Hwang, S. J., Ahn, C. C., & Vajo, J. J. (2004). NMR and X-ray diffraction studies of phases in the destabilized LiH-Si system. *MRS Online Proceedings Library Archive, 837*.
13. Bruster, E., Dobbins, T. A., Tittsworth, R., & Anton, D. (2004). Decomposition behavior of Ti-doped $NaAlH_4$ studied using x-ray absorption spectroscopy at the titanium K-edge. *MRS Online Proceedings Library Archive, 837*.
14. Burke, A., & Gardiner, M. (2005). Hydrogen storage options: technologies and comparisons for light-duty vehicle applications. *Institute of Transportation Studies*.
15. Carpetis, C. (1980). A system consideration of alternative hydrogen storage facilities for estimation of storage costs. *International Journal of Hydrogen Energy, 5*(4), 423-437.
16. Carpetis, C. (1982). Estimation of storage costs for large hydrogen storage facilities. *International Journal of Hydrogen Energy, 7*(2), 191-203.
17. Chambers, A., Park, C., Baker, R. T. K., & Rodriguez, N. M. (1998). Hydrogen storage in graphite nanofibers. *The Journal of Physical Chemistry B, 102*(22), 4253-4256.
18. Chrissafis, K. (2007). Multicyclic study on the carbonation of CaO using different limestones. *Journal of Thermal Analysis and Calorimetry, 89*(2), 525-529.
19. Chuang, S. S. (2005). Catalysis of solid oxide fuel cells. *Catalysis, 18*, 186-198.
20. Chuang, S. S., Mirzababaei, J., & Rismanchian, A. (2014).*Development of a 5 kW Prototype Coal-based Fuel Cell* (No. DOE-AKRON-GO86055). Columbus, OH (United States): The Ohio Coal Development Office.
21. Crabtree, G. W., & Dresselha, M. S. (2005). Challenges for the Hydrogen Economy. *Physics Today, January, 1*.
22. Crabtree, G. W., Dresselhaus, M. S., & Buchanan, M. V. (2004). The hydrogen economy. *Physics Today, 57*(12), 39-44.
23. Das, L. M. (1990). Hydrogen engines: a view of the past and a look into the future. *International Journal of Hydrogen Energy, 15*(6), 425-443.
24. DeLuchi, M. A. (1989). Hydrogen vehicles: an evaluation of fuel storage, performance, safety, environmental impacts, and cost. *International Journal of Hydrogen Energy, 14*(2), 81-130.
25. Dillon, A. C., Blackburn, J. L., Parilla, P. A., Zhao, Y., Kim, Y. H.,

Zhang, S. B., & Heben, M. J. (2004). Discovering the mechanism of H_2 adsorption on aromatic carbon nanostructures to develop adsorbents for vehicular applications. *MRS Online Proceedings Library Archive, 837*.

26. Dorner, R. W., Hardy, D. R., Williams, F. W., & Willauer, H. D. (2010). K and Mn doped iron-based CO 2 hydrogenation catalysts: detection of $KAlH_4$ as part of the catalyst's active phase. *Applied Catalysis A: General, 373*(1), 112-121.
27. Escribano Sanz, C. (2014). *Study of chemical looping and later applications* (Bachelor's thesis, Universitat Politècnica de Catalunya).
28. Fan, L. S., & Gupta, H. (2006). *U.S. Patent No. 7,067,456*. Washington, DC: U.S. Patent and Trademark Office.
29. Fan, L. S., & Jadhav, R. A. (2002). Clean coal technologies: OSCAR and CARBONOX commercial demonstrations. *AIChE Journal, 48*(10), 2115-2123.
30. Fan, L. S., Li, F., Zeng, L., & Sridhar, D. (2016). *U.S. Patent No. 9,371,227*. Washington, DC: U.S. Patent and Trademark Office.
31. Fan, L. S., Ramkumar, S., Wang, W., & Statnick, R. (2008). Separation of carbon dioxide from gas mixtures by calcium based reaction separation process. *Provisional Patent Application, 61*(116,172).
32. Fan, Y. Y., Liao, B., Liu, M., Wei, Y. L., Lu, M. Q., & Cheng, H. M. (1999). Hydrogen uptake in vapor-grown carbon nanofibers. *Carbon, 37*(10), 1649-1652.
33. Fennell, P. S., Pacciani, R., Dennis, J. S., Davidson, J. F., & Hayhurst, A. N. (2007). The effects of repeated cycles of calcination and carbonation on a variety of different limestones, as measured in a hot fluidized bed of sand. *Energy & Fuels, 21*(4), 2072-2081.
34. Gao, M., & Krishnamurthy, R. (2008). Hydrogen transmission in pipelines and storage in pressurized and cryogenic tanks. *Hydrogen Fuel*, 341-379.
35. Garberoglio, G., Skoulidas, A. I., & Johnson, J. K. (2005). Adsorption of gases in metal organic materials: comparison of simulations and experiments. *The Journal of Physical Chemistry B, 109*(27), 13094-13103.
36. Garcia-Labiano, F., Adánez, J., de Diego, L. F., Gayán, P., & Abad, A. (2006). Effect of pressure on the behavior of copper-, iron-, and nickel-based oxygen carriers for chemical-looping combustion. *Energy & Fuels, 20*(1), 26-33.
37. García-Labiano, F., de DIEGO, L. F., Adánez, J., Abad, A., & Gayán, P. (2004). Reduction and oxidation kinetics of a copper-based oxygen carrier

prepared by impregnation for chemical-looping combustion. *Industrial & Engineering Chemistry Research, 43*(26), 8168-8177.

38. Grasa, G. S., & Abanades, J. C. (2006). CO_2 capture capacity of CaO in long series of carbonation/calcination cycles. *Industrial & Engineering Chemistry Research, 45*(26), 8846-8851.
39. Gupta, B. K., Tiwari, R. S., & Srivastava, O. N. (2004). Studies on synthesis and hydrogenation behaviour of graphitic nanofibres prepared through palladium catalyst assisted thermal cracking of acetylene. *Journal of Alloys and Compounds, 381*(1), 301-308.
40. Gupta, H., Benson, S. A., Fan, L. S., Laumb, J. D., Olson, E. S., Crocker, C. R., …& Tibbets, J. E. (2004). Pilot-scale studies of NO X reduction by activated high-sodium lignite chars: a demonstration of the CARBONOX process. *Industrial & Engineering Chemistry Research, 43*(18), 5820-5827.
41. Gupta, R. B. (Ed.). (2008). *Hydrogen fuel: production, transport, and storage*. CRC Press.
42. Hallberg, P., Rydén, M., Mattisson, T., & Lyngfelt, A. (2014). $CaMnO_3$-δ made from low cost material examined as oxygen carrier in chemical-looping combustion. *Energy Procedia, 63*, 80-86.
43. Heung, L. K. (2003). *Using metal hydride to store hydrogen*. United States: Department of Energy.
44. Heung, L. K., & Wicks, G. G. (1999). Silica embedded metal hydrides. *Journal of Alloys and Compounds, 293*, 446-451.
45. Hildebrandt, D., Glasser, D., Hausberger, B., Patel, B., & Glasser, B. J. (2009). Producing transportation fuels with less work. *Science, 323*(5922), 1680-1681.
46. Hong, S. E., Kim, D. K., Jo, S. M., Kim, D. Y., Chin, B. D., & Lee, D. W. (2007). Graphite nanofibers prepared from catalytic graphitization of electrospun poly (vinylidene fluoride) nanofibers and their hydrogen storage capacity. *Catalysis Today, 120*(3), 413-419.
47. Jin, H., & Ishida, M. (2004). A new type of coal gas fueled chemical-looping combustion. *Fuel, 83*(17), 2411-2417.
48. Jung, D. H., Kim, D., Lee, T. B., Choi, S. B., Yoon, J. H., Kim, J., …& Choi, S. H. (2006). Grand canonical Monte Carlo simulation study on the catenation effect on hydrogen adsorption onto the interpenetrating metal–organic frameworks. *The Journal of Physical Chemistry B, 110*(46), 22987-22990.
49. Kronberger, B., Johansson, E., Löffler, G., Mattisson, T., Lyngfelt, A.,

& Hofbauer, H. (2004). A two-compartment fluidized bed reactor for CO_2 capture by chemical-looping combustion. *Chemical Engineering & Technology, 27*(12), 1318-1326.

50. Kronberger, B., Lyngfelt, A., Löffler, G., & Hofbauer, H. (2005). Design and fluid dynamic analysis of a bench-scale combustion system with CO_2 separation−chemical-looping combustion. *Industrial & Engineering Chemistry Research, 44*(3), 546-556.
51. Lee, K. B., Verdooren, A., Caram, H. S., & Sircar, S. (2007). Chemisorption of carbon dioxide on potassium-carbonate-promoted hydrotalcite. *Journal of Colloid and Interface Science, 308*(1), 30-39.
52. Lee, Y. W., Deshpande, R., Dillon, A. C., Hebe, M. J., Dai, H., & Clemens, B. M. (2004). The role of metal catalyst in near ambient hydrogen adsorption on multi-walled carbon nanotubes. *MRS Online Proceedings Library Archive, 837*.
53. Leion, H., Lyngfelt, A., & Mattisson, T. (2009). Solid fuels in chemical-looping combustion using a NiO-based oxygen carrier. *Chemical Engineering Research and Design, 87*(11), 1543-1550.
54. Leion, H., Mattisson, T., & Lyngfelt, A. (2007). The use of petroleum coke as fuel in chemical-looping combustion. *Fuel, 86*(12), 1947-1958.
55. Leion, H., Mattisson, T., & Lyngfelt, A. (2009). Using chemical-looping with oxygen uncoupling (CLOU) for combustion of six different solid fuels. *Energy Procedia, 1*(1), 447-453.
56. Li, S., Jena, P., Araujo, C. M., & Ahuja, R. (2004). Electronic structure and hydrogen desorption in NaAlH 4. *MRS Online Proceedings Library Archive, 837*.
57. Li, Y., & Yang, R. T. (2006). Hydrogen storage in metal−organic frameworks by bridged hydrogen spillover. *Journal of the American Chemical Society, 128*(25), 8136-8137.
58. Li, Y., Yang, F. H., & Yang, R. T. (2007). Kinetics and mechanistic model for hydrogen spillover on bridged metal−organic frameworks. *The Journal of Physical Chemistry C, 111*(8), 3405-3411.
59. Lu, D. Y., Hughes, R. W., & Anthony, E. J. (2008). Ca-based sorbent looping combustion for CO 2 capture in pilot-scale dual fluidized beds. *Fuel Processing Technology, 89*(12), 1386-1395.
60. Malyshenko, S. P., Borzenko, V. I., Dunikov, D. O., Nazarova, O. V., Yankov, G. G., Artemov, V. I., & Sung, J. S. (2000). Modeling of thermophysical processes in Me-H cleaning systems. *Hydrogen Energy Progress, 2*, 1323.

61. Manovic, V., & Anthony, E. J. (2008). Parametric studies on the CO_2 capture capacity of CaO-based sorbents in looping cycles. *Energy & Fuels, 22*(3), 1851-1857.

62. Manovic, V., & Anthony, E. J. (2008). Sequential SO_2/CO_2 capture enhanced by steam reactivation of a CaO-based sorbent. *Fuel, 87*(8), 1564-1573.

63. Manovic, V., & Anthony, E. J. (2008). Thermal activation of CaO-based sorbent and self-reactivation during CO_2 capture looping cycles. *Environmental Science & Technology, 42*(11), 4170-4174.

64. Mattisson, T., Leion, H., & Lyngfelt, A. (2009). Chemical-looping with oxygen uncoupling using CuO/ZrO_2 with petroleum coke. *Fuel, 88*(4), 683-690.

65. Michel, F., Fieseler, H., Meyer, G., & Theiβen, F. (1998). On-board equipment for liquid hydrogen vehicles. *International Journal of Hydrogen Energy, 23*(3), 191-199.

66. Newson, E., Haueter, T., Hottinger, P., Von Roth, F., Scherer, G. W. H., & Schucan, T. H. (1998). Seasonal storage of hydrogen in stationary systems with liquid organic hydrides. *International Journal of Hydrogen Energy, 23*(10), 905-909.

67. Pant, K., & Gupta, R. B. (2009). Fundamentals and use of hydrogen as a fuel. In *Hydrogen Fuel: Production, Transport, and Storage*, 3-32.

68. Park, A. H., Gupta, P., Li, F., Sridhar, D., & Fan, L. S. (2010). Novel applications of chemical looping technologies. *Chemical Looping Systems for Fossil Energy Conversions*, 363-401.

69. Park, C., Tan, C. D., Hidalgo, R., Baker, R. T. K., & Rodriguez, N. M. (1998). Hydrogen storage in graphite nanofibers. In *Proceedings of the US DOE Hydrogen Program Review* (p. 525).

70. Patel, B., Hildebrandt, D., Glasser, D., & Hausberger, B. (2007). Synthesis and integration of chemical processes from a mass, energy, and entropy perspective. *Industrial & Engineering Chemistry Research, 46*(25), 8756-8766.

71. Pröll, T., Schmid, J. C., Pfeifer, C., & Hofbauer, H. (2010, September). Design considerations for direct solid fuel chemical looping combustion systems. In *High temperature solid looping cycles network, 2nd Network Meeting*, Alkmaar, Netherlands.

72. Riedel, T., Claeys, M., Schulz, H., Schaub, G., Nam, S. S., Jun, K. W., & Lee, K. W. (1999). Comparative study of Fischer–Tropsch synthesis with H_2/CO and H_2/CO_2 syngas using Fe-and Co-based catalysts. *Applied*

Catalysis A: General, 186(1), 201-213.

73. Riedel, T., Schaub, G., Jun, K. W., & Lee, K. W. (2001). Kinetics of CO2 hydrogenation on a K-promoted Fe catalyst. *Industrial & Engineering Chemistry Research, 40*(5), 1355-1363.
74. Rosi, N. L., Eckert, J., Eddaoudi, M., Vodak, D. T., Kim, J., O'keeffe, M., & Yaghi, O. M. (2003). Hydrogen storage in microporous metal-organic frameworks. *Science, 300*(5622), 1127-1129.
75. Rowsell, J. L., Millward, A. R., Park, K. S., & Yaghi, O. M. (2004). Hydrogen sorption in functionalized metal−organic frameworks. *Journal of the American Chemical Society, 126*(18), 5666-5667.
76. Ruff, O., Ebert, F., & Stephan, E. (1929). An article on highly fire resistant ceramic substances II the ZrO_2-CaO system. *Zeitschrift fur anorganische und allgemeine Chemie, 180*, 215-224.
77. Rydén, M., & Lyngfelt, A. (2006). Using steam reforming to produce hydrogen with carbon dioxide capture by chemical-looping combustion. *International Journal of Hydrogen Energy, 31*(10), 1271-1283.
78. Rydén, M., Lyngfelt, A., & Mattisson, T. (2006). Synthesis gas generation by chemical-looping reforming in a continuously operating laboratory reactor. *Fuel, 85*(12), 1631-1641.
79. Satyapal, S., Petrovic, J., Read, C., Thomas, G., & Ordaz, G. (2007). The US Department of Energy's National Hydrogen Storage Project: Progress towards meeting hydrogen-powered vehicle requirements. *Catalysis Today, 120*(3), 246-256.
80. Satyapal, S., Petrovic, S., Thomas, G., Read, C., & Ordaz, G. (2006, June). The US national hydrogen storage project. In *Proceedings of the 16th World Hydrogen Energy Conference* (pp. 13-16).
81. Scherer, G. W. H., Newson, E., & Wokaun, A. (1999). Economic analysis of the seasonal storage of electricity with liquid organic hydrides. *International Journal of Hydrogen Energy, 24*(12), 1157–1169.
82. Schüth, F., Bogdanović, B., & Felderhoff, M. (2004). Light metal hydrides and complex hydrides for hydrogen storage. *Chemical Communications*, (20), 2249-2258.
83. Scott, S. A., Dennis, J. S., Hayhurst, A. N., & Brown, T. (2006). In situ gasification of a solid fuel and CO2 separation using chemical looping. *AIChE Journal, 52*(9), 3325-3328.
84. Ströhle, J., Orth, M., & Epple, B. (2014). Design and operation of a 1MW th chemical looping plant. *Applied Energy, 113*, 1490-1495.

85. Sun, P., Lim, C. J., & Grace, J. R. (2008). Cyclic CO_2 capture by limestone-derived sorbent during prolonged calcination/carbonation cycling. *AIChE Journal, 54*(6), 1668-1677.

86. Taerakul, P., Sun, P., Golightly, D. W., Walker, H. W., Weavers, L. K., Zand, B., …& Fan, L. S. (2007). Characterization and re-use potential of by-products generated from the Ohio State Carbonation and Ash Reactivation (OSCAR) process. *Fuel, 86*(4), 541-553.

87. Tong, A., Sridhar, D., Sun, Z., Kim, H. R., Zeng, L., Wang, F.,& Fan, L. S. (2013). Continuous high purity hydrogen generation from a syngas chemical looping 25kW th sub-pilot unit with 100% carbon capture. *Fuel, 103*, 495-505.

88. Verbetsky, V. N., Malyshenko, S. P., Mitrokhin, S. V., Solovei, V. V., & Shmal'ko, Y. F. (1998). Metal hydrides: properties and practical applications. Review of the works in CIS-countries. *International Journal of Hydrogen Energy, 23*(12), 1165-1177.

89. Wang, W., Ramkumar, S., Li, S., Wong, D., Iyer, M., Sakadjian, B. B., & Fan, L. S. (2010). Subpilot demonstration of the carbonation−calcination reaction (CCR) process: High-temperature CO_2 and sulfur capture from coal-fired power plants. *Industrial & Engineering Chemistry Research, 49*(11), 5094-5101.

90. Wang, W., Ramkumar, S., Wong, D., & Fan, L. S. (2012). Simulations and process analysis of the carbonation–calcination reaction process with intermediate hydration. *Fuel, 92*(1), 94-106.

91. Wang, Y., & Iqbal, Z. (2004). Electrochemical hydrogen adsorption/storage in pure and functionalized single wall carbon nanotubes. *MRS Online Proceedings Library Archive, 837*.

92. White, C. M., Strazisar, B. R., Granite, E. J., Hoffman, J. S., & Pennline, H. W. (2003). Separation and capture of CO_2 from large stationary sources and sequestration in geological formations—coalbeds and deep saline aquifers. *Journal of the Air & Waste Management Association, 53*(6), 645-715.

93. Zhang, Y., Jacobs, G., Sparks, D. E., Dry, M. E., & Davis, B. H. (2002). CO and CO_2 hydrogenation study on supported cobalt Fischer–Tropsch synthesis catalysts. *Catalysis Today, 71*(3), 411-418.

CHAPTER 8

NEXT-GENERATION SEQUENCING CHEMICAL TECHNOLOGIES AND APPLICATIONS

CONTENTS

8.1 INTRODUCTION

Presently, high-output next-generation sequencing (NGS) is quickly adapting to numerous phases of biomedical research and initiated to involve in the clinical practice. The latter phase will aid the use of genomic knowledge into clinical practice in present and several next decades and will greatly alter the diagnosis, prognosis, and treatment of various human diseases. Moreover, it will also demand reforms in both medical and philosophical curricula for the training of our future physicians. Nonetheless, substantial efforts are needed to overcome certain challenges before the final application of NGS in genomic medicine can be made fruitful and practical.

In 2003, as a result of the human genome sequencing project, the molecular basis to understand processes of several diseases at the genetic level (International Human Genome Sequencing Consortium, 2004; Hattori, 2005) was established. As a result of this, the accessibility of reference sequence of the human genome has driven the rise of a new era of genomic medicine (Cancer Genome Atlas Research Network, 2008; Chin, 2013; Ley et al., 2008). Advancement in modern technology of high-output next-generation sequencing (NGS), which is also identified as multiplex cyclic sequencing or massively parallel, is the chief element that will facilitate the use of genomic knowledge into clinical practice (Pao et al., 2004; Dietz, 2010; Guttmacher & Dietz, 2010).

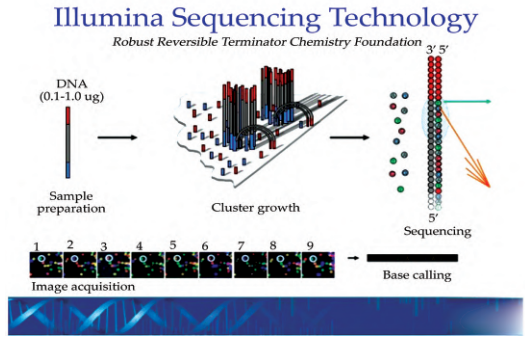

Figure 67. Next-generation Illumina-based sequencing technology

[https://www.slideshare.net/AustralianBioinformatics/ken-mcgrath-next-gen-sequencing-game-of-thrones-edition]

Nevertheless, DNA sequencing and other associated genomic informatics should be made more informative, cost-effective, and readily and easily

applicable for the ultimate switching from empirical practice to precision medicine (Green & Guyer, 1947; Hawkins, Hon, & Ren, 2010). Presently, the pace of evolution of NGS technology is spectacular, and it is expected that soon, it will result in the delivery of high-output, economical, and even portable DNA sequencing appliances to be used in clinical laboratories. Ngs has already started the production of apparatuses for clinical benefits in few healthcare settings (Shendure & Ji, 2008; Mardis, 2008; Metzker, 2010). Perhaps in the coming decades, genomic medicine driven by NGS will greatly alter the processes of prognosis, diagnosis, and therapy of human diseases. It will require both philosophical alterations and reform in the curriculum for the training of our potential physicians in the future as well.

With the purpose of getting there, there are certain challenges which need to be overcome, for instance, development of computational biology techniques as well as sophisticated bioinformatics for the analysis of huge volume of sequencing data, understanding both non-genetic and genetic centers of human ailments, understanding discrepancies in the genome, and instituting effective methods for the delivery of evidence-based genomic medicine. Lastly, resolution of legal and ethical problems in the exercise of genomic medicine is also significant (Pozo, Casas, Ruiz, Falcon, & Pérez-Breña, 2008; Martinez & Nelson, 2010; Liu & Li, 2011). This chapter presents technological background and chemistry of NGS. In the end, it will be concluded by the path of technological development of the future in these aspects (Voelkerding, Dames, & Durtschi, 2009).

8.2 CHEMISTRY OF MATERIALS

The Human Genomic Project undertook DNA sequencing which was concluded in 2003 almost completely by Sanger's procedure, the first-generation sequencing. DNA sequencing was taken to the new heights in 2007, when the Illumina genome analyzer was presented for the first time, foreshowing the age of next-generation sequencing. After that, within one year, in 2008, NGS has employed effectively to sequence the first individual human genome (Wheeler et al., 2008). Presently, NGS technology has been growing at an unprecedented speed along with a reducing cost. It is anticipated that in the coming years, the price will be reduced down to less than $10,000 per human diploid genome (Niedringhaus, Milanova, Kerby, Snyder, & Barron, 2011). During the time of writing, it is possible for a typical platform to produce almost 600-giga-base data in a sequencing course that continues for 7–10 days. The data characterize almost 6,000,000,000 sequencing reads

having a length of 100 bases. Commonly, NGS uses ligation chemistry (sequencing-by-synthesis) or DNA synthesis to read through several free templates of DNA at the similar time in a highly parallel manner to produce a massive quantity of DNA sequence data (Fuller et al., 2009). The strategy of sequencing-by-synthesis involves ensemble approach (sequencing of several clonally amplified DNA targets on secluded beads or surfaces) or a single-molecule approach. Both of the mentioned approaches can be accomplished in either synchronous-controlled fashion (in this approach, DNA polymerase is manufactured using "stop-and-go" technique by controlling the delivery of nucleotides or by limiting extension temporarily through metal catalysts or modified nucleotides) or real-time fashion (DNA polymerase is manufactured without disruption). The detection of the signal can be accomplished by enzyme-coupled chemiluminescence assays for pyrophosphate, fluorescent labeling of nucleotides, and pH change which results from the release of proton during incorporation of each nucleotide.

One major difference between the first-generation Sanger sequencing and NGS is that NGS produces short reads of commonly less than 500 bp, unlike 1000 bp. Nevertheless, the huge depth of coverage, that is, many reads over the similar template DNA region, provides compensation for the limitations induced by short reads. NGS technologies have several advantages such as they have significantly increased the throughput capacities and speed over Sanger sequencing at the same time decreasing price, even as we write. NGS may be categorized into second and third generations as per their years of chemistry and availability. Second-generation sequencing fundamentally employs DNA synthesis chemistry; the same is employed by the conventional Sanger's sequencing. On the other hand, third-generation sequencing (single-polymerase sequencing platforms of PacBioRS, Inc and Ion Torrent of Life Technologies, Inc) makes use of unique chemistries, which will be elaborated in the following technology section.

8.3 GENERAL WORKFLOW OF NGS

Irrespective of several sequencing chemistries, both second and third generations of NGS need highly complicated presequencing target preparation techniques plus data analysis of postsequencing bioinformatics (Fig. 68). The presequencing procedure consists of targeting DNA enrichment as well as library preparation of NGS. Target enrichment can be achieved by different amplification procedures (PCR, RainDance Fluidigm PCR, or

Long Ranger PCR) or hybridization capture techniques (in solution or by solid phase). NGS library preparation step usually includes the following:

- The disintegration of the enriched target DNA using different physical methods (acoustic wave, sonication, or nebulization) into a dimension of 150–500 length base pairs (library sequences) commonly,
- Ligation of the pieces to adaptor primers, and
- Clonal amplification of the library carried out by either surface cluster amplification or emulsion bead PCR.

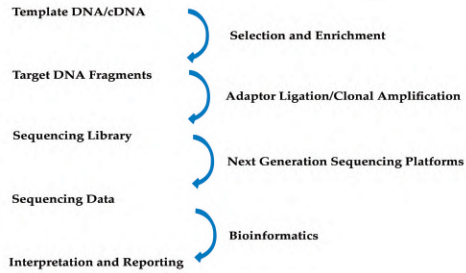

Figure 68. General workflow of next-generation sequencing technology

[https://www.ncbi.nlm.nih.gov/pubmed/22648865]

Following a sequencing reaction, several billions of reads are produced. Each read comprises the sequence of a single template clone, normally ~100 bases in length (Staplet et al., 2010; Rekadwad & Gonzalez, 2017). The bioinformatics analysis after sequencing commonly includes sequence image processing for the generation of base sequences, conversion of sequence files into readable files, and alignment of sequence with reference DNA sequence for ultimate variant identification and annotation. Suitability of NGS depends on the depth and sequence coverage. Adequate coverage of DNA regions of concern is required, and the appropriate depth of coverage (how many reads of the similar region) is significant for interpretation and accuracy. Few normally occurring complications related to NGS include sequencing reads being too short, which results in difficulties in mapping or assembly of final sequence; not each one of the sequences is processed in the same manner at homopolymers and high GC-rich regions, amplification bias is innate in few target enrichment processes, and sequencing errors (predominantly longer reads) take place from 0.01 to 16 per 100 bases' read (Ekblom & Galindo, 2011).

8.4 EVOLUTION OF SEQUENCING CHEMICAL TECHNOLOGY

8.4.1 First-Generation Sequencing

Before 2008, Sanger sequencing method was the dominated method in the biomedical research field (Maxam & Gilbert, 1977; Sanger et al., 1977). Typical fluorescent labeling is having four-color, where each of the colors is associated with one of the four bases of DNA, has been the chosen method for detection through automated capillary electrophoresis (CE) platforms, which are available commercially from Life Technologies Inc., Applied Biosystems Inc., and Beckman Coulter Inc. In 2007, the first comprehensive human diploid genome (known as Craig Venter) was sequenced using Sanger's method (Levy et al., 2007; Wang et al., 2008; Wheeler et al., 2008). Even though tasks of sequencing in huge comprehensive research ventures have now been shifted to NGS platforms, the platform of Sanger sequencing CE will probably continue to be of significant usage for clinical diagnostic applications and targeted sequencing projects (pathway analysis and biomarker identification) unless small-scale NGS platforms come to be economical and sufficiently fast; this is a fast-developing area of industrial development.

8.4.2 Second-Generation Sequencing

Reversible terminator sequencing is represented by Illumina, second-generation sequencing by Roche 454 pyrosequencing, and single-molecule sequencing by Helicos. Employing DNA ligase or DNA polymerase as their nuclear chemistry, such platforms deliver substantial performance in massive comprehensive whole-genome sequencing projects (Shendure & Ji, 2008; Margulies et al., 2006). Roche 454 employs emulsion PCR for achieving clonal amplification of target sequence. The sequencing machine is composed of numerous picoliter-volume wells, each of which contains a single bead and sequencing enzymes (Schuster, 2008). Pyrosequencing employs luciferase for the generation of light for detecting the distinct nucleotide that is merged into the nascent DNA (Ronaghi, Karamohamed, Pettersson, Uhlén, & Nyrén, 1996; Ronaghi, Uhlén, & Nyren, 1998; Ahmadian et al., 2000). Illumina (Solexa) employs cluster target sequence amplification on surfaces that are solid (known as bridge amplification). Sequencing is carried out by the addition of four kinds of nucleotides, each of which has been labeled by one of four fluorophores and contains a 30 reversible terminator. Unlike

pyrosequencing, in the Illumina-based approach, DNA can be extended by just one nucleotide at a time. After the recording of the fluorescent image of the incorporated nucleotide, the fluorophore, together with the 30 reversible terminators, is removed chemically from the DNA molecule, which permits the next cycle to occur (Mardis, 2008).

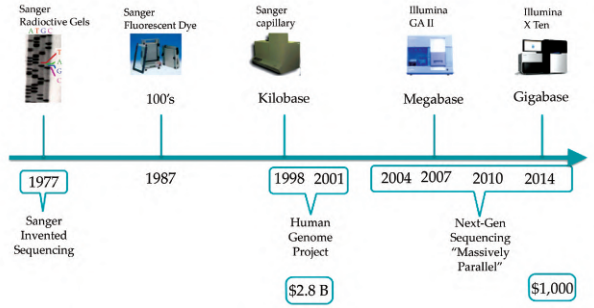

Figure 69. Progressive generations of the sequencing technologies

[Source: https://databricks.com/blog/2016/05/24/genome-sequencing-in-a-nutshell.html]

Applied Biosystems' SOLiD technology uses ligation reaction to carry out sequencing by employing a stock of all possible oligonucleotides having a fixed length that are categorized according to the position of the sequence. The ligation of oligonucleotides is done after annealing. The first ligation done by DNA ligase for matching sequences makes a record of the position of nucleotide. The clonal amplification of DNA is carried out by emulsion PCR on beads, which leads to each bead having just copies of the same molecule of DNA. These beads are placed on a glass slide and sequenced afterward (Valouev et al., 2008). These sequences are comparable regarding lengths and quantities to Illumina sequencing (Schuster, 2008; Wu, Irizarry, & Bravo, 2010).

HeliScope sequencer uses a technology known as "true single-molecule sequencing" (Efcavitch & Thompson, 2010; Thompson & Milos, 2011; Thompson, Ozsolak, & Milos, 2012). DNA fragments together with extra polyA tail adapters are joined to the surface of flow cell; this is followed by extension-based sequencing using fluorescently labeled nucleotides for cyclic washes of the flow cell just like in the case of Sanger sequencing. Even though the reads are short, current upgrading of the methodology has increased the accuracy of reading using homopolymers and also permits

for RNA sequencing (Harris et al., 2008; Thompson & Milos, 2011). The second-generation sequencing platforms differ considerably regarding their read length, throughput, and operating cost (Niedringhaus et al., 2011). They usually have high throughput, but extremely costly machines have ranged from US$0.5 to 1.0 million. The method used for signal recording is either pyrophosphate chemical conversion or fluorescence labeling; both methods need optical detection. The second-generation sequencing platforms, while being effective in several research applications, suffer consistently from high rates of the instrument, complexities of instrumentation and optics, difficulties in the preparation of sample and chemistry (enzyme–substrate reaction and fluorescent labeling), and read length restrictions (Foquet et al., 2008).

8.4.3 Third-Generation Sequencing

High demand for sequencing technology results in higher prices of technology. The final target goal aimed by NIH/NHGRI is $1000 per genome which invited grant challenge in 2004 for the development of advanced technologies. In line with this, presently the third-generation sequencing platforms have been characterized by less operation time, new chemistry, desktop design, and reduced operating cost. Three major third-generation sequencers have emerged at the time of writing, which comprise of Complete Genomics' combined pro-anchor hybridization and ligation (cPAL), Pacific Biosciences' real-time single-molecule sequencing (PacBioRS), and Ion Torrent of Life Technologies, Inc.

PacBioRS is a single-molecule single-polymerase sequencing platform operating in real time and can produce 1000-bp read (Eid et al., 2009; Munroe & Harris, 2010). Each chip contains zero-mode wave-guided (ZMW) nanostructures having 100-nm holes; inside these holes, DNA polymerase executes sequencing by amalgamation with phosphor-linked nucleotides which are characterized with sequentially introduced fluorophores (Fig. 70) (Lundquist et al., 2008; Korlach et al., 2008; 2010). Besides the production of DNA sequence, monitoring of the kinetics of nucleotide integration may prove helpful in the future for extracting epigenetic information (e.g., methylation configuration) of the native DNA strands (Flusberg et al., 2010). The platform has the capacity to sequence mRNA by employing ribosome in place of DNA polymerase (Uemura et al., 2010). However, the instrument having such configuration will be costly.

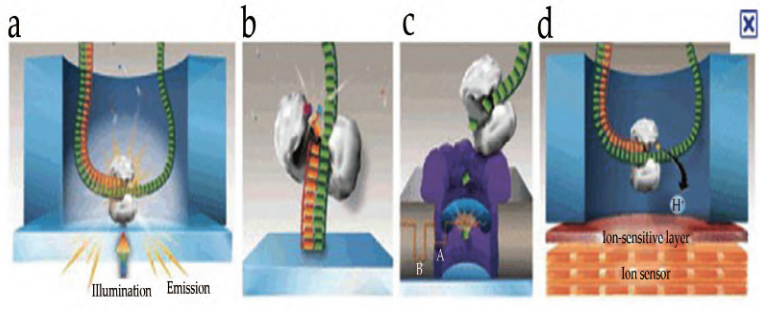

Figure 70. PacBioRS-based real-time single-polymerase, single-molecule sequencing. The sequencing of a single-stranded template of DNA is performed by manufacturing in a nanostructure hole.

[https://www.ncbi.nlm.nih.gov/pubmed/22648865]

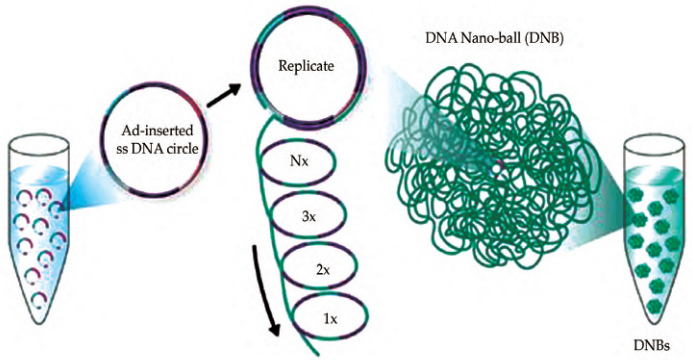

Figure 71. Complete development of Complete Genomics' nanoballs after magnification of the rolling cycle. Ligation is used for carrying out sequencing of these DNB

[https://www.ncbi.nlm.nih.gov/pubmed/22648865]

A combinatorial methodology of ligation (cPAL) sequencing and probe/anchor hybridization was pronounced by Complete Genomics with the claim of the largest throughput amid third-generation sequencers (Fig. 71). The technique employs rolling circle amplification of small DNA sequences into alleged nanoballs. Afterward, unchained sequencing by ligation is employed for determining the nucleotide sequence (Drmanac et al., 2010). This specific methodology allows sequencing of large numbers of DNA nanoballs per run

and at reduced consumable prices (Porreca, 2010; Namiot, Batyanovskii, Filatov, Tumanyan, & Esipova, 2011). The platform has successfully been employed in applications of clinical genome sequencing including whole-genome sequencing of individuals (Lee et al., 2010; Roach et al., 2010). It can prove difficult to map the short sequencing reads to the database of a genomic reference, particularly during the analysis of tumor DNA.

Presently, the most flexible and cost-effective method is perhaps Ion Torrent technology (Life Technologies, Inc). This method has been supplied as a personal genomic machine (PGM) in the form of a benchtop apparatus to clinical and research laboratories (Rothberg et al., 2011). The sequencing methodology of Ion Torrent technology involves the discharge of proton through DNA polymerase, in the course of incorporation of each nucleotide. The thick microarray of individual microwell permits DNA polymerase to perform on target DNA fragments that are clonally amplified. Underneath each microwell, the detection of a change in pH is carried out by the ion-sensitive field effect transistor (ISFET); this change in pH takes place as a result of the release of each proton, and a potential change (DV) is noted as direct measurement of nucleotide integration events (Fig. 72). In this system, no optical detection is involved; moreover, the system does not need any nucleotide labeling. The cost of Ion Torrent's PGM is less than 100 K with sequencing ability sufficient for clinical diagnostic laboratories or small-scale research projects. After its introduction in the market, NGS has started to be considered as a commodity for clinical and biomedical applications. As a general feature of several other systems, it contains multiplex barcoding adaptors which permit simultaneous testing of many samples.

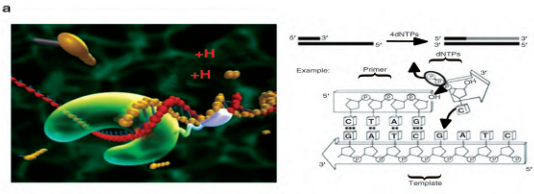

Figure 72. Ion Torrent technology illustrating the release of proton after the incorporation of the nucleotide by the DNA

[https://www.ncbi.nlm.nih.gov/pubmed/22648865]

The chip sizes that are available (314–318) capture 10–1000 MB of sequence data per run. Even though the present Ion Torrent operation is labor-demanding, recently the availability of automation with one-step

library preparation has simplified the whole process. Few limitations exist such as short read length (around 100–200 bp) and technical complications in reading by highly repetitive homopolymers and sequences, for which some progress has been made recently.

8.4.4 Next-Generation Sequencing Technology

The sequencing approach of Oxford's nanopore technology is different and is presently in the developmental phase. It employs the tunneling electron microscope (TEM) which assessed changes in conductivity across a nanopore at the time of passage of a single DNA molecule. The total current that can pass through the nanopore at any specified moment differs depending on the size, shape, and length of the nucleotide that is hindering the flow of ion through the pore. With the passage of the DNA molecule, the resultant alteration in current through the nanopore represents a direct reading of the DNA sequence. For splitting of individual molecules of nucleotide from the DNA, an exonuclease enzyme is employed; moreover, these nucleotides can be identified in the proper sequence when coupled to a suitable detection system (Branton et al., 2008; Clarke et al., 2009). Oxford's nanopore technology might also be appropriate for incorporation into a system for analyses of epigenetic modifications.

The nanopore known as "a hemolysin nanopore" is a capable sensor for ultrafast sequencing of DNA strands inside nanopores, which might deliver further sequence information by employing two recognition sites instead of one (Stoddart, Heron, Mikhailova, Maglia, & Bayley, 2009). Additionally, nanopore technology does not have the problems related to some of the other platforms by eliminating the requirement for the synthesis of DNA and optical detection and even target DNA amplifications (Ashkenasy, Sánchez-Quesada, Bayley, & Ghadiri, 2005; Astier, Braha, & Bayley, 2006; Bayley, 2006; Wu, Astier, Maglia, Mikhailova, & Bayley, 2007).

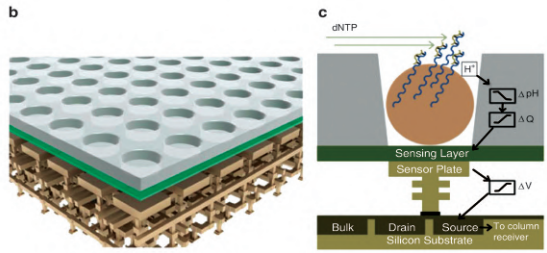

Figure 73. Advanced Ion Torrent technology. (a) The Ion Torrent exclusive mi-

crochip design. (b) Cross-sectional outlook of a single well which houses ionic sphere particles possessing a clonal amplified template of DNA. The incorporation of nucleotide by DNA poly

[https://www.ncbi.nlm.nih.gov/pubmed/22648865]

8.5 COMMON PROBLEMS WITH NGS DATA

Few general technical problems are related to several NGS platforms. Short reads in several NGS systems lead to complications in mapping and assembling to the reference sequences, especially at constant regions. All sequences are not necessarily equally sequenced and processed, and DNA regions that are supplemented with GC content are mainly susceptible to low coverage. For platforms of NGS with target enrichment or amplification, it is possible to introduce amplification bias. Finally, sequencing errors essentially exist in all NGS platforms. Longer reads are susceptible to error readings, mainly toward the ends. For some third-generation sequencers, homopolymers and repetitive sequences, too, are of concern; nevertheless, rapid improvement has been made in last few months to resolve these problems. To resolve few of these problems, deep sequencing and increase of coverage are significant measures. In Table 1, a summary of main characteristics of the present NGS platforms has been provided.

8.6 APPLICATIONS

Genomic medicine motivated by the modern development of NGS technologies will deeply influence our understanding of the developmental stages of the human disease and various phases of clinical practice in the future: prognostics, diagnostics, and therapeutics. A rough division of such clinical applications can be done according to the distinct target sequences: targeted sequencing of exomes (whole or selected) or selected genes that are associated with a specific disorder or class of disease, whole-genome sequencing, transcriptome sequencing, epigenetic mapping, and microbial population sequencing.

8.6.1 Whole-Genome Sequencing

Whole-genome sequencing can be employed for the identification of somatic mutations or germline, indels (insertion and deletion), single-nucleotide

polymorphisms (SNPs), and copy number variations. Throughout the past five years of using NGS, studies of the genomewide association have started to provide excellent information of the connection that exists between genetics and different disorders (Manolio, 2010). For instance, a similar approach has recently facilitated in the identification of new genomic loci for vulnerability to Crohn's disease, a constant draining intestinal disease of which there was no proper understanding of pathogenesis (Rioux et al., 2007). The identification of these innovative loci has greatly increased our understanding of the pathophysiology of the syndrome; moreover, it has implications for the treatment of the patient (Van Limbergen, Wilson, & Satsangi, 2009). Genomewide association studies have also resulted in producing data of non-coding sequences associated with the pathogenesis of complex human syndromes (Manolio, 2010). Whole-genome sequencing now allows the compiling of refined databanks of the full spectrum of germline variants deliberating possibilities for genetic diseases and various somatic mutations underlying all phases of human cancer (Hoffmann et al., 2011). Recently, $48 million has been granted by the National Institutes of Health which has opened the door to the usage of NGS for analyzing the genomes of hundreds and thousands of patients who are suffering from more than 6000 rare genetic syndromes, several of which are following Mendelian inheritance patterns with mutations that involve a single gene.

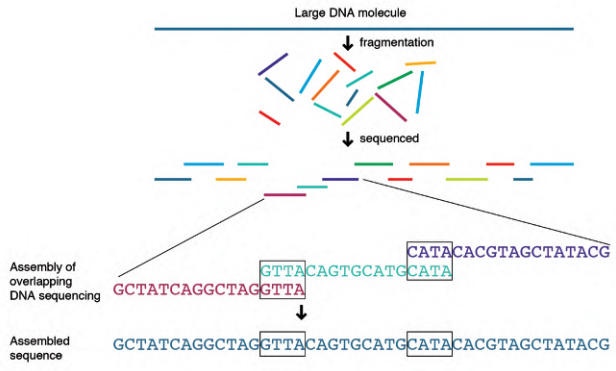

Figure 74. A typical schematic of whole-genome sequencing

[Source: http://knowgenetics.org/whole-genome-sequencing/]

It is imperative to note that as research on human genomics has been developing into the whole-genome sequencing epoch by utilizing NGS, it is imperious to first identify and afterward document the genetic discrepancies

which occur across human populations to make sure that diverse ancestry is included in our genomic studies in order to curtail the healthcare disparities that are introduced by genetics community (Need & Goldstein, 2009). Besides human studies, NGS has also been employed for studying genetic population structures and diversities of endangered species of animals. Moreover, it also has substantial applications in the plant as well (Miller et al., 2011; 2012; Zalapa et al., 2012).

8.6.2 Targeted Sequencing

At present, NGS has enabled several forms of clinical diagnostic testing through targeting selected genes or gene exons to facilitate specific clinical needs. Numerous human syndromes arise due to dysfunctions in one of many causative genes. Mutations in genes that are involved in the similar signaling or metabolic pathways may lead to similar disease phenotypes. In contrast, different mutations that involve the same gene can carry subtle to significantly different clinical manifestation of the syndrome, and several syndromes may contain overlapping mutation profiles. For instance, genetic erythrocyte syndromes can involve any of the 27 genes that are associated with the red cell enzyme deficiency, red cell membrane structure, and hemoglobin metabolism (Mohandas & Gallagher, 2008; Hershberger & Siegfried, 2011; Kingsmore et al., 2011). Phenotypic overlap between numerous involved genes needs an accurate diagnosis of these disorders by identifying the corresponding gene mutations (Hu et al., 2009; Jones et al., 2011; Schraders et al., 2011; Tsurusaki et al., 2011). Certainly, several medical centers have started to offer the facility of clinical mutation analysis through NGS. Few examples include X-linked congenital syndromes, extensive panels for detecting mutations in one of the 10–30 genes for cardiomyopathy diagnosis, comprehensive mutation detection in 24 genes that have been identified to give rise to congenital disorders of glycosylation, and several other autosomal disorders (Doi et al., 2011; Artuso et al., 2012; Guergueltcheva, et al., 2012).

For identification of mutations, whole-exome capture, as well as sequencing by NGS, has been effectively applied by employing several tissue sources (Choi et al., 2009; 2011; Bowne et al., 2011; Scholl et al., 2012). Given the extent of the burden of the carrier in human population and progressively increasing the availability of economic NGS platforms, targeted screening of carrier is also now possible in clinical practice for reducing the incidence and pain in severe receding childhood disorders (Bell et al., 2011). The significance of analysis of targeted gene mutation

panel for oncology is increasing as it is becoming more economical for cancer diagnosis, precision therapy, and prognosis. Presently, numerous popular medical centers in the United States are authenticating such cancer sequencing panels through NGS.

8.6.3 Epigenetic Applications

Epigenetic applications of NGS might contain platforms such as histone modification and CHIP-seq-protein-DNA binding (Park, 2009). Technology such as this has been recently employed to plot the methylome of the diploid human genome (Fouse, Nagarajan, & Costello, 2010). Epigenetic applications of NGS are starting to deliver essential insights into human diseases and biology. For instance, the discovery of extensive allele-particular epigenetic variation in the human genome will probably play a part in our understanding of some general diseases having a complex genetic background (Ku, Naidoo, Wu, & Soong, 2011; Kobayashi et al., 2012; Meaburn & Schulz, 2012).

8.6.4 Transcriptome Analysis

Targeted RNA sequencing (RNA-Seq) has proved to be an effective and economical method for the analysis of particular subsets of transcriptome at the same time for structural alteration, mutation, and expression (Gibbons et al., 2009; Hittinger, Johnston, Tossberg, & Rokas, 2010). This technique has been applied by a combination of next-generation sequencing and hybridization capture of cDNAs. NGS technologies having suitable assembly algorithms have aided the reconstruction of the complete transcriptome when a reference genome is not present (Martin & Wang, 2011). Similarly, targeted RNA sequencing is a dominant tool appropriate for an extensive range of large-scale tumor-profiling studies for the identification of sequence variations as well as innovative fusion gene products (Levin et al., 2009).

8.6.5 Microbial Population Analysis

NGS is perfectly suitable for whole bacterial, viral, and yeast genome sequencing due to its high output, a suitable size of most microbial genomes, and depth of sequencing. Presently, a large quantity of NGS data have become accessible that will help us greatly in increasing our understanding of interactions of host pathogen with the discovery of new splice variants, transcripts, regulatory elements, mutations, and epigenetic controls (Tripathy & Jiang, 2012). For instance, NGS was applied successfully for

characterization of the genome of the enterohemorrhagic *E. coli* O104: H4 outbreak (Mellmann et al., 2011). The capability to perform whole-genome comparisons has allowed us further to link phenotypic variations between closely linked organisms and their core genetic mechanisms and hence has enabled us to achieve a better understanding of the evolution of pathogen (Hu, Xie, Lo, Starkenburg, & Chain, 2011). NGS techniques have led us to a different field of study known as "metagenomics." Now, detection of numerous unanticipated disease-related viruses as well as emerging new human viruses is possible, such as cancer-related ones (Barzon, Lavezzo, Militello, Toppo, & Pal , 2011; Capobianchi, Giombini, & Rozera, 2013). Few other applications include HPV typing owing to its high detection sensitivity and its wide-ranging spectrum coverage of HPV subtypes, types, and variants (Barzon, Militello, Lavezzo, Franchin, Peta, Squarzon, & Palù, 2011).

8.7 LIMITATIONS OF NGS IN CLINICAL PRACTICE

Various technical limitations of NGS in genomic medicine or genomic studies have already been described in the previous sections. To pay an emphasis on the clinical sides of NGS application in medicine, the below mentioned are significant perplexing factors that will probably be the subjects of many upcoming discussions:

- Quality assurance/quality control programs are difficult prospective programs for standardization from the preliminary technical operation to clinical validation;
- Data storage and management (examination, management, and instrumentation for storage of data) need electronic devices having exceptionally high capacity;
- Intimidating challenges during the analysis of sequence data intended for clinical interpretation (e.g., formerly unknown genetic variants) are significant issues which need to be tackled;
- Reporting difficult results might be exceptionally challenging concerning clinical implication in the diagnosis of any disease, its prognosis, and managing precision therapy;
- Incidental findings having important biomedical consequences may pose ethical duties for pathologists (duty to report);
- Infringement of patent might affect laboratories that are reporting genes or using NGS or DNA sequences under patent protection;

- Adequate reimbursement of NGS will require the commercial laboratories, academic institutions, and governing agencies to develop consensus facilities, and fee codes (such as CPT codes) in partnership with service providers, clinicians, and insurance industry.

8.8 CURRENT TRENDS

Challenging Moore's law in the computer business, NGS has been rather outclassing its previous forecast of doubling affordability and technical improvement every two years. The exponential development of speed and the associated astronomical decline in prices are rapidly driving NGS from the research arena to the bedside of patients. NGS will principally impact all aspects of clinical care matters allowing numerous diagnostic tests that have never been thought possible before. In the coming years, we will probably witness the arrival of NGS platforms that will be accurate, versatile, affordable, as well as portable for clinical use. Still, a substantial obstacle in the clinical application of NGS is bioinformatics analyzation of the sequencing data. Data mining into several databases is needed for sequence variant annotation (e.g., HGMD/Biobase, locus-specific database, SeattleSeq, OMIM, and 1000 Genome program); moreover, functional prediction programs such as SIFT and PolyPhen are necessary for clinical and biological interpretation of unusual or new sequence variants. As we have been transitioning from the analysis of single gene in the past, to analysis of multigene panel, to complete exome sequencing, and soon, in the future, to the whole-genome approach, the complexity of the bioinformatics and technology has increased drastically; moreover, their clinical applications have turned out to be far more challenging than previously supposed. Progress from base pairs of DNA of the human genome to the bedside of patients will remain dependent on novel technologies such as genomic bioinformatics sciences, NGS, wide-scale collective exertions, and a multidisciplinary team approach including hospitals, academic institutions, industries, and government agencies.

REFERENCES

1. Ahmadian, A., Gharizadeh, B., Gustafsson, A. C., Sterky, F., Nyrén, P., Uhlén, M., & Lundeberg, J. (2000). Single-nucleotide polymorphism analysis by pyrosequencing. *Analytical Biochemistry, 280*(1), 103-110.
2. Artuso, R., Fallerini, C., Dosa, L., Scionti, F., Clementi, M., Garosi, G., & Longo, I. (2012). Advances in Alport syndrome diagnosis using next-generation sequencing. *European Journal of Human Genetics, 20*(1), 50.
3. Ashkenasy, N., Sánchez-Quesada, J., Bayley, H., & Ghadiri, M. R. (2005). Recognizing a single base in an individual DNA strand: a step toward DNA sequencing in nanopores. *Angewandte Chemie, 117*(9), 1425-1428.
4. Astier, Y., Braha, O., & Bayley, H. (2006). Toward single molecule DNA sequencing: direct identification of ribonucleoside and deoxyribonucleoside 5‘-monophosphates by using an engineered protein nanopore equipped with a molecular adapter. *Journal of the American Chemical Society, 128*(5), 1705-1710.
5. Barzon, L., Lavezzo, E., Militello, V., Toppo, S., & Palù, G. (2011). Applications of next-generation sequencing technologies to diagnostic virology. *International Journal of Molecular Sciences, 12*(11), 7861-7884.
6. Barzon, L., Militello, V., Lavezzo, E., Franchin, E., Peta, E., Squarzon, L., & Palù, G. (2011). Human papillomavirus genotyping by 454 next generation sequencing technology. *Journal of Clinical Virology, 52*(2), 93-97.
7. Bayley, H. (2006). Sequencing single molecules of DNA. *Current Opinion in Chemical Biology, 10*(6), 628-637.
8. Bell, C. J., Dinwiddie, D. L., Miller, N. A., Hateley, S. L., Ganusova, E. E., Mudge, J., & Sheth, V. (2011). Carrier testing for severe childhood recessive diseases by next-generation sequencing. *Science Translational Medicine, 3*(65), 65ra4.
9. Bowne, S. J., Sullivan, L. S., Koboldt, D. C., Ding, L., Fulton, R., Abbott, R. M., & Liu, Q. (2011). Identification of disease-causing mutations in autosomal dominant retinitis pigmentosa (adRP) using next-generation DNA sequencing. *Investigative Ophthalmology & Visual Science, 52*(1), 494-503.
10. Branton, D., Deamer, D. W., Marziali, A., Bayley, H., Benner, S. A.,

Butler, T., & Jovanovich, S. B. (2008). The potential and challenges of nanopore sequencing. *Nature Biotechnology, 26*(10), 1146-1153.

11. Cancer Genome Atlas (TCGA) Research Network. (2008). Comprehensive genomic characterization defines human glioblastoma genes and core pathways. *Nature, 455*(7216), 1061.
12. Capobianchi, M. R., Giombini, E., & Rozera, G. (2013). Next-generation sequencing technology in clinical virology. *Clinical Microbiology and Infection, 19*(1), 15-22.
13. Chin, L. (2013). Comprehensive genomic characterization defines human glioblastoma genes and core pathways (vol 455, pg 1061, 2008). *Nature, 494*(7438), 506-506.
14. Choi, M., Scholl, U. I., Ji, W., Liu, T., Tikhonova, I. R., Zumbo, P., & Nelson-Williams, C. (2009). Genetic diagnosis by whole exome capture and massively parallel DNA sequencing. *Proceedings of the National Academy of Sciences, 106*(45), 19096-19101.
15. Choi, M., Scholl, U. I., Yue, P., Björklund, P., Zhao, B., Nelson-Williams, C., & Lolis, E. (2011). K+ channel mutations in adrenal aldosterone-producing adenomas and hereditary hypertension. *Science, 331*(6018), 768-772.
16. Clarke, J., Wu, H. C., Jayasinghe, L., Patel, A., Reid, S., & Bayley, H. (2009). Continuous base identification for single-molecule nanopore DNA sequencing. *Nature Nanotechnology, 4*(4), 265-270.
17. Dietz, H. C. (2010). New therapeutic approaches to mendelian disorders. *New England Journal of Medicine, 363*(9), 852-863.
18. Doi, H., Yoshida, K., Yasuda, T., Fukuda, M., Fukuda, Y., Morita, H., & Saitsu, H. (2011). Exome sequencing reveals a homozygous SYT14 mutation in adult-onset, autosomal-recessive spinocerebellar ataxia with psychomotor retardation. *The American Journal of Human Genetics, 89*(2), 320-327.
19. Drmanac, R., Sparks, A. B., Callow, M. J., Halpern, A. L., Burns, N. L., Kermani, B. G., & Dahl, F. (2010). Human genome sequencing using unchained base reads on self-assembling DNA nanoarrays. *Science, 327*(5961), 78-81.
20. Efcavitch, J. W., & Thompson, J. F. (2010). Single-molecule DNA analysis. *Annual Review of Analytical Chemistry, 3*, 109-128.
21. Eid, J., Fehr, A., Gray, J., Luong, K., Lyle, J., Otto, G., & Bibillo, A. (2009). Real-time DNA sequencing from single polymerase molecules.

Science, 323(5910), 133-138.

22. Ekblom, R., & Galindo, J. (2011). Applications of next generation sequencing in molecular ecology of non-model organisms. *Heredity, 107*(1), 1.
23. Flusberg, B. A., Webster, D. R., Lee, J. H., Travers, K. J., Olivares, E. C., Clark, T. A., …& Turner, S. W. (2010). Direct detection of DNA methylation during single-molecule, real-time sequencing. *Nature Methods, 7*(6), 461-465.
24. Foquet, M., Samiee, K. T., Kong, X., Chauduri, B. P., Lundquist, P. M., Turner, S. W., & Roitman, D. B. (2008). Improved fabrication of zero-mode waveguides for single-molecule detection. *Journal of Applied Physics, 103*(3), 034301.
25. Fouse, S. D., Nagarajan, R. P., & Costello, J. F. (2010). Genome-scale DNA methylation analysis. *Epigenomics, 2*(1), 105-117.
26. Fuller, C. W., Middendorf, L. R., Benner, S. A., Church, G. M., Harris, T., Huang, X., …& Vezenov, D. V. (2009). The challenges of sequencing by synthesis. *Nature Biotechnology, 27*(11), 1013-1023.
27. Gibbons, J. G., Janson, E. M., Hittinger, C. T., Johnston, M., Abbot, P., & Rokas, A. (2009). Benchmarking next-generation transcriptome sequencing for functional and evolutionary genomics. *Molecular Biology and Evolution, 26*(12), 2731-2744.
28. Green, E. D., & Guyer, M. S. (1947). Genomics charting a course for genomic medicine from base pairs to bedside. *Nature-London, 470*(7333), 204-213.
29. Guergueltcheva, V., Azmanov, D. N., Angelicheva, D., Smith, K. R., Chamova, T., Florez, L., & Kaprelyan, A. (2012). Autosomal-recessive congenital cerebellar ataxia is caused by mutations in metabotropic glutamate receptor 1. *The American Journal of Human Genetics, 91*(3), 553-564.
30. Guttmacher, A. E., & Dietz, H. C. (2010). New therapeutic approaches to mendelian disorders genomic medicine. *The New England Journal of Medicine, 363*(9), 852.
31. Harris, T. D., Buzby, P. R., Babcock, H., Beer, E., Bowers, J., Braslavsky, I., & Giladi, E. (2008). Single-molecule DNA sequencing of a viral genome. *Science, 320*(5872), 106-109.
32. Hattori, M. (2005). Finishing the euchromatic sequence of the human genome. *Tanpakushitsu kakusan koso, 50*(2), 162–168.

33. Hawkins, R. D., Hon, G. C., & Ren, B. (2010). Next-generation genomics: an integrative approach. *Nature Review Genetics, 11*(7), 476-486.

34. Hershberger, R. E., & Siegfried, J. D. (2011). Update 2011: clinical and genetic issues in familial dilated cardiomyopathy. *Journal of the American College of Cardiology, 57*(16), 1641-1649.

35. Hittinger, C. T., Johnston, M., Tossberg, J. T., & Rokas, A. (2010). Leveraging skewed transcript abundance by RNA-Seq to increase the genomic depth of the tree of life. *Proceedings of the National Academy of Sciences, 107*(4), 1476-1481.

36. Hoffmann, T. J., Kvale, M. N., Hesselson, S. E., Zhan, Y., Aquino, C., Cao, Y., & Ewing, M. (2011). Next generation genome-wide association tool: design and coverage of a high-throughput European-optimized SNP array. *Genomics, 98*(2), 79-89.

37. Hu, B., Xie, G., Lo, C. C., Starkenburg, S. R., & Chain, P. S. (2011). Pathogen comparative genomics in the next-generation sequencing era: genome alignments, pangenomics and metagenomics. *Briefings in Functional Genomics, 10*(6), 322-333.

38. Hu, H., Wrogemann, K., Kalscheuer, V., Tzschach, A., Richard, H., Haas, S. A., & Van Bokhoven, H. (2009). Mutation screening in 86 known X-linked mental retardation genes by droplet-based multiplex PCR and massive parallel sequencing. *The HUGO Journal, 3*(1-4), 41-49.

39. International Human Genome Sequencing Consortium. (2004). Finishing the euchromatic sequence of the human genome. *Nature, 431*(7011), 931-945.

40. Jones, M. A., Bhide, S., Chin, E., Ng, B. G., Rhodenizer, D., Zhang, V. W., & Hegde, M. R. (2011). Targeted polymerase chain reaction-based enrichment and next generation sequencing for diagnostic testing of congenital disorders of glycosylation. *Genetics in Medicine, 13*(11), 921-932.

41. Kingsmore, S. F., Dinwiddie, D. L., Miller, N. A., Soden, S. E., Saunders, C. J., & Children's Mercy Genomic Medicine Team*. (2011). Adopting orphans: comprehensive genetic testing of Mendelian diseases of childhood by next-generation sequencing. *Expert Review of Molecular Diagnostics, 11*(8), 855-868.

42. Kobayashi, H., Sakurai, T., Imai, M., Takahashi, N., Fukuda, A., Yayoi,

O., & Suzuki, Y. (2012). Contribution of intragenic DNA methylation in mouse gametic DNA methylomes to establish oocyte-specific heritable marks. *PLoS Genetics, 8*(1), e1002440.

43. Korlach, J., Bjornson, K. P., Chaudhuri, B. P., Cicero, R. L., Flusberg, B. A., Gray, J. J., & Turner, S. W. (2010). Real-time DNA sequencing from single polymerase molecules. *Methods in Enzymology, 472*, 431-455.
44. Korlach, J., Marks, P. J., Cicero, R. L., Gray, J. J., Murphy, D. L., Roitman, D. B., …& Turner, S. W. (2008). Selective aluminum passivation for targeted immobilization of single DNA polymerase molecules in zero-mode waveguide nanostructures. *Proceedings of the National Academy of Sciences, 105*(4), 1176-1181.
45. Ku, C. S., Naidoo, N., Wu, M., & Soong, R. (2011). Studying the epigenome using next generation sequencing. *Journal of Medical Genetics, 48*(11), 721-730.
46. Lee, W., Jiang, Z., Liu, J., Haverty, P. M., Guan, Y., Stinson, J., & Ha, C. (2010). The mutation spectrum revealed by paired genome sequences from a lung cancer patient. *Nature, 465*(7297), 473.
47. Levin, J. Z., Berger, M. F., Adiconis, X., Rogov, P., Melnikov, A., Fennell, T., & Gnirke, A. (2009). Targeted next-generation sequencing of a cancer transcriptome enhances detection of sequence variants and novel fusion transcripts. *Genome Biology, 10*(10), R115.
48. Levy, S., Sutton, G., Ng, P. C., Feuk, L., Halpern, A. L., Walenz, B. P., & Lin, Y. (2007). The diploid genome sequence of an individual human. *PLoS Biology, 5*(10), e254.
49. Ley, T. J., Mardis, E. R., Ding, L., Fulton, B., McLellan, M. D., Chen, K., …& Cook, L. (2008). DNA sequencing of a cytogenetically normal acute myeloid leukemia genome. *Nature, 456*(7218), 66.
50. Liu, Z., & Li, D. (2011). Epigenetic silencing of floral genes. In *The science of gene flow in agriculture and its role in co-existence* (pp. 69-70). Washington, DC: University of California at Davis, Department of Plant Sciences.
51. Lundquist, P. M., Zhong, C. F., Zhao, P., Tomaney, A. B., Peluso, P. S., Dixon, J., & Maxham, M. (2008). Parallel confocal detection of single molecules in real time. *Optics Letters, 33*(9), 1026-1028.
52. Manolio, T. A. (2010). Genomewide association studies and assessment of the risk of disease. *New England Journal of Medicine, 363*(2), 166-

176.

53. Mardis, E. R. (2008). Next-generation DNA sequencing methods. *Annu. Rev. Genomics Hum. Genet., 9*, 387–402.
54. Margulies, M., Egholm, M., Altman, W. E., Attiya, S., Bader, J. S., Bemben, L. A., & Dewell, S. B. (2006). Corrigendum: Genome sequencing in microfabricated high-density picolitre reactors. *Nature, 441*(7089), 120-121.
55. Martin, J. A., & Wang, Z. (2011). Next-generation transcriptome assembly. *Nature Reviews Genetics, 12*(10), 671-682.
56. Martinez, D. A., & Nelson, M. A. (2010). The next generation becomes the now generation. *PLoS Genetics, 6*(4), e1000906.
57. Maxam, A. M., & Gilbert, W. (1977). A new method for sequencing DNA. *Proceedings of the National Academy of Sciences, 74*(2), 560-564.
58. Meaburn, E., & Schulz, R. (2012). Next generation sequencing in epigenetics: insights and challenges. *Seminars in Cell and Developmental Biology, 23*(2) 192-199.
59. Mellmann, A., Harmsen, D., Cummings, C. A., Zentz, E. B., Leopold, S. R., Rico, A., & McLaughlin, S. F. (2011). Prospective genomic characterization of the German enterohemorrhagic Escherichia coli O104: H4 outbreak by rapid next generation sequencing technology. *PloS One, 6*(7), e22751.
60. Metzker, M. L. (2010). Sequencing technologies--the next generation. *Nature Reviews Genetics, 11*(1), 31.
61. Miller, W., Hayes, V. M., Ratan, A., Petersen, C., Wittekindt, N. E., Miller, J., & Wang, Q. (2012). Genetic diversity and population structure of the endangered marsupial Sarcophilus harrisii (Tasmanian devil). *Proceedings of the National Academy of Sciences, 108*(30), 12348-12353.
62. Mohandas, N., & Gallagher, P. G. (2008). Red cell membrane: past, present, and future. *Blood, 112*(10), 3939-3948.
63. Munroe, D. J., & Harris, T. J. (2010). Third-generation sequencing fireworks at Marco Island. *Nature Biotechnology, 28*(5), 426-428.
64. Namiot, V. A., Batyanovskii, A. V., Filatov, I. V., Tumanyan, V. G., & Esipova, N. G. (2011). General theory of the long-range interactions in protein folding. *Physics Letters A, 375*(32), 2911-2915.

65. Need, A. C., & Goldstein, D. B. (2009). Next generation disparities in human genomics: concerns and remedies. *Trends in Genetics, 25*(11), 489-494.

66. Niedringhaus, T. P., Milanova, D., Kerby, M. B., Snyder, M. P., & Barron, A. E. (2011). Landscape of next-generation sequencing technologies. *Analytical Chemistry, 83*(12), 4327-4341.

67. Pao, W., Miller, V., Zakowski, M., Doherty, J., Politi, K., Sarkaria, I., & Mardis, E. (2004). EGF receptor gene mutations are common in lung cancers from "never smokers" and are associated with sensitivity of tumors to gefitinib and erlotinib. *Proceedings of the National Academy of Sciences of the United States of America, 101*(36), 13306-13311.

68. Park, P. J. (2009). ChIP-seq: advantages and challenges of a maturing technology. *Nature Reviews Genetics, 10*(10), 669.

69. Porreca, G. J. (2010). Genome sequencing on nanoballs. *Nature Biotechnology, 28*(1), 43-44.

70. Pozo, F., Casas, I., Ruiz, G., Falcon, A., & Pérez-Breña, P. (2008). Application of molecular methods in the diagnosis and epidemiological study of viral respiratory infections. *Enfermedades infecciosas y microbiologia clinica, 26*, 15-25.

71. Rekadwad, B., & Gonzalez, J. M. (2017). New generation DNA sequencing (NGS): mining for genes and the potential of extremophiles. In *Microbial Applications Vol. 1* (pp. 255-268). Springer International Publishing.

72. Rioux, J. D., Xavier, R. J., Taylor, K. D., Silverberg, M. S., Goyette, P., Huett, A., & Shugart, Y. Y. (2007). Genome-wide association study identifies five novel susceptibility loci for Crohn's disease and implicates a role for autophagy in disease pathogenesis. *Nature Genetics, 39*(5), 596.

73. Roach, J. C., Glusman, G., Smit, A. F., Huff, C. D., Hubley, R., Shannon, P. T., & Shendure, J. (2010). Analysis of genetic inheritance in a family quartet by whole-genome sequencing. *Science, 328*(5978), 636-639.

74. Ronaghi, M., Karamohamed, S., Pettersson, B., Uhlén, M., & Nyrén, P. (1996). Real-time DNA sequencing using detection of pyrophosphate release. *Analytical Biochemistry, 242*(1), 84-89.

75. Ronaghi, M., Uhlén, M., & Nyren, P. (1998). A sequencing method based on real-time pyrophosphate. *Science, 281*(5375), 363.

76. Rothberg, J. M., Hinz, W., Rearick, T. M., Schultz, J., Mileski, W.,

Davey, M., & Hoon, J. (2011). An integrated semiconductor device enabling non-optical genome sequencing. *Nature, 475*(7356), 348.

77. Sanger, F., Nicklen, S., & Coulson, A. R. (1977). DNA sequencing with chain-terminating inhibitors. *Proceedings of the National Academy of Sciences, 74*(12), 5463-5467.
78. Scholl, U. I., Nelson-Williams, C., Yue, P., Grekin, R., Wyatt, R. J., Dillon, M. J., & Wang, W. H. (2012). Hypertension with or without adrenal hyperplasia due to different inherited mutations in the potassium channel KCNJ5. *Proceedings of the National Academy of Sciences, 109*(7), 2533-2538.
79. Schraders, M., Haas, S. A., Weegerink, N. J., Oostrik, J., Hu, H., Hoefsloot, L. H., & Kalscheuer, V. M. (2011). Next-generation sequencing identifies mutations of SMPX, which encodes the small muscle protein, X-linked, as a cause of progressive hearing impairment. *The American Journal of Human Genetics, 88*(5), 628-634.
80. Schuster, S. C. (2008). Next-generation sequencing transforms today's biology. *Nature Methods, 5*(1), 16.
81. Shendure, J., & Ji, H. (2008). Next-generation DNA sequencing. *Nature Biotechnology, 26*(10), 1135.
82. Stapley, J., Reger, J., Feulner, P. G., Smadja, C., Galindo, J., Ekblom, R., & Slate, J. (2010). Adaptation genomics: the next generation. *Trends in Ecology & Evolution, 25*(12), 705-712.
83. Stoddart, D., Heron, A. J., Mikhailova, E., Maglia, G., & Bayley, H. (2009). Single-nucleotide discrimination in immobilized DNA oligonucleotides with a biological nanopore. *Proceedings of the National Academy of Sciences, 106*(19), 7702-7707.
84. Thompson, J. F., & Milos, P. M. (2011). The properties and applications of single-molecule DNA sequencing. *Genome Biology,* 12(2), 217.
85. Thompson, J. F., Ozsolak, F., & Milos, P. M. (2012). Recent Advances in Sequencing Technology. In *Detection of non-amplified genomic DNA* (pp. 281–308). Springer: Netherlands.
86. Tripathy, S., & Jiang, R. H. (2012). Massively parallel sequencing technology in pathogenic microbes. *Plant Fungal Pathogens: Methods and Protocols,* 271–294.
87. Tsurusaki, Y., Okamoto, N., Suzuki, Y., Saitsu, H., Miyake, N., & Matsumoto, N. (2011). Exome sequencing of two patients in a family with atypical X-linked leukodystrophy. *Clinical Genetics, 80*(2), 161-

166.

88. Tsurusaki, Y., Osaka, H., Hamanoue, H., Shimbo, H., Tsuji, M., Doi, H., & Miyake, N. (2011). Rapid detection of a mutation causing X-linked leucoencephalopathy by exome sequencing. *Journal of Medical Genetics, 48*(9), 606-609.
89. Uemura, S., Aitken, C. E., Korlach, J., Flusberg, B. A., Turner, S. W., & Puglisi, J. D. (2010). Real-time tRNA transit on single translating ribosomes at codon resolution. *Nature, 464*(7291), 1012.
90. Valouev, A., Ichikawa, J., Tonthat, T., Stuart, J., Ranade, S., Peckham, H., …& Sidow, A. (2008). A high-resolution, nucleosome position map of C. elegans reveals a lack of universal sequence-dictated positioning. *Genome Research, 18*(7), 1051-1063.
91. Van Limbergen, J., Wilson, D. C., & Satsangi, J. (2009). The genetics of Crohn's disease. *Annual Review of Genomics and Human Genetics, 10*, 89-116.
92. Voelkerding, K. V., Dames, S. A., & Durtschi, J. D. (2009). Next-generation sequencing: from basic research to diagnostics. *Clinical Chemistry, 55*(4), 641-658.
93. Wang, J., Wang, W., Li, R., Li, Y., Tian, G., Goodman, L., & Guo, Y. (2008). The diploid genome sequence of an Asian individual. *Nature, 456*(7218), 60.
94. Wheeler, D. A., Srinivasan, M., Egholm, M., Shen, Y., Chen, L., McGuire, A., & Gomes, X. (2008). The complete genome of an individual by massively parallel DNA sequencing. *Nature, 452*(7189), 872.
95. Wu, H. C., Astier, Y., Maglia, G., Mikhailova, E., & Bayley, H. (2007). Protein nanopores with covalently attached molecular adapters. *Journal of the American Chemical Society, 129*(51), 16142-16148.
96. Wu, H., Irizarry, R. A., & Bravo, H. C. (2010). Intensity normalization improves color calling in SOLiD sequencing. *Nature Methods, 7*(5), 336-337.
97. Zalapa, J. E., Cuevas, H., Zhu, H., Steffan, S., Senalik, D., Zeldin, E., & Simon, P. (2012). Using next-generation sequencing approaches to isolate simple sequence repeat (SSR) loci in the plant sciences. *American Journal of Botany, 99*(2), 193-208.

INDEX

W

X

Z